AN ASSESSMENT OF THE SHORT-TERM RESPONSE OF THE CUYAHOGA RIVER TO THE REMOVAL OF THE LEFEVER DAM, CUYAHOGA FALLS, OHIO

A Thesis

Presented to

The Graduate Faculty of The University of Akron

In Partial Fulfillment

of the Requirements for the Degree

Master of Science

Christopher J. Biro

December, 2015

AN ASSESSMENT OF THE SHORT-TERM RESPONSE OF THE CUYAHOGA RIVER TO THE REMOVAL OF THE LEFEVER DAM, CUYAHOGA FALLS, OHIO

Christopher J. Biro

Thesis

Approved:	Accepted:
______________________	______________________
Advisor Dr. John A. Peck	Interim Dean of the College Dr. John C. Green
______________________	______________________
Faculty Reader Dr. LaVerne M. Friberg	Dean of the Graduate School Dr. Chand Midha
______________________	______________________
Faculty Reader Dr. James McManus	Date
______________________	
Department Chair Dr. James McManus	

ABSTRACT

In recent years, the removal of dams from U.S. rivers has become a more frequent method of river restoration. The August 2013 removal of the 4.1-m-tall LeFever Dam in Cuyahoga Falls, Ohio was the fourth dam removed on the middle Cuyahoga River in an attempt to improve water quality. The LeFever Dam removal has also provided an excellent opportunity to study the effects of low head dam removal on the fluvial environment. Previous studies on the middle Cuyahoga River have provided a comprehensive characterization of the former LeFever dam pool and the pre-LeFever removal conditions. Previous studies have also quantified the effect of the 2005 Munroe Falls Dam removal which served as predictive tool for the LeFever Dam removal located ~ 5.5 km downstream. This study has incorporated new findings from 2011 through 2015 to quantify the rate and magnitude of the geomorphic, sedimentologic and hydraulic changes induced by the LeFever Dam removal. These new findings furthered the understanding of the long-term channel adjustments induced by the Munroe Falls Dam removal as well. The six stage channel evolution model of Doyle et al. (2003) was used as the framework for describing the first-order changes brought about by the LeFever Dam removal and the long-term changes caused by the Munroe Falls removal. However, this study has found site-specific dissimilarities in the channel evolution model that have greatly influenced channel morphology. In addition, the former LeFever Dam pool has progressed through channel evolution at a faster rate than the former Munroe Falls Dam pool because the Cuyahoga River has more slope energy near the former LeFever Dam. The presence of large woody debris and the occurrence of high discharge events have significantly increased the rate of channel erosion in the study reach. Channel coarsening has resulted from both dam removals as well as pronounced degradation of the former LeFever Dam pool sediment and prolonged channel widening upstream of the former Munroe Falls Dam. Based on the river response to the Munroe Falls and LeFever Dam removals, the future conditions within the former LeFever Dam pool have been predicted.

ACKNOWLEDGEMENTS

This thesis research simply could not have been possible without the help of the dedicated individuals who supported me from the very beginning of this endeavor. First, I would like to extend my deepest gratitude to my professor and advisor Dr. John A. Peck. From my undergraduate days through my time as graduate student, he has accepted nothing but my best. I have learned more from him than any instructor in my academic career and without his knowledge, guidance, and patience I would not be where I am today.

I would also like to sincerely thank my committee members Dr. LaVerne M. Friberg and Dr. James McManus for their insights and advice and for helping me compose a quality Master's Thesis. Dr. Friberg was my very first Geology professor and I am very grateful to have worked him during my time at the University of Akron. I would also like to thank Tom Quick for his genius in building the field equipment I utilized and for always being a beacon of positivity and kindness. Elaine Butcher has been there for me since I decided to peruse geology and has always been extremely helpful, patient and hilarious. This department could not function without Tom or Elaine and I thank you both for all you have done for me and for everyone in the Geosciences Department.

I would also like to offer a special thanks to Stephanie Mitchell for her countless hours of field and lab work, friendship and support through times both good and bad. Thank you also to my fellow graduate students Carl Medvid, Charles Spurr, Zack Strong, Natalie Murray, Justin Gilbow, Gina Filliano Kunkel and Paul Krasner for your friendship and academic support. Thank you to Michael Humphreys and the Szalay Family and crew for a great season on the farm.

Finally, I would like to thank my mother Jan and father Mark for giving me the love, support and tools to complete this master's degree long before I knew I was even capable doing it. Thank you also to my brother Mark and sister-in-law Monica for always being there for me. And thank you to my amazing girlfriend Hae Nim Cho. Her unwavering love, support and friendship have been paramount in my success. I will always be grateful to have her in my life and for all she has done to for me. Thank you everyone, I am eternally grateful.

TABLE OF CONTENTS

Page

LIST OF FIGURES

LIST OF TABLES

CHAPTER I

INTRODUCTION

1.1 Significance of Dam Removal

The construction of dams on U.S. waterways has been prolific over the past two centuries and their presence has influenced the natural course of American rivers and streams in the past and present (Heinz Center, 2002). Dams are of great economic, environmental and historical value and provide many societal benefits. Dams are a vital part of American infrastructure because they are used for generating hydroelectric power, irrigation, flood control; navigation for the shipment of goods, municipal water supplies and recreational activities (American Rivers, 2002). There is no doubt that dams can be invaluable resources and fulfill the basic necessities of many people but their implementation has a profound impact on the rivers they exploit.

Dams can significantly impact river channel morphology, sedimentation and biological systems (Doyle et al., 2003; Peck and Kasper, 2013). Dams increase the upstream water depth, creating an unnatural, low-energy slack water impoundment. Within this impoundment, flow regime, temperature and dissolved oxygen levels are altered; often negatively affecting aquatic life (Burroughs et al., 2009; Csiki and Rhoads, 2010). Dams impede the natural flow of rivers and trap sediment, nutrients, and pollutants (Bednarek, 2001; Stanley and Doyle, 2002; Doyle et al., 2005; Green et al., 2013). Dams also block the movement of migratory taxa and cause degradation of downstream sediments.

Many of the dams occupying waterways today were built in the early 1900s and are reaching or have exceeded their life expectancy of ~ 50 years (American Rivers and Trout Unlimited, 2002; Heinz Center, 2002). Many of these dams are no longer needed for their intended purposes and have become obsolete. For this reason, dams are abandoned and left to deteriorate over time; giving rise to serious safety risks for downstream communities of both humans and wildlife (American Rivers and Trout Unlimited, 2002). In many cases, complete removal of the weakened structures is more cost effective than making the necessary repairs. In light of these negative impacts on the fluvial environment and hazard potential; dam removal is now viewed as a viable method of river restoration (ICF, 2005).

In recent years, the removal of manmade dams from U.S. rivers has become a more frequent method of river restoration (Doyle et al., 2002; Csiki and Rhoads, 2013). There are nearly 87,000 (NID, 2013) dams greater than 25 feet tall and potentially a total of ~ two million dams (Heinz Center, 2002) including the smallest of structures nationwide. 1,185 dams have been removed for various reasons to date; 72 of which were removed in 2014 alone (American Rivers, 2014). With the multitude of dams in the U.S and the growing trend to remove them, it is important to understand how a river system will adjust and equilibrate once a dam is removed. Doyle et al., (2003) developed a six stage, channel evolution model based on two small dam removals in Wisconsin to describe how a river system equilibrates in response to dam removal (base level lowering) (Doyle et al., 2002).

The August 2013 removal of the LeFever Dam from the Cuyahoga River in Cuyahoga Falls, Ohio provided an excellent opportunity to study the effects of dam removal on the fluvial environment. The pre-removal hydrologic, geomorphic and sedimentological conditions upstream of the LeFever dam have been extensively studied by Rumschlag and Peck (2007), Kasper (2010) and Peck and Kasper (2013). The objective of this study is to quantify the rate and magnitude of change induced by the removal of the LeFever Dam. This objective was addressed by conducting repeated field surveys to measure stream flow, geomorphic profiles and channel floor sediment characteristics. The channel evolution model of Doyle et al. (2003) describes the first-order hydrologic, geomorphic, and sedimentologic response of the river to the removal of the LeFever Dam. However, this study has found some site specific dissimilarities with the model. This study addresses the physical response of the river to dam removal. The results of this study can be of benefit to biologic studies because channel sediment serves as the habitat for benthic communities. In addition, the results of this study can be applied to other low-head dam removal projects on streams similar to the Cuyahoga River.

1.2 Geologic Setting

The Cuyahoga River is located in northeast Ohio (Figure 1). The river begins in Geauga County, takes a U-shaped course for nearly 160 kilometers, and discharges into Lake Erie. The Cuyahoga River watershed is ~1,300 km^2 and contains many different land use types ranging from highly industrial to rural land uses (OEPA, 2003; Peck and Kasper, 2013). Northeast Ohio has been subject to several glacial advances and retreats during the Pleistocene epoch (Szabo et al., 2013) The Cuyahoga River flows through a complex, interlobate zone where ice from the Erie Lobe was divided into three, Late Wisconsinan glacial lobes (Szabo and Ryan, 1981). The Cuyahoga, Grand River and Killbuck glacial lobes were topographically controlled by the resistant Pennsylvanian sandstones of the Allegheny Plateau. As the late Wisconsinan Hiram ice retreated, a northward drainage direction was established due to the regional slope of the Cuyahoga lowland (Szabo, 1986). The ancestral Cuyahoga River migrated southward by headward erosion, dissecting major morainic complexes and capturing the southward draining,

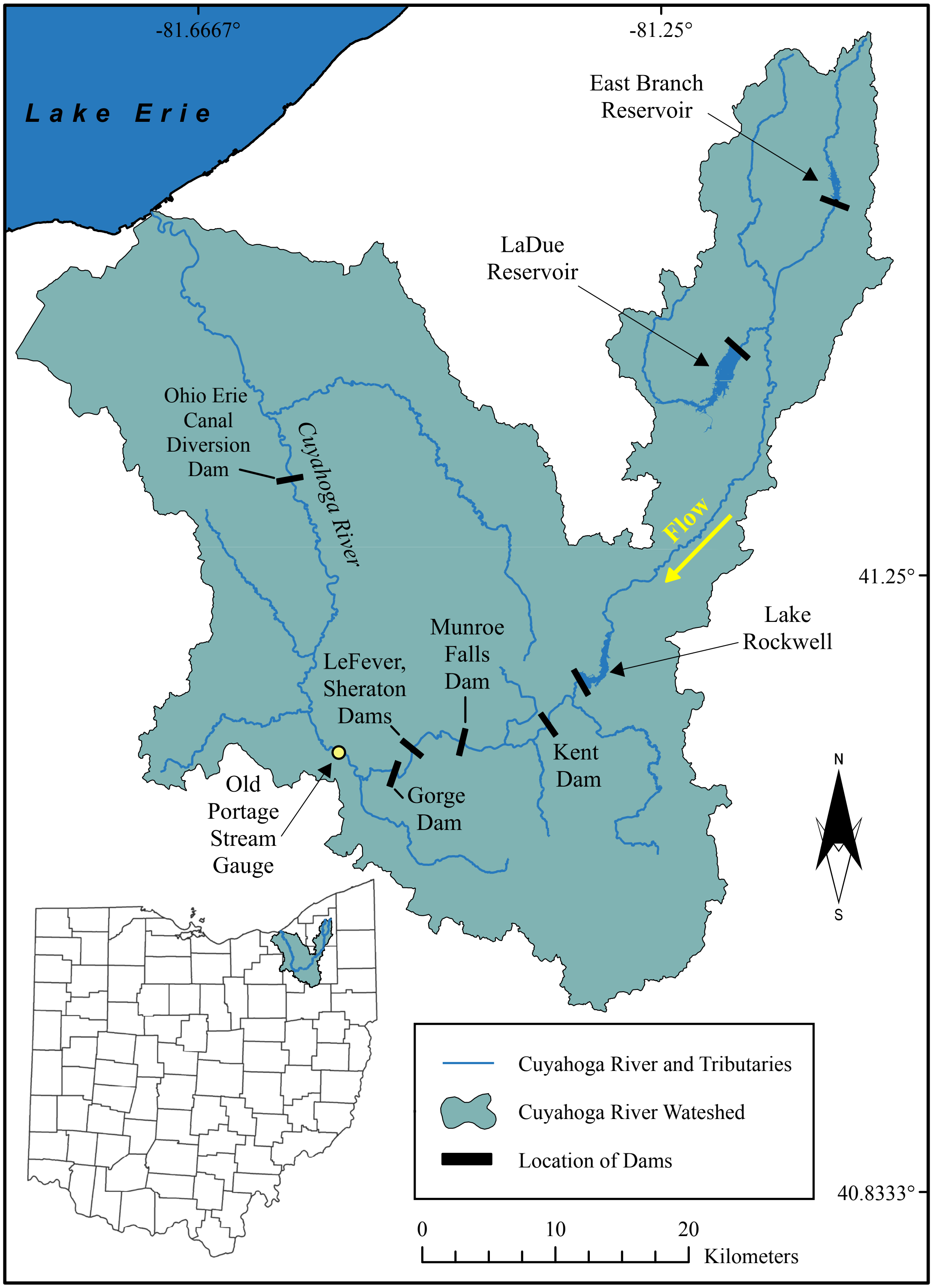

Figure 1. Location of the Cuyahoga River and major tributaries, dams and reservoirs within Northeast Ohio. The study area spans the reach from the LeFever Dam in Cuyahoga Falls to the reach upstream of the Munroe Falls Dam in Munroe Falls, OH along the Middle Cuyahoga River (USGS and Summit County GIS databases).

more mature, middle and upper reaches of the Cuyahoga River (Szabo, 1986). Glacial deposits consist of tills, lacustrine and outwash sediments (Szabo, 1986). These glacial deposits range in thicknesses from a few meters to greater than 60 m (Szabo and Ryan, 1981). The dominant soils of the Cuyahoga River watershed are the Mahoning, Canfield, Rittman, and Chili soils. They are generally derived from till and lacustrine deposits and are moderately to highly erodible (ODNR, 2002; OEPA 2003). The outwash sands and gravels are highly permeable and provide a valuable groundwater resource (ODNR, 2002).

Within the middle Cuyahoga River, near the vicinity of the former LeFever Dam, the Cuyahoga River flows directly on Pennsylvanian through Mississippian-aged siliciclastic sedimentary rocks. Where the river flows over more resistant sandstone beds of the Pennsylvanian Sharon Formation and Mississippian Cuyahoga Group, rapids and waterfalls are present. It was the waterpower of these falls that lead to the development and establishment of the city of Cuyahoga Falls and the construction of dams on the Cuyahoga River (Raub, 1984).

Upstream of the former LeFever Dam there are abundant exposures of the Sharon Formation composed of quartz arenite beds with minor quartzose conglomerate interbeds. The exposed bedrock is present as near-vertical cliffs on river left downstream of Waterworks Park and on both sides of the river downstream of the Doodlebug railroad bridge (Figure 2). At Waterworks Park, the Cuyahoga River dissects the north-south trending buried valley of Mud Brook and flows over the Wisconsinan sands and gravels of the valley fill (Szabo et al., 2013). Along this river reach, the absence of the Sharon Formation on the channel margins marks an unconfined boundary of the river, leading to an increased sinuosity of the meander bends. Other unconsolidated glacial sediment and soils comprise the banks of the former LeFever Dam impoundment where the Sharon

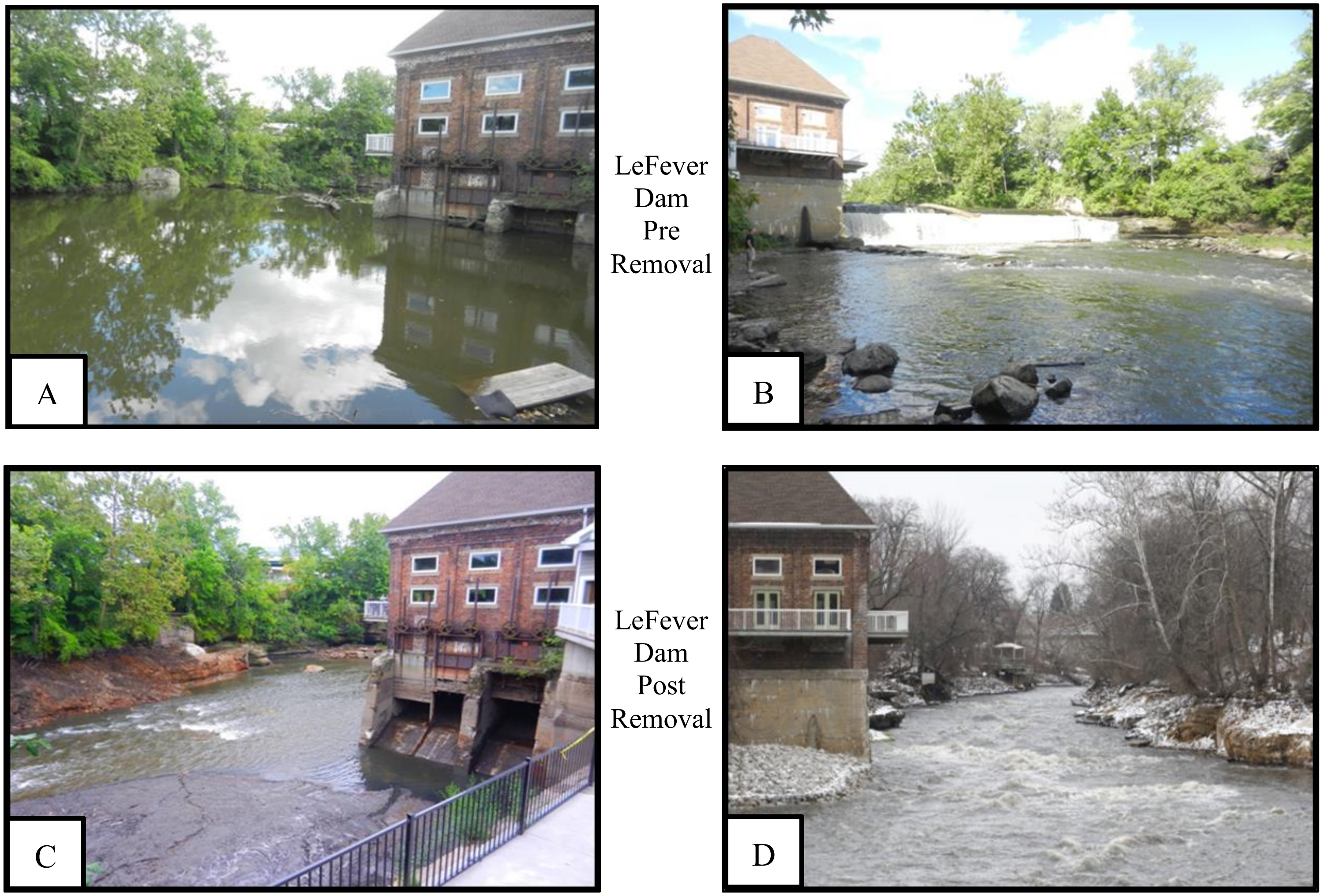

Figure 2. Photos A and B are the upstream and downstream views of the LeFever Dam pre-removal taken August 8, 2013. Photos C and D (cuyahogafalls.ohio.com) are the upstream and downstream views of the LeFever Dam site post-removal. Photo C was taken August 24, 2013 and photo D is was taken in the winter of 2013/2014.

Formation is absent and in areas outside the limits of the buried valley. These banks of sediment and soil are stabilized by the growth of well-established vegetation.

1.3 Study Area

The study area encompasses a 10.6 km stretch of the middle Cuyahoga River which spans Portage and Summit counties in northeastern Ohio (Figure 3). The boundaries of the study reach extend 4.5 km upstream of the Former Munroe Falls Dam down to the former LeFever Dam. The LeFever Dam (also known as the Powerhouse Dam) was 4.1 m tall, 30.5 m wide and once stood at river kilometer (RK) 74.5 (HDC, 2011) (Figures 1,2 and 3). The structure was a poured-concrete, curved weir dam, supported by concrete abutments on both sides (HDC, 2011). The dam was built in 1914 to replace a timber dam located just upstream that had been destroyed in the flood of 1913 (Raub, 1984). The LeFever Dam supplied hydroelectric power to the Falls Hollow Staybolt Company until 1953 when the company went out of business (HDC, 2011). Since then, the dam was no longer needed by industry; however, the dam retained structural integrity (HDC, 2011).

Even though the LeFever Dam posed no imminent social or economic risks, it was negatively affecting water quality and wildlife communities (OEPA, 2007). The low velocity impoundment extended ~2.4 km upstream of the dam and contained more than 52,000 m^3 of sediment (Kasper, 2010; Peck and Kasper, 2013). The dam pool contained 1-3 m of fine-grained sand and mud in the shallow water margins and 0.5-1 m of coarser sand and gravel in the thalweg (Kasper, 2010). The impounded sediment contained elevated concentrations of the anthropogenic metals Cr, Pb, Cu and Zn (Kasper, 2010; Peck and Kasper, 2013).

The OEPA Environmental Assessment (2011) of the lower Cuyahoga River and OEPA (2007) biological surveys conducted in the vicinity of the former LeFever Dam

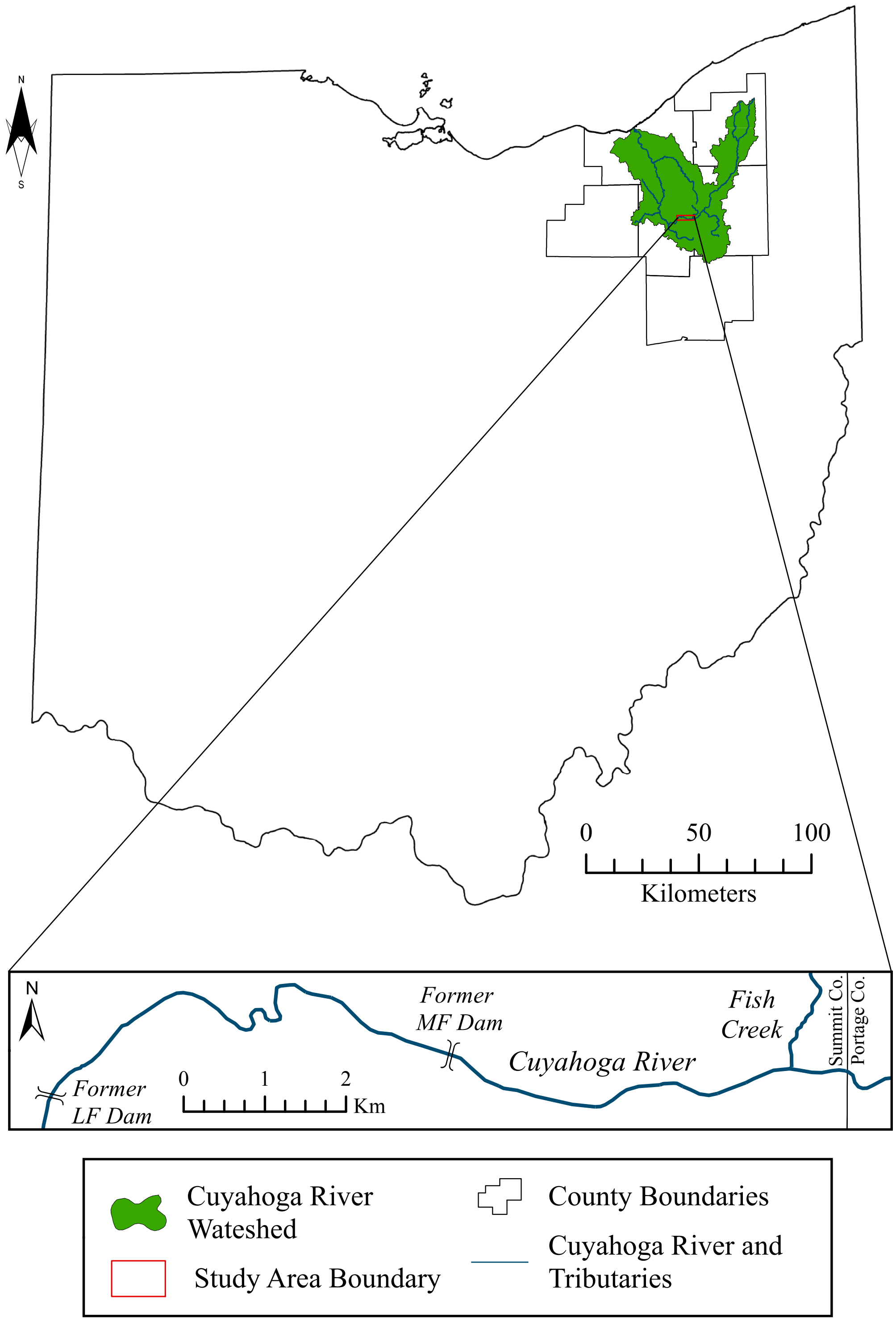

Figure 3. The location of the Cuyahoga River, its watershed and tributaries within Northeast Ohio. The watershed spans six counties. The inset map shows the middle Cuyahoga River within the study area and the location of the former LeFever (LF) and Munroe Falls (MF) Dams. Flow is from east to west.

concluded that water quality, and fish and macroinvertebrate health standards were not met in accordance with the 2003 Total Maximum Daily Load (TMDL) report. To improve water quality and the health of fish and macroinvertebrate communities, the City of Cuyahoga Falls and the Northeast Ohio Regional Sewer District (NEORSD) were funded by the Ohio Water Pollution Control Loan Fund (OWPCLF) to remove the LeFever Dam between August 12 and 19, 2013 (Figure 2). In addition, the low-head Sheraton Dam, located further downstream, was removed between July 30 and August 7, 2013. These dams were the third and fourth dams to be removed from the Cuyahoga River in the past 9 years (OEPA, 2011). The bypass of the Kent Dam in 2004 and the removal of the Munroe Falls Dam in 2005 successfully improved water quality and habitat conditions upstream of those dams (OEPA, 2011).

Based on studies of the removal of two low-head dams in Wisconsin, a channel evolution model describing the river response to dam removal has been developed by Doyle et al. (2003) (Figure 4). This model describes the geomorphic change in six sequential stages (A to F) resulting from a lowered base level, instantaneous increase in slope and decrease in water cross sectional area. The model also incorporates grain size and cohesion of the impoundment sediment because these factors can control the rate and magnitude of channel adjustment (Doyle et al., 2005). The stages of channel evolution are as follows:

- Stage A: Pre-Removal – The channel upstream of the dam is submerged under the low velocity and low energy dam pool.
- Stage B: Lowered water surface – The dam has been breached and causes a rapid decrease in water level. The drop in water level increases the slope of the river which increases the boundary shear stress. The decrease in water area results in an increase in flow velocity as expressed by the continuity equation; discharge equals the flow velocity multiplied by the cross sectional area of water in the

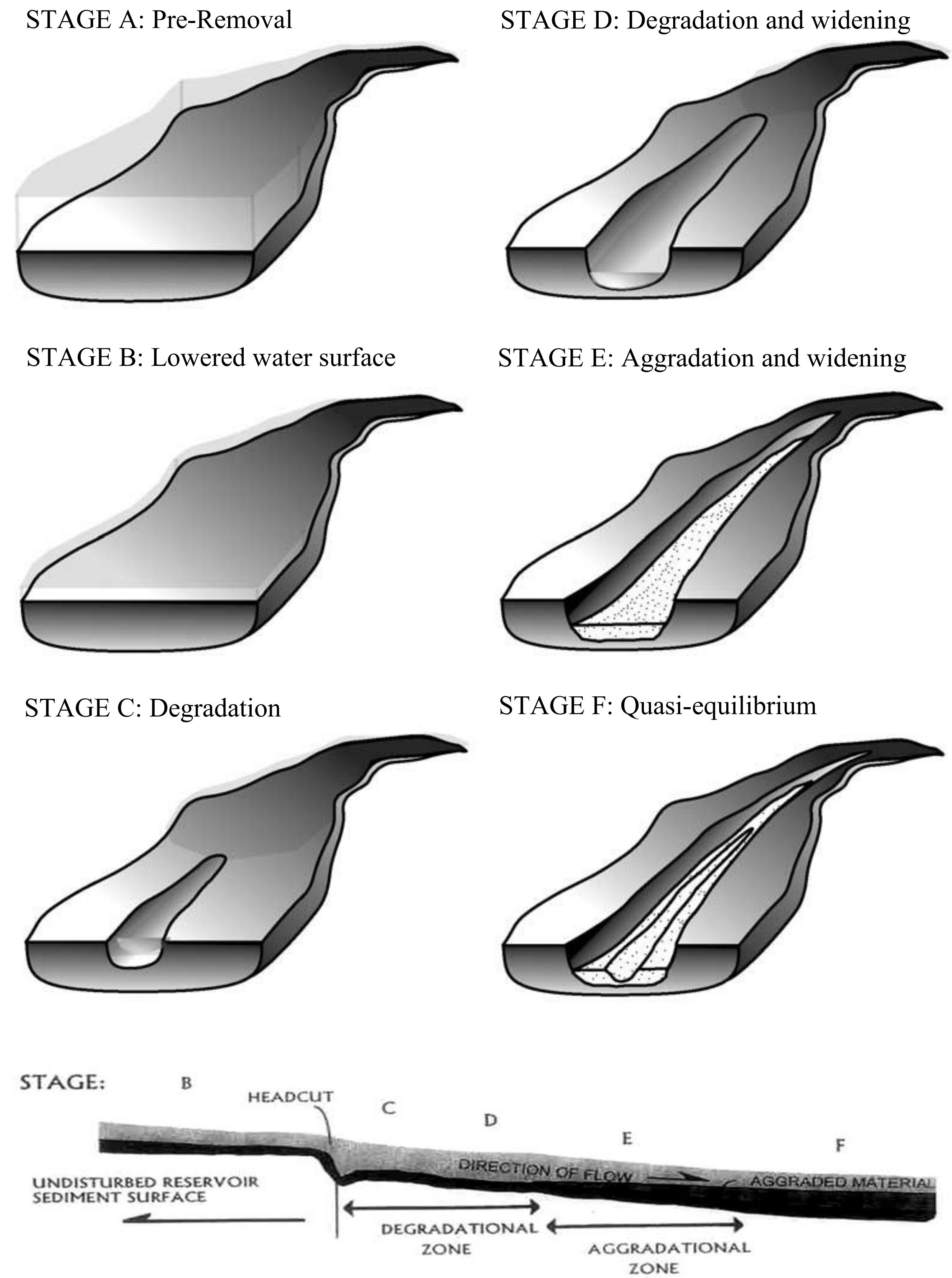

Figure 4. Channel evolution model of Stanley and Doyle (2003) based on the response of two Wisconsin rivers to the removal of low-head dams. The lower illustration shows the corresponding change along the longitudinal profile (Stanley and Doyle, 2003).

channel. Increased flow velocity and boundary shear stress initiates the first stage of geomorphic change within the channel itself (Stanley and Doyle, 2002).

- Stage C: Degradation – Due to the increased energy of the free flowing river, the channel erodes vertically into the impoundment sediment to the depth of the pre-dam substrate. This vertical erosion creates a deeply incised channel. The upstream end of the incision is called a headcut or knick point which migrates upstream by headward erosion. The rate of headcut migration controls the rate of overall change throughout the reservoir. Vertical incision occurs almost immediately after the dam is removed so Stage C may occur while Stage B dewatering is progressing (Stanley and Doyle, 2002).
- Stage D: Degradation and widening – Prolonged incision produces over steepened banks, particularly in impoundments consisting of fine-grained cohesive sediments. These banks become unstable and are prone to mass wasting. Stage D is characterized by channel widening due to slumping of the steep banks. As these banks erode, the sediment is transported downstream, while upstream sediments begin to move through the newly formed, high energy channel. As upstream sediment and eroded bank material are deposited within the impoundment, Stage E aggradation begins.
- Stage E: Aggradation and widening – Stage E is characterized by sediment deposition within the newly formed channel. During this stage, new flood plains are established and significant, non-seasonal erosion events have stopped.
- Stage F: Quasi-equilibrium – Major geomorphic adjustments within the impoundment no longer occur due to bank stabilization from the growth of riparian vegetation (Stanley and Doyle, 2002). The channel form is now stabilized within the former impoundment and the free flowing river reach has reached a state of near-equilibrium.

The degree and rate to which a stream progresses through these six stages depends largely on the local geologic and hydrologic conditions of the dammed river reach and associated impoundment (Evans, 1994; Stanley and Doyle, 2002). The response of the middle Cuyahoga River to the 2005 removal of the Munroe Falls Dam has been well documented and can be used to predict the response of the river to the removal of the LeFever Dam (Rumschlag 2007; Rumschlag and Peck 2007; Kasper, 2010; Peck and Kasper, 2013). Incision to the pre-dam substrate (Stage C) occurred within one month after the removal of the Munroe Falls Dam and lateral erosion (Stage D) continued for nearly three years after removal (Kasper, 2010). Stage E was reached downstream at Water Works Park within ~2.5 years post-removal. A similar sequence of channel evolution is expected within the former LeFever Dam impoundment.

1.4 Objectives

Rumschlag and Peck (2007), Kasper (2010) and Peck and Kasper (2013) extensively studied the hydrology, sedimentology and geomorphology of the LeFever Dam pool and the immediate upstream reach. Their work provides a quantitative characterization of the pre-removal conditions within the LeFever Dam pool.

The objective of this study is to quantify the rate and magnitude of hydrologic, sedimentologic and geomorphic change within the former LeFever Dam pool in response to the removal of the LeFever Dam. It is hypothesized that the channel evolution model of Doyle et al. (2003) will predict the first-order sequence of hydrologic, sedimentologic and geomorphic changes to occur within the former LeFever Dam pool. It is also hypothesized that the hydrologic, sedimentologic and geomorphic changes to the former LeFever Dam pool will occur at faster rates than within the former Munroe Falls Dam pool because the slope of the Cuyahoga River is greater near the former LeFever Dam pool.

CHAPTER II

METHODS

2.1 Sedimentology

To assess the changes in channel floor sedimentation, transport and erosion, sediment samples were collected from upstream of the former Munroe Falls Dam to downstream to the former LeFever Dam pool. Sites previously sampled between 2003 and 2010 by Peck et. al. (2007), Rumschlag (2007), Rumschlag and Peck (2007), Kasper (2010) and Peck and Kasper (2013) were resampled to assess the sedimentologic changes resulting from the LeFever Dam Removal. By resampling this stretch of the middle Cuyahoga River, pre and post-removal changes in sediment characteristics resulting from the Munroe Falls and LeFever Dam removals can be quantified.

The uppermost 1 cm of channel floor sediment was collected from the deep water channel using a pole-mounted scoop. The geographic coordinates of each sample were recorded using a hand held GPS. The GIS data from the previous years of sampling were included in the new sample location maps so that data coverage through time could be assessed (Figures 5-10; Tables 1-3). Water depth at each location was measured with a meter stick. Sampling took place in the summer of 2012, the fall of 2013 and the summer and winter of 2014. The grain size of each sample was visually examined in the field and the samples were placed in labeled plastic bags. These samples were then refrigerated until grain size analysis and loss-on-ignition were performed.

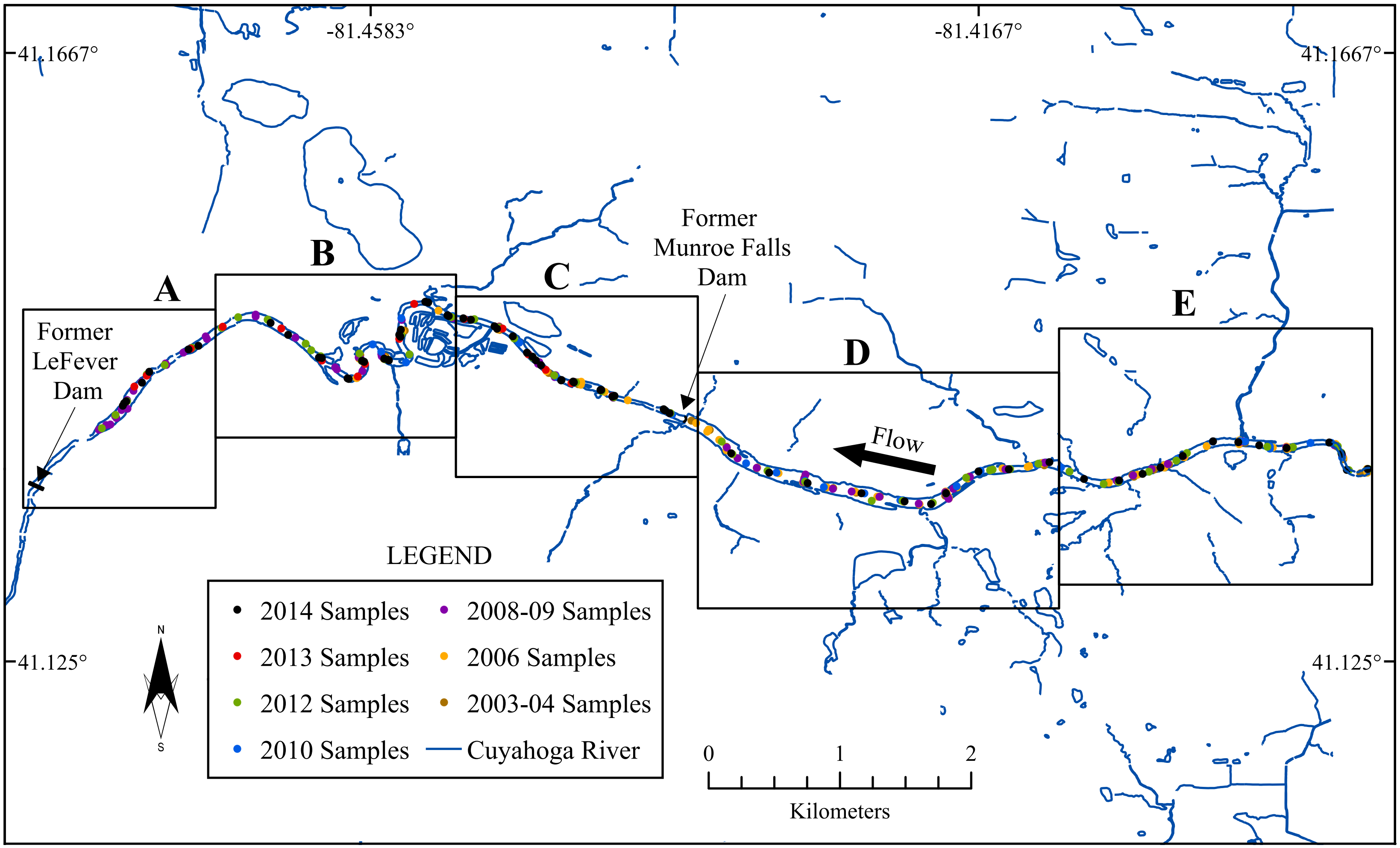

Figure 5. Location of all Cuyahoga River sediment samples collected within the study area in 2003-04, 2006 2008-09, 2010, 2012 and 2014. The inset boxes outline the enlarged areas in Figs. 6-10. Water boundaries were obtained from Summit County Geographic Information Services (SCGIS) et al. (2000).

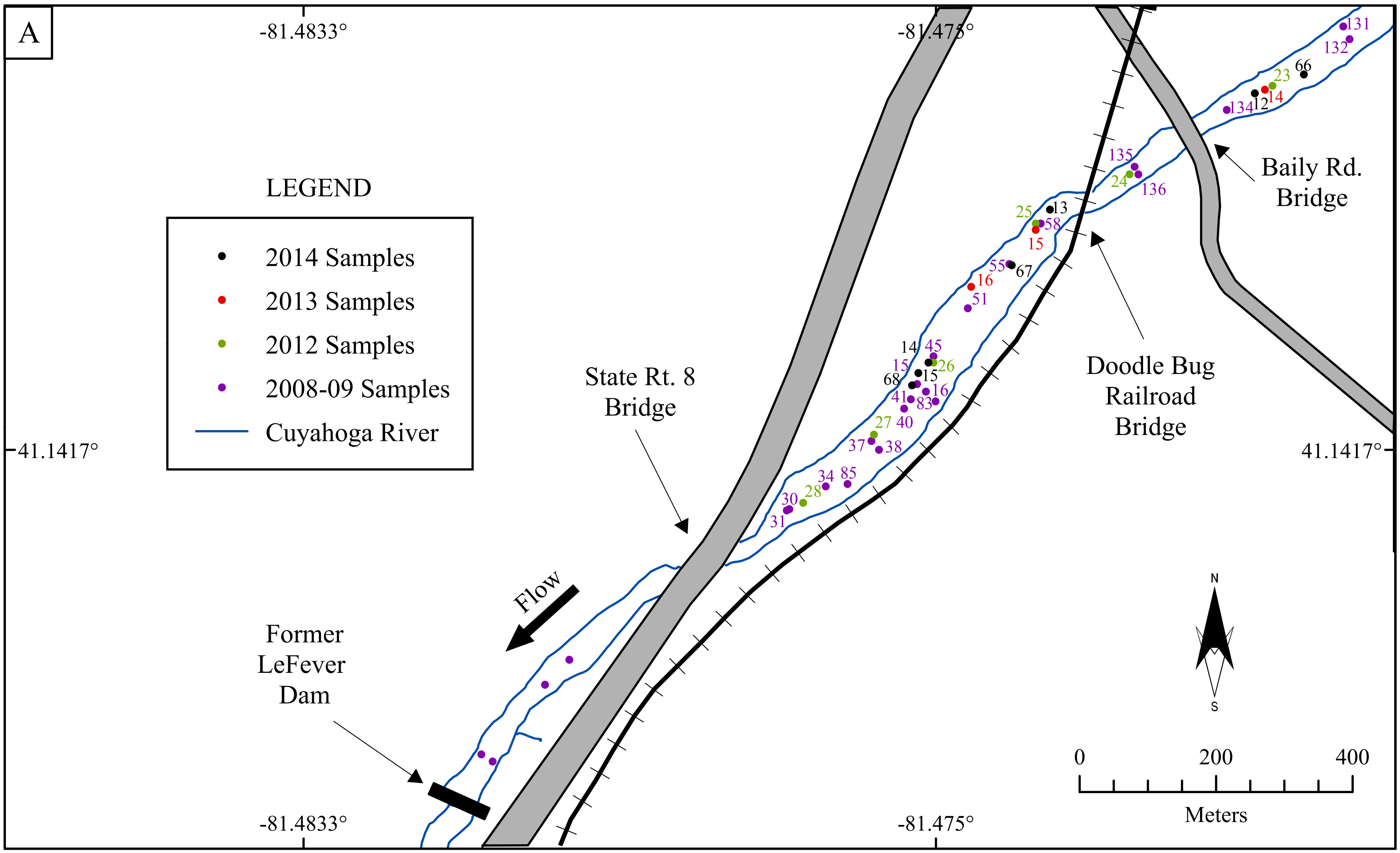

Figure 6. Location of Cuyahoga River sediment samples collected in 2008-09, 2012, 2013 and 2014. See inset box A on Figure 5 for the location within the study area. Water boundaries were obtained from Summit County Geographic Information Services (SCGIS) et al. (2000). The unlabeled dots from 2008-09 are core locations from Kasper (2010) used for water depth values.

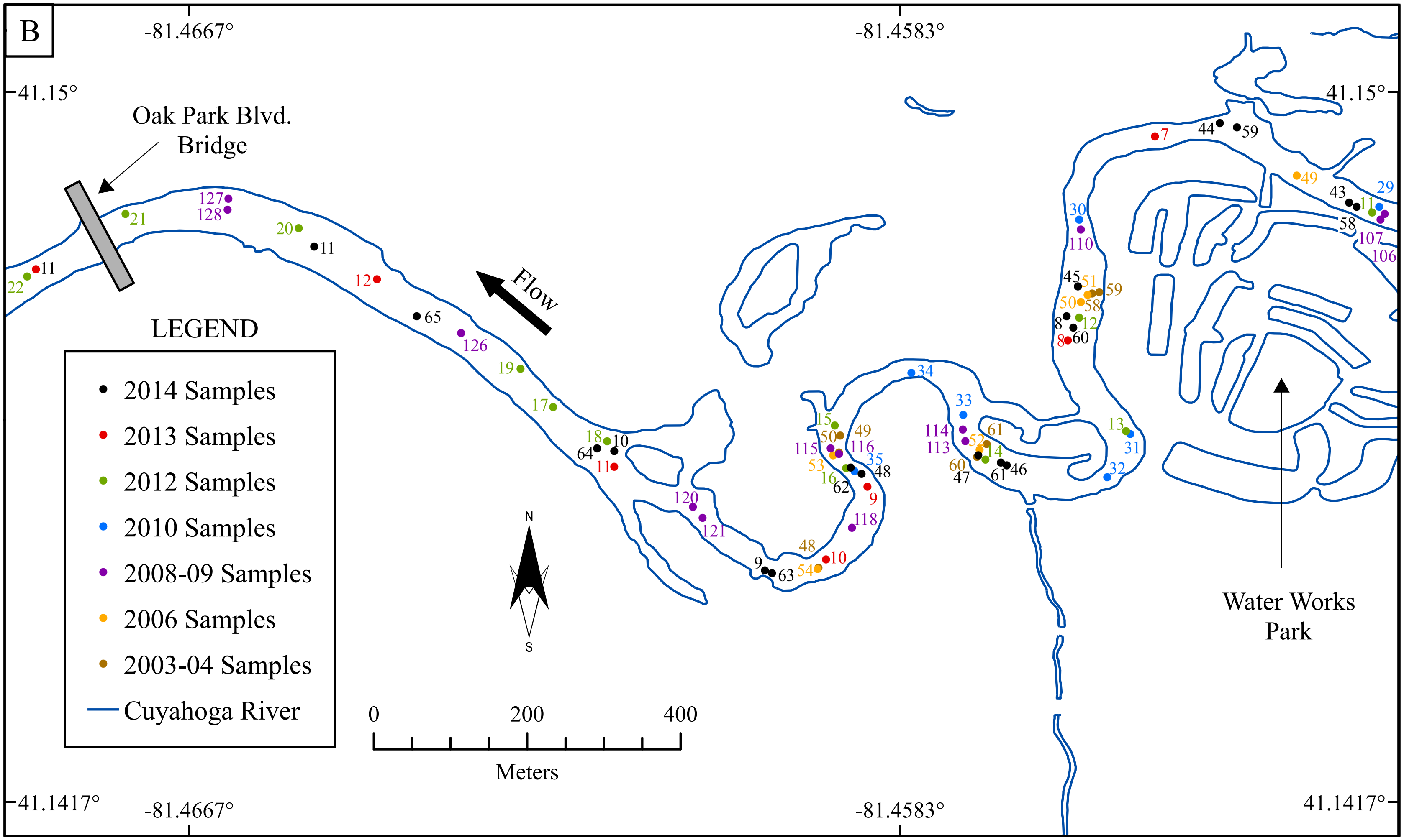

Figure 7. Location of Cuyahoga River sediment samples collected in 2003-04, 2006, 2008-09, 2010, 2012, 2013 and 2014. See inset box B on Figure 5 for the location within the study area. Water boundaries were obtained from Summit County Geographic Information Services (SCGIS) et al. (2000).

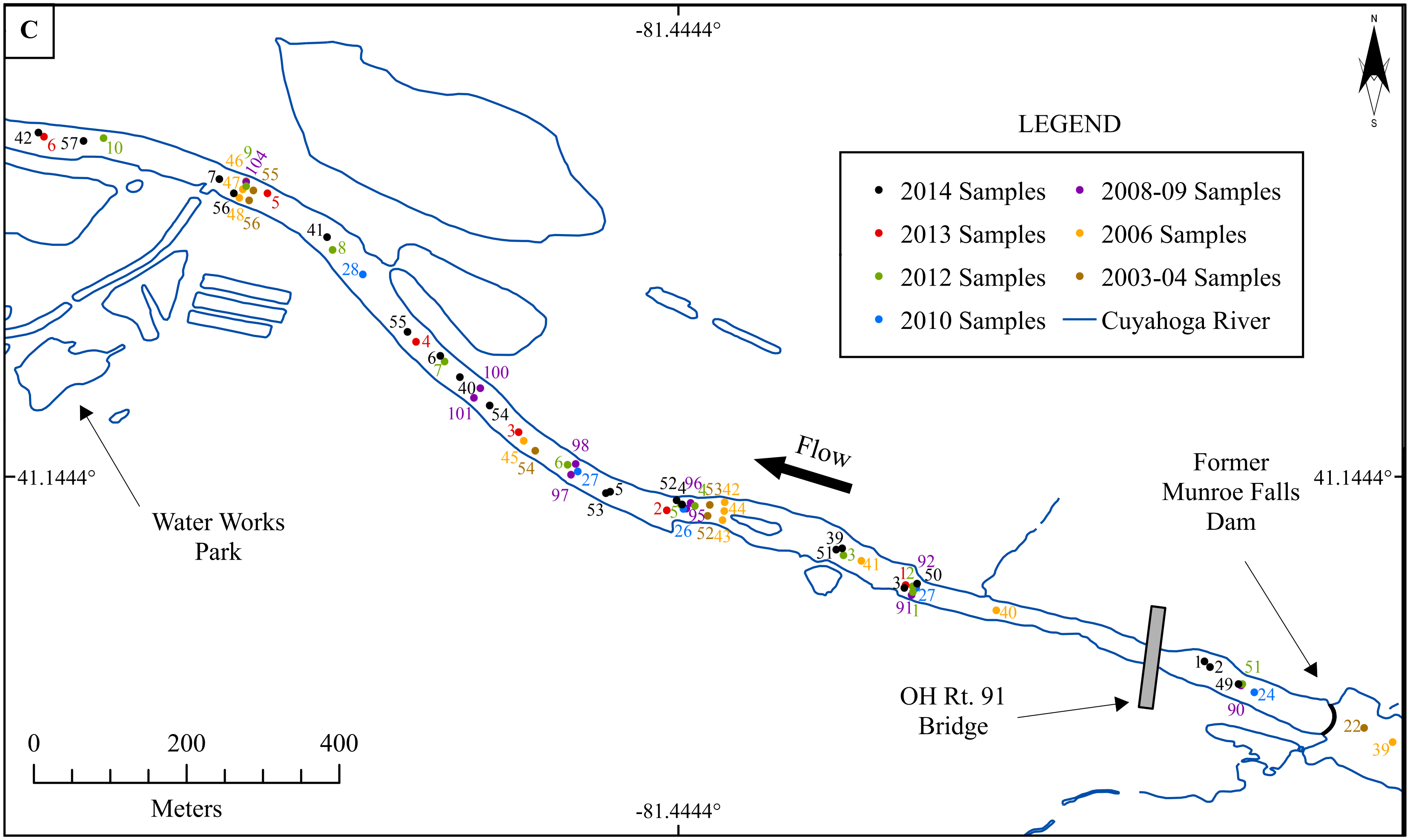

Figure 8. Location of Cuyahoga River sediment samples collected in 2003-04, 2006, 2008-09, 2010, 2012, 2013 and 2014. See inset box C on Figure 5 for the location within the study area. Water boundaries were obtained from Summit County Geographic Information Services (SCGIS) et al. (2000).

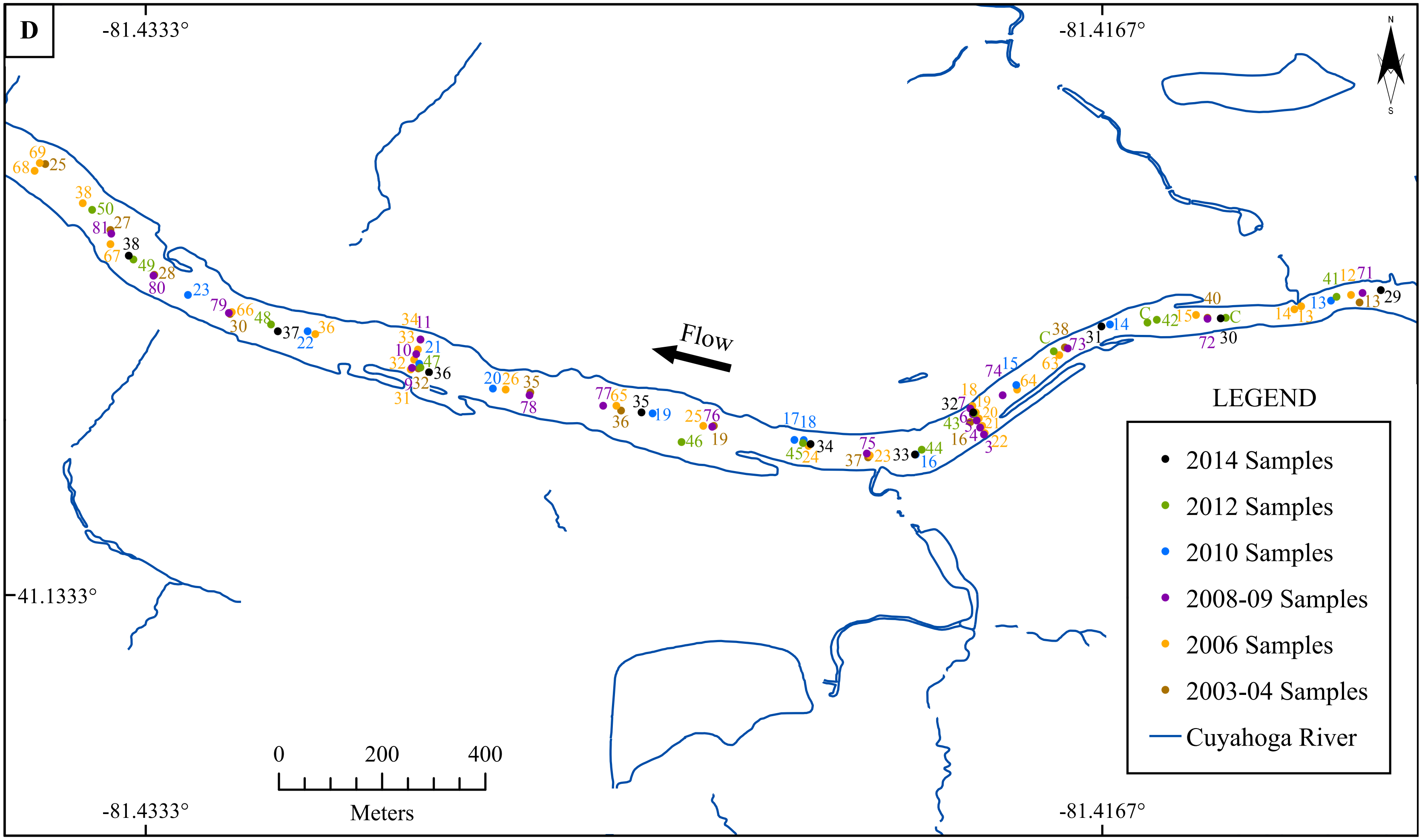

Figure 9. Location of Cuyahoga River sediment samples collected in 2003-04, 2006, 2008-09, 2010, 2012 and 2014. See inset box D on Figure 5 for the location within the study area. Water boundaries were obtained from Summit County Geographic Information Services (SCGIS) et al. (2000).

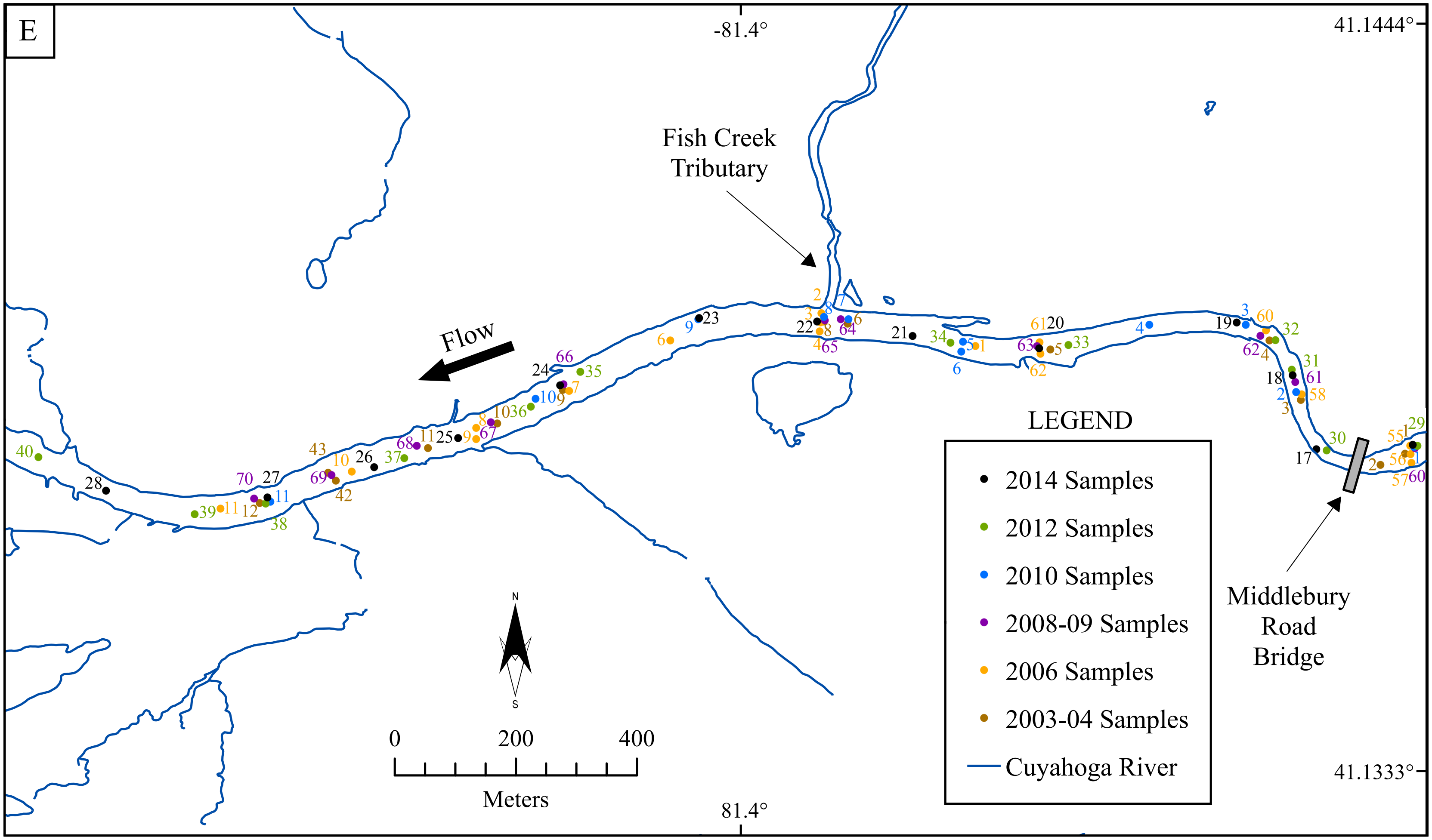

Figure 10. Location of Cuyahoga River sediment samples collected in 2003-04, 2006, 2008-09, 2010, 2012 and 2014. See inset box E on Figure 5 for the location within the study area. Water boundaries were obtained from Summit County Geographic Information Services (SCGIS) et al. (2000).

Table 1. Geographic coordinates, water depth and upstream distance from the former LeFever Dam of Cuyahoga River sediment samples collected in 2012.

Sample ID	Latitude	Longitude	Water Depth (m)	Distance from LeFever (m)	Comments
CR12-G1	41.1431	-81.4417	-	5764	Gravel
CR12-G2	41.1432	-81.4417	0.89	5762	Sand
CR12-G3	41.1435	-81.4425	-	5682	Pebbly sand
CR12-G4	41.1441	-81.4443	-	5523	Gravel
CR12-G5	41.1441	-81.4444	0.56	5509	Sand with pebbles
CR12-G6	41.1443	-81.4462	1.18	5380	Sand with gravel
CR12-G7	41.1458	-81.4472	0.69	5198	Sand
CR12-G8	41.1471	-81.4485	1.15	5008	Sand with granules
CR12-G9	41.1479	-81.4495	0.56	4893	Sand with granules
CR12-G10	41.1484	-81.4512	0.83	4739	Sand with granules
CR12-G11	41.1486	-81.4528	1.3	4603	Sand
CR12-G12	41.1474	-81.4562	1.08	4071	Sand
CR12-G13	41.1460	-81.4557	0.76	3908	Sand
CR12-G14	41.1457	-81.4573	0.86	3719	Sand
CR12-G15	41.1461	-81.4591	1.32	3453	Coarse sand
CR12-G16	41.1456	-81.4590	0.41	3398	Sand
CR12-G17	41.1463	-81.4624	1.14	2887	Sand
CR12-G18	41.1459	-81.4618	0.14	2962	Sand
CR12-G19	41.1468	-81.4628	0.76	2831	Sand
CR12-G20	41.1484	-81.4654	0.76	2546	Sand
CR12-G21	41.1486	-81.4674	2.7	2372	Gravel, boulders on bedrock
CR12-G22	41.1478	-81.4686	1.55	2248	Boulders, gravel on bedrock
CR12-G23	41.1465	-81.4706	1.9	2023	Mud
CR12-G24	41.1453	-81.4725	2.48	1818	Sand and leaves
CR12-G25	41.1447	-81.4737	2.75	1687	Sand
CR12-G26	41.1428	-81.4750	1.3	1455	Sand
CR12-G27	41.1419	-81.4758	1.65	726	Mud
CR12-G28	41.1410	-81.4768	2.04	603	Mud
CR12-G29	41.1382	-81.3900	0.764	10719	Mud
CR12-G30	41.1381	-81.3913	1.146	10587	Sand, gravel with shells
CR12-G31	41.1393	-81.3918	1.35	10443	Sand and pebbles
CR12-G32	41.1400	-81.3918	0.81	10401	Sand gravel with shells
CR12-G33	41.1397	-81.3951	1.35	10130	Sand, gravel with shells
CR12-G34	41.1397	-81.3969	1.35	9980	Sand and pebbles
CR12-G35	41.1393	-81.4024	0.81	9491	No sample, cobbles-boulders
CR12-G36	41.1388	-81.4031	0.81	9411	Boulders with gravely bars
CR12-G37	41.1380	-83.4031	0.81	9235	Sand to gravel with shells

Table 1. Geographic coordinates, water depth and upstream distance from the former LeFever Dam of Cuyahoga River sediment samples collected in 2012 (Continued).

Sample ID	Latitude	Longitude	Water Depth (m)	Distance from LeFever (m)	Comments
CR12-G38	41.1374	-83.4068	0.81	9043	Sand, gravel with shells
CR12	41.1381	-81.4159	0.54	8252	No sample, all cobbles
CR12-G39	41.1372	-81.4081	0.68	8952	Sand and granules
CR12-G40	41.1380	-81.4104	0.58	8736	Gravel
CR12-G41	41.1385	-81.4126	0.84	8537	Sand, pebbles with shells
CR12	41.1382	-81.4145	0.37	8367	Cobbles
CR12-G42	41.1381	-81.4157	0.1	8267	Gravel with shells
CR12	41.1376	-81.4175	0.58	8102	Gravel and cobbles
CR12-G43	41.1365	-81.4189	0.47	7934	Sand and gravel
CR12-G44	41.1359	-81.4198	0.68	7831	Sand and gravel
CR12-G45	41.1360	-81.4219	0.3	7658	Sand and gravel
CR12-G46	41.1470	-81.4242	0.42	7473	Sand with pebbles
CR12-G47	41.1373	-81.4286	0.77	7070	Sand, gravel with shells
CR12-G48	41.1381	-81.4312	0.53	6839	Sand
CR12-G49	41.1392	-81.4336	0.58	6599	Sand and pebbles
CR12-G50	41.1401	-81.4343	0.78	6489	Sand to boulders on bedrock
CR12-G51	41.1420	-81.4378	0.22	6116	Sand, gravel with shells

Table 2. Geographic coordinates, water depth and upstream distance from the former LeFever Dam of Cuyahoga River sediment samples collected on 9-7-2013.

Sample ID	Latitude	Longitude	Water Depth (m)	Distance from LeFever (m)	Comments
CR13-G1	41.14317	-81.44177	0.65	5150	Sand with pebbles
CR13-G2	41.14417	-81.44453	0.79	4887	Sand with pebbles
CR13-G3	41.14485	-81.44640	0.84	4707	Sand, pebbles with shells
CR13-G4	41.14603	-81.44753	0.28	4547	Sand and granules
CR13-G5	41.14778	-81.44928	1.2	4305	Sand to pebbles
CR13-G6	41.14845	-81.45192	0.54	4069	Sand, granules with shells
CR13-G7	41.14952	-81.46048	0.45	3742	Sand
CR13-G8	41.14708	-81.45637	0.52	3430	Coarse sand and granules
CR13-G9	41.14537	-81.45872	0.6	2751	Sand
CR13-G10	41.14642	-81.46168	0.24	2337	Sand
CR13-G11	41.14560	-81.46168	0.4	2378	Small dunes.
CR13-G12	41.14780	-81.46447	0.48	2039	Coarse sand and granules
CR13-G13	41.14792	-81.46847	0.36	1655	Sand
CR13-G14	41.14642	-81.47067	0.55	1406	Little sand, no bed forms.
CR13-G15	41.14457	-81.47368	0.65	1076	Mud, sand with some leaves
CR13-G16	41.14382	-81.47453	0	964	Mud

Table 3. Geographic coordinates, water depth and upstream distance from the former LeFever Dam of Cuyahoga River sediment samples collected from 7-25-2014 to 12-15-2014.

Sample ID	Latitude	Longitude	Water Depth (m)	Distance from LeFever (m)	Comments
CR14-G1	41.14227	-81.43825	0.5	5466	Sand, pebbles with shells
CR14-G2	41.14220	-81.43818	0.5	5473	Sand, gravel with shells
CR14-G3	41.14313	-81.44178	0.56	5154	Sand and pebbles
CR14-G4	41.14412	-81.44440	0.54	4907	Sand and gravel
CR14-G5	41.14427	-81.44525	0.78	4831	Sand with cobbles
CR14-G6	41.14587	-81.44725	0.42	4588	Sand to pebbles with shells
CR14-G7	41.14795	-81.44985	0.76	4262	Sand and granules
CR14-G8	41.14737	-81.45638	0.57	3473	Sand and 2.5-D ripples
CR14-G9	41.14438	-81.45992	0.5	2582	Sand, gravel with leaves
CR14-G10	41.14578	-81.46168	0.42	2366	Sand
CR14-G11	41.14818	-81.46520	0.38	1957	Sand
CR14	41.14742	-81.46907	0.2	1581	Bedrock
CR14-G12	41.14637	-81.47080	0.28	1391	Sandy granules
CR14-G13	41.14483	-81.47350	1.08	1106	Sand
CR14-G14	41.14282	-81.47510	0	847	Sand, gravel and mud
CR14-G15	41.14252	-81.47527	0.91	811	Sand and gravel
CR14-G16	41.13818	-81.39002	0.72	10104	Sand to fine cobbles
CR14-G17	41.13812	-81.39145	0.96	9969	Cobbles and bigger
CR14-G18	41.13922	-81.39180	0.84	9854	Sand with pebbles and shells
CR14-G19	41.14000	-81.39263	0.72	9738	All cobbles
CR14-G20	41.13962	-81.39557	0.81	9486	Sand to fine cobbles
CR14-G21	41.13980	-81.39745	0.79	9319	Sand and pebbles
CR14-G22	41.14002	-81.39887	0.54	9199	Sand to fine cobbles
CR14-G23	41.14007	-81.40062	0.6	9056	Coarse with sand inbetween
CR14-G24	41.13907	-81.40268	0.61	8849	Sand with pebbles and mud
CR14-G25	41.13828	-81.40420	0.8	8700	Sand
CR14-G26	41.13785	-81.40545	0.6	8584	Cobbles and boulders
CR14-G27	41.13740	-81.40703	0.78	8440	Gravel with sand
CR14-G28	41.13750	-81.40943	0.88	8229	Gravel on bedrock.
CR14-G29	41.13865	-81.41182	0.91	7997	Sand to gravel
CR14-G30	41.13833	-81.41462	0.48	7755	Cobbles
CR14-G31	41.13802	-81.41668	0.69	7581	Cobbles and fines inbetween
CR14-G32	41.13652	-81.41892	0.59	7331	Sand to fine cobbles, shells
CR14-G33	41.13578	-81.41993	0.8	7213	Gravel with sand and shells
CR14-G34	41.13597	-81.42175	0.41	7059	Fine cobbles
CR14-G35	41.13652	-81.42470	0.53	6804	Sand, mud, Macrophytes

Table 3. Geographic coordinates, water depth and upstream distance from the former LeFever Dam of Cuyahoga River sediment samples collected from 7-25-2014 to 12-15-2014 (Continued).

Sample ID	Latitude	Longitude	Water Depth (m)	Distance from LeFever (m)	Comments
CR14-G36	41.13722	-81.42840	1.01	6480	Sand and gravel
CR14-G37	41.13793	-81.43103	0.64	6246	Cobbles and big boulder
CR14-G38	41.13925	-81.43363	0.74	5984	Red pebbley sand on bedrock
CR14-G39	41.14360	-81.44252	0.5	5076	Sand to gravel
CR14-G40	41.14562	-81.44702	0.63	4622	Sand to gravel with shells
CR14-G41	41.14727	-81.44858	0.66	4393	Sand, granules with shells
CR14-G42	41.14850	-81.45198	0.54	4073	Sand, gravel with shells
CR14-G43	41.14870	-81.45307	0.96	3976	Sand to pebbles with shells
CR14-G44	41.14963	-81.45458	1.27	3819	Cobbles and sand
CR14-G45	41.14772	-81.45625	0.84	3513	Sand, granules with shells
CR14-G46	41.14562	-81.45708	0.6	3139	Sand and gravel
CR14-G47	41.14573	-81.45742	-	3108	Gravel with sand
CR14-G48	41.14552	-81.45878	0.56	2774	Sand to pebbles with shells
CR14-G49	41.14200	-81.43785	0.56	5507	Sand to fine cobbles
CR14-G50	41.14318	-81.44163	0.84	5162	Sand with gravel
CR14-G51	41.14358	-81.44258	0.74	5070	Sand with gravel
CR14-G52	41.14417	-81.44447	0.76	4902	Sand to pebbles
CR14-G53	41.14425	-81.44530	1.18	4829	All cobbles
CR14-G54	41.14528	-81.44667	1.08	4667	Sand to pebbles
CR14-G55	41.14615	-81.44763	0.56	4540	Sand, pebbles with shells
CR14-G56	41.14778	-81.44968	1.1	4281	Sand, granules with shells
CR14-G57	41.14840	-81.45145	0.94	4118	Sand, granules with shells
CR14-G58	41.14865	-81.45298	1.38	3985	Sand, coarse pebbles, shells
CR14-G59	41.14958	-81.45438	0.96	3834	Sand with leaves and shells
CR14-G60	41.14723	-81.45630	0.71	3458	Sand and granules
CR14-G61	41.14565	-81.45715	0.42	3132	Sand and pebbles
CR14-G62	41.14560	-81.45877	0.72	2778	Coarse sand
CR14-G63	41.14435	-81.45983	-	2590	Gravel
CR14-G64	41.14582	-81.46188	0.62	2356	Sand and gravel
CR14-G65	41.14737	-81.46400	0.71	2095	Sand, granules with shells
CR14-G66	41.14662	-81.47015	0.9	1457	Little sand on bedrock
CR14-G67	41.14410	-81.47400	0.74	1016	Sand and granules
CR14-G68	41.14252	-81.47532	0.97	809	Coarse sand

Sediment grain size was measured following the methodology of Folk (1980). Varying amounts of each sediment sample were used for analysis based on the sample grain size; 45 g for wet mud, 90 g for wet sand and 150 g for pebbly samples. Each sample then received six 10 ml treatments of 30% hydrogen peroxide to oxidize the organic matter in the sediment. After the six treatments when effervescence was minimal, the samples were air-dried at room temperature to obtain the starting weight for grain size analysis. Cobble samples were air-dried at room temperature and did not receive any hydrogen peroxide treatments because any organic matter attached to the cobble contributes a negligible amount of mass.

Sandy and gravely samples were sieved at half-phi intervals from 4 ϕ to -5.5 ϕ using a Tyler Rotap. The long, intermediate and short axes of clasts coarser than -5.5 ϕ were measured with a ruler, weighed and the ϕ size was calculated. The statistical mean, median, sorting and skewness as well as the percentages of sand, gravel and mud were calculated using the template made available by Rumschlag (2007) (Appendix A). Muddy samples were measured by settling using the pipette method of Folk (1980). Representative sand and mud samples were measured in duplicate to assess reproducibility.

Sediment wet and dry bulk density and organic content were measured by Dean's (1974) method of loss on ignition (Appendix B). Approximately 10% of the samples were measured in replicate.

2.2 Geomorphic Profiles

To measure the changes in channel morphology, Cuyahoga River transects previously established by Rumschlag (2007), Rumschlag and Peck (2007), Kasper (2010) and Peck and Kasper (2013) were resurveyed ~4 times per year (Figure 11, Table 4). Two new

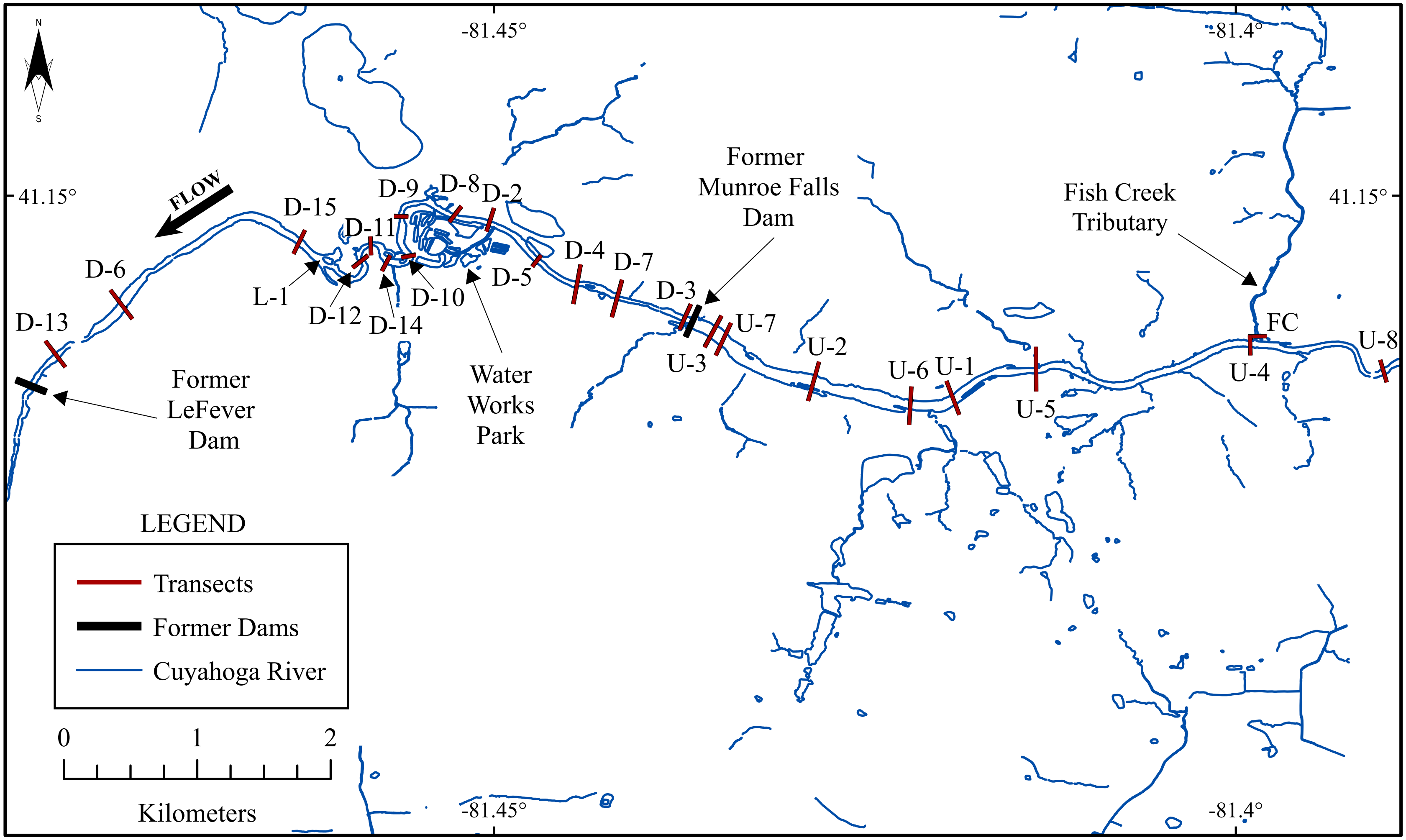

Figure 11. Location of all Cuyahoga River transects where geomorphic profiles were measured within the study area. Transects D-14 and D-15 were added to the preexisting data sets of Rumschlag (2007), Rumschlag and Peck (2007), Kasper (2010) and Peck and Kasper (2013). Water boundaries were obtained from Summit County Geographic Information Services (SCGIS) et al. (2000).

Table 4. Survey dates for geomorphic profiles at each transect along the Cuyahoga River study area. Transect D-13 is closest to the former dam and U-8 is at the upstream limit of the study area. L-1 represents the LeFever Impoundment Delta. The survey dates have been grouped by season. The "X" indicates that the profile was measured on that date.

Surveys	D-13	D-6	D-15	L-1	D-12	D-14	D-10	D-2	D-8	D-5	D-4	D-7	D-3	U-3	U-7	U-2	U-6	U-1	U-4	FC	U-8
30-Aug-13	-	-	-	X	-	-	-	-	-	-	-	-	-	-	-	-	-	-	-	-	-
7-Sep-13	-	X	X	X	X	X	X	X	X	X	X	X	-	-	-	-	-	-	-	-	-
29-Oct-13	-	-	-	-	-	X	-	-	-	-	-	-	-	-	-	-	-	-	-	-	-
17-Dec-13	-	X	X	X	-	-	-	-	-	-	-	-	-	-	-	-	-	-	-	-	-
23-Mar-14	-	X	X	X	X	-	-	-	-	-	-	-	-	-	-	-	-	-	-	-	-
24-Mar-14	-	-	-	-	-	X	X	X	X	X	-	X	-	-	-	-	-	-	-	-	-
1-Apr-14	-	X	-	-	-	-	-	-	-	-	-	-	-	-	-	-	-	-	-	-	-
23-May-14	-	X	X	X	-	-	-	-	-	-	-	-	-	-	-	-	-	-	-	-	-
25-Jul-14	-	-	X	X	-	X	-	-	-	X	-	X	-	-	-	-	-	-	-	-	-
9-Aug-14	-	-	-	-	-	-	-	X	-	-	-	-	-	-	-	-	-	-	-	-	-
11-Aug-14	X	X	-	-	-	-	-	-	-	-	-	-	X	X	-	-	-	-	-	-	-
19-Aug-14	-	-	-	-	X	-	X	-	X	-	-	-	-	-	X	-	X	X	X	X	X
14-Dec-14	-	-	-	-	X	X	X	-	X	X	-	X	-	-	-	-	-	-	-	-	-
15-Dec-14	-	X	X	X	-	-	-	-	-	-	-	-	-	-	-	-	-	-	-	-	-
22-Dec-14	-	-	-	-	-	-	-	X	-	-	-	-	-	-	-	-	-	-	-	-	-
12-Apr-15	-	X	-	-	X	X	-	-	-	-	-	-	-	-	-	-	-	-	-	-	-
18-Apr-15	-	-	-	-	-	-	-	X	-	-	-	-	-	-	-	-	-	-	-	-	-
3-May-15	-	-	-	X	-	-	X	-	X	X	-	X	-	-	-	X	-	-	X	-	-

transects were established in the fall of 2013; one at the head of the former LeFever Dam pool (Transect D-15) and one further upstream at Water Works Park (Transect D-14). All transects were marked by placing a semi-permanent reference stake (reinforced steel bar with a washer cap) on each bank of the river. The geographic coordinates of each reference stake were recorded with a handheld GPS unit and field maps were produced so that the transects could be relocated (Table 5, Appendix C). Geomorphic profiles were surveyed using a CST/Burger PAL Automatic Level (26x magnification), Stadia Rod and tape measure (rope with 1 m tape markings) (Appendix D). Transect D-8 was surveyed twice on May 3, 2015 to assess reproducibility (Figure 12). Reading the Stadia Rod to the nearest quarter centimeter provides a horizontal resolution of 25 cm for each survey point. All of the profiles were graphed so that they are viewed looking downstream with distance and elevation measured relative to the local reference stakes (Table 6). The depth of pre-removal substrate was measured by pushing a metal probe rod through the bank/channel material until the underlying substrate could no longer be penetrated. If bedrock was determined to be the pre-removal substrate it was listed as such on the profiles. If former floodplain or pre-removal gravel lag deposits composed the pre-removal substrate, then that surface was denoted “depth of refusal” or “refusal” on the profiles.

The river downstream of the former LeFever Dam was not studied because this area is characterized by a bedrock gorge having a steep gradient and little to no sediment deposition. Upon removal of the LeFever Dam, sediment eroded from the impoundment was transported further downstream to the Gorge Dam pool.

2.3 Hydrology

The removal of the LeFever Dam induced significant hydrologic changes to the previously dammed reach of the middle Cuyahoga River. The pre and post-removal flow

Table 5. Geographic coordinates and upstream distance from the former LeFever Dam of all geomorphic profiles within the study area. L-1 is at the LeFever impoundment delta and FC is located at the mouth of Fish Creek Tributary.

Transect	Latitude	Longitude	Distance from LeFever Dam (m)	Zone
D-13	41.1390	-81.4794	273	5
D-6	41.1425	-81.4748	843	
D-15	41.1470	-81.4630	2216	
L-1	41.1460	-81.4610	2415	
D-12	41.1455	-81.4591	2795	4
D-11	41.1466	-81.4583	2947	
D-14	41.1455	-81.4573	3146	
D-10	41.1459	-81.4559	3310	
D-9	41.1486	-81.4561	3610	
D-8	41.1489	-81.4525	4023	
D-2	41.1490	-81.4500	4254	
D-5	41.1458	-81.4470	4607	
D-4	41.1442	-81.4443	4916	
D-7	41.1433	-81.4416	5169	
D-3	41.1420	-81.4370	5554	
U-3	41.1405	-81.4354	5765	3
U-7	41.1399	-81.4348	5858	
U-2	41.1379	-81.4283	6476	
U-6	41.1362	-81.4218	7056	2
U-1	41.1366	-81.4191	7325	
U-5	41.1385	-81.4134	7859	
U-4	41.1403	-81.3989	9204	
FC	41.1403	-81.3989	9217	
U-8	41.1383	-81.3901	10107	1

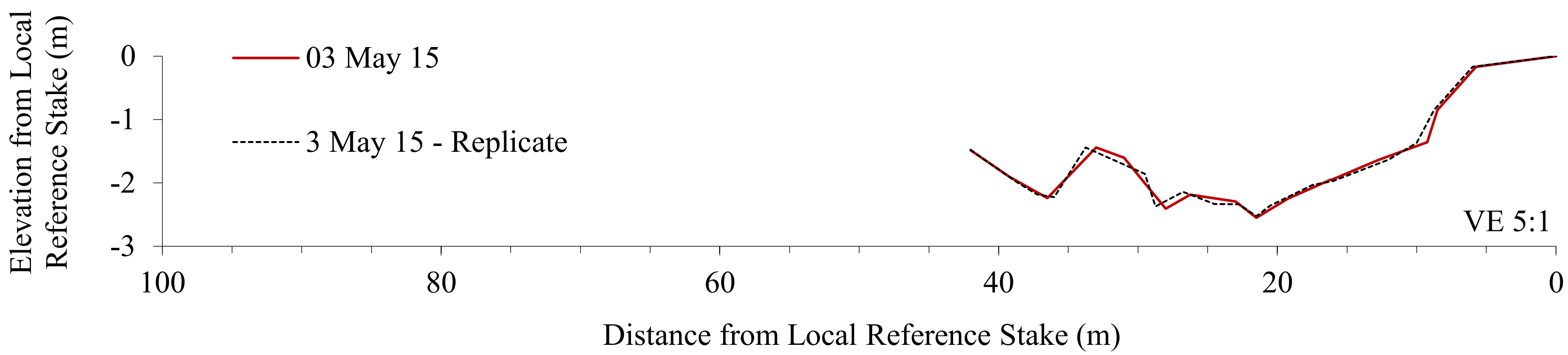

Figure 12. Geomorphic profile and replicate survey of transect D-8 located 4,023 m upstream of the LeFever Dam, surveyed on May 3, 2015.

Table 6. Cross section, distance, elevation and location of all local reference stakes used for plotting of Cuyahoga River geomorphic profiles.

Transect	Distance (m)	Elevation (m)	Location
D-13	0	0	Left bank
D-6	66.1	0	Right bank
D-15	0	0	Right bank, top of scarp is at 1.5 m distance
D-12	0	0	Right bank
D-11	0	12.5	Left bank
D-14	0	0	Left bank, rebar is 0.81 m below deck
D-10	3	0.1	Right bank
D-9	0	0	Left bank
D-2	0	1.55	Right bank
D-8	0	0	Right bank
D-5	45	0	Right bank
D-4	0	0	Right bank
D-7	0	0	Left bank
D-3	-11.75	0.43	Right bank
U-3	31.5	-2.756	Left bank
U-7	0	0	Left bank
U-2	91.3	-1.825	Right bank
U-6	0	0	Right bank
U-1	0	0	Right bank
U-5	0	0	Right bank
U-4	0	0	Right bank
FC	10.12	-0.58	Right bank
U-8	0	0	Right bank

velocity, channel cross-sectional area, river discharge and river slope were all evaluated 843 m upstream of the former LeFever Dam at transect D-6 (Figure 11).

2.4 Flow Velocity

Flow velocity measurements were recorded every meter across the channel using a Gurley pygmy current meter held at 0.6 of the water depth (measured from the water surface) which is equal to 0.4 of the water depth measured from the channel floor. The pre-removal flow velocity was measured within the former LeFever Dam pool at transect D-6 on May 17, 2012 (J. Peck, written communication, 2013) when the mean daily discharge was 5.26 m^3/s at the Old Portage stream gauging station (Table 7) (waterdata.usgs.gov). The post-removal flow velocity was measured at the same location on August 11, 2014 when the mean daily discharge was 8.32 m^3/s at the Old Portage stream gauging station (waterdata.usgs.gov). The mean daily discharge pre and post-removal was similar so it was appropriate to make comparisons between the two conditions.

2.5 Channel Cross-Sectional Area

The channel cross-sectional area was determined by dividing the channel into rectangles bounded by the water surface and channel floor. Each field measurement of water depth served as the midpoint of the individual rectangles. The area of the individual rectangles were summed to obtain the total channel area. The number of rectangles and therefore the accuracy of the estimated area were controlled by the number of data points collected. Because all of the geomorphic profiles were not graphed using a smooth curve, any over estimation of cross sectional area was reduced by subtracting the area of the

Table 7. Mean daily discharge at the Old Portage stream gauging station USGS 04206000 on the days surveys were conducted (waterdata.usgs.gov).

Survey Date	Mean Daily Discharge (ft^3/s)	Mean Daily Discharge (m^3/s)
14-May-09	317	8.98
7-Jul-11	179	5.07
14-May-12	296	8.39
17-May-12	175	4.96
20-May-13	147	4.17
30-Aug-13	199	5.64
7-Sep-13	171	4.85
29-Oct-13	368	10.43
17-Nov-13	205	5.81
23-Mar-14	822	23.29
24-Mar-14	735	20.83
1-Apr-14	963	27.29
23-May-14	710	20.12
25-Jul-14	173	4.90
9-Aug-14	304	8.61
11-Aug-14	284	8.05
19-Aug-14	251	7.11
14-Oct-14	347	9.83
15-Oct-14	323	9.15
22-Dec-14	314	8.90
12-Apr-15	1,350	38.26
2-May-15	223	6.32
3-May-15	214	6.06

portions of the individual rectangles that extended beyond the channel boundaries. The channel cross sectional area was assessed within the former dam pool and at transects further upstream. Pre and post-removal comparisons were made only on days of similar discharge because changes in discharge alter the river's cross-sectional area (Table 7).

2.5 Cuyahoga River Discharge

Cuyahoga River discharge was calculated using the continuity equation:

$$Q = V \times A \qquad \text{(Eq. 1)}$$

where Q is the river discharge in m^3/s, V is the flow velocity in m/s and A is the cross sectional area of the river channel in m^2. The river discharge in the former dam pool was determined using a technique similar to the one used for estimating channel cross-sectional area. Discharge was calculated within each of the previously described rectangles, and the summation of the discharge through the individual rectangles yielded the total river discharge through the channel. The discharge values at D-6 differ from those recorded at the Old Portage stream gauging station because Old Portage is located further downstream and the little Cuyahoga River discharges into the Cuyahoga River between the gauging station and Transect D-6 (Figure 1).

2.6 Slope of the Cuyahoga River

The change in the slope of the Cuyahoga River after the removal of the LeFever Dam is directly related to the boundary shear stress and the erosive capability of the river.

The pre-removal slope of 0.00029 m/m was determined using the 7.5 minute Hudson Quadrangle 2 ft. topographic contour map (USGS, 1994). The 990 ft. contour line crossed the river at the location of transect D-15 (Figure 11). The upstream distance from the former LeFever Dam to this transect was already determined using the ruler tool in ArcGIS (Table 5), so it was used to calculate the change in distance. The elevation change was determined using the elevation of the aforementioned contour line crossing and the 988 ft. elevation of the former LeFever Dam determined by BBC&M Engineering (2008). The post removal slope was surveyed on August 11, 2014 using a Stadia Rod and Transit 843 m upstream of the former dam at Transect D-6 (Figure 11).

2.7 LeFever Impoundment Delta Survey

The deltaic deposit at the head of the former LeFever impoundment was surveyed using a handheld GPS unit. The GPS points were measured in a grid around the deltaic feature to map its position, shape, and spatial extent (Figure 13). Water depth was measured at each of the GPS locations using a meter stick. Water depth was converted into a height measurement relative to the local reference stake so that the geomorphic change between surveys could be assessed (Appendix E). In order to quantify the rate and magnitude of geomorphic change to the delta following the removal of the LeFever Dam, the delta was resurveyed in the summer and winter of 2013, the spring, summer and winter of 2014 and in the spring of 2015 (Table 4). Raster surfaces of the delta were generated by using Natural Neighbors interpolation in ArcMap 10.2 (Figure 14). Using the same field data, contour maps were also drawn by hand and later digitized in ArcMap 10.2 (Figure 15). The accuracy of the interpolated raster surface was limited by the number of data points collected in the field. For example, a deep water channel observed in the field along river right disappears in the interpolated raster surface (Figure 14). The

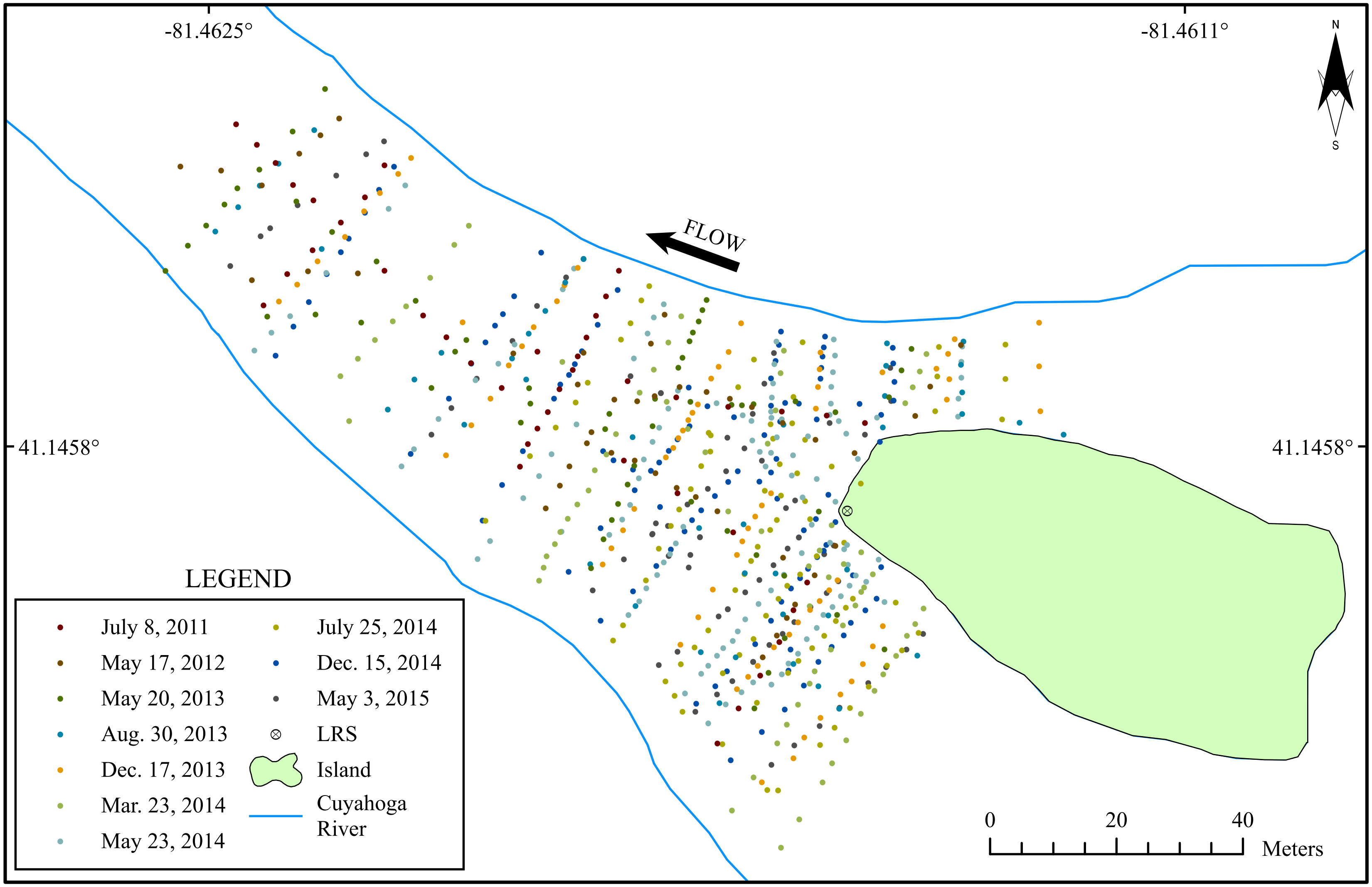

Figure 13. Spatial distribution of geomorphic survey points of the LeFever Impoundment Delta located 2,415 m (ULFD). Survey data was measured relative to the local reference stake (LRS) from July 8, 2011 to May 3, 2015.

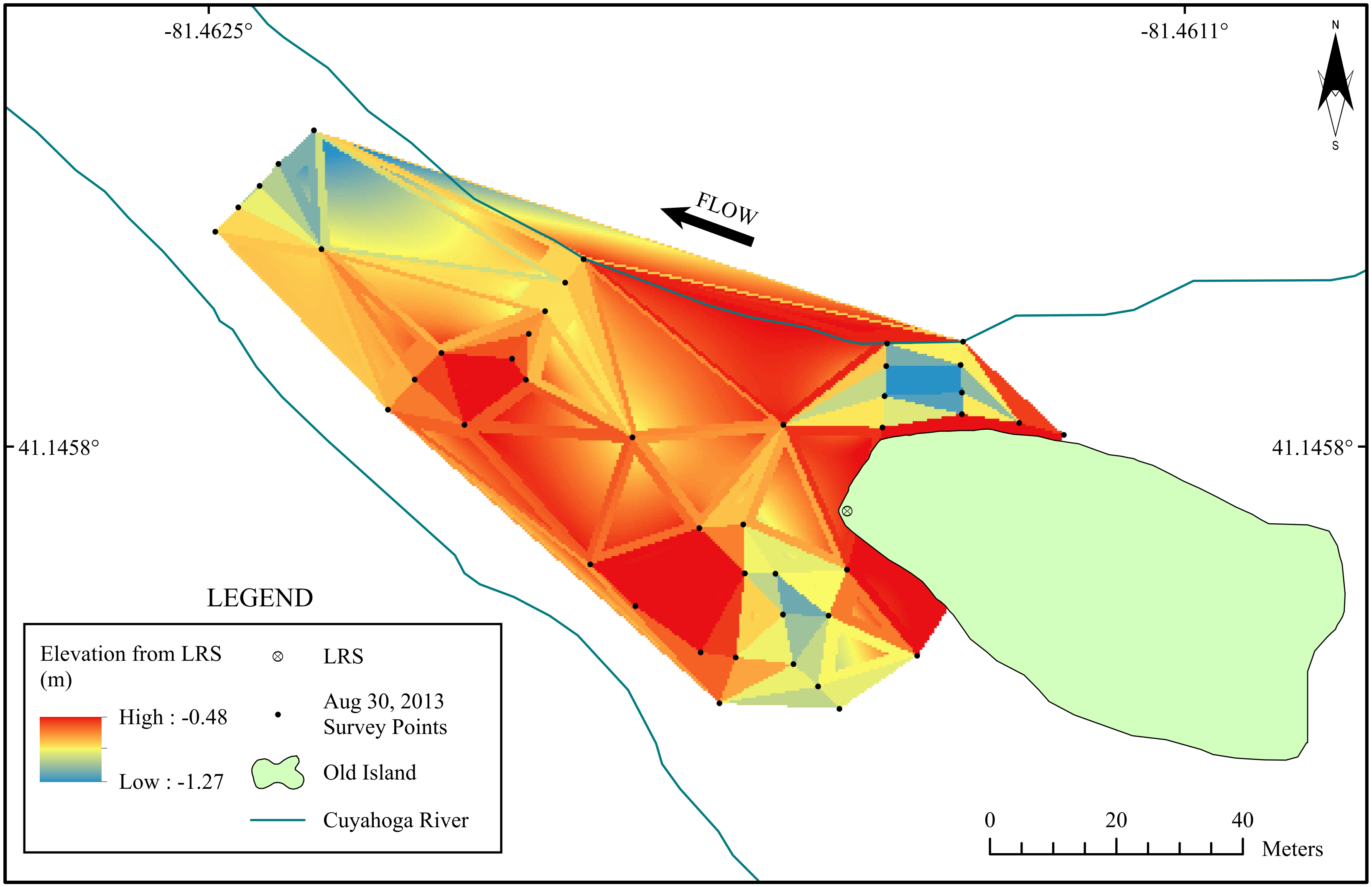

Figure 14. Raster surface of the LeFever impoundment delta using Natural Neighbors interpolation on August 30, 2013. Elevations were measured relative to the Local Reference Stake (LRS). The water surface is -0.94 m from the LRS.

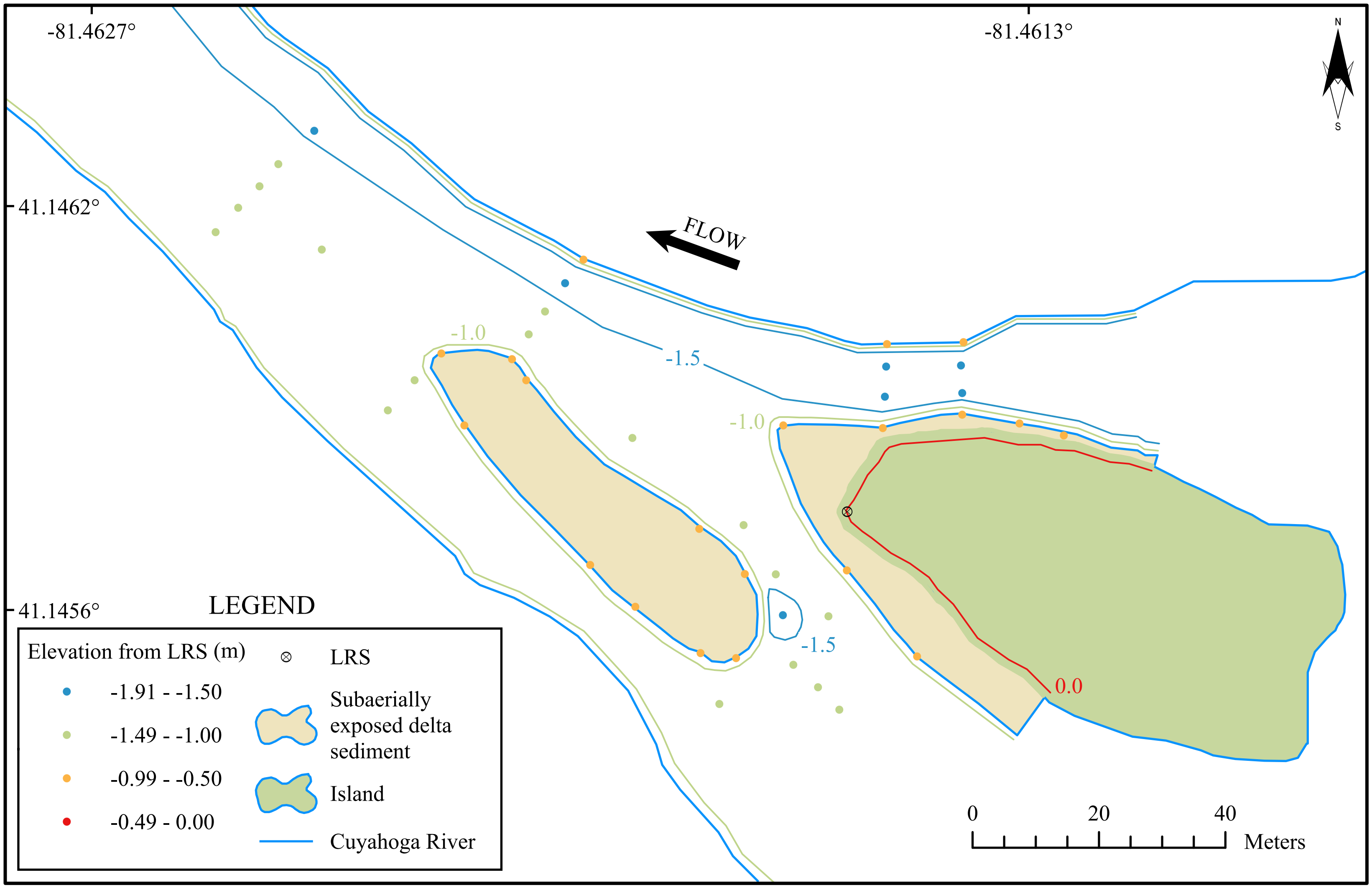

Figure 15. Map view of the geomorphology at the head of the former LeFever Dam pool on 8-30-2013. Elevations relative to the local reference stake (LRS) and contoured at a 0.5 m contour interval. The water surface is -0.94 m from the LRS.

hand-drawn contour maps provided a more realistic depiction of the geomorphology of the delta because it uses field observations to connect widely spaced data points.

CHAPTER III

RESULTS

3.1 Sediment Characteristics of the Deep Water Channel

The middle Cuyahoga River study reach has been grouped into five Zones of similar physical characteristics (Figure 16). Zone 1 begins at the upstream limit of the study area which is located 10,615 m upstream of the former LeFever Dam m (ULFD) and extends downstream to the Zone 1-2 boundary at 9,315 m (ULFD). Zone 3 extends from the Zone 2-3 boundary at 6,615 m (ULFD) downstream to the site of the former Munroe Falls Dam at 5,615 m (ULFD). Zone 4 ends at the upstream limit of the LeFever Dam pool at 2,670 m (ULFD). Zone 5 encompasses the former LeFever Dam pool and ends at the site of the former LeFever Dam at 0 m (ULFD).

Grain size data has been collected throughout this reach of the middle Cuyahoga River from 2003 to 2014. These results characterize the sedimentologic changes before and after the 2005 removal of the Munroe Falls Dam and the 2013 removal of the LeFever Dam. A detailed characterization of the former Munroe Falls Dam pool sediment, and pre-removal conditions can be found in Rumschlag (2007), Rumschlag and Peck (2007), and Peck et al. (2007). Kasper (2010) and Peck and Kasper (2013) provided a comprehensive assessment of the sedimentologic changes associated with the removal of the Munroe Falls Dam as well and the characteristics of the former LeFever impoundment fill. These existing data were added and reinterpreted. The study area was regrouped into five new Zones based on varying sedimentologic and geomorphic

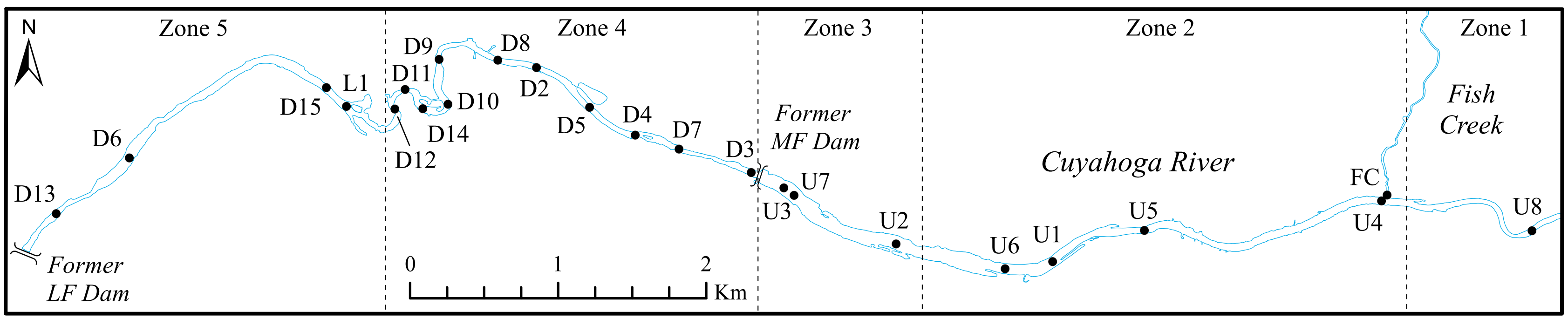

Figure 16. Location of geomorphic transects and 5 Zones boundaries within the Middle Cuyahoga River study reach. The location of the former LeFever (LF) and Munroe Falls (MF) Dams are also shown and flow is from east to west.

properties. Although the previous studies addressed the sediment characteristics of both channel margins and the thalweg of the former dam pools, this study only evaluated the deep water channel environment.

Twelve sedimentologic parameters were analyzed and averaged by each of the 5 Zones to characterize the sedimentologic change throughout the study reach (Tables 8, 9) (Figures 17-20). The following section describes the sedimentologic results beginning furthest upstream and moving downstream towards the LeFever Dam.

3.1.1 Zone 1

Zone 1 is located at the upstream limit of the study area from 10,615 to 9,315 m upstream of the LeFever Dam m (ULFD). Zone 1 is located at the upstream end of the former Munroe Falls Dam impoundment. While the Munroe Falls Dam was in place, the deep water channel contained mostly gravel (≈ 67%) with some sand (≈ 31%) and a trace amount of mud (≈ 1%) (Table 8, Figure 17). The average water depth was 1.91 m and the organic content of the sediment was relatively low (≈ 4%) (Table 8). Following the 2005 removal of the Munroe Falls Dam, the average water depth rapidly decreased by 1.05 m in 2006 (Figure 17). The average sand content in the channel increased by 21% with a subsequent decrease (-20%) in the average gravel content (Table 8, Figure 17). The channel sediment became more poorly sorted and the average organic content decreased by 3% (Figures 17-18). By 2008-09, the proportion of gravel to sand returned to its pre-removal condition. By 2012, the gravel content increased to 84% while the sand content decreased to 15% (Table 9).

No data was collected in this zone immediately following the removal of the LeFever Dam so the post-removal changes were evaluated using only the data from 2014. Between 2012 and 2014 the average sand and gravel content remained nearly the same (Table 9, Figure 19).

Table 8. Average surficial sediment characteristics of the deep water channel environment for each Zone in the study reach. The sample sets are grouped by their collection dates pre (Rumschlag, 2007) and post removal (Kasper, 2010) of the Munroe Falls Dam. N.D. denotes no data collection.

Sample Set	Zone	*n*	Water Depth (m)	Gravel (%)	Sand (%)	Mud (%)	D_{50}	Mean (Φ)	Sorting (Φ)	Skewness (Φ)	WBD (g/cc)	DBD (g/cc)	Water (%)	Organics (%)
	1	4	0.68	66	34	0.21	-1.79	-2.53	1.35	2.74	1.38	1.44	20	2
Post	2	20	0.64	75	25	0.21	-2.66	-2.84	1.57	4.63	1.49	1.54	19	3
Removal	3	6	0.86	55	45	0.19	-1.11	-1.67	1.59	2.99	1.44	1.48	20	2
2008-09	4	18	1.09	53	46	1	-0.84	-1.78	1.47	4.47	1.44	1.46	21	2
	5	25	2.11	10	73	17	2.18	1.99	1.78	2.98	0.94	0.62	56	11
	1	6	0.86	47	52	0.31	N.D.	-1.13	1.34	5.53	2.22	1.80	19	1
Post	2	25	0.86	29	69	2	N.D.	-0.30	1.19	1.67	2.11	1.64	22	3
Removal	3	10	0.99	17	83	1	N.D.	0.37	0.78	-0.74	2.05	1.59	23	4
2006	4	16	1.06	23	76	2	N.D.	0.31	0.70	0.47	2.06	1.60	23	2
	5	0	N.D.	N.D.	N.D.	N.D.	N.D.	N.D.	N.D.	N.D.	N.D.	N.D.	N.D.	N.D.
	1	5	1.91	67	31	1	N.D.	-1.40	0.73	2.99	1.80	1.40	19	4
Pre	2	17	1.95	8	87	5	N.D.	1.15	0.67	-1.22	1.80	1.35	25	6
Removal	3	15	2.70	9	71	20	N.D.	2.41	2.84	0.84	1.41	0.71	48	12
2003-04	4	9	1.57	81	17	2	N.D.	-1.85	0.44	1.25	1.97	1.58	20	3
	5	0	N.D.	N.D.	N.D.	N.D.	N.D.	N.D.	N.D.	N.D.	N.D.	N.D.	N.D.	N.D.

Table 9. Average surficial sediment characteristics of the deep water channel environment for each Zone in the study reach. The sample sets are grouped by their collection dates pre (Kasper, 2010) and post removal of the LeFever Dam. N.D. denotes no data collection.

Sample Set	Zone	*n*	Water Depth (m)	Gravel (%)	Sand (%)	Mud (%)	D_{50}	Mean (Φ)	Sorting (σ)	Skewness (Φ)	WBD (g/cc)	DBD (g/cc)	Water (%)	Organics (%)
	1	6	0.81	82	18	0.11	-4.71	-3.54	1.85	4.31	2.10	1.72	22	2
Post	2	14	0.66	83	17	0.15	-4.59	-3.26	1.73	7.43	2.15	1.77	22	2
Removal	3	3	0.80	84	16	0.06	-4.64	-3.39	2.25	9.06	2.16	1.78	22	1
2014	4	32	0.74	54	46	0.22	-1.84	-1.61	1.52	4.07	2.11	1.71	24	3
	5	13	0.59	49	51	0.76	-1.49	-1.26	1.51	3.42	2.01	1.54	32	3
	1	0	N.D.	N.D.	N.D.	N.D.	N.D.	N.D.	N.D.	N.D.	N.D.	N.D.	N.D.	N.D.
Post	2	0	N.D.	N.D.	N.D.	N.D.	N.D.	N.D.	N.D.	N.D.	N.D.	N.D.	N.D.	N.D.
Removal	3	0	N.D.	N.D.	N.D.	N.D.	N.D.	N.D.	N.D.	N.D.	N.D.	N.D.	N.D.	N.D.
2013	4	9	0.65	35	65	0.36	-0.58	-0.35	1.57	1.20	2.04	1.64	20	2
	5	6	0.45	10	89	2	1.10	1.00	1.17	-0.55	1.76	1.27	29	8
	1	8	1.05	84	15	0.44	-3.57	-2.97	2.01	9.42	2.14	1.78	17	2
Pre	2	15	0.57	80	20	0.23	-3.61	-2.67	1.99	5.46	2.16	1.77	18	2
Removal	3	6	0.62	62	38	0.26	-2.56	-2.23	1.73	3.99	2.11	1.72	18	2
2012	4	16	0.85	17	83	0.30	0.47	0.35	1.13	-0.26	2.03	1.60	21	4
	5	9	1.90	25	71	3.79	0.54	0.51	1.31	2.12	1.57	0.91	46	12
	1	0	N.D.	N.D.	N.D.	N.D.	N.D.	N.D.	N.D.	N.D.	N.D.	N.D.	N.D.	N.D.
Pre	2	7	1.19	85	15	0.16	-3.21	-2.86	1.40	5.01	1.98	1.61	19	5
Removal	3	3	0.99	73	26	0.22	-2.55	-1.93	1.93	6.16	2.05	1.73	16	1
2010	4	12	1.19	68	32	0.16	-2.49	-2.22	1.95	6.35	2.05	1.69	17	2
	5	7	1.30	10	90	0.10	0.65	0.65	1.01	-1.17	1.97	1.55	21	2

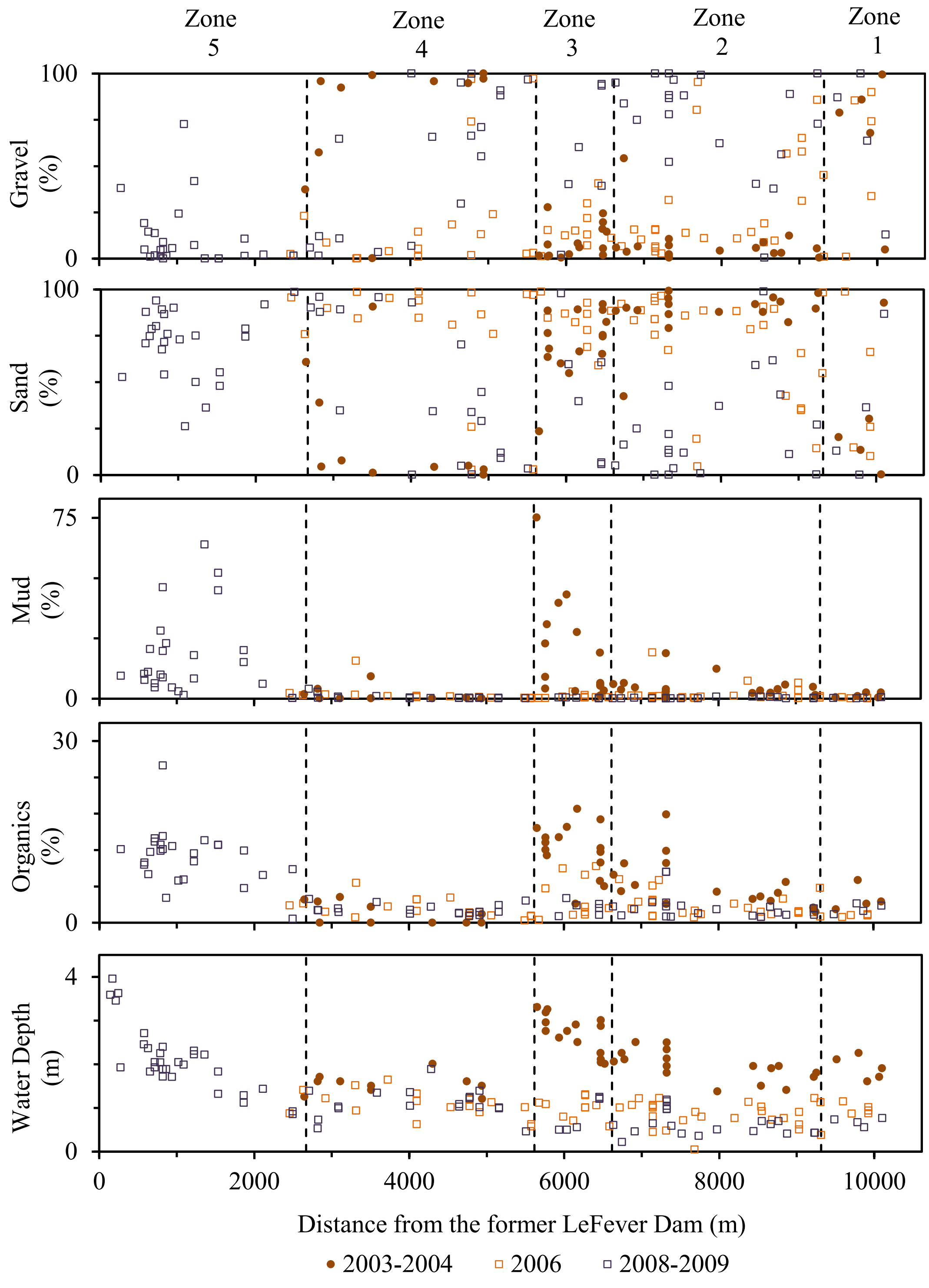

Figure 17. Deep channel sediment characteristics pre (closed circles) (Kasper, 2010; Rumschlag, 2007) and post-removal (open squares) (Kasper, 2010) of the former Munroe Falls Dam. Zone boundaries are shown by vertical dashed lines and are modified from Kasper (2010) such that the Former LeFever Dam lies at 0 m and the former Munroe Falls Dam lies at 5615 m.

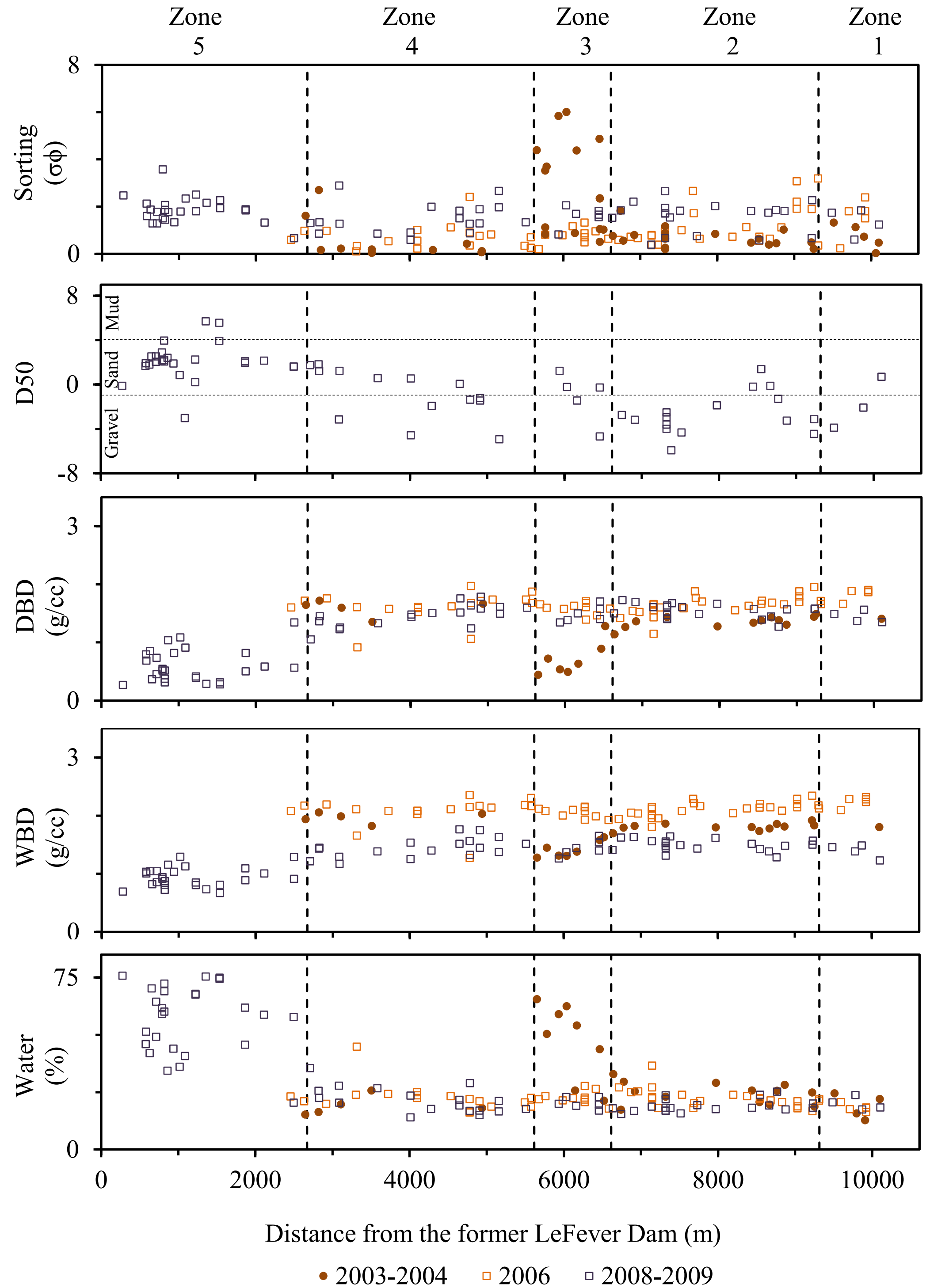

Figure 18. Deep channel sediment characteristics pre (closed circles) (Kasper 2013, Rumschlag, 2007) and post-removal (open squares) (Kasper, 2010) of the former Munroe Falls Dam. Zone boundaries are shown by vertical dashed lines and are modified from Kasper (2010) such that the Former LeFever Dam lies at 0 m and the former Munroe Falls Dam lies at 5615 m.

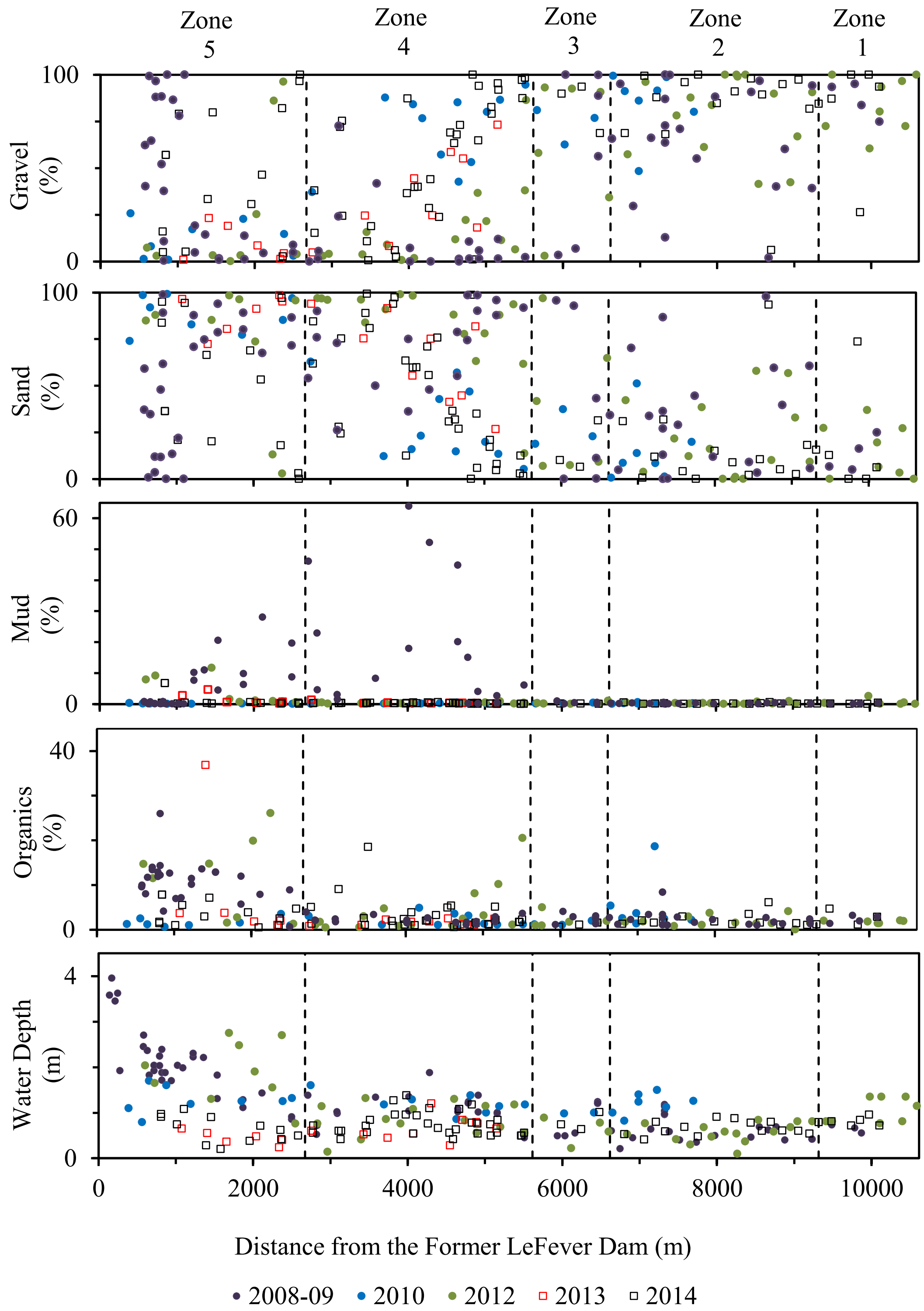

Figure 19. Deep channel sediment characteristics pre (closed circles) and post-removal (open squares) (Kasper, 2010) of the former LeFever Dam. Zone boundaries are shown by vertical dashed lines and are modified from (Kasper, 2010) such that the Former LeFever Dam lies at 0 m and the former Munroe Falls Dam lies at 5615 m.

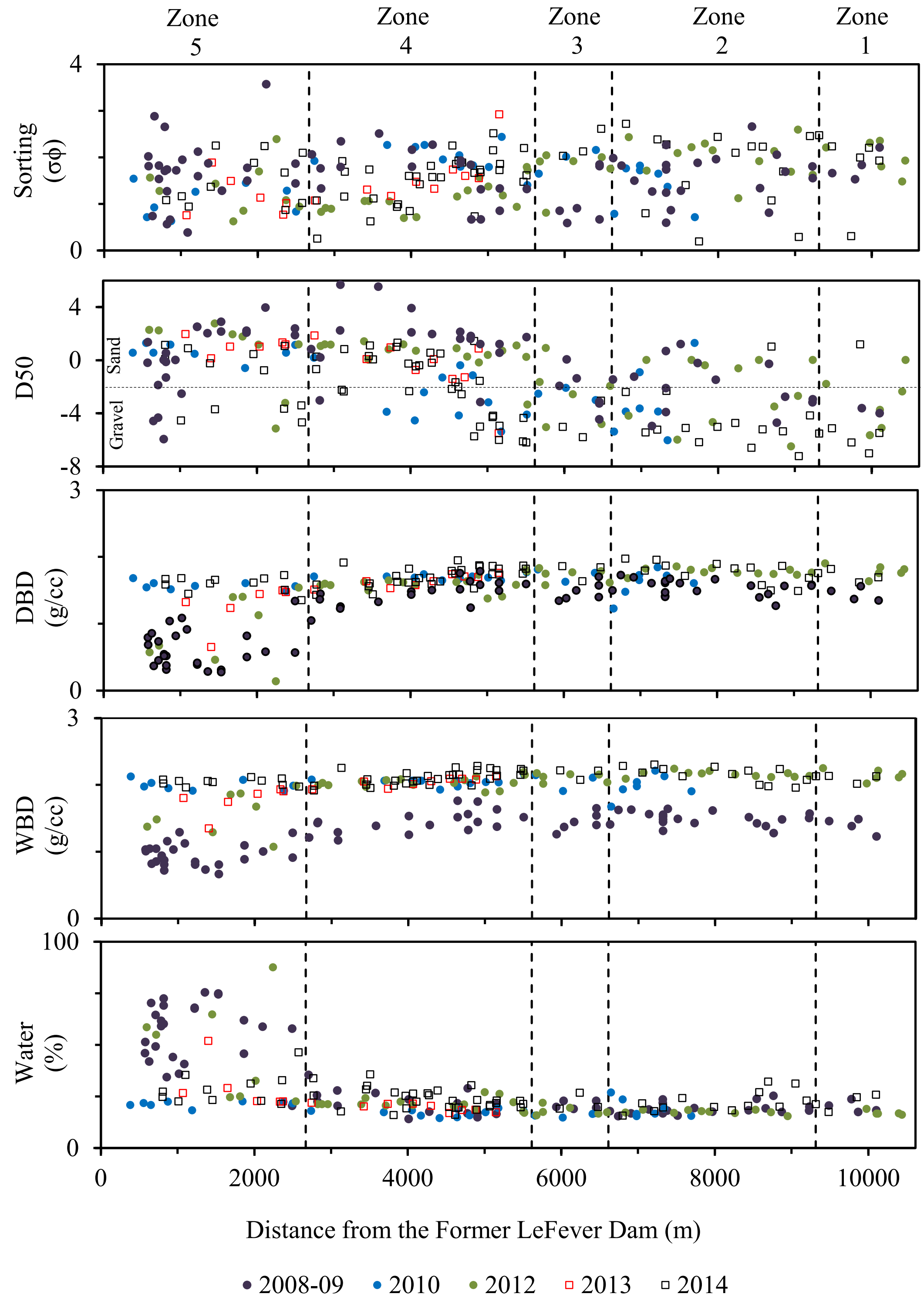

Figure 20. Deep channel sediment characteristics pre (closed circles) and post-removal (open squares) (Kasper, 2010) of the former LeFever Dam. Zone boundaries are shown by vertical dashed lines and are modified from Kasper (2010) such that the Former LeFever Dam lies at 0 m and the former Munroe Falls Dam lies at 5615 m.

3.1.2 Zone 2

Continuing downstream into Zone 2 the sedimentologic change during the study period has been quite substantial. Zone 2 is located between 9,315 and 6,615 m (ULFD) and comprises the largest portions of the former Munroe Falls Dam impoundment. When the Munroe Falls Dam was in place, the thalweg was composed mainly of moderately well sorted, medium sand (≈ 87%) with lesser amounts of gravel (≈ 8%) and mud (≈ 5%) (Table 8, Figure 17). The average water depth was slightly deeper than in Zone 1 (1.95 m) and the channel sediment was more organic rich (≈ 6%). Once the dam was removed, the amount of gravel increased to 29% whereas sand decreased to 69% and mud decreased to 2% by 2006 (Figure 17). The increase in gravel content was also reflected in the shift of mean grain size from medium sand (1.15 ϕ) to granules (-0.30 ϕ) post-removal (Table 8). Accompanying this channel coarsening was a 1.09 m decrease in average water depth and a 50% decrease in organic matter. By 2008, the amount of gravel increased to 75%, the sand content decreased to 25% and the mean grain size coarsened substantially.

The majority of the sedimentologic change induced by the Munroe Falls Dam removal had taken place by 2010 because the 2010, 2012, and 2014 grain size data show similar gravel contents (80-85%) and similar mean grain sizes (Tables 8-9). The 2013 LeFever Dam removal had no effect on Zone 2 because it is located well above the LeFever Dam pool.

2.1.3 Zone 3

Further downstream in Zone 3, the sedimentological change was quite significant following the removal of the Munroe Falls Dam. The former Munroe Falls Dam marks the downstream limit of this zone at 5,615 m (ULFD). While the Munroe Falls Dam was in place, the average water depth was 2.70 m and fine sand (mean 2.41 ϕ) dominated the deep water channel (≈ 71%) (Table 8, Figure 17). Zone 3 had the greatest mud content (≈

20%) and was the most organic rich (≈ 12 %) among all the Zones upstream of the former Munroe Falls Dam (Figure 17).

After the Munroe Falls Dam was removed, Zone 3 experienced a marked decrease (-1.71 m) in the average water depth, mud content (-19%) and organic matter (-66%) (Figure 17). The average gravel content rose from 17% in 2006 to 73% in 2010 as the average sand content fell from 83% to 26% (Figure 17, 19). Within a year of the Munroe Falls Dam removal the mud had all been transported downstream of Zone 3.

Although no data was collected immediately following the removal of the LeFever Dam, channel coarsening did continue through 2014. From 2012 to 2014, channel sands declined by 22% (Table 9, Figure 19). The mean grain size steadily increased from fine sand (2.41 ϕ) in 2003-04 to pebbles (-3.39 ϕ) in 2014 (Tables 8, 9).

2.1.4 Zone 4

Zone 4 extends downstream from the former Munroe Falls Dam site to the upstream limit of the former LeFever Dam pool (5,615 – 2,670 m ULFD). This zone has shown a different pattern of sedimentologic change than Zones 1,2 and 3. Pre-Munroe Falls removal, the channel sediment was composed of 81% well sorted granules (mean -1.85 ϕ) and the channel had an average water depth of 1.57 m (Table 8, Figure 17). Compared to Zones 1,2 and 3, Zone 4 had the least amount of sand, mud and organic matter prior to the removal of the removal of the Munroe Falls Dam (Figure 17).

By 2006 following the removal of the Munroe Falls Dam, moderately well sorted, coarse sands (mean 0.31 ϕ) accounted for 76% of the channel sediment and average gravel content decreased to just 23% (Table 8, Figure 17). Two years later in 2008-09, the Zone 4 sediment becomes coarser (mean -1.78 ϕ) with an average of 53% gravel. The coarsening of Zone 4 sediment continued in 2010 when the mean grain size reached its maximum of -2.22 ϕ (Table 9). These poorly sorted pebbles accounted for 68% of the bed sediment (Table 9, Figure 19). There have been trace amounts of mud in the Zone 4 sediment since 2010.

The trend of channel sediment coarsening in Zone 4 from 2006 to 2010 changed markedly in 2012. In 2012, the average sand content reached its maximum (83%) as poorly sorted, coarse sand (mean 0.35 ϕ) dominated the channel (Table 9, Figure 17). The amounts of mud and organic matter also doubled.

Following the LeFever Dam removal, the average gravel content of the Zone 4 sediment increased from 17% to 35% (Table 9, Figure 19). The amount of organic matter also decreased by 50% but the proportion of mud in the channel sediment remained constant. Channel coarsening continued between 2012 and 2014 as the mean grain size increased to -1.61ϕ. By 2014 the bed sediment contained almost equal parts sand (46%) and gravel (54%) with trace amounts of mud (Table 9, Figure 19).

2.1.5 Zone 5

The furthest downstream zone in the study reach is Zone 5 which extends from 2,670 m (ULFD) downstream to the site of the former LeFever Dam. No data was collected in this zone until 2008-09 so the impact of the Munroe Falls Dam removal on the Zone 5 sediment could not be assessed. However, field observations indicate that most of the mobilized sediment from the former Munroe Falls impoundment was deposited within Zone 4 (Kasper, 2010). Following the removal of the LeFever Dam, no sediment samples were collected in the first 843 m upstream of the former dam because of the swift current and limited access.

After the Munroe Falls Dam removal but before the LeFever Dam removal (2008-09), Zone 5 had an average water depth of 2.11 m and a maximum depth of about 4 m close to the dam. The channel sediment in Zone 5 was composed of poorly sorted sand (73%) with a mean grain size of 1.99 ϕ (Table 8, Figure 17). The mean grain size reflected the elevated sand content and organic rich (≈ 11%) mud was present in higher concentrations (≈ 17%) than gravel.

In 2010, the thalweg contained 90% sand having a mean grain size of 0.65 ϕ (Table 9, Figure 19). Because sampling did not continue all the way down to the LeFever Dam the Zone 5 average water depths were 1.3 m and 1.9 m in 2010 and 2012 respectively (Table 9). In 2012 the thalweg contained 71% sand having a mean grain size of 0.51 ϕ. The organic rich mud content in 2012 is comparable to that in 2008-09. The survey one month after the LeFever Dam was removed indicated the average water depth in Zone 5 had decreased by 1.45 m (Table 9, Figure 19). The sand content in 2013 (89%) was comparable to that between 2008 and 2012 (71 – 90%). By 2014 the mean grain size in Zone 5 was the coarsest (-1.26 ϕ) of all the survey years.

3.2 Fluvial Geomorphology

In order to assess the impact of the Munroe Falls (2005) and LeFever (2013) Dam removals on the Cuyahoga River, geomorphic profiles were measured along flow-perpendicular transects. Geomorphic data has been collected from 2003 to 2015 throughout this reach of the middle Cuyahoga River. These results describe the geomorphic changes before and after the removal of the Munroe Falls Dam and the LeFever Dam. Rumschlag (2007), Rumschlag and Peck (2007), and Peck et al. (2007) described the initial morphologic changes pre and post-Munroe Falls removal primarily upstream of that dam. Kasper (2010) and Peck and Kasper (2013) further assessed the ongoing changes post-Munroe Falls removal upstream of that dam and along the reach extending down to the former LeFever Dam. This study revisits the geomorphic profiles of the aforementioned authors in addition to two new transects in Zones 4 and 5. These results will be described starting with the upstream profiles of Zone 1, ending with the downstream profiles of Zone 5.

3.2.1 Zone 1

Transect U-8 is located furthest upstream from 10,615 to 9,315 m ULFD (Figure 16). Measurements at this location began in 2006 after the removal of the Munroe Falls Dam. Little geomorphic change has occurred during the subsequent 8 years. What little geomorphic change did occur was in the form of minor lateral erosion and minor fluctuations (≤ 10 cm) in the mid-channel reflecting sediment aggradation and degradation (Figure 21). The right bank laterally eroded 1.65 m from the 2011 to 2014 surveys as slumped bank material was eroded away during high flows.

3.2.2 Zone 2

Zone 2 encompasses the river reach from 9,315 to 6,615 m (ULFD) (Figure 16). This zone is characterized by rapid downcutting soon after the Munroe Falls Dam was removed followed by slower rates of lateral erosion in the subsequent years. Transects at the mouth of Fish Creek tributary (FC), U-4, U-5, U-1, and U-6 are located in Zone 2 and generally exhibit this pattern of channel adjustment.

The confluence of Fish Creek and the Cuyahoga River is located at the upstream end of Zone 2 at 9,217 m (ULFD). Fish Creek has experienced significant downcutting and channel widening. From the 2004 to 2005 surveys, the channel rapidly downcut ~ 0.5 m after the Munroe Falls Dam was removed (Figure 22). The newly incised channel continued downcutting as well as laterally eroding through 2011. By 2014, the channel had downcut an additional ~ 0.19 m and the right bank laterally eroded 2.25 m between 2011 and 2014. The main channel of Fish Creek tributary has experienced a total of ~ 0.9 m of downcutting and a total channel widening of ~ 3.25 m since the removal of the

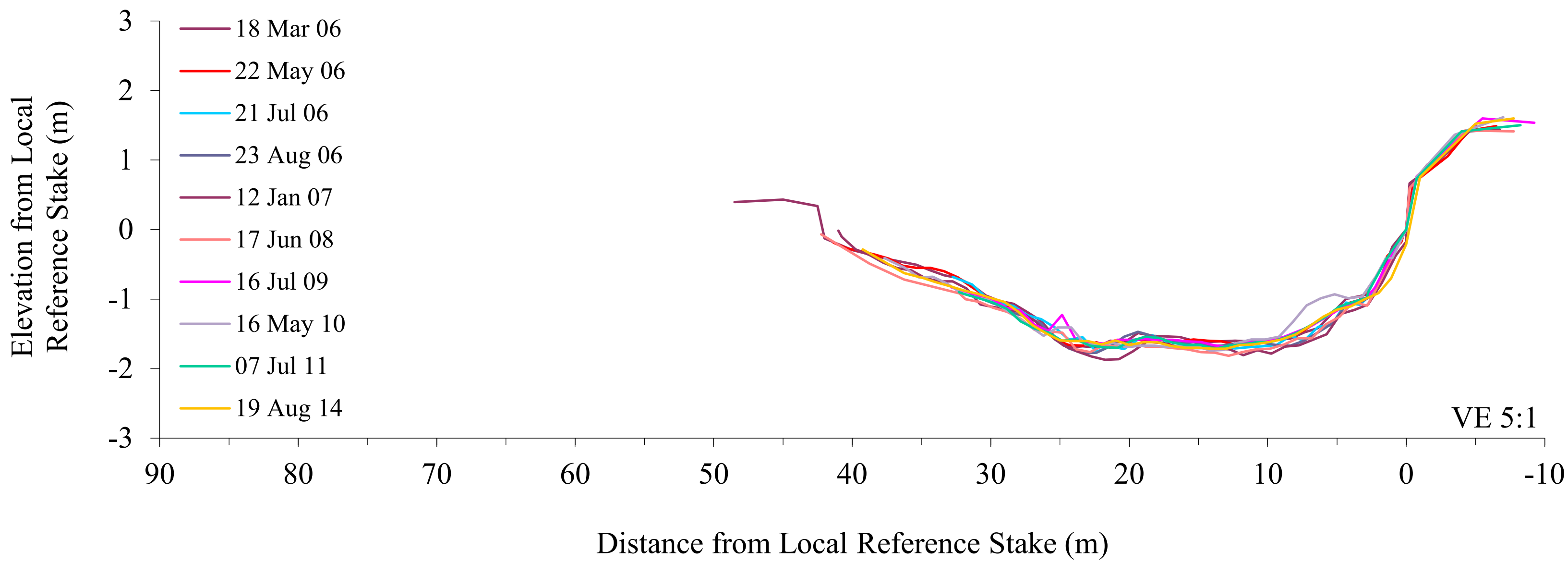

Figure 21. Geomorphic profile of transect U-8 located 10,107 m upstream of the former LeFever Dam, surveyed from March 2006 to August 2014.

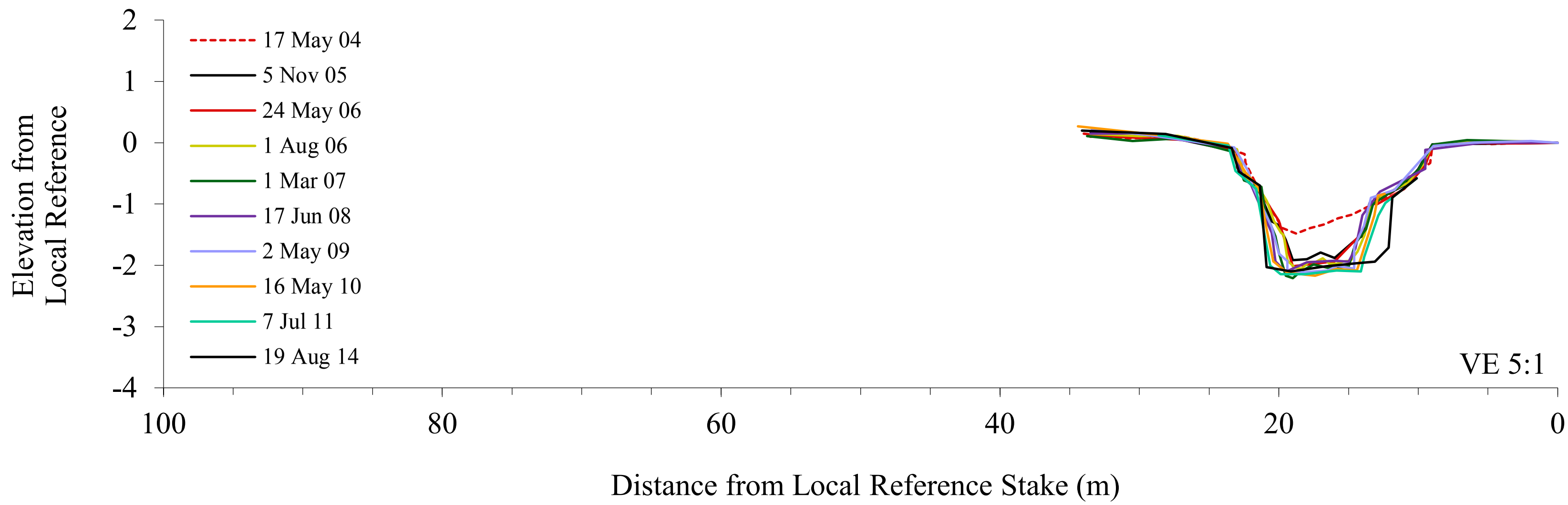

Figure 22. Geomorphic profile of the transect at Fish Creek tributary located 9,217 m upstream of the former LeFever Dam, surveyed from May 2004 to August 2014.

Munroe Falls Dam. However, significant lateral erosion has occurred to the right bank since 2011. Immediately downstream of the Fish Creek tributary is transect U-4 located at 9,204 m (ULFD). In November 2005, after the Munroe Falls Dam was removed, a linear sand bar on river left was deposited in the lee of large woody debris (LWD) (Figure 23). The sand bar was completely eroded by the August 2006 survey because the LWD had moved further downstream. Between the 2010 and 2011 surveys, Fish Creek had incised a 4 m wide channel on river right resulting in a total of ~ 0.57 m of downcutting since the 2005 survey. Minor fluctuations (≤ 10 cm) of mid-channel aggradation and degradation also occurred between 2005 and 2014.

Continuing downstream in Zone 2 is transect U-5 located 7,859 m (ULFD). The large deposit of sand and gravel of the Pambi Farms delta can be seen in the November 2005 survey (Figure 24). By May 2009 the deltaic feature was substantially eroded away and the bedrock-floored channel on river left had increased in width. Between 2009 and 2011, continued erosion reduced the size of the Pambi Farms delta deposit. Because the river channel rests on bedrock at this location further erosion will not produce significant downcutting so this transect was no longer surveyed.

Further downstream in Zone 2, at about 7,500 m (ULFD), the channel of the Cuyahoga River was much wider and substantial amounts of muddy sediment accumulated in the channel margins from when the Munroe Falls Dam was in place (Rumschlag and Peck, 2007). Transects U-1 and U-6 are located at 7,325 and 7,056 m (ULFD) respectively and exhibit these channel characteristics (Figures 25, 26).

At transect U-1, significant change occurred in the ~ 2.5 years following the Munroe Falls Dam removal (2005-2008) whereas geomorphic change has been less extensive after 2008 (Figure 25). After the Munroe Falls Dam was removed, it took the Cuyahoga River ~ 10 months to incise through impoundment sediments in the channel and reach the pre-dam substrate (Figure 25). The large sediment accumulation present at 30-35 m

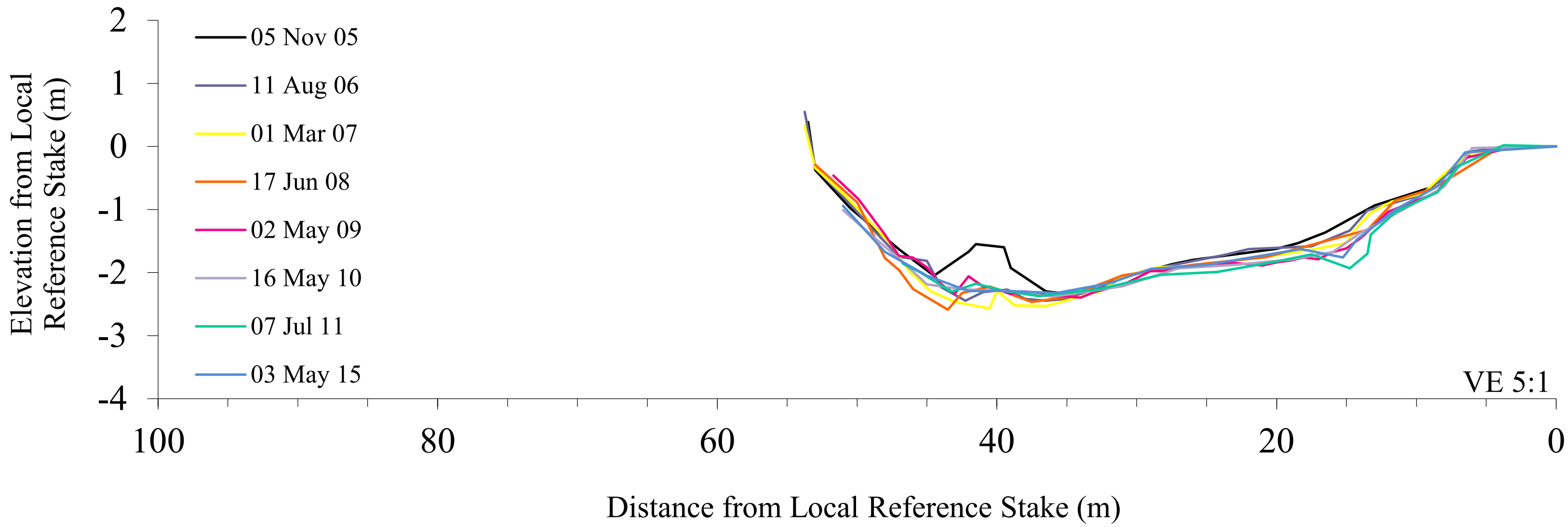

Figure 23. Geomorphic profile of transect U-4 located 9,204 m upstream of the former LeFever Dam, surveyed from November 2005 to August 2014.

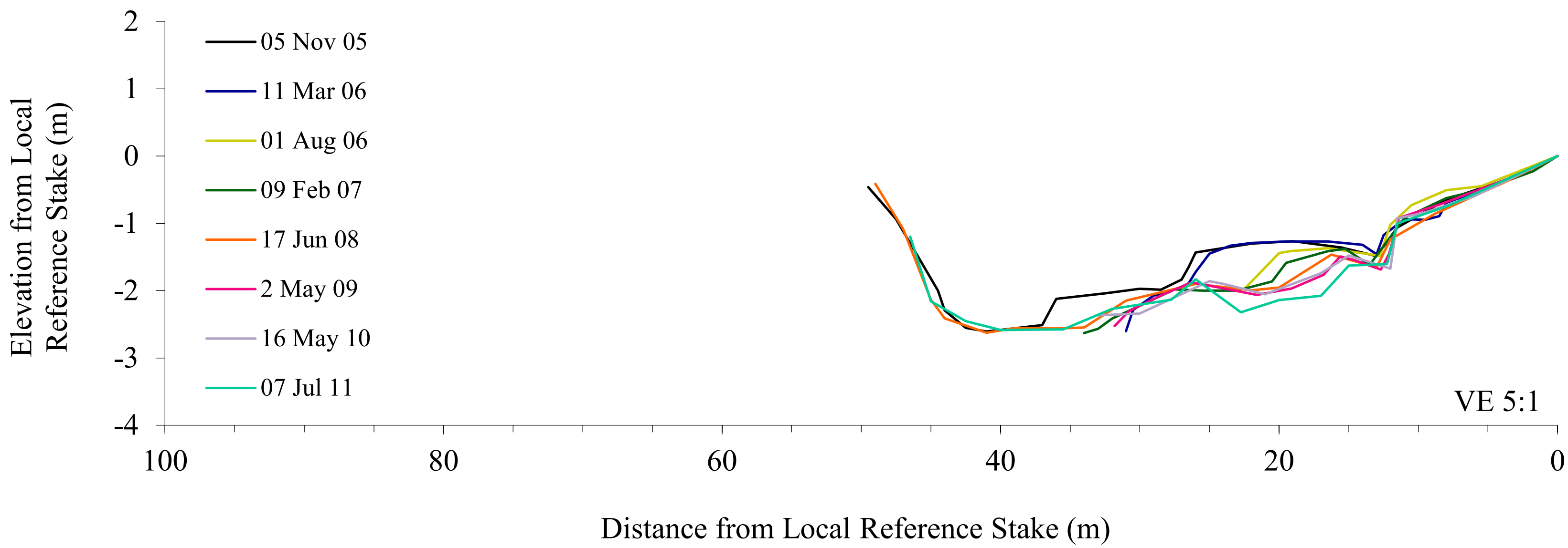

Figure 24. Geomorphic profile of transect U-5 located 7,859 m upstream of the former LeFever Dam, surveyed November 2005 to July 2011.

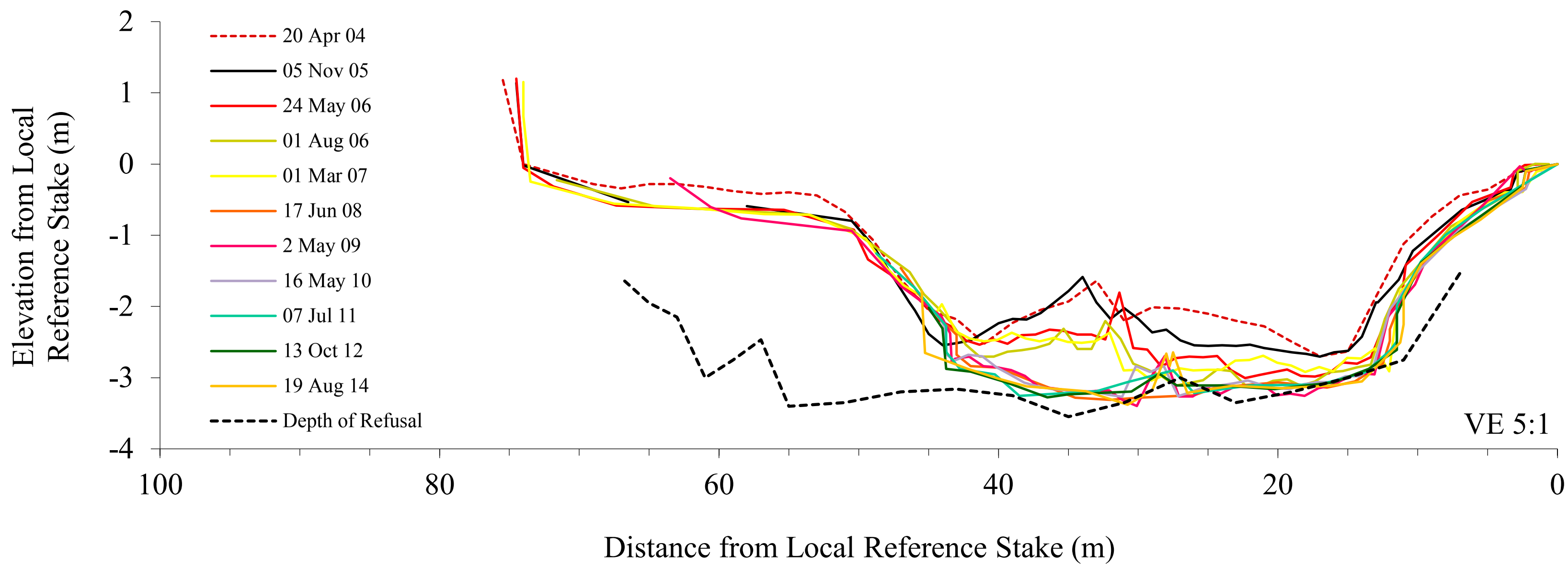

Figure 25. Geomorphic profile of transect U-1 located 7,325 m upstream of the former LeFever Dam, surveyed from April 2004 to August 2014.

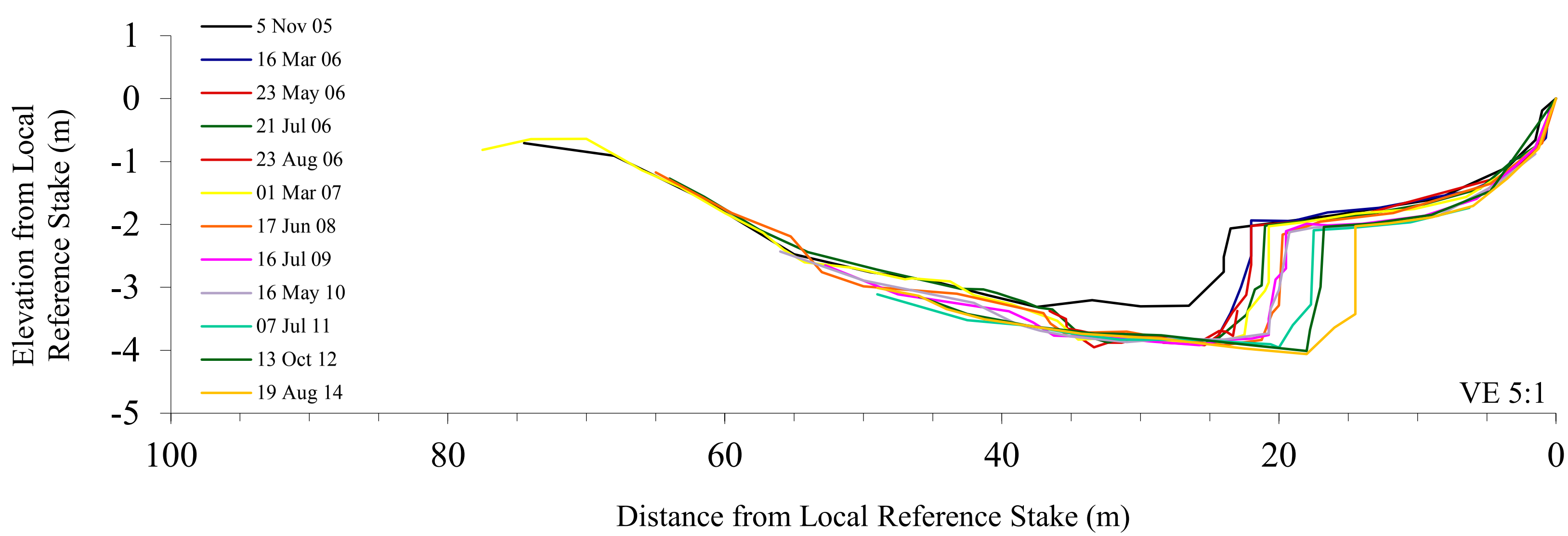

Figure 26. Geomorphic profile of transect U-6 located 7,056 m upstream of the former LeFever Dam, surveyed from November 2005 to August 2014.

on the profile resulted from the presence of submerged LWD in the former dam pool. Between 2008 and 2014, minor fluctuations in erosion/deposition characterize the channel floor. From 2008 to 2014, the channel widened a total of ~3.5 m producing near vertical banks on either side of the channel. The small sediment deposit present at 27.75 m on the profile accumulated next to LWD and a metal boat hull present at that location. Following the Munroe Falls Dam removal, the effect of dewatering of the exposed impounded muddy sediment is evident on the left bank (Figure 25). The left bank vertically compacted ~ 21 cm between 2004 and 2005 at a rate of ~1.12 cm/month. The impounded mud was 3 m thick on the left bank before dewatering occurred.

Transect U-6 is located 7,056 m (ULFD) near the downstream end of Zone 2 (Figure 16). At this location the former Dam pool had a wide channel with substantial deposits of impounded mud (Figure 26). Significant lateral erosion and compaction have occurred exclusively on the right bank at this transect. Geomorphic data was first collected along this transect about one month (Nov. 2005) after the Munroe Falls Dam was removed. Seven months following the removal of the Munroe Falls Dam, the Cuyahoga River downcut an additional 0.53 m to the pre-dam substrate (25-35 m on profile) and laterally eroded 2 m on the right bank (Figure 26). By 2012 (74 months later), the river downcut 0.4 m through the pre-dam flood plain sediments on river left. This slower rate of erosion is due to the substrate type. The left bank is comprised of more cohesive pre-dam flood plain sediments with tree trunks in growth position. The right bank of U-6 displays a progressive back-stepping in the form of vertical slump blocks since the removal of the Munroe Falls Dam (Figure 26). The right bank has receded 9.5 m since the Munroe Falls Dam was removed in 2005. Between the 2005 and 2008 surveys the right bank receded 4 m whereas the right bank only eroded 0.5 m from 2008-2009. Between the 2010 and 2011 surveys the right bank receded 3.05 m. Between the 2011 and 2012 surveys the right bank receded 0.7 m and from 2012 to 2014 it eroded an additional 2.5 m.

The vertical compaction of dewatered impoundment mud is clearly shown on the upland portion of the right bank. A rapid rate of compaction was observed immediately following dam removal and this rate diminished in the subsequent years. Compaction was assessed at 10 m distance on the profile (Figure 26). The right bank vertically compacted 0.23 m between 2005 and 2008. From 2008 to 2009 the right bank vertically compacted 0.04 m and only compacted 0.03 m from 2009 to 2014. The thickness of the underling mud was 2.2 m. Significant vertical compaction was completed by the July 2009 survey.

3.2.3 Zone 3

Zone 3 extends from 6,615 m ULFD to the upstream end of the former Munroe Falls Dam at 5,615 m (ULFD) (Figure 16). Geomorphic profiles U-2, U-7 and U-3 are located within this Zone. The most upstream profile measured in Zone 3 is located at 6,476 m (UFLD) at transect U-2 (Figure 27). The initial response of the Cuyahoga River to the removal of the Munroe Falls Dam was rapid vertical incision (~ 0.8 m from ~ 69-79 m distance) to the pre-dam substrate by March 2006 (Figure 27). The channel was also widened by lateral erosion. Between 2008 and 2009 a tree trunk lining the left bank was transported downstream and enhanced lateral erosion of the left bank by 2.75 m that year (Peck and Kasper, 2013). The right bank consists of a vertical scarp cut into the impoundment sediment. Erosion of this scarp has been episodic. From 2010 to 2011 the right bank scarp was stationary while the central channel (65-80 m) downcut 0.15 m. Between the 2011 and 2012 surveys, the right bank laterally eroded 1.3 m. Transect U-2 was resurveyed in 2015 and no significant morphologic change had took place between 2012 and 2015.

Transect U-2 also clearly shows the effect of vertical compaction of the impounded sediment following the removal of the Munroe Falls Dam. At 45 m on the U-2 profile the impounded sediment was 2.85 m thick. In the 2 months following the Munroe Falls

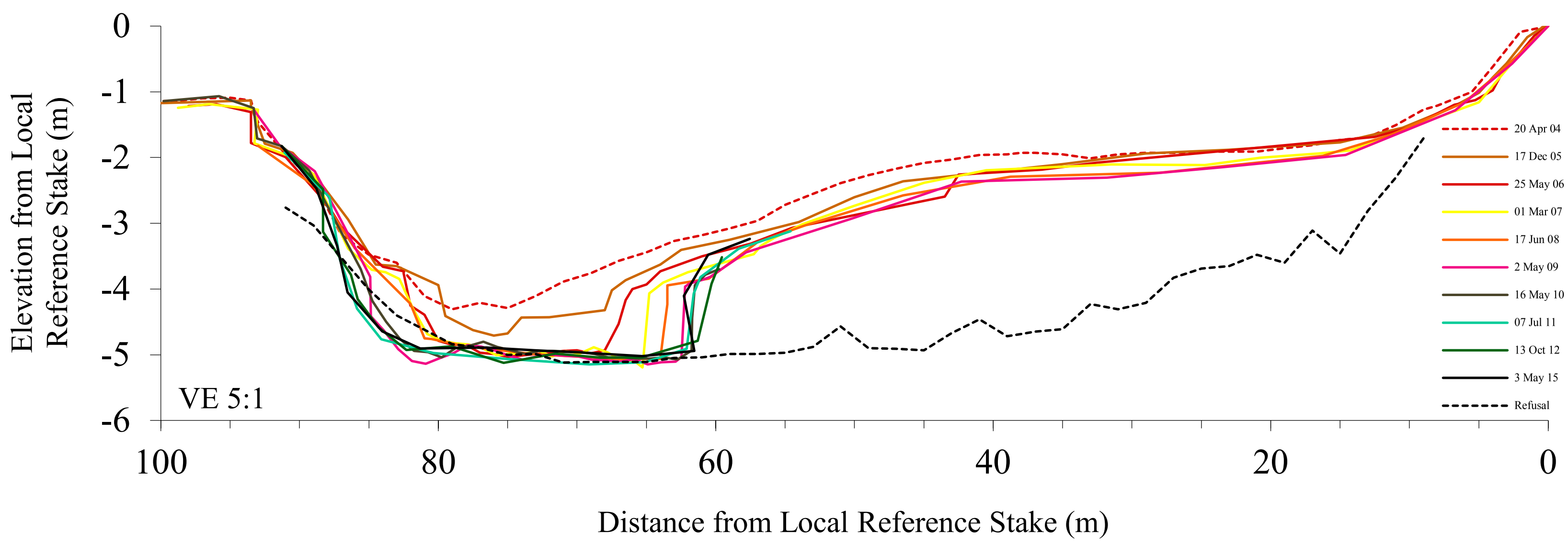

Figure 27. Geomorphic profile of transect U-2 located 6,476 m upstream of the former LeFever Dam, surveyed from April 2004 to May 2015.

Dam removal the sediment compacted 0.28 m. By 2009 it had compacted an additional m 0.33 m. Closer to the upland at 25 m distance on the profile, the impoundment fill was 1.9 m thick. Here the total amount of compaction was 0.23 m between 2005 and 2008. By the July 2009 survey, vertical compaction all along the right bank was complete and no further change was observed in 2010.

Transect U-7 is located further downstream at 5,858 m (ULFD) (Figure 16). Transect U-7 exhibits a similar sequence of behavior as transect U-2. The Cuyahoga River incised to the pre-dam substrate by May 2006 (Figure 28). Between 2011 and 2012 more significant lateral erosion of 1.5 m occurred. Lateral erosion then became the dominant form of geomorphic change resulting in a total channel widening of ~ 9.6 m (~ 8.1 m on the right bank and ~ 1.5 m on the left bank) since the Munroe Falls Dam removal. The lateral erosion on the right bank occurred as a progressive back stepping in the form of vertical slump blocks. From 2010 to 2011 the right bank laterally eroded 0.34 m. No significant geomorphic change has occurred at this transect between 2012 and 2014.

Vertical compaction on the right bank was comparable to that of transect U-2. At transect U-7, the thickness of the impoundment sediment was about 2 m at 65 m distance on the profile and the impounded sediment compacted about 0.30 m between 2005 and 2007.

Transect U-3 is located near the downstream end of Zone 3 just upstream of the former Munroe Falls Dam at 5,765 m (ULFD) (Figure 16). The maximum width (90 m) of the former dam pool is represented at this transect as well (Figure 29). By December 2005, the channel downcut to the pre-dam substrate (bedrock) and began to laterally erode both banks (Figure 29). By August 2014 the channel had widened a total of 7 m. From May 2010 to July 2011 the right bank laterally eroded 0.5 m whereas the left bank eroded 0.75 m resulting in a total channel widening of 1.25 m. From July 2011 to October 2012 the right bank receded 1 m whereas the left bank remained unchanged.

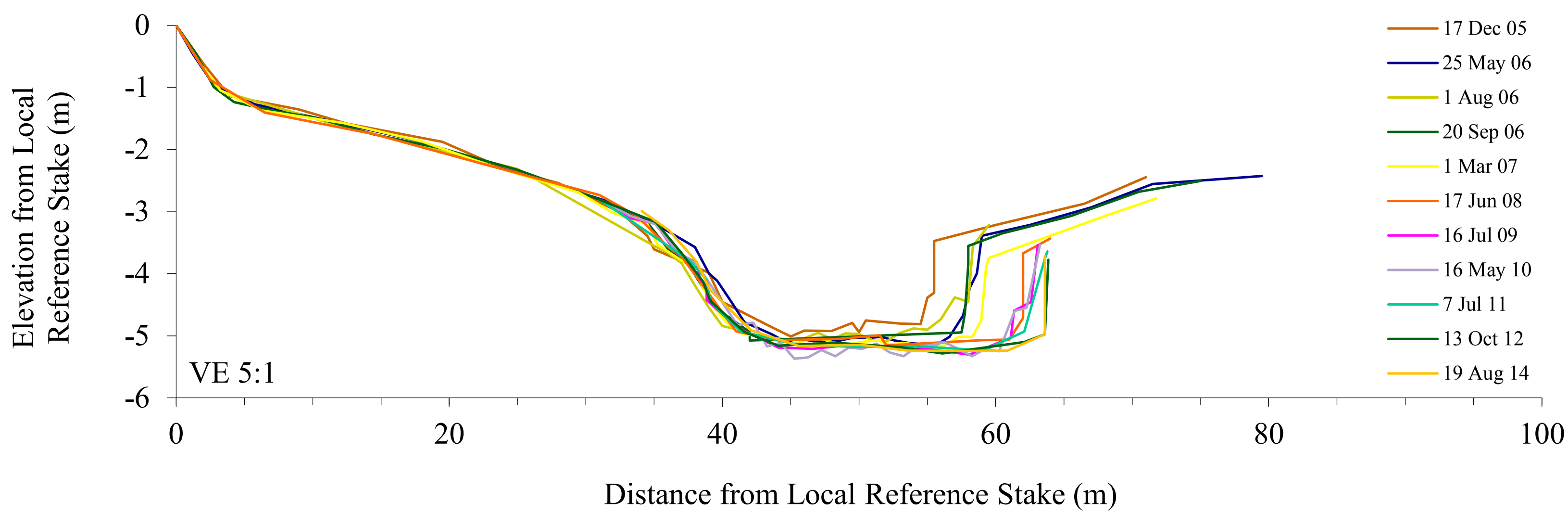

Figure 28. Geomorphic profile of transect U-7 located 5,858 m upstream of the former LeFever Dam, surveyed from December 2005 to August 2014.

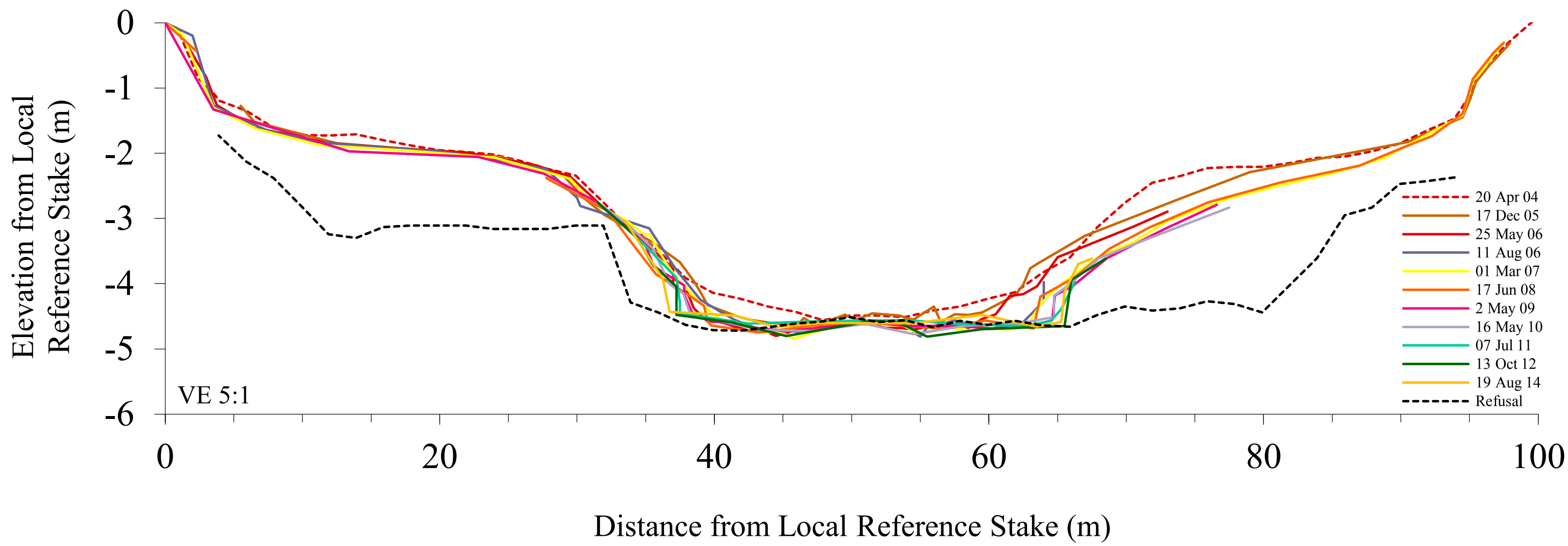

Figure 29. Geomorphic profile of transect U-3 located 5,765 m upstream of the former LeFever Dam, surveyed from April 2004 to August 2014.

From the October 2012 to August 2014 surveys, the left bank laterally eroded ~ 1 m whereas the right bank remained unchanged. The minor variations in elevation within the channel reflect irregularities in the bedrock channel floor and the placement of the stadia rod during the individual surveys. The geomorphic change at this transect also displays significant bank subsidence associated with the dewatering and compaction of the impounded mud following the removal of the Munroe Falls Dam. The following compaction values were calculated between the April 2004 and March 2007 surveys. The right bank vertically compacted ~59 cm at 72 m distance and ~32 cm at 82 m distance on the profile. The thickness of the underlying mud at these distances was ~1.96 m and ~1.87 m, respectively. The left bank displays much less vertical compaction; ~ 0.08 m at 18 m distance and ~0.05 m at 25 m distance. The thickness of the underlying mud at these distances was ~1.23 m and ~1.14 m respectively. A major difference between the left and right banks is that the right bank receives significant water from upland seeps and was notably wetter than the left bank.

3.2.4 Zone 4

Zone 4 begins at the former Munroe Falls Dam (6,615 m ULFD) and ends at the upstream limit of the former LeFever Dam pool (2,670 m ULFD) (Figure 16). The nature of the middle Cuyahoga River in this zone differs from the upstream zones as it meanders more extensively and contains cut bank, point bar, and chute sub-environments (Peck and Kasper, 2013). Because this zone is downstream of the former Munroe Falls Dam the trends in morphologic change are different than the upstream zones.

Zone 4 is generally characterized as sediment starved while the Munroe Falls Dam existed, by aggradation following the Munroe Falls removal and by degradation following the LeFever Dam removal. Transects D-3, D-7, D-4, D-5, D-8, D-2, D-9, D-10, D-14, D-11 and D-12 are located within this zone and generally exhibit these characteristics.

Transects D-3 and D-7 are located near the upstream end of Zone 4 at 5,554 and 5,169 m (ULFD) respectively (Figure 30, 31). Both of these transect show little geomorphic change following both dam removals. At transect D-3 a 0.17 m high sand levee was deposited on the right bank between the January 2007 and June 2008 surveys (Figure 30). At transect D-7 a 0.14 m levee deposit also accumulated on the right bank between the May 2009 and July 2011 surveys (Figure 31). Transect D-3 remained fairly stable from 2008 to 2014 (Figure 30). At D-7 however, 0.14 m of additional levee sands were deposited on the right bank between the July 2011 and May 2015 surveys (Figure 31). The right bank at D-7 underwent a total of 0.5 m of lateral erosion between May 2009 and May 2015.

Continuing downstream is the location of transect D-4 (4,916 m ULFD) which is located downstream of an island in the Cuyahoga River. This transect was established ~3.5 years after the Munroe Falls Dam removal so sediment released from the former Munroe Falls impoundment had already accumulated along the left side at this location (Figure 32). Little change occurred in response to the LeFever Dam removal (0.10 m of downcutting between May 2009 and Sept. 2013) and no geomorphic data has been collected since (Figure 32).

Further downstream is transect D-5 located at 4,607 m (ULFD) (Figure 16). A sediment bar occupied the channel from 12-40 m on the profile and maintained its maximum size from May 2009 to September 2013. By March 2014 the bar began to erode and continued to do so through 2015. By December 2014, the bar only spanned 10-20 m distance on the profile (Figure 33). Between the 2012 and 2015 surveys, the bar was downcut a total of 0.62 m at 19 m on the profile. A new sand bar appeared in the lee of LWD on river left at 7 to 12 m distance between December 2014 and May 2015

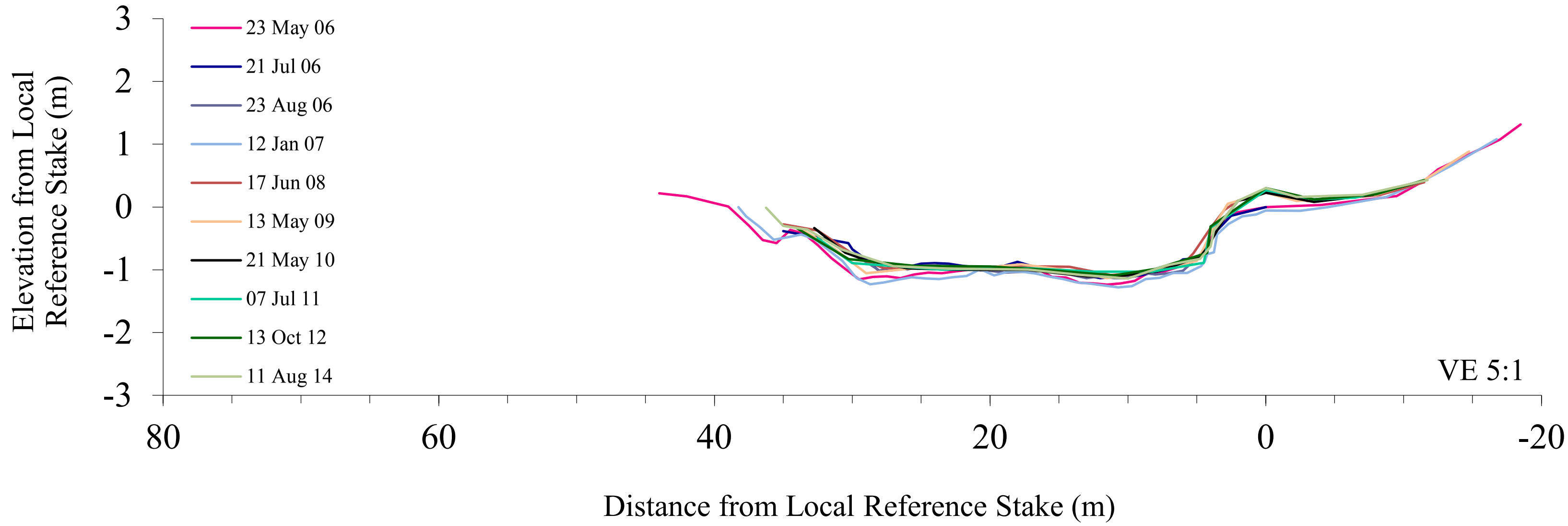

Figure 30. Geomorphic profile of transect D-3 located 5,554 m upstream of the former LeFever Dam, surveyed from May 2006 to August 2014.

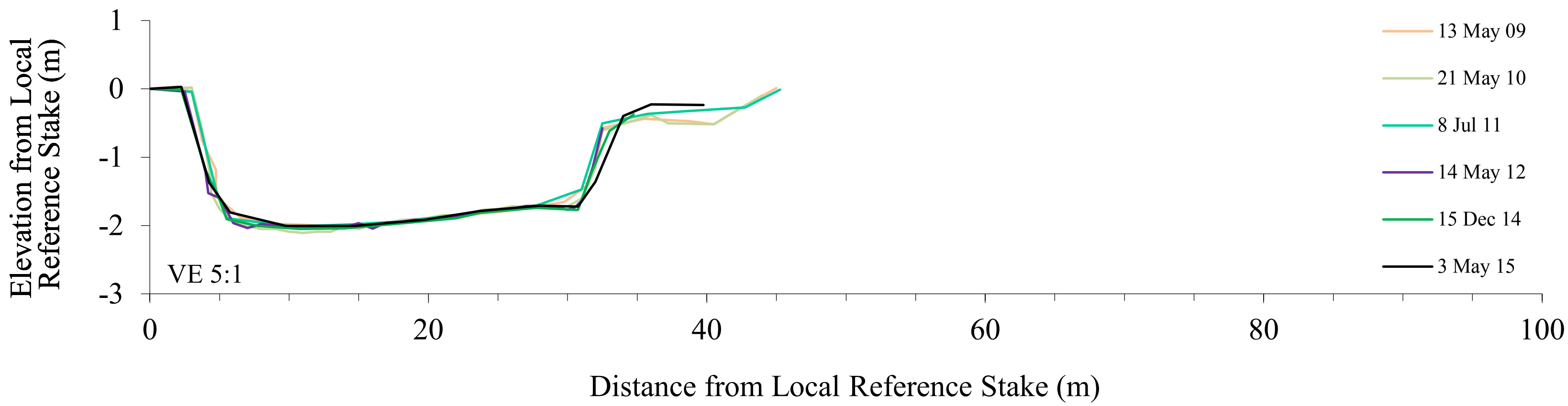

Figure 31. Geomorphic profile of transect D-7 located 5,169 m upstream of the former LeFever Dam, surveyed from January 2005 to May 2015.

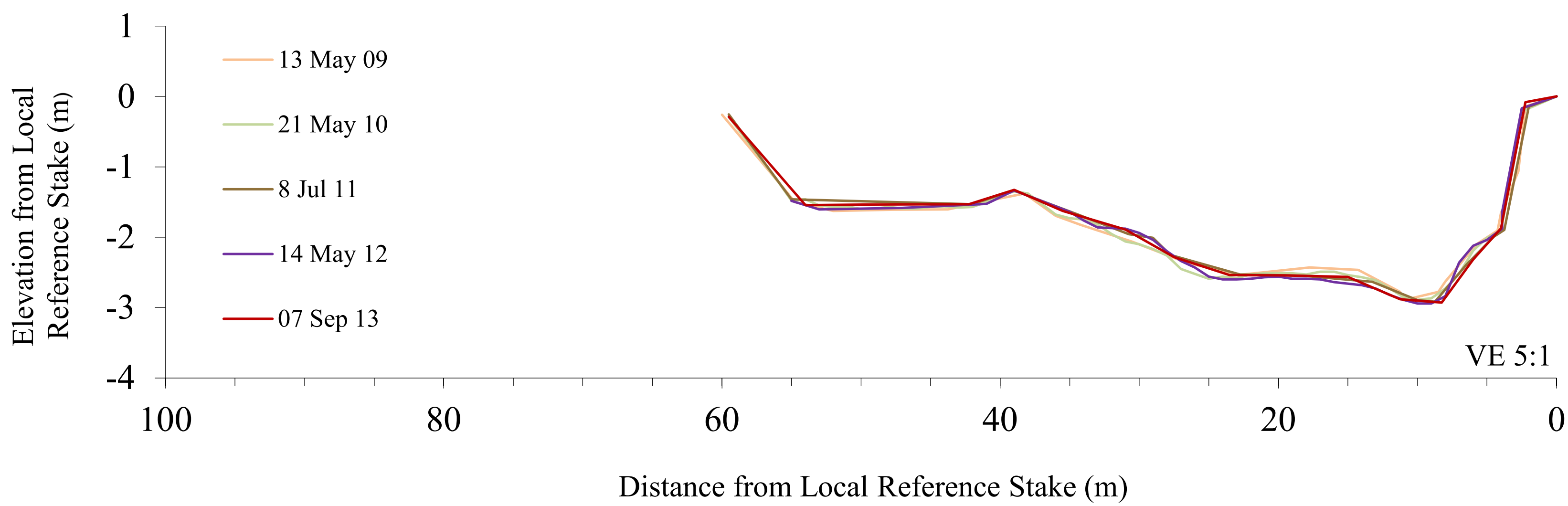

Figure 32. Geomorphic profile of transect D-4 located 4,916 m upstream of the former LeFever Dam, surveyed from May 2009 to September 2013.

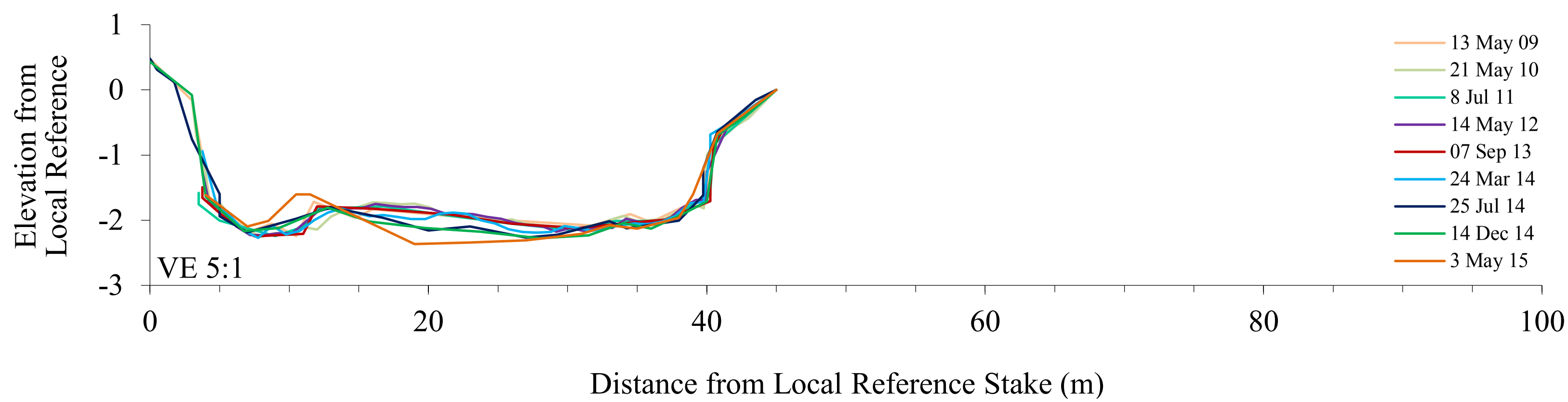

Figure 33. Geomorphic profile of transect D-5 located 4,607 m upstream of the former LeFever Dam, surveyed from May 2005 to May 2015.

surveys (Figure 33). The elevation of this bar exceeded the maximum elevation in 2010 by 0.14 m. The sediment accumulation in the channel between 33-40 m on the profile has remained unchanged since 2009 (Figure 33).

Continuing downstream is the location of transect D-2 which is located 4,254 m (ULFD) adjacent to Water Works Park (Figure 16). This profile is unique among the profiles downstream of the former Munroe Falls Dam because the profile was surveyed pre-Munroe Falls removal (Rumschlag and Peck 2007). The channel was deep and gravely prior to the Munroe Falls removal. Bed elevation changes were evaluated at 27 m on the profile (Figure 34).

Between the January 2005 and December 2006 surveys the channel aggraded with 0.96 m of sand eroded from the Munroe Falls impoundment fill (Figure 34). By January 2013, the channel down cut through the aggraded sediment by 0.14 m. Following the removal of the LeFever Dam, the channel incised an additional 0.18 m by the September 2013 survey. The channel sands continued to be downcut through the winter of 2014 (0.12 m by December 2014) and spring of 2015 (0.25 m by May 2015). The channel reached the pre-Munroe Falls removal substrate at 25 m on the profile in 2015 as well. Nearly two thirds of the sand deposited following the Munroe Falls Dam removal was eroded (72% decrease in elevation) and transported downstream between December 2006 and May 2015 (Figure 34).

Further downstream in Zone 4 is transect D-8 located 4,023 m (ULFD) (Figure 16). The impoundment sediment from the former Munroe Falls Dam was deposited in the channel by May 2009 and the channel was stable through May 2012. The accumulation of sand was right of the center of the channel between 30-10 m on the profile. The thalweg was on river left at about 35 m on the profile and the thalweg was composed of cobbles reflecting the pre-Munroe Falls removal conditions (Figure 35). One month after the LeFever Dam removal (September 2013 survey) 0.5 m of sand was eroded at 20 m on

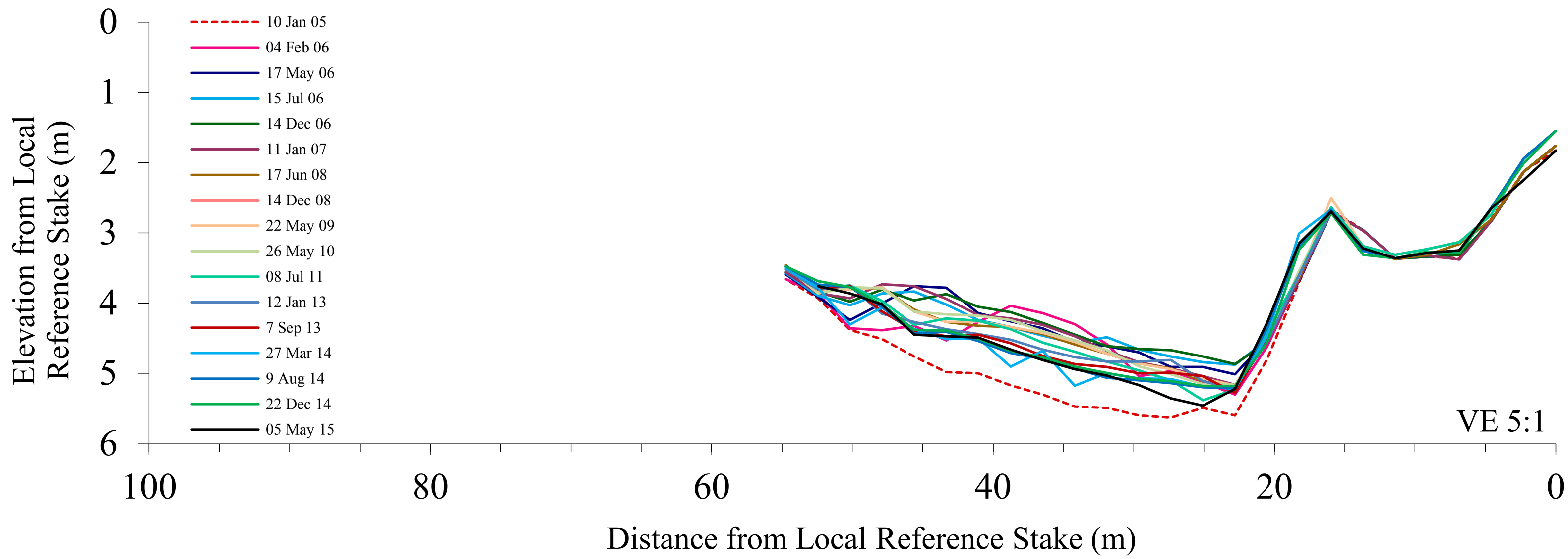

Figure 34. Geomorphic profile of transect D-2 located 4,254 m upstream of the former LeFever Dam, surveyed from January 2005 to May 2015.

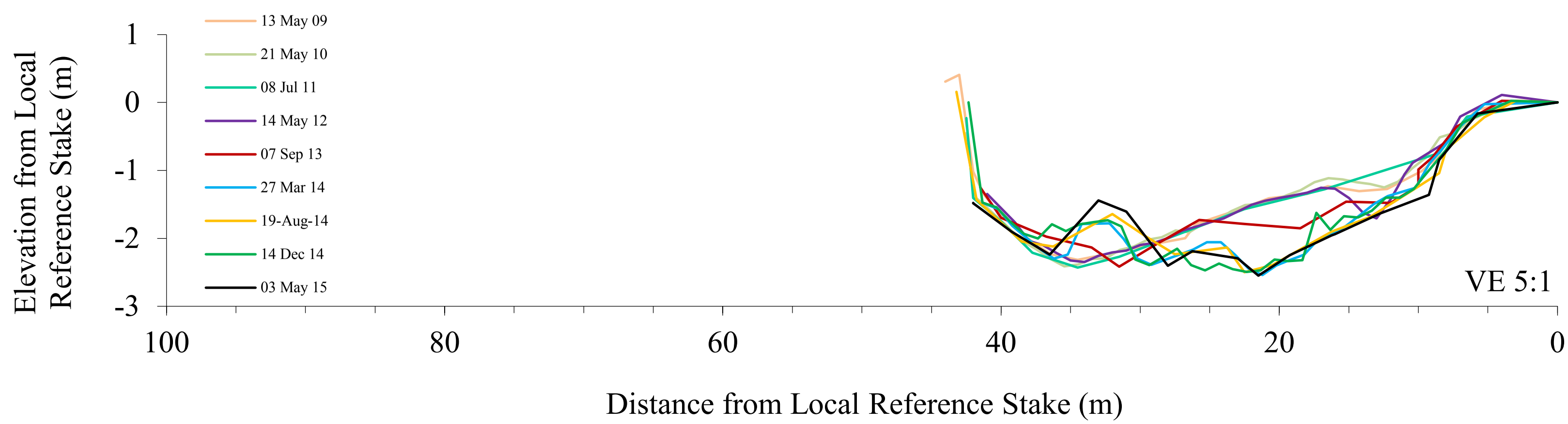

Figure 35. Geomorphic profile of transect D-8 located 4,023 m upstream of the former LeFever Dam, surveyed from May 2009 to May 2015.

the profile (Figure 35). By the March 2014 survey, an additional ~ 0.7 m of downcutting occurred and the channel reached the pre-Munroe Falls removal substrate. In addition to this downcutting, 0.68 m of sand accumulated on river left due to the transport of LWD to this location (30-35 m on profile) between September 2013 and March 2014. From March to December 2014 more sediment was deposited in the lee of this LWD aggrading the channel at 30-35 m on the profile.

Moving further downstream is the location of transect D-10 located 3,310 m (ULFD) (Figure 16). Similar to the previously described transects in Zone 4, significant deposition of sands eroded from the Munroe Falls impoundment span the channel by the time of the May 2009 surveys (Figure 36). The maximum elevation of sand is maintained between the 2009-2010 surveys except on river left where the thalweg was scoured ~ 0.46 m. After the 2010 survey, extensive sand deposition occurred on the point bar and adjacent chutes located on river right. As a result, the local reference stake was buried and new one had to be emplaced. All of the surveys from 2011-2015 were measured from the new, local reference stake on the left bank. By May 2013, ~ 0.23 m of downcutting through the sand deposit occurred at 22-30 m on the profile (Figure 36). Between May 2013 and September 2013, the channel downcut an additional ~ 0.27 m. The LeFever Dam was also removed between these dates. From September 2013 to December 2014 the channel continued to downcut a total of ~ 0.17 m. Between the December 2014 and May 2015 surveys the 0.26 m of downcutting occurred in the thalweg while the channel on river right at 10-20 m on the profile aggraded 0.15 m.

Further downstream in Zone 4, is transect D-14 located 3,146 m (ULFD) at Water Works Park (Figure 16). This transect was not established until May 2013 so the initial aggradation of Munroe Falls sand is not recorded. However, field observations at this location following the removal of the Munroe Falls Dam showed that the right bank aggraded substantially with sand released from the former Munroe Falls Impoundment

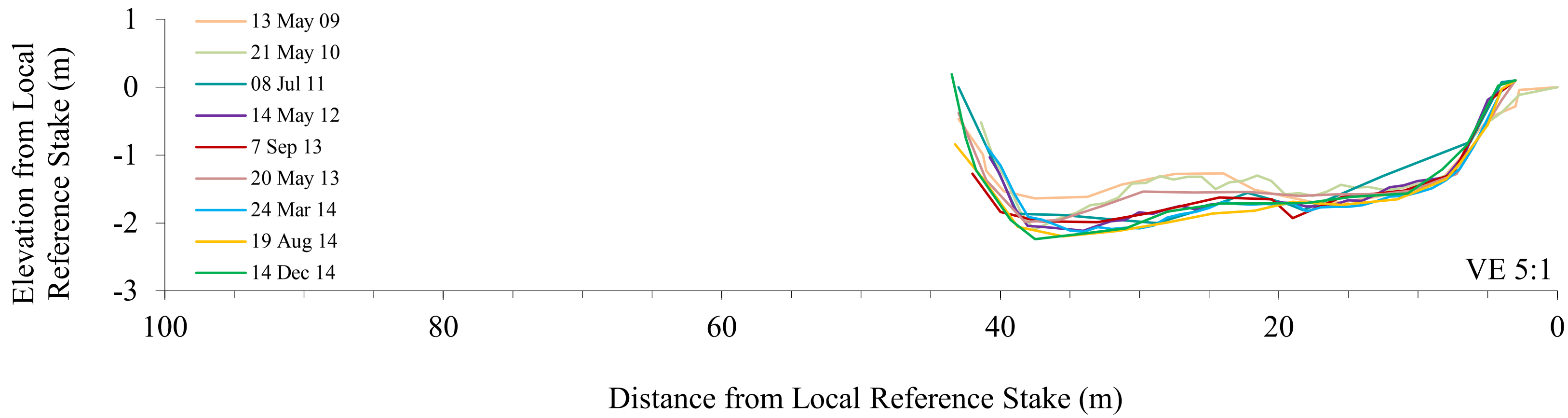

Figure 36. Geomorphic profile of transect D-10 located 3,310 m upstream of the former LeFever Dam, surveyed from May 2009 to December 2014.

(J. Peck personal communication). As of the May 2013 survey, Munroe Falls sand deposits comprised the right side of the profile and the thalweg was on river left between 0-17 m (Figure 37). Following the removal of the LeFever Dam in September 2013 the right bank was scoured ~ 0.38 m between ~ 29-39 m on the profile while the left bank remained stable. No significant geomorphic change occurred between September 2013 and October 2013. The right bank and mid-channel sediment bar laterally eroded (~1.77 m) toward river right between October 2013 and March 2014. Between the March 2014 and July 2014 surveys, the sediment bar was largely eroded away leaving a small bar-form at about 20 m on the profile. Downcutting and lateral erosion continued from July to December 2014 and resulted in a ~ 2.23 m recession of the right bank and the lowest incision at 27 m distance. The erosion recorded on the December 2014 survey was enhanced by the presence of a tree that had moved from upstream to the profile location. This log was angled in such a way as to direct the flow of the Cuyahoga River toward the right bank and this accelerated the erosion. The thalweg is now at 27 m at the same location as the log on the profile line that created obstacle scour of the bed.

Substantial geomorphic change took place between the December 2014 and May 2015 surveys as the trend of post-removal downcutting was reversed. At 29 m on the profile, the right bank aggraded 0.76 m with sand transported to this location from upstream. Sand stored in chutes to the right of transect D-14 likely deposited along the right bank because a small chute channel was observed to be actively discharging on the right bank. In the center of the channel between 25-35 m about 1 m of sediment accumulated. This extensive deposition of sand resulted from the seasonal high flows of the winter and spring that caused a sediment bar to migrate downstream to the profile location.

Transect D-11 located at 2,947 m (ULFD) coinciding with a meander bend having a cut bank and point bar. Following the Munroe Falls Dam removal, sands were deposited

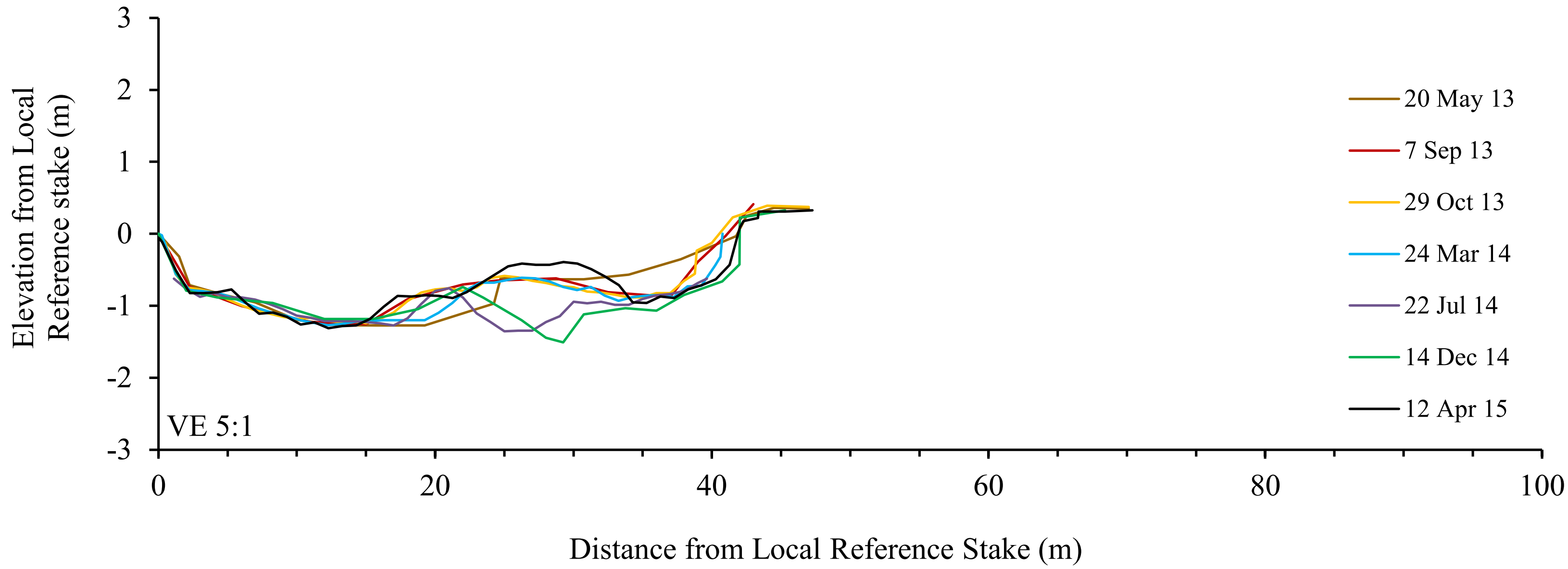

Figure 37. Geomorphic profile of transect D-14 located 3,146 m upstream of the former LeFever Dam, surveyed from May 2013 to April 2015.

on the point bar on river left (Figure 38). From 2009 to 2010 the point bar was eroded slightly. By July 2011 the bar is nearly eroded away and by May 2013 the sands have been removed. The erosion of this sandy point bar is not related to the removal of the LeFever Dam because the LeFever Dam was removed after May 2013.

The furthest downstream geomorphic profile measured in Zone 4 is transect D-12 at 2,795 m (UFLD) (Figure 16). This transect was established in 2009 after the deposition of sediment from the Munroe Falls impoundment following the removal of the Munroe Falls Dam (Figure 39). The maximum bed elevation of the channel deposit was maintained from the May 2009 to the May 2013 surveys. Surveys during these four years display minor fluctuations in erosion/deposition across the channel as sandy dunes migrated downstream. For example between May 2010 and July 2011, sediment accumulated on both river right and river left. One month after the LeFever Dam was removed, the transect was surveyed in September 2013 and was found to resemble the May 2013 profile. However, by March 2014, the bed incised an average of ~ 0.42 m across the channel. Downcutting continued through December 2014 scouring sand from river right and incising portions of the central channel and left bank by 10-20 cm.

3.2.5 Zone 5

Zone 5 begins at the head of the LeFever Dam pool (2,670 m ULFD) and ends at the site of the former LeFever Dam (0 m ULFD) (Figure 16). This zone has shown rapid incision to the pre-dam substrate following the removal of the LeFever Dam. The LeFever impoundment delta and transects D-15, D-6, and D-13 are located in this zone and display this trend in geomorphic change. The furthest upstream geomorphic measurements made in Zone 5 are at the LeFever impoundment delta (2,415 m ULFD) but will be discussed in more detail in section 3.3 because a dense network of 3-D measurements were made rather than a channel cross section.

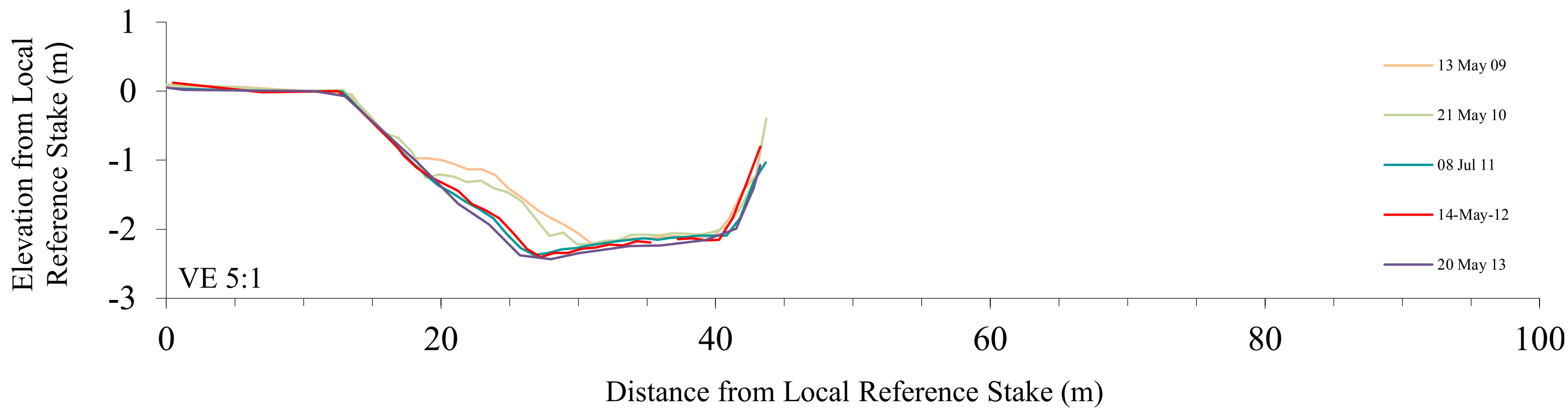

Figure 38. Geomorphic profile of transect D-11 located 2.947 m upstream of the former LeFever Dam, surveyed from May 2009 to May 2013.

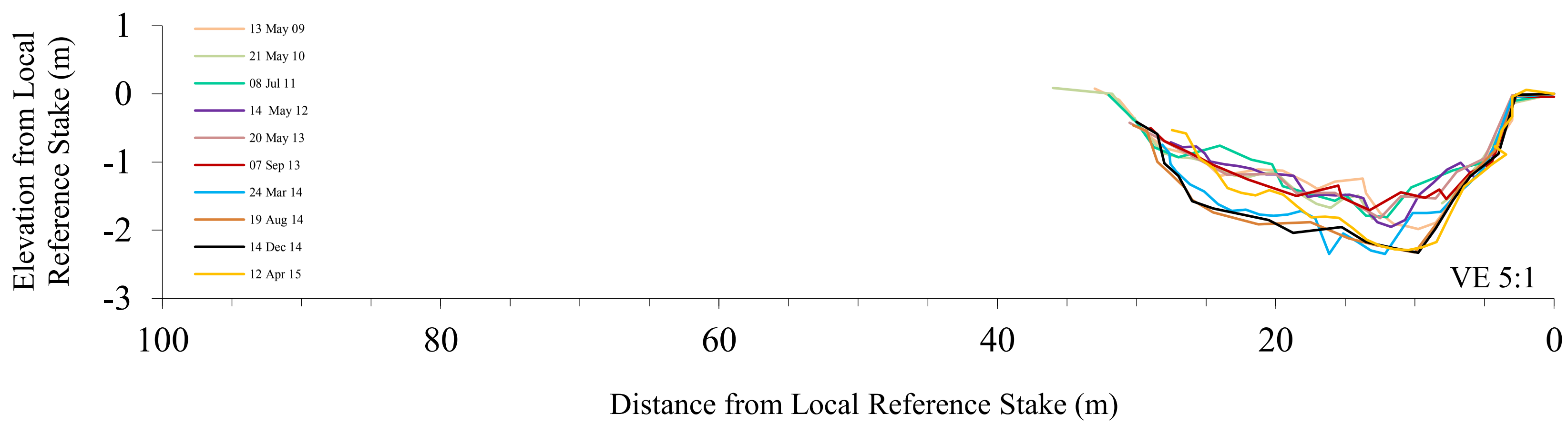

Figure 39. Geomorphic profile of transect D-12 located 2,795 m upstream of the former LeFever Dam, surveyed from May 2009 to April 2015.

Just downstream of the delta is transect D-15 located at 2,216 m (ULFD) (Figure 16). Transect D-15 was established in September 2013 following the removal of the LeFever Dam. The channel bed is underlain by bedrock and the maximum, measured sediment thickness was ~ 0.67 m at 23 m on the September 2013 profile (Figure 40). In December 2013, ~ 4 months after the LeFever Dam was removed, about half of the sediment was eroded and transported downstream. The Cuyahoga River incised to bedrock by the March 2014 survey and bedrock continued to be exposed on the channel floor through the December 2014 survey. The channel floor at this location is primarily bedrock with patchy deposits of sand and gravel that are being actively transported downstream.

Much farther downstream is the widest geomorphic profile measured in Zone 5 (Figure 16). Transect D-6 is located 843 m (ULFD) and contains formerly impounded muddy sediment in the channel margins and a thalweg on river right (Figure 41). The December 2008 to May 2012 surveys were measured before the removal of the LeFever Dam and show very little geomorphic change when the dam was in place. The first post-removal survey was conducted one month after the LeFever Dam was removed in September 2013. This survey however, was not accurately referenced to the rebar on river right so the elevation of the channel floor is not a reliable measurement even though the channel width is accurate.

Four months after the LeFever Dam removal in December 2013, the Cuyahoga River had incised 1.02 m to bedrock at transect D-6 (Figure 41). By March 2014 the newly incised channel aggraded ~ 0.60 m with sand and gravel. Following the LeFever Dam removal the river formed wide and shallow channel. The channel at D-6 remains wide and shallow through the December 2014 survey, however the river continued to slowly erode the newly aggraded thalweg as well as the muddy channel margin on river left. Between March 2014 and May 2014 the thalweg downcut by 0.2 m with the most erosion on river left. The channel between ~20-45 m is composed of a thin layer of actively

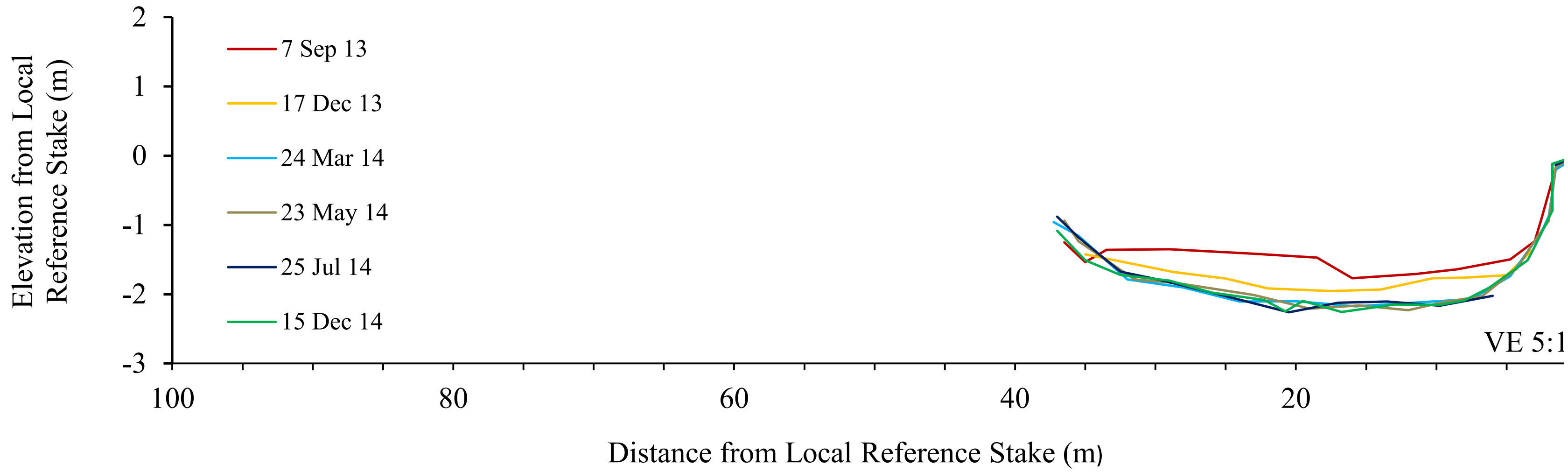

Figure 40. Geomorphic profile of transect D-15 located 2,216 m upstream of the former LeFever Dam, surveyed from September 2013 to December 2014.

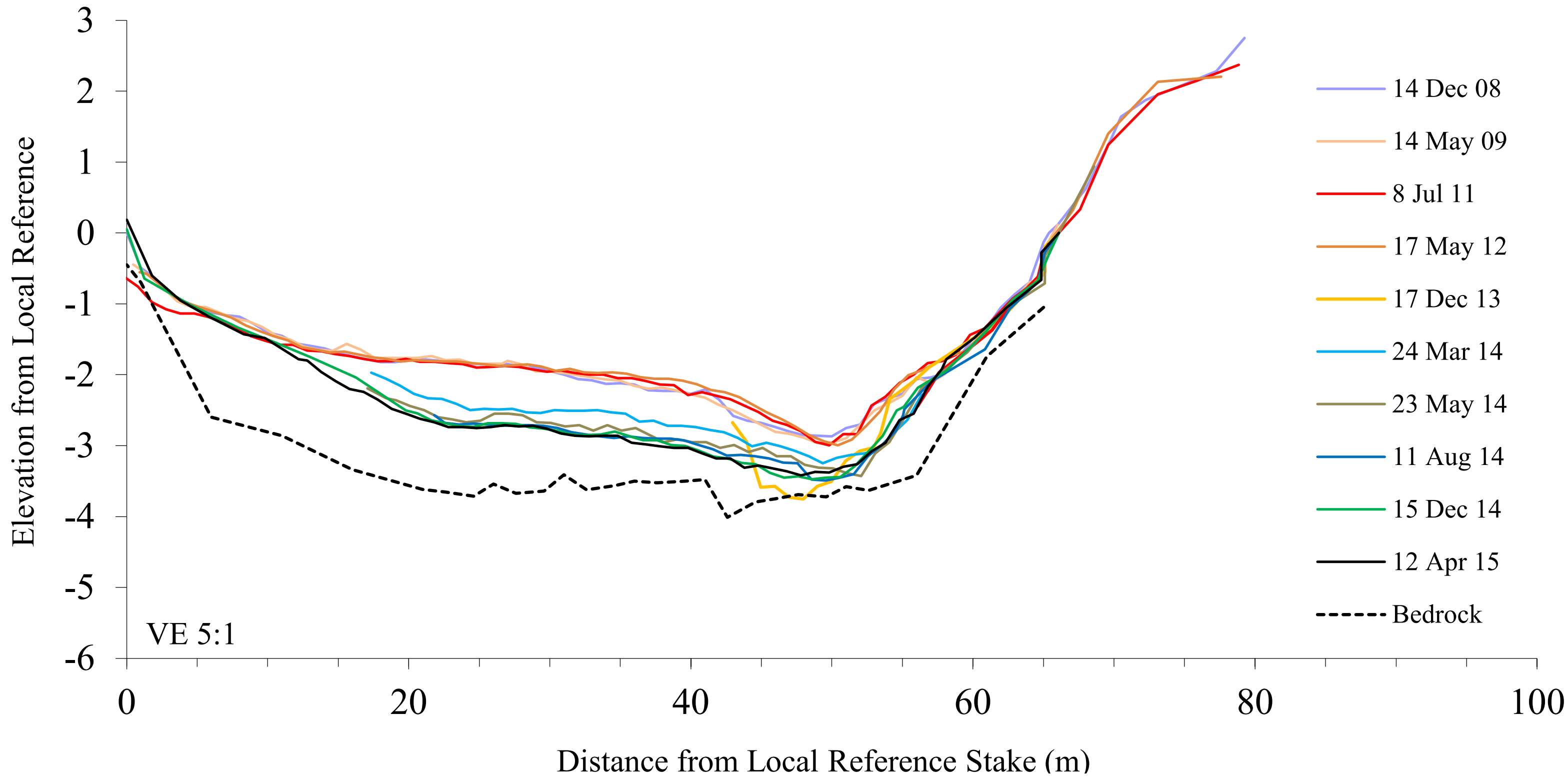

Figure 41. Geomorphic profile of transect D-6 located 843 m upstream of the former LeFever Dam, surveyed from December 2008 to April 2015.

transporting sand and gravel that was deposited on top of the impoundment mud. The channel floor lowered by an average of 0.22 m between 20-45 m on the profile (Figure 41). Between May 2014 and August 2014, the main channel downcut an average of 0.18 m. From August 2014 to December 2014 the main channel downcut and additional 0.2 m at 45-48 m on the profile.

The total channel widening is difficult to determine at this transect because the left bank in not marked by a vertical scarp. The right bank has laterally eroded ~ 3.2 m from the December 2013 to December 2014 surveys. The channel at D-6 in December 2014 was 36.6 m wide with sand and gravel in bed load transport. The mud on the left bank (10-20 m on profile) experienced 0.16 m of lowering between the December 2014 and May 2015 surveys. The thalweg remained stable between these surveys as well. Former LeFever Dam pool mud is still present and is the thickest on the channel margins.

The final geomorphic profile measured in Zone 5 is transect D-13 (273 m ULFD) (Figure 16). When the LeFever Dam was in place, the channel was 41 m wide and ~ 3.5 m deep in May 2009 (Figure 42). Mud to gravel sized sediment comprised the left bank. After the LeFever Dam was removed, the channel narrowed to about 13.5 m wide and ~ 0.94 m deep on the August 2014 survey (Figure 42). No additional geomorphic data was collected here in 2015.

3.3 The LeFever Impoundment Delta

Before the 2005 Munroe Falls and 2013 LeFever Dam removals, two, deep water, low velocity impoundments existed within the middle Cuyahoga River. The initial sediment release following the Munroe Falls Dam removal was transported downstream, causing extensive sand deposition in Zone 4. Sand sedimentation was prevented from continuing downstream by the low velocity LeFever Dam pool (Zone 5) located 3.2 km downstream

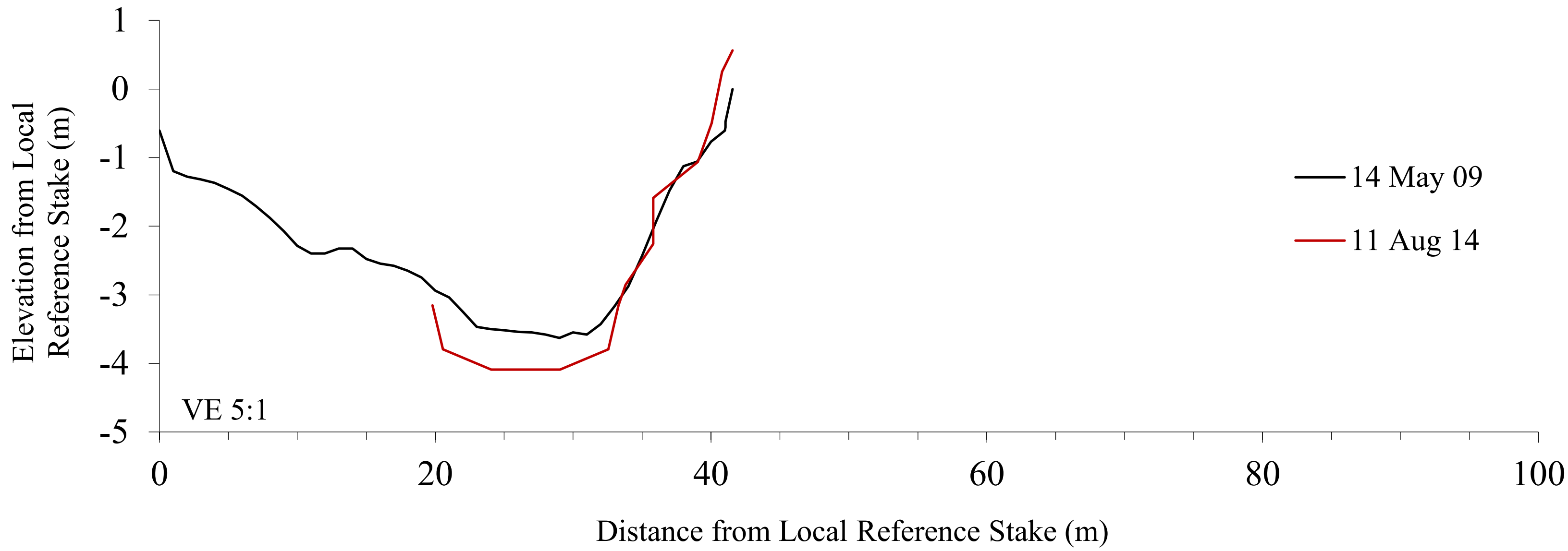

Figure 42. Geomorphic profile of transect D-13 located 273 m upstream of the former LeFever Dam, surveyed from May 2009 to August 2014.

of the former Munroe Falls Dam. This forced deposition of sandy sediment resulted in the formation of a large deltaic feature at the head of the former LeFever Dam pool known in this study as the LeFever impoundment delta.

Kasper and Peck (2013) observed the initial deposition of this deltaic feature several months after the Munroe Dam removal and determined that the deposit was ~1.35 m thick by 2009. High river discharge through March 2010 caused erosion of the delta top and subsequent downstream migration of 25 m (Peck and Kasper, 2013). Geomorphic surveys of this delta have since continued through 2015 and document the profound impacts of the LeFever Dam removal on the morphology and spatial extent of the deposit.

The deltaic deposit was dynamic in terms of its spatial extent and sedimentation/erosion prior to the LeFever Dam removal as well. In July 2011, the deposit occupied the main channel of the Cuyahoga River while the chute on river right and downstream end of the delta had minimal amounts of sediment (Figure 43). By the May 2012 survey, the delta top aggraded 0.56 m in the lee of the mid-channel island (Figure 44). At the downstream end, the channel floor aggraded 0.81 m as migrating 2-D dunes with superimposed 2.5-D ripples moved downstream (Figure 44). However, between the May 2012 and May 2013 surveys, the delta top eroded 0.45 m while the downstream end eroded 0.70 m (Figure 45). Changes in bed elevation of the chute on river right were negligible between the July 2011 and May 2013 surveys. The spatial extent of the subaerially exposed delta sediment was dependent upon the discharge and water surface elevation on each survey date as well.

Eleven days after the LeFever Dam removal, the August 2013 survey revealed significant changes to the geomorphology of the impoundment delta. The water surface elevation dropped 0.48 m between the May and August 2013 surveys (Figure 46). Because discharge at Old Portage Path (waterdata.usgs.gov) was higher in August (5.64 m^3/s) than in May (4.17 m^3/s) the lowered water surface can be attributed to the

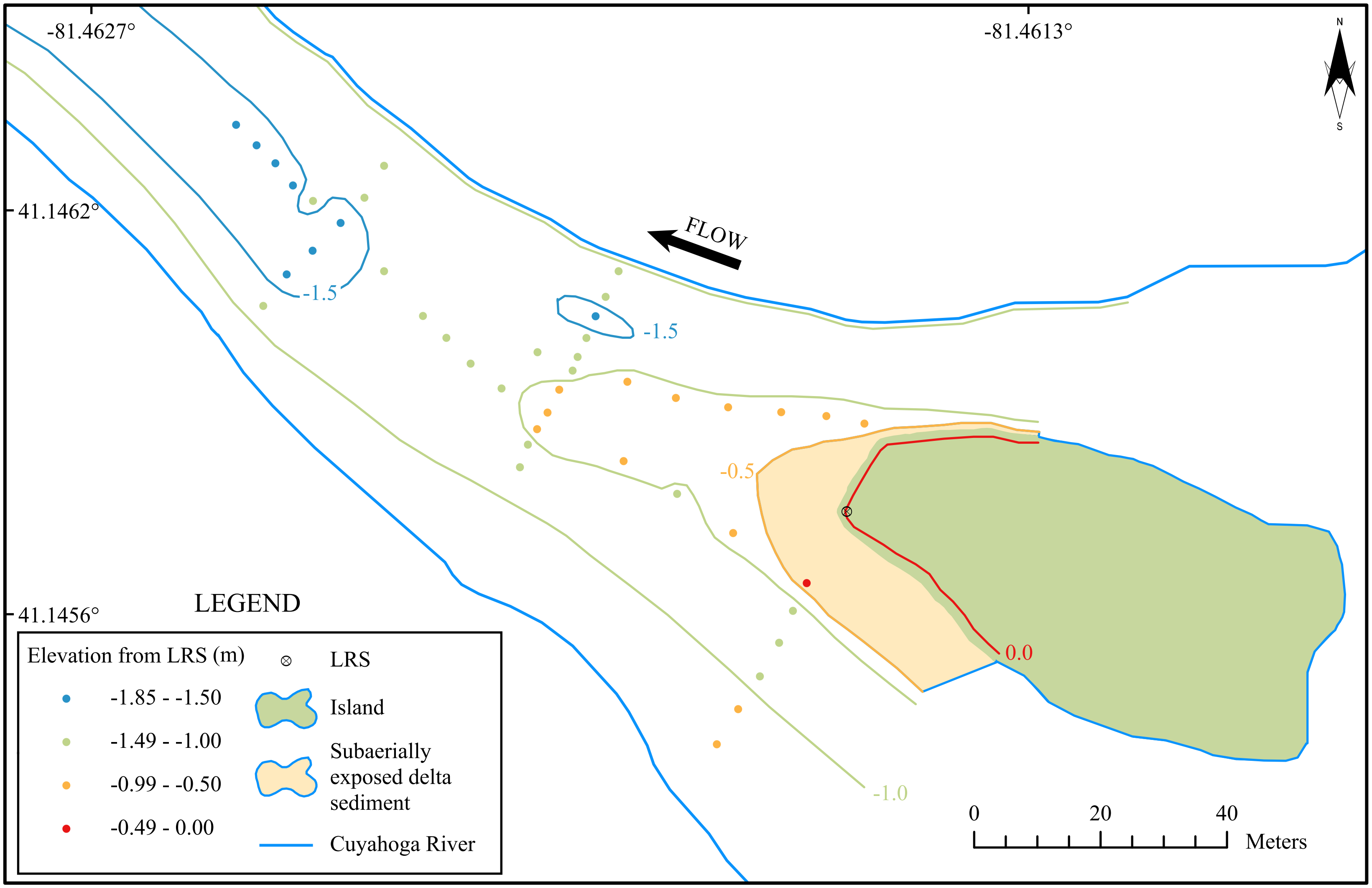

Figure 43. Map view of the geomorphology at the head of the former LeFever Dam pool on 7-8-11. Elevations relative to the local reference stake (LRS) and contoured at a 0.5 m interval. The water surface is -0.50 m from the LRS.

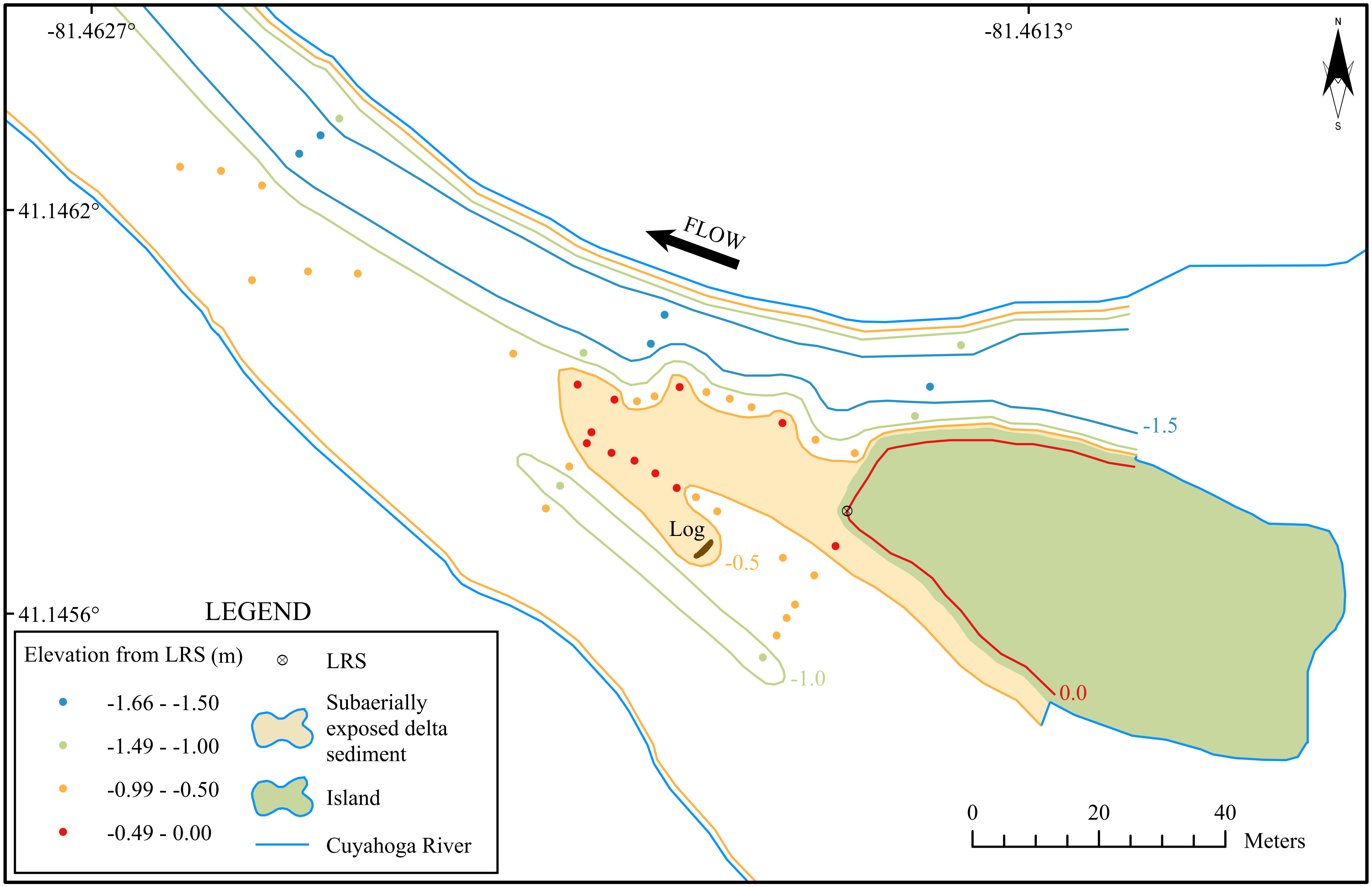

Figure 44. Map view of the geomorphology at the head of the former LeFever Dam pool on 5-17-12. Elevations relative to the local reference stake (LRS) and contoured at a 0.5 m interval. The water surface is -0.43 m from the LRS.

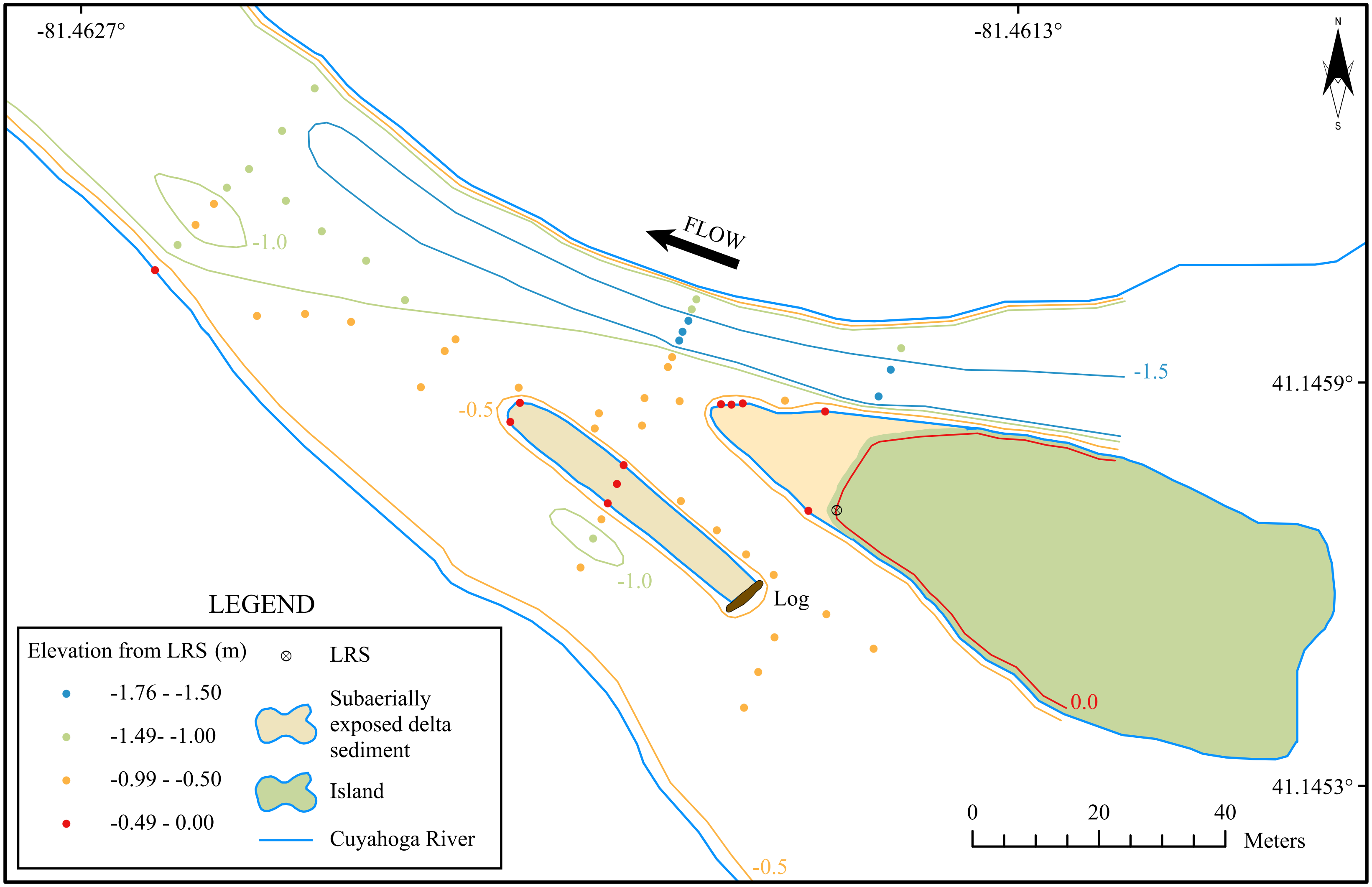

Figure 45. Map view of the geomorphology at the head of the former LeFever Dam pool on 5-20-2013. Elevations relative to the local reference stake (LRS) and contoured at a 0.5 m interval. The water surface is -0.46 m from the LRS.

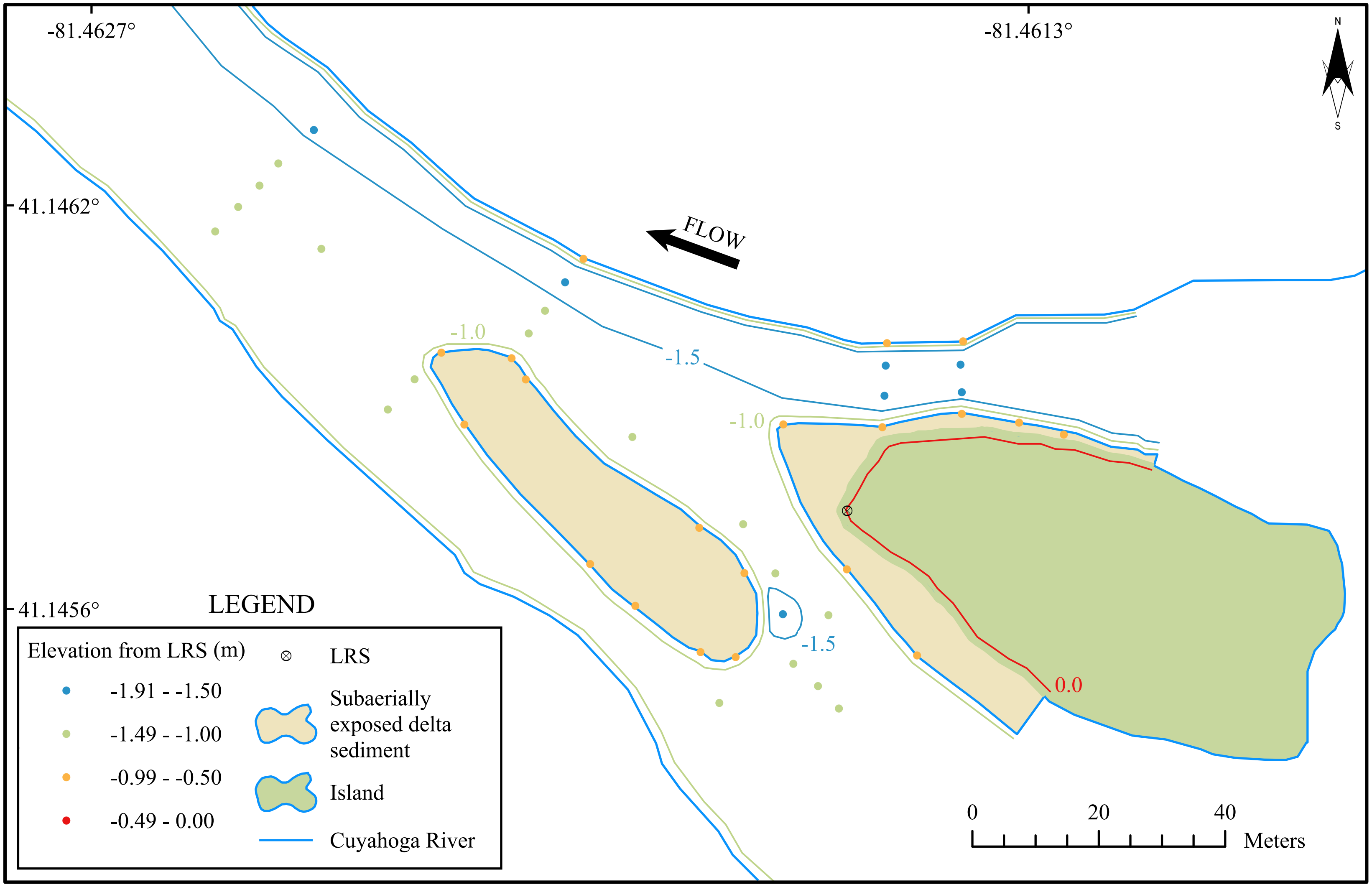

Figure 46. Map view of the geomorphology at the head of the former LeFever Dam pool on 8-30-2013. Elevations relative to the local reference stake (LRS) and contoured at a 0.5 m contour interval. The water surface is -0.94 m from the LRS.

dewatering of the LeFever Dam pool. The upstream end of the delta top vertically eroded an average of 0.25 m. The downstream end then aggraded 0.35 m as did the chute on river right by an average of 0.24 m (Figure 46).

By the December 2013 survey the post-removal thalweg is well established between the vegetated island and mid-channel sediment bar (Figure 47). The 1.5 m wide thalweg incised into the underlying LeFever impoundment sediment creating mud furrows and 0.2-0.5 m tall scarps on the channel margins. The new thalweg aggraded 0.05 m with sand and gravel in active transport. The chute on river right also aggraded 0.36 m as a sand bar migrated downstream. The channel on river right and the downstream end of the delta contained sandy bedforms in active transport resulting in 0.17 m and 0.15 m of aggradation respectively. Bedrock was exposed at the upstream and downstream ends of the delta on river left as well.

Erosion of the delta sediment was prominent between December 2013 and March 2014. The thalweg experienced 0.71 m of vertical erosion as a sand bar eroded away and just downstream of the mid-channel sediment bar, 0.57 m vertical erosion occurred as well (Figure 48). On the downstream end of the delta, the sandy bedforms in transport during the December 2013 survey had moved downstream resulting in an average decrease in bed elevation of 0.42 m. Sand continued to be transported through the chute on river right.

Erosion continued through the May 2014 survey. The upstream end of the delta eroded further as the post-removal thalweg became deeper and wider (Figure 49). Bedrock was also exposed in the center channel downstream of the mid-channel sediment bar and in portions of the farthest left and right bank downstream of the vegetated island. LeFever impoundment clay was also exposed on the downstream end of the mid channel sediment bar. By the July 2014 survey the thalweg was very well established and spanned the entire length of the delta (Figure 50). The former mid-channel sand

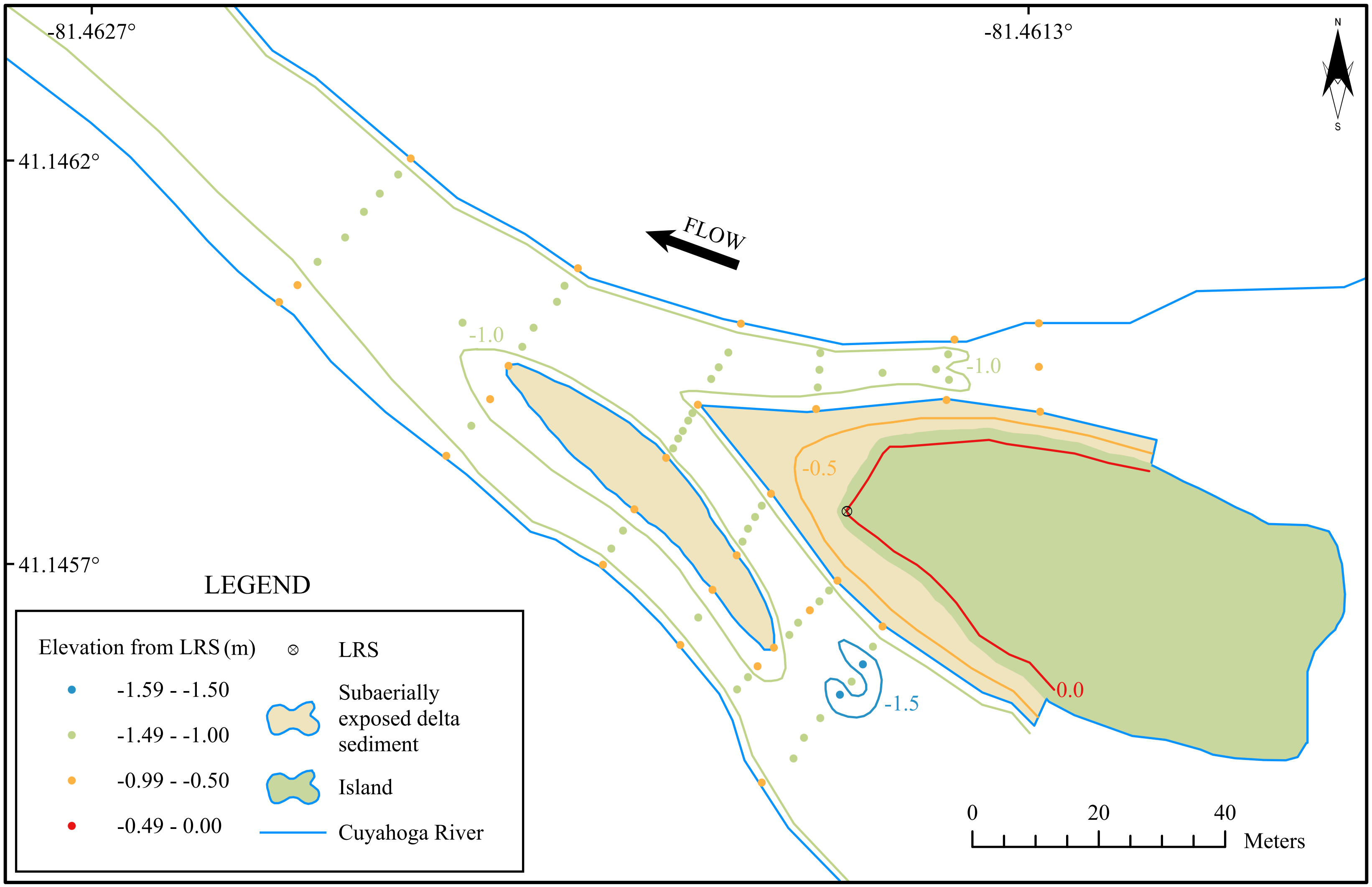

Figure 47. Map view of the geomorphology at the head of the former LeFever Dam pool on 12-17-13. Elevations relative to the local reference stake (LRS) and contoured at a 0.5 m interval. The water surface is -0.78 m from the LRS.

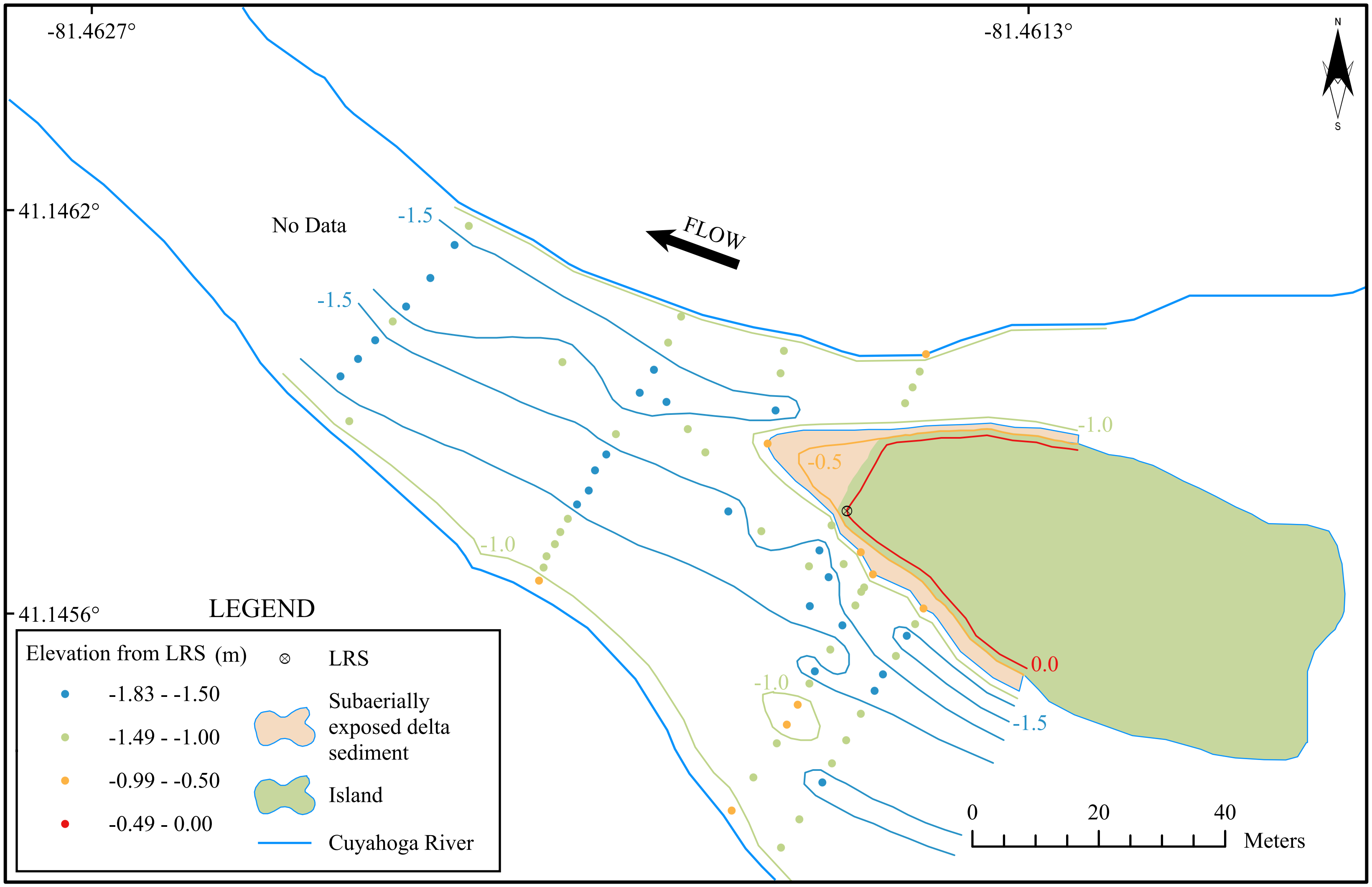

Figure 48. Map view of the geomorphology at the head of the former LeFever Dam pool on 3-23-2014. Elevations relative to the local reference stake (LRS) and contoured at a 0.5 m interval. The water surface is -0.67 m from the LRS.

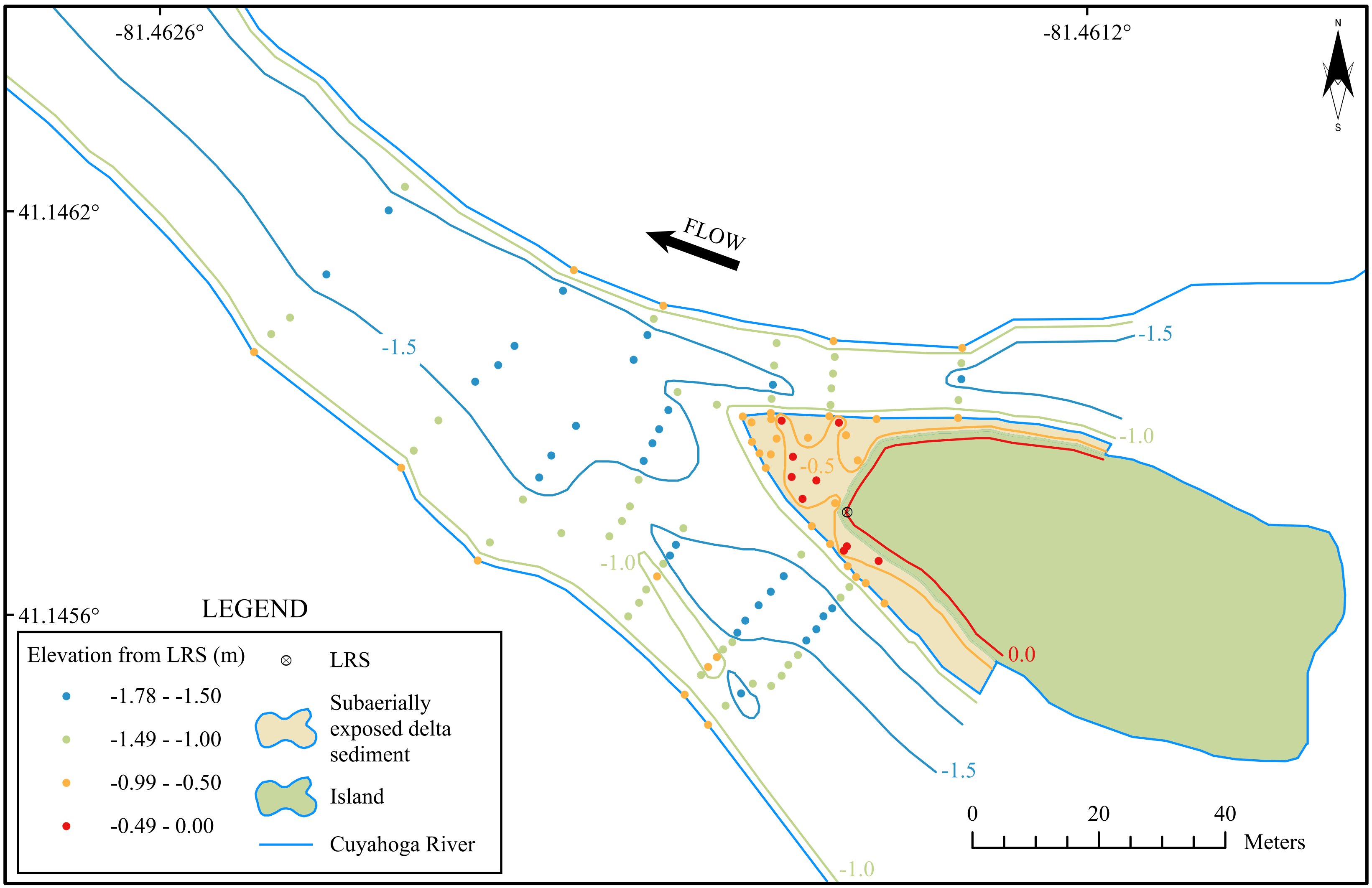

Figure 49. Map view of the geomorphology at the head of the former LeFever Dam pool on 5-23-14. Elevations relative to the local reference stake and contoured at a 0.5 m interval. The water surface is -0.83 m from the LRS.

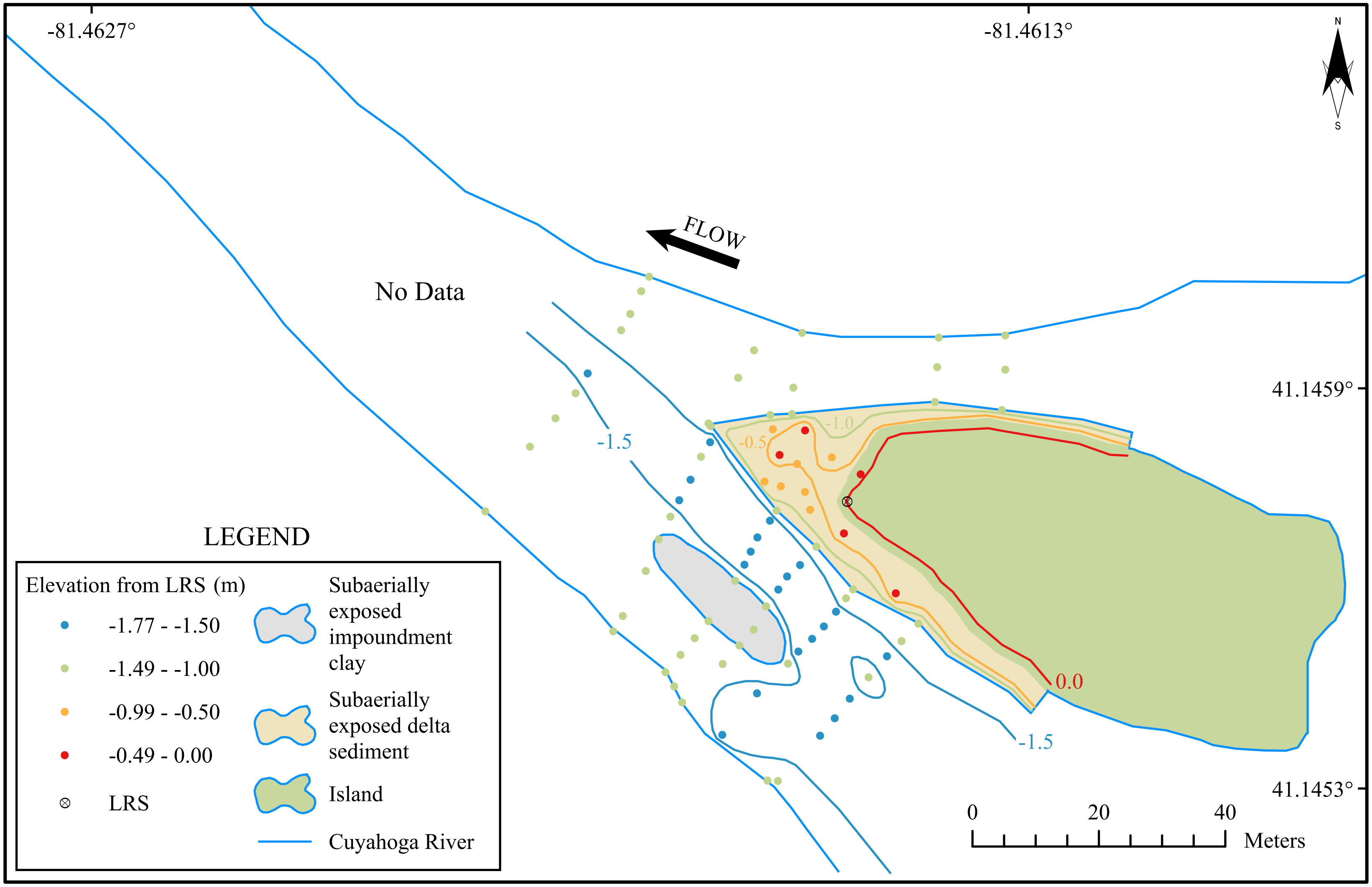

Figure 50. Map view of the geomorphology at the head of the former LeFever Dam pool on 7-25-14. Elevations relative to the local reference stake (LRS) and contoured at a 0.5 m interval. The water surface is -1.2 m from the LRS.

bar has been completely eroded leaving a small island of impoundment clay. The delta sediments continued to be eroded on river left through the December 2014 survey (Figure 51) and by the May 2015 survey only two small remnants of the clay island remained (Figure 52). Bedrock with very thin deposits of sand in gravel in active transport comprised the majority of the channel floor at the downstream end of the delta and near the clay remnants. The former impoundment clay will likely be eroded by the winter of 2015/2016.

3.4 Hydrologic Adjustments

The presence of the LeFever Dam induced major changes in the hydrology of the middle Cuyahoga River during its ~100 year existence. The dam created a wide, deep and low velocity pool that extended 2.67 km upstream to Water Works Park in Cuyahoga Falls. A detailed description of the dam pool characteristics can be found in Kasper (2010). Just as the presence of the LeFever Dam affected the hydrology of the middle Cuyahoga River; the removal of the dam caused significant changes to occur as well.

The August 2013 removal of the LeFever Dam resulted in a marked decrease in the cross sectional area of the channel and an accompanying increase in flow velocity within the former dam pool. Base level lowering resulted in an increase in the slope of the river, which increased the boundary shear stress under the new, free flowing conditions. Transects D-13 (273 m ULFD) and D-6 (843 m ULFD) are located closest to the former dam and best exhibit these hydrologic changes.

3.4.1 Cross Sectional Area and Velocity Changes in Zone 5

Transect D-13 is located closest to the former dam (273 m ULFD) and experienced the greatest change in channel cross sectional area following the LeFever Dam removal

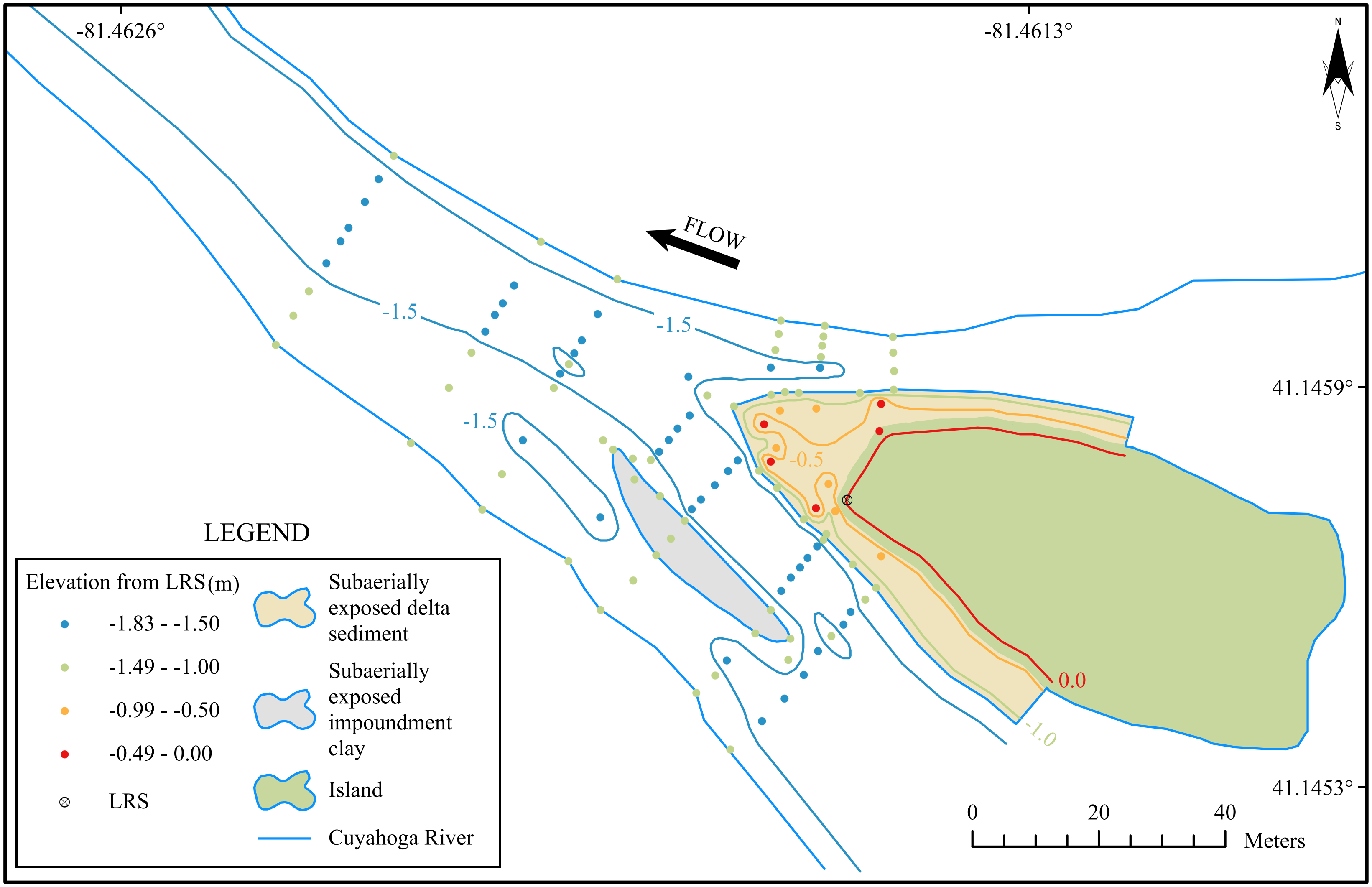

Figure 51. Map view of the geomorphology at the head of the former LeFever Dam pool on 12-15-14. Elevations relative to the local reference stake and contoured at a 0.5 m interval. The water surface is -1.11 m from the LRS.

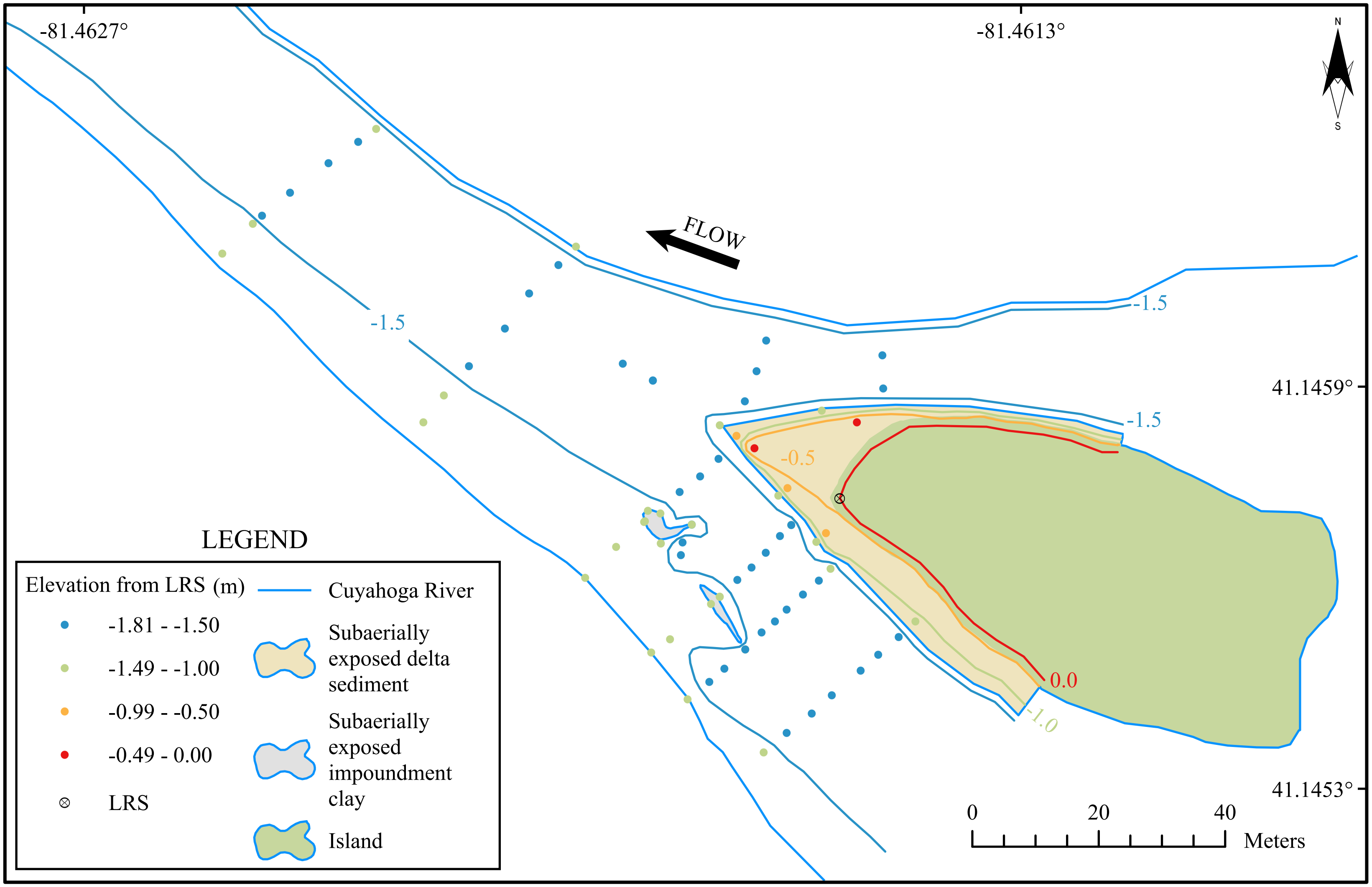

Figure 52. Map view of the geomorphology at the head of the former LeFever Dam pool on 5-3-15. Elevations relative to the local reference stake (LRS) and contoured at a 0.5 m interval. The water surface is -1.22 m from the LRS.

(Figure 53). It is important to note that the channel cross sectional area varies daily depending on the river discharge (Q) so pre and post-removal comparisons were made only on days of similar discharge. Pre-removal on May 14, 2009 the river discharge was 8.98 m^3/s and post-removal on August 11, 2014 the river discharge was 8.04 m^3/s. Therefore it is appropriate to compare these two survey dates. The cross sectional area of the channel on May 14, 2009 was 79.87 m^2 and decreased by 86.6% to 10.7 m^2 on August 11, 2014 following the removal of the dam (Figure 53). Although flow velocity data was not collected at this transect, field observations showed that the post-removal velocity increased from a slack-water impoundment to a stream flowing too fast to be waded across.

Transect D-6 is located further upstream from D-13 at 843 m (ULFD) and underwent similar hydrologic change. Pre-removal on May 17, 2012 the river discharge was 4.96 m^3/s and post-removal on August 11, 2014 the river discharge was 8.04 m^3/s. These discharge rates are comparable. Even though the post-removal cross sectional area was measured on a day when discharge was greater than the pre-removal discharge, the decrease in area was still quite substantial. The pre-removal cross sectional area was 84.3 m^2 and decreased by 84.5% to 13.1 m^2 following the removal of the LeFever Dam (Figure 54). The peak flow velocity also increased considerably. While the dam was in place, the maximum flow velocity through the deep water channel was only 0.06 m/s (Figure 54, Table 10). Post-removal the flow velocity became ~ nine times faster reaching 0.53 m/s in the thalweg (Figure 54, Table 11).

3.4.2 Changes in River Slope in Zone 5

The pre and post-removal slopes of the Cuyahoga River were measured within the former dam pool near transect D-6 (843 m UFLD). The pre-removal slope was calculated using the 7.5 minute Hudson Quadrangle 2 ft. topographic contour map (USGS, 1994).

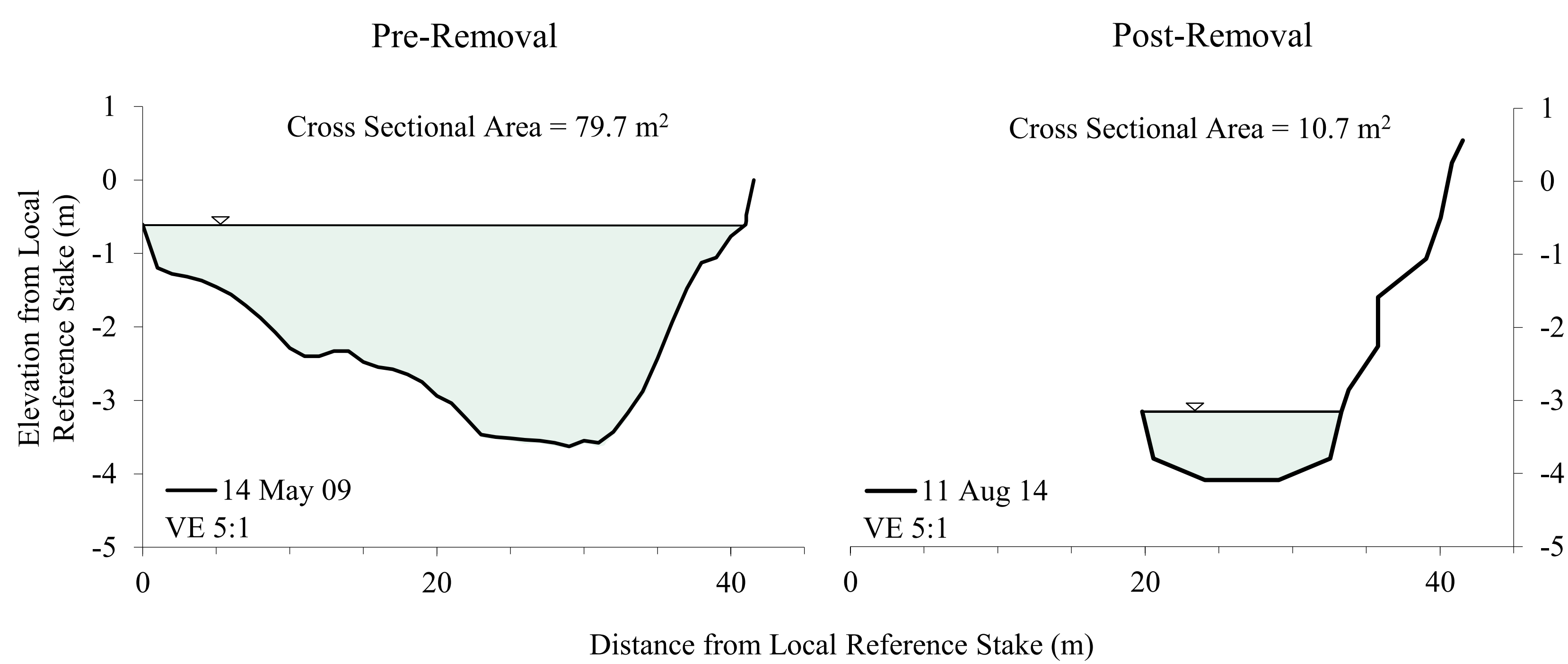

Figure 53. Comparison of the pre (left) and post (right) removal geomorphic profiles and cross-sectional areas at transect D-13 located 273 m upstream of the former LeFever.

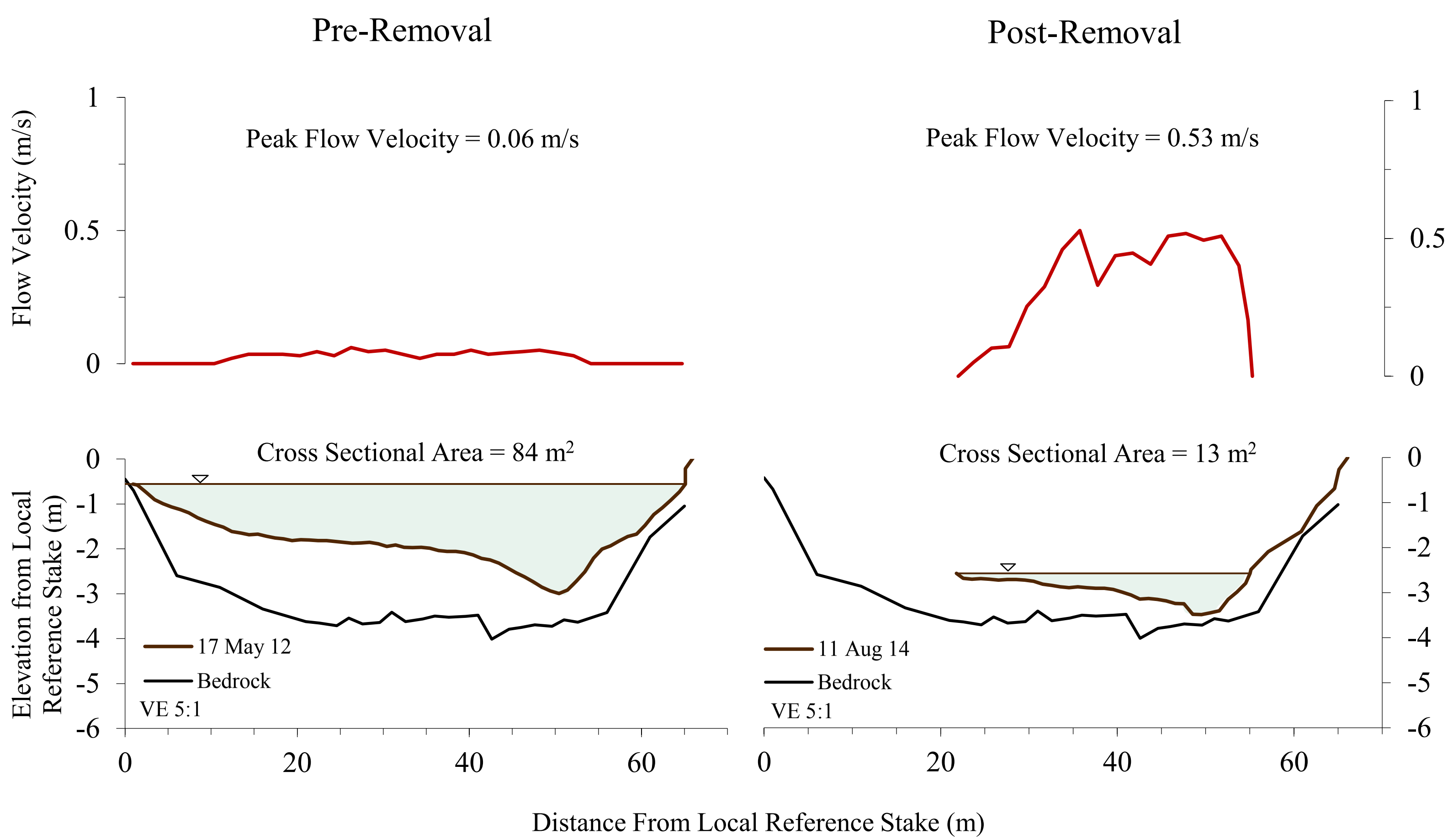

Figure 54. Comparison of pre (left) and post (right) removal velocity (top) and geomorphic (bottom) profiles measured at transect D-6 located 843 m ULFD on 5-17-12 (pre-removal) and 8-11-14 (post-removal).

Table 10. Combined survey and flow data used to calculate Cuyahoga River discharge at transect D-6 on 5-17-12. The number of clicks per minute is multiplied by the constant 0.0050813 to obtain flow velocity (m/s).

Distance (m)	Elevation (m)	Water Depth (m)	# Clicks per minute	0.4 Water Depth (m)	Segment Width (m)	Area (m^2)	Velocity (m/s)	Discharge (m^3/sec)
65.1	-0.55	0.00	0	0.00	-	-	0.00	0.00
62.42	-1.09	0.53	0	0.21	3.68	1.95	0.00	0.00
60.42	-1.48	0.92	0	0.37	2.00	1.84	0.00	0.00
58.42	-1.73	1.17	0	0.47	2.00	2.34	0.00	0.00
54.42	-2.21	1.65	0	0.66	4.00	6.60	0.00	0.00
52.42	-2.73	2.17	6	0.87	2.00	4.34	0.03	0.13
50.42	-3.00	2.44	8	0.98	2.00	4.88	0.04	0.20
48.42	-2.86	2.3	10	0.92	2.00	4.60	0.05	0.23
46.42	-2.63	2.07	9	0.83	2.00	4.14	0.05	0.19
44.42	-2.43	1.87	8	0.75	2.00	3.74	0.04	0.15
42.42	-2.25	1.69	7	0.68	2.00	3.38	0.04	0.12
40.42	-2.14	1.58	10	0.63	2.00	3.16	0.05	0.16
38.42	-2.06	1.5	7	0.60	2.00	3.00	0.04	0.11
36.42	-2.04	1.48	7	0.59	2.00	2.96	0.04	0.11
34.42	-1.97	1.41	4	0.56	2.00	2.82	0.02	0.06
32.42	-1.97	1.41	7	0.56	2.00	2.82	0.04	0.10
30.42	-1.95	1.39	10	0.56	2.00	2.78	0.05	0.14
28.42	-1.86	1.3	9	0.52	2.00	2.60	0.05	0.12
26.42	-1.88	1.32	12	0.53	2.00	2.64	0.06	0.16
24.42	-1.84	1.28	6	0.51	2.00	2.56	0.03	0.08
22.42	-1.82	1.26	9	0.50	2.00	2.52	0.05	0.12
20.42	-1.80	1.24	6	0.50	2.00	2.48	0.03	0.08
18.42	-1.78	1.22	7	0.49	2.00	2.44	0.04	0.09
16.42	-1.72	1.16	7	0.46	2.00	2.32	0.04	0.08
14.42	-1.69	1.13	7	0.45	2.00	2.26	0.04	0.08
12.42	-1.62	1.06	4	0.42	2.00	2.12	0.02	0.04
10.42	-1.46	0.9	0	0.36	2.00	1.80	0.00	0.00
8.42	-1.31	0.75	0	0.30	2.00	1.50	0.00	0.00
6.42	-1.13	0.57	0	0.23	6.50	3.71	0.00	0.00
0.92	-0.56	0.00	0	0.00	-	-	0.00	0.00
					TOTAL	84.29	TOTAL	2.54

Table 11. Combined survey and flow data used to calculate Cuyahoga River discharge at transect D-6 on 8-11-14. The number of clicks per minute is multiplied by the constant 0.0050813 to obtain flow velocity (m/s).

Distance (m)	Elevation (m)	Water Depth (m)	# Clicks per minute	0.4 Water Depth (m)	Segment Width (m)	Area (m^2)	Velocity (m/s)	Discharge (m^3/sec)
55.05	-2.57	0.00	0.0	0.00	-	-	0.00	0.00
54.55	-2.79	0.22	40.0	0.09	1.00	0.22	0.20	0.04
53.55	-2.99	0.42	79.0	0.17	1.00	0.42	0.40	0.17
51.55	-3.40	0.83	100.0	0.33	2.00	1.66	0.51	0.84
49.55	-3.49	0.92	97.0	0.37	2.00	1.84	0.49	0.91
47.55	-3.25	0.68	102.0	0.27	2.00	1.36	0.52	0.70
45.55	-3.18	0.61	100.0	0.24	2.00	1.22	0.51	0.62
43.55	-3.13	0.56	80.0	0.22	2.00	1.12	0.41	0.46
41.55	-3.05	0.48	88.0	0.19	2.00	0.96	0.45	0.43
39.55	-2.93	0.36	86.0	0.14	2.00	0.72	0.44	0.31
37.55	-2.90	0.33	65.0	0.13	2.00	0.66	0.33	0.22
35.55	-2.87	0.3	104.0	0.12	2.00	0.60	0.53	0.32
33.55	-2.87	0.3	90.5	0.12	2.00	0.60	0.46	0.28
31.55	-2.81	0.24	64.0	0.10	2.00	0.48	0.33	0.16
29.55	-2.72	0.15	50.0	0.06	2.00	0.30	0.25	0.08
27.55	-2.71	0.14	21.0	0.06	2.00	0.28	0.11	0.03
25.55	-2.70	0.13	20.0	0.05	2.00	0.26	0.10	0.03
23.55	-2.70	0.13	10.0	0.05	2.75	0.36	0.05	0.02
21.80	-2.57	0.00	0.0	0.00	-	-	0.00	0.00
					TOTAL	13.06	TOTAL	5.61

The post-removal slope was surveyed on August 11, 2014. The removal of 4.1 m high LeFever Dam resulted in a base level lowering comparable to the height of the dam and was responsible for the increase in river slope. The slope more than doubled as it increased from 0.00029 m/m to 0.00066 m/m.

CHAPTER IV

DISCUSSION

4.1 Changing Energy of the Cuyahoga River

After the LeFever Dam was removed in 2013, the channel width and depth upstream of the former dam decreased, whereas the river slope increased due to base level lowering. These physical changes yielded an increase in erosive energy that resulted in the post-removal erosion of the impoundment sediment. Pre and post-removal stream power and boundary shear stress were calculated to quantify the erosive capabilities in the upper and lower portions of the dam pool. The most significant physical changes occurred immediately upstream of the former dam whereas physical changes were less extensive further upstream (Table 12). The following describes (downstream to upstream) how the energy of the Cuyahoga River has changed following the LeFever Dam removal.

The increased erosive energy can be expressed in terms of boundary shear stress (τ_o) which is calculated using the DuBoys equation

$$\tau_o = \lambda g R_h S \qquad \text{Eq. (2)}$$

where; λ is the fluid density, g is the acceleration due to gravity, Rh is the hydraulic radius (cross-sectional area/wetted perimeter) and S is the river slope (Boggs, 2011). The fluid density of the river water did not change following dam removal so it did

Table 12. Measured and calculated parameters used to calculate the pre and post-LeFever Dam (LFD) removal boundary shear stress (τ_o) and stream power (Ω) at transects D-13, D-6 and D-12. These variables are channel width (w), water depth (d) river discharge (Q), river slope (S), flow velocity (V), cross-sectional area (A) and hydraulic radius (R_h). Average values were used for the measured depth and velocity. Q_{OP} is the discharge at Old Portage stream gauging station (waterdata.usgs.gov) and Q_{OP}^* was normalized by the ratio of the Q at Old Portage and the measured Q at D-6 on 11 Aug 14. Q_{OP}^* is used in the calculated velocity relationship.

Variables and energy parameters		Transect D-13			Transect D-6			Transect D-12		
		Pre LFD 14 May 09	Post LFD 11 Aug 14	% Change	Pre LFD 17 May 12	Post LFD 11 Aug 14	% Change	Pre LFD 14 May 12	Post LFD 19 Aug 14	% Change
Measured variables	w (m)	41.55	13.7	-67	64.18	33.25	-48	21.7	19.75	-9
	d (m)	1.93	0.93	-52	1.28	0.4	-69	0.63	0.47	-24
	Q (m^3/s)	-	-	-	2.54	5.61	121	-	-	-
	Q_{OP}	8.98	8.05	-10	4.96	8.05	62	8.39	7.11	-15
	Q_{OP}*	6.26	5.61	-10	-	-	-	5.85	4.95	-15
	S (m/m)	0.00029	0.0072	2383	0.00029	0.00066	128	0.00029	0.00029	0
	V (m/s)	-	-		0.03	0.32	1081	-	-	-
Calculated variables	A (m^2)	79.7	10.7	-87	84.29	13.06	-85	14.24	13.66	-4
	R_h (m)	1.76	0.69	-61	1.26	0.38	-70	0.62	0.66	6
Calculated velocity relationship	V = Q/A	0.08	0.52	568	0.03	0.43	1325	0.41	0.36	-12
Boundary Shear Stress	τ_o (N/m)	4.99	48.57	873	3.59	2.48	-31	1.76	1.88	6
Stream Power per unit width	Ω (W/m^2)	1.08	28.50	2541	0.14	0.42	195	0.71	0.76	8

not change τ_o. The slope on the other hand, increased from 0.00029 m/m to 0.00066-0.0072 m/m (BBCM, 2008) in Zone 5 and remained unchanged (0.00029) m/m in Zone 4 (Peck personal measurement at Water Works Park, Sept. 2015). At transect D-13 (273 m ULFD) the cross-sectional area decreased by 87% and the calculated average velocity increased from 0.08 to 0.52 m/s (Table 12). Both of these changes yielded an increase in τ_o from 4.99 to 48.57 N/m. Similarly, at transect D-6 (843 m ULFD) the cross-sectional area decreased by 85% and the measured average velocity increased from 0.03 to 0.32 m/s. τ_o actually decreased from 3.59 to 2.48 N/m post-removal because the pre-removal hydraulic radius (Rh) was more than three times greater than the post-removal hydraulic radius. (Table 12). Within the former dam pool, the channel at transects D-13 and D-6 experienced similar decreases in cross-sectional area which was the dominant factor for increasing τ_o.

Just upstream of the former dam pool (Zone 4) at transect D-12 (2,795 m ULFD), the cross-sectional area decreased by only 4% but the calculated velocity decreased by 10% (Table 12) (Figure 55). However, the mean daily discharge was less on the day the post-removal survey was conducted compared to the pre-removal survey so the calculated velocity will also be less post-removal. The river slope did not increase either, meaning the dominant mechanism for sediment erosion was the decrease in cross sectional area (Figure 55). Sediment no longer accumulates at the LeFever impoundment delta so Zone 4 sediments can be freely transported downstream as well.

While boundary shear stress is sufficient for quantifying the erosive energy of the Cuyahoga River, stream power (Ω) expresses how the river does work on the bed per unit area across the channel. Because the channel has become substantially narrower and shallower within the former dam pool, the increased erosive energy is now concentrated within the channel. Stream power was calculated at the same three transects above using the equation;

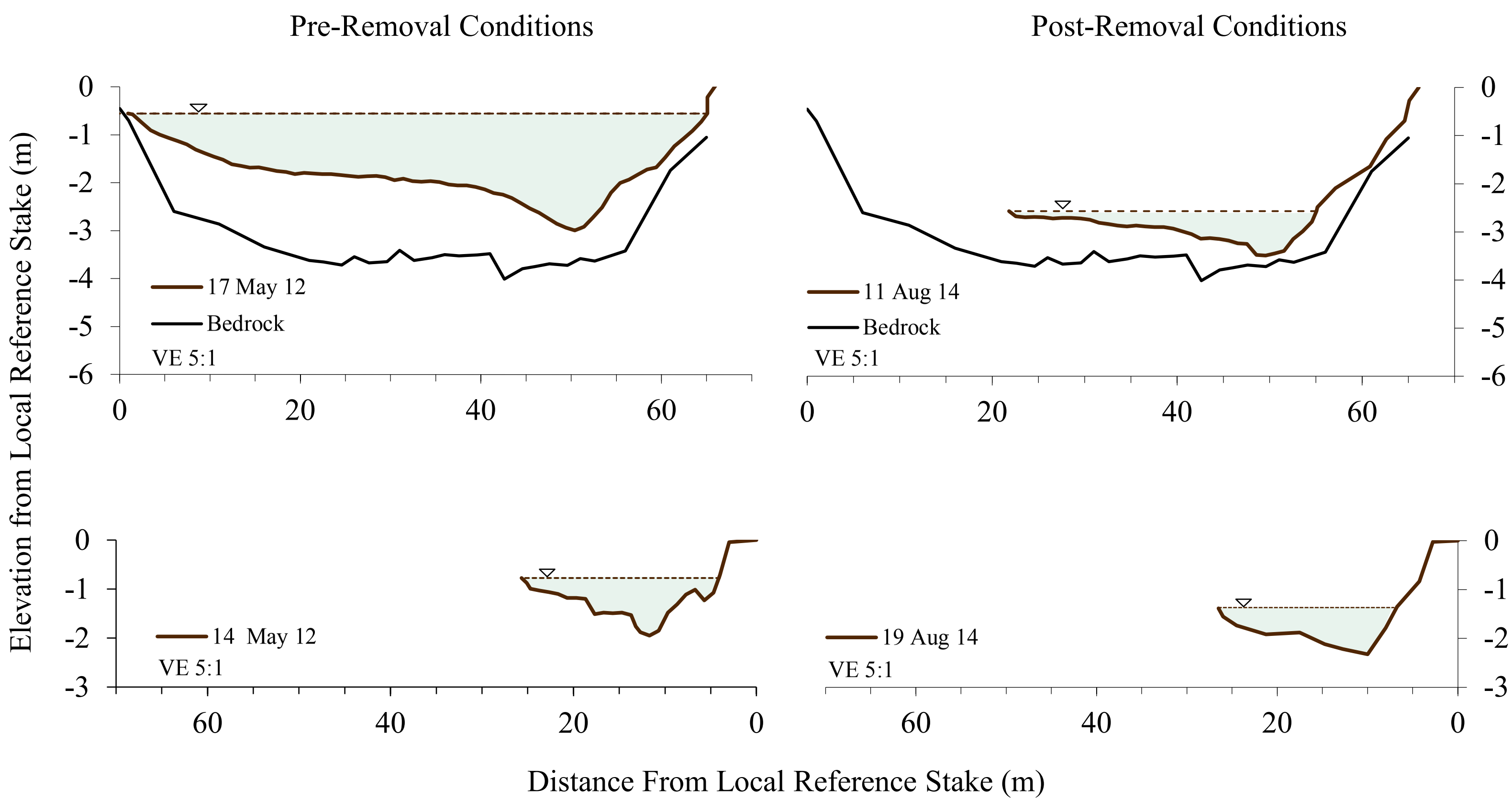

Figure 55. Comparison between the pre (left) and post-removal (right) cross-sectional areas within the former LeFever Dam pool and farther upstream. Transect D-6 (843 m ULFD) is located within the former dam pool and (top) transect D-12 (2,795 m ULFD) is located farther upstream near Water Works Park (bottom). The cross-sectional area at transect D-6 decreased by 85% post-removal and transect D-12 decreased by 4%.

$$\Omega = \rho g R_h S Q \qquad \text{Eq. (3)}$$

where; ρ is the fluid density, g is the acceleration due to gravity, R_h is the hydraulic radius (cross-sectional area/wetted perimeter), S is the river slope, Q is the river discharge and w is the channel width (Boggs, 2011). Stream power increased substantially within the former dam pool at transects D-13 and D-6 (Table 12). The channel at D-13 experienced the greatest increase in Ω from 1.08 to 28.50 W/m^2 and is evident in the narrow, high velocity channel floored by bedrock (Table 12). Stream power at transect D-6 increased comparably from 0.14 to 0.42 W/m^2 post-removal. Upstream of the former dam pool at D-12, Ω slightly increased from 0.71 to 0.76 W/m^2.

The changes in fluvial energy and resulting impact on sedimentary processes can be described by the Hjulström Diagram. This diagram shows the relationship between flow velocity and the erosion, transport and deposition of sediment of varying grain size (Press and Siever, 1986). Although the Hjulström Diagram is limited to a channel with one meter flow depth and a bed composed of quartz spheres of uniform size, it can be used to predict the behavior of sediments under certain flow conditions (Boggs, 2011). At transect D-6 the post-removal bed was composed of 85% quartz and 15% lithic fragments with trace amounts of anthropogenic slag and cinders. The mean grain size was -1.26 ϕ and on August 11, 2014 the maximum flow velocity was 53 cm/s. These conditions plotted on the Hjulström Diagram at the boundary of erosion and transport of granules (Figure 56). The flow velocity of river in the former dam pool is great enough to erode and transport consolidated mud to granules and transport pebbles as bedload. Pre-removal the river was only capable of transporting unconsolidated mud up to coarse sand as bedload (Figure 56).

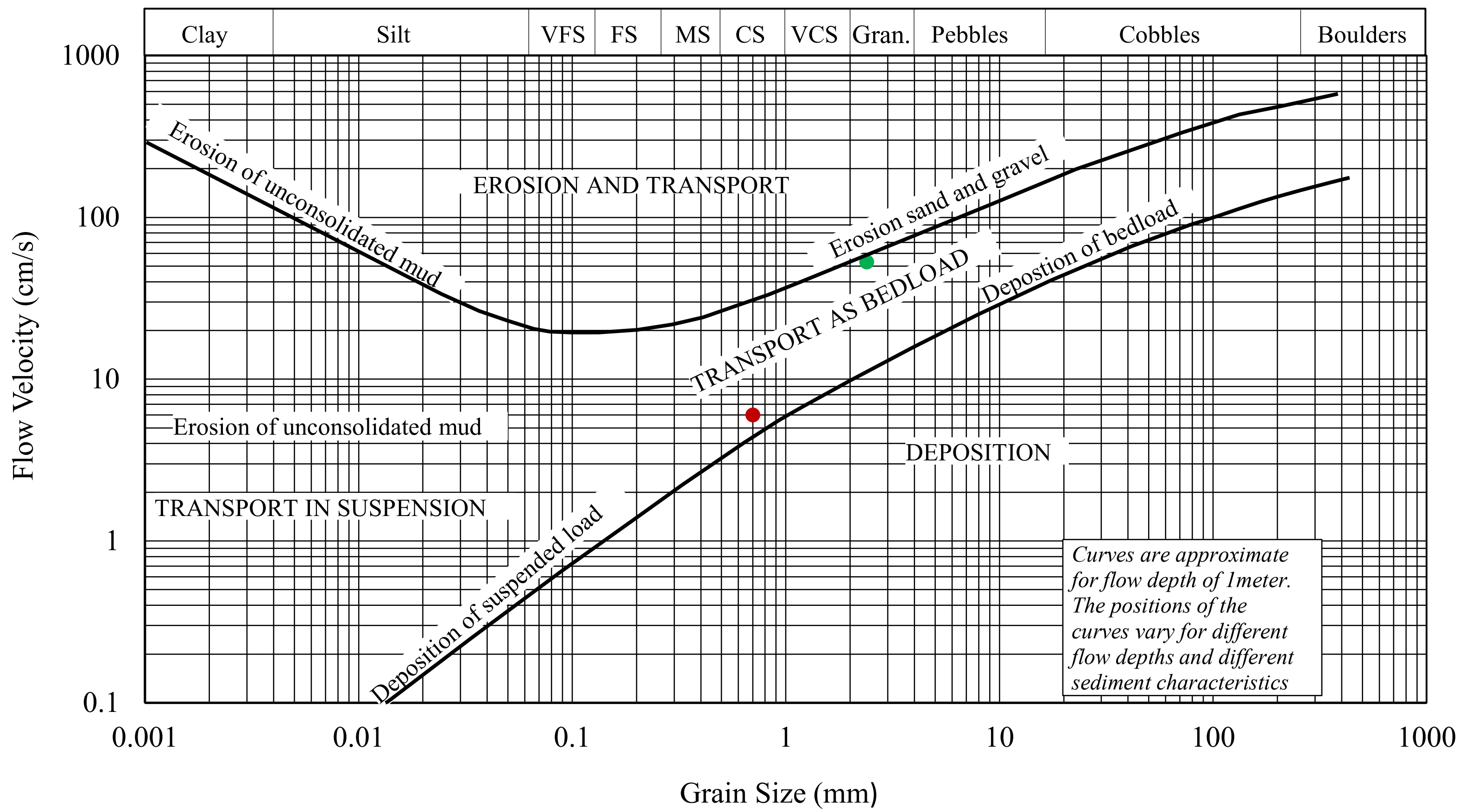

Figure 56. Hjulström diagram showing the relationship between flow velocity and the behavior of different sized sediments in a stream under 1 meter flow depth (modified from Press and Siever, 1986). The pre (red dot) and post-LeFever flow (green dot) velocities were measured on 5-17-2012 and 8-11-2014 at transect D-6 (843 m ULFD). The mean grain size for all of Zone 5 in those years was used for the grain sizes plotted above.

4.2 Geomorphic and Sediment Response to Dam Removal

Channel evolution models describe how a fluvial system progressively returns to equilibrium following dam removal. Channel evolution models are also beneficial for predicting how the channel will respond after a dam is removed as well as the rate at which channel adjustments progress through time (Doyle et al., 2002). Doyle et al. (2003) developed a channel evolution model based on the study of two low-head dam removals in Wisconsin (Figure 4). This model describes the geomorphic change in six sequential stages (A to F) resulting from a lowered base level, instantaneous increase in slope and decrease in water cross sectional area. The model incorporates grain size and cohesion of the impoundment sediment because these factors can control the rate and magnitude of channel adjustments (Doyle et al., 2005).

The 2013 removal of the LeFever Dam has brought about significant increases in fluvial energy that eroded and coarsened the channel sediments upstream of the former dam. The LeFever Dam removal impacted the channel in Zones 4 and 5 only, while Zones 1-3 continued long-term adjustments following the 2005 Munroe Falls Dam removal. The following sections discuss the long-term geomorphic and sedimentologic response in Zones 1-3 to the Munroe Falls Dam removal followed by an in-depth discussion of the response in Zones 4 and 5 to the LeFever Dam removal.

4.2.1 Long-Term Changes in the former Munroe Falls Dam Pool

Previous studies have been conducted upstream of the former Munroe Falls Dam (Zones 1, 2, 3) but the present thesis research incorporates new findings from the years 2011 through 2015. Rumschlag (2007) and Rumschlag and Peck (2007) concluded that the channel evolution model of Doyle et al. (2003) generally described the short-term morphologic change of the middle Cuyahoga River in response to the removal of the

Munroe Falls Dam. Stage A impoundment spanned the 113 year existence of the Munroe Falls Dam, trapping sediment upstream and eliminating the sediment supply downstream. Pre-removal in 2003-04 the sediment stored behind the dam (Zone 3) contained 71% sand and 20% organic rich mud (Table 8). Post-removal the channel upstream of the former dam (Zone 3) progressed from Stage A to Stage C (incision to the pre-dam substrate) in less than two months. Once the river eroded to the pre-dam substrate, Stage D degradation and widening commenced and persisted for ~ 2 years (Rumschlag, 2007; Rumschlag and Peck 2007). By March 2007, Zone 4 transitioned from Stage D to Stage E aggradation and widening as the former Munroe Falls impoundment sediment was transported downstream (Rumschlag, 2007; Rumschlag and Peck, 2007). As a result the gravel content decreased from 81% to 23% by 2008-09 as fine, well sorted sand occupied the channel (Table 8). Due to the prolonged erosion of the sandy impoundment upstream, the mean grain size and gravel content in Zone 4 increased to -1.78 ϕ and 55% by 2008-09 (Figure 57).

Five years after the removal of the Munroe Falls Dam the Cuyahoga River was still laterally eroding and Stage F quasi-equilibrium had not yet been reached (Kasper, 2010; Peck and Kasper, 2013). The upstream reach (Zones 1-3) hardly aggraded with sand, rather the channel floor became a gravel lag deposit composed of 73% – 85% gravel having a mean grain size -1.92 to -2.86 ϕ (Kasper, 2010) (Table 9) (Figure 57). It took ~ 2 years after the Munroe Falls Dam was removed for the mean grain size to increase from sand to gravel whereas former LeFever Dam pool coarsened to gravel within one year post-removal (Figure 57). The channel downstream of the former Munroe Falls Dam experienced significant aggradation resulting from the upstream erosion and transport of the Munroe Falls impoundment sediment to the LeFever Dam pool (Zones 4,5). By 2012 the channel sediment contained 71% – 83 % sand in Zones 4 and 5 (Table 9)

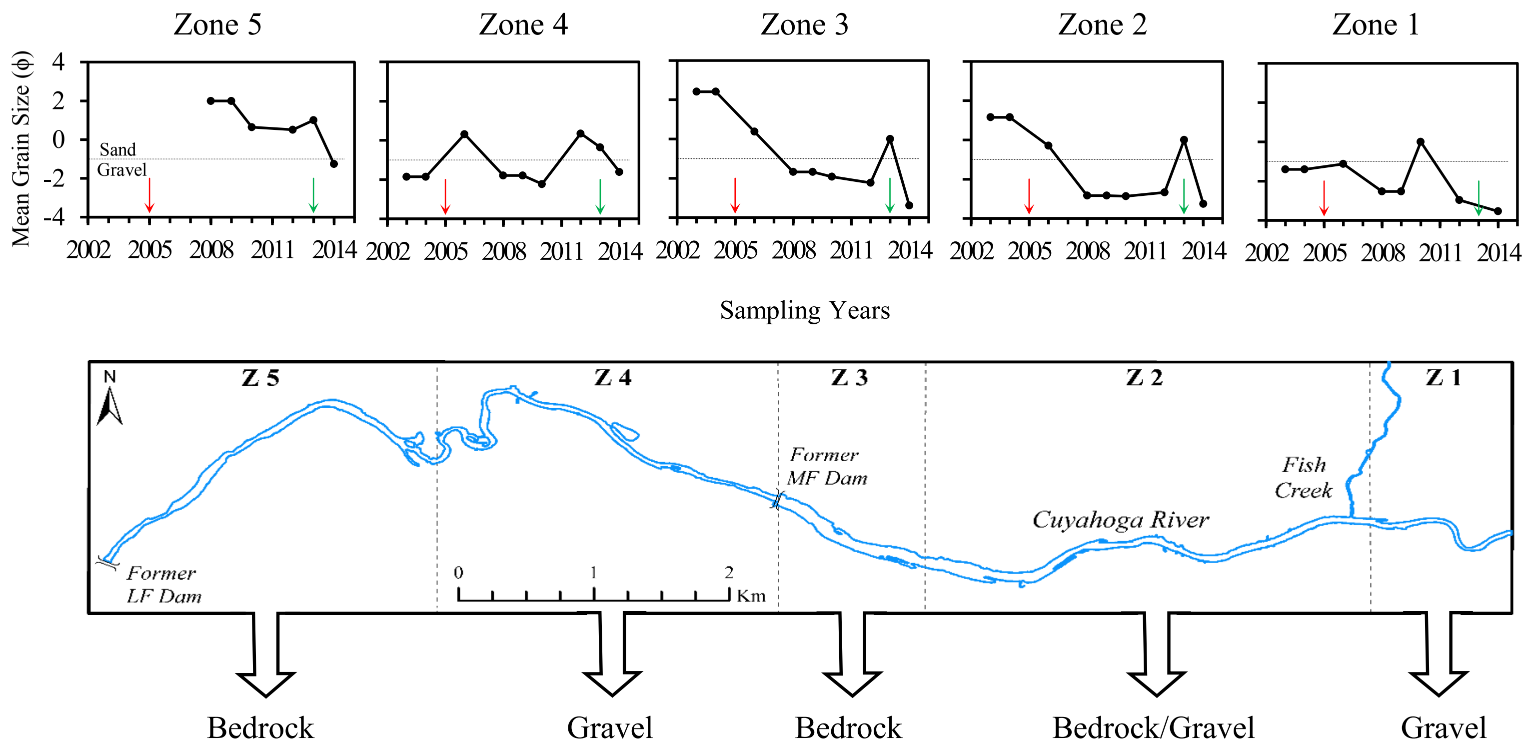

Figure 57. Mean grain size (ϕ) per sampling year of all five zones in the study reach (top). The red arrow indicates the 2005 removal of the Munroe Falls Dam and the green arrow indicates the 2013 removal of the LeFever Dam. The dashed horizontal line represents the grain size boundary between sand and gravel. (Center) Map view of the Cuyahoga River showing the locations of the former LeFever (LF) and Munroe Falls Dam as well as the Zone boundaries (Z 1 – Z 5). The grain size listed on the bottom of the figure indicates the future channel substrate once the river reaches a state of near-equilibrium.

The new findings from 2011 through 2015 have furthered the understanding of the long-term channel adjustments following the Munroe Falls Dam removal. Channel widening has been the prevailing form of geomorphic change while downcutting occurred in minor amounts because the post-removal channel is coarse grained and flows on resistant bedrock (Figure 57). Channel widening has occurred as episodic slump block erosion of the remnant Munroe Falls impoundment mud that composes the vegetated channel margins in Zones 1-3. The channel sediment has also coarsened significantly in the long-term and was composed of ~ 80% gravel and 20% sand with trace amounts of organic rich mud in 2014. Factors unrelated to the Munroe Falls Dam removal have also affected these geomorphic and sedimentologic changes in Zones 1-3 and are discussed in sections 4.3 and 4.4.

4.2.2 Geomorphic and Sediment Changes in the former LeFever Dam Pool (Zone 5)

The LeFever Dam was in place from 1914 to 2013 and represents the Stage A pre-removal impoundment. The channel sediment was composed of 71% sand and 17% organic rich mud in Zone 5 due to ~100 years of sediment storage (Table 9). Stage B dewatering commenced as soon the dam removal process began on August 12, 2013 and ended by the completion of dam removal on August 19, 2013. Stage C incision then began when a headcut/knickpoint formed and migrated upstream by headward erosion. Kasper (2010) predicted that downcutting to the underlying bedrock would occur within days to weeks following the removal of the LeFever Dam. About four months post-removal on the December 17, 2013 survey the location of a 0.64 m tall headcut was discovered 1,000 m (ULFD) on river right (Figure 58). Upstream of the former LeFever Dam to the State Rt. 8 bridge (0-450 m ULFD), the thalweg had a thin deposit (<0.5 m) (Kasper, 2010), so the rate of headcut migration was calculated using the State Rt. 8 bridge as the starting point. The headcut propagated upstream at a rate of 117 m/mo,

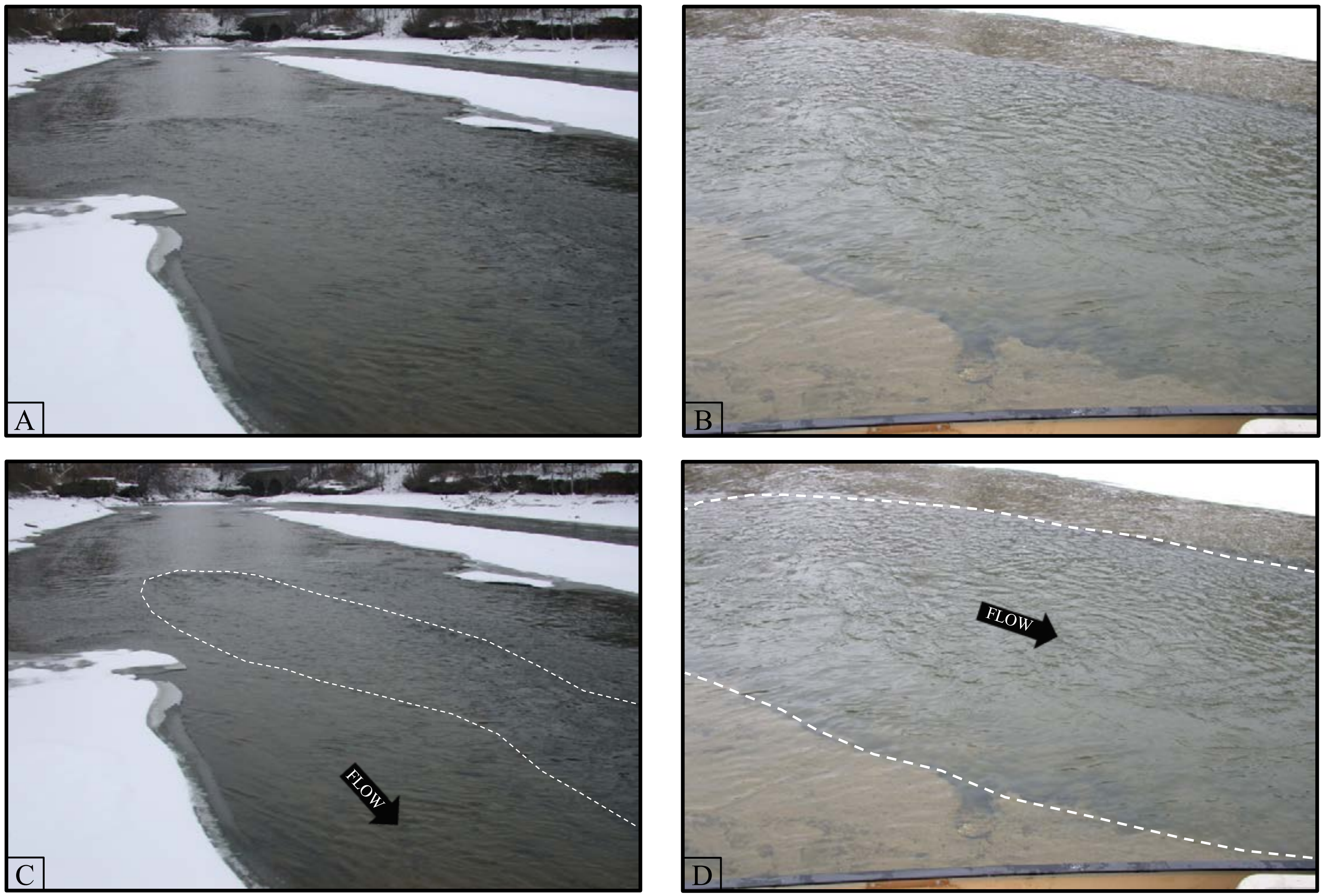

Figure 58. Photographs of the former LeFever Dam pool viewed looking upstream ~ 4 mo. post removal. Photos A and B show the location of the headcut within the former dam pool (1,000 m ULFD) on December 17, 2013. Photos C and D show the same as A and B but with the 0.64 m tall headcut is outlined with a white dashed line.

eroding the impoundment sediment and exposing the underlying bedrock (Stage C). Downstream of the headcut on the December 17, 2013 survey at transect D-6 (843 m ULFD) bedrock was exposed on the channel floor (Figure 59). Stage C was met two months sooner in the former LeFever Dam pool than at a comparable location (U-3) in the former Munroe Falls Dam pool. The headcut could not be found on any subsequent survey most likely because it had completely migrated upstream through the impounded sediment and reached the location of the Doodlebug railroad bridge. With a headcut migration rate of 117 m/mo Stage C incision was completed through the wide dam pool section (0-1,146 m ULFD) by mid-February 2014.

The reach closest to the former LeFever Dam completed Stage C incision within days to weeks post removal based upon visual observations. It took 1-5 months longer to reach stage C at a similar location in the former Munroe Falls Dam pool (U-7). Subaerially exposed impoundment muds comprise the new channel margins. The exposed impoundment muds were slowly dewatered and underwent mass wasting by rotational slumping. Mass wasting of these muddy channel margins marks the onset of Stage D degradation and widening which was first observed 9 days post-removal (Figure 60). It is very unlikely that significant deposition will occur throughout Zone 5 in the future because a high velocity, bedrock channel with a steep slope was formed post-removal. The channel may widen during episodic slump block erosion of the muddy bank material during high discharge events (Stage E widening). Stage E aggradation is not likely to occur along this reach because the high energy channel acts a zone of transport.

Although Stage E aggradation has not occurred downstream of the St. Rt. 8 bridge, the middle and upper dam pool did undergo extensive aggradation as upstream sediment was eroded following the LeFever Dam removal. The sand content in Zone 5 increased by 18% while and sand content in Zone 4 decreased by 18% within one month post-removal. On December 19, 2013, (~4 months post removal) a sand wave

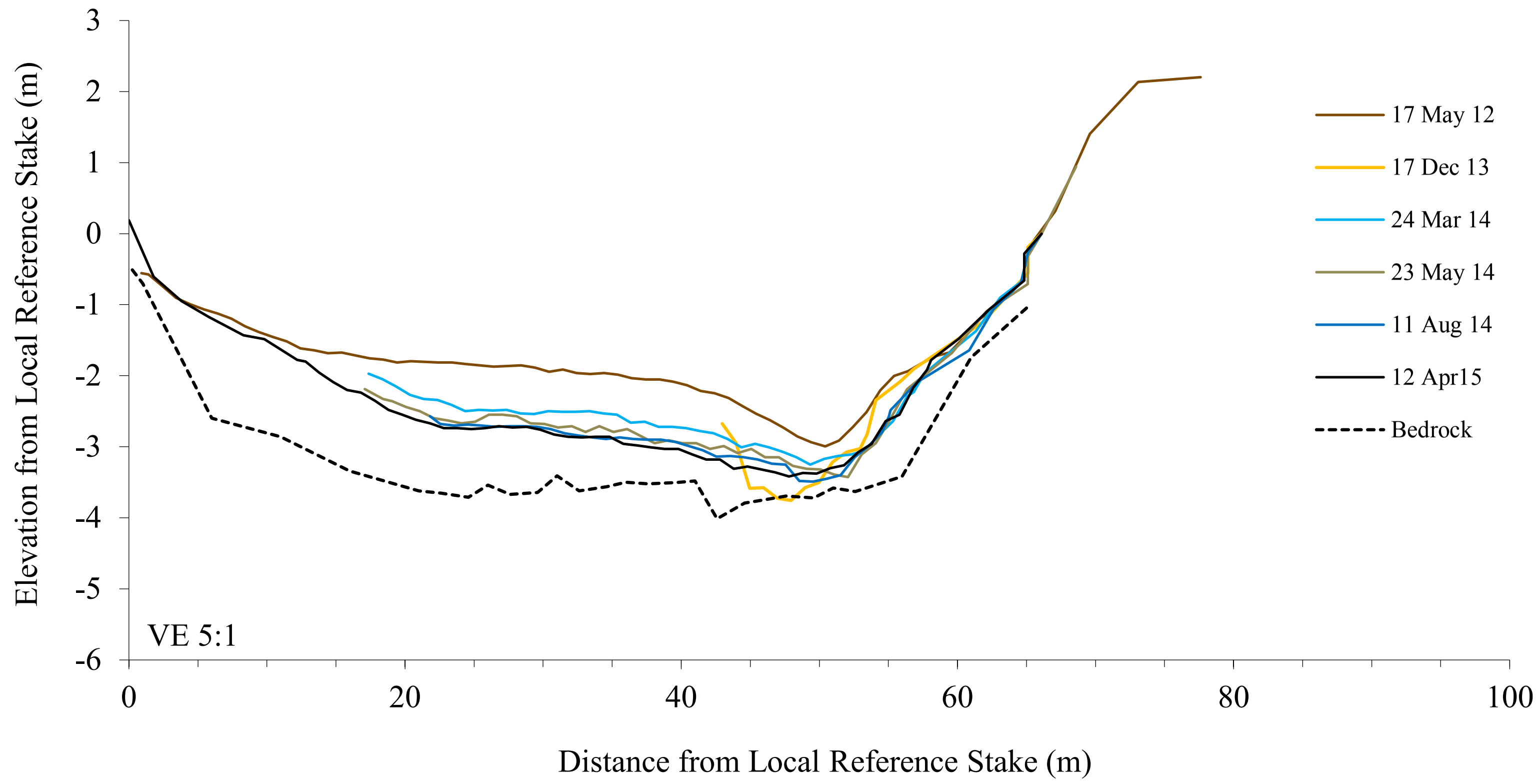

Figure 59. Geomorphic profile of transect D-6 located 843 m upstream of the former LeFever Dam, surveyed from May 2012 to April 2015.

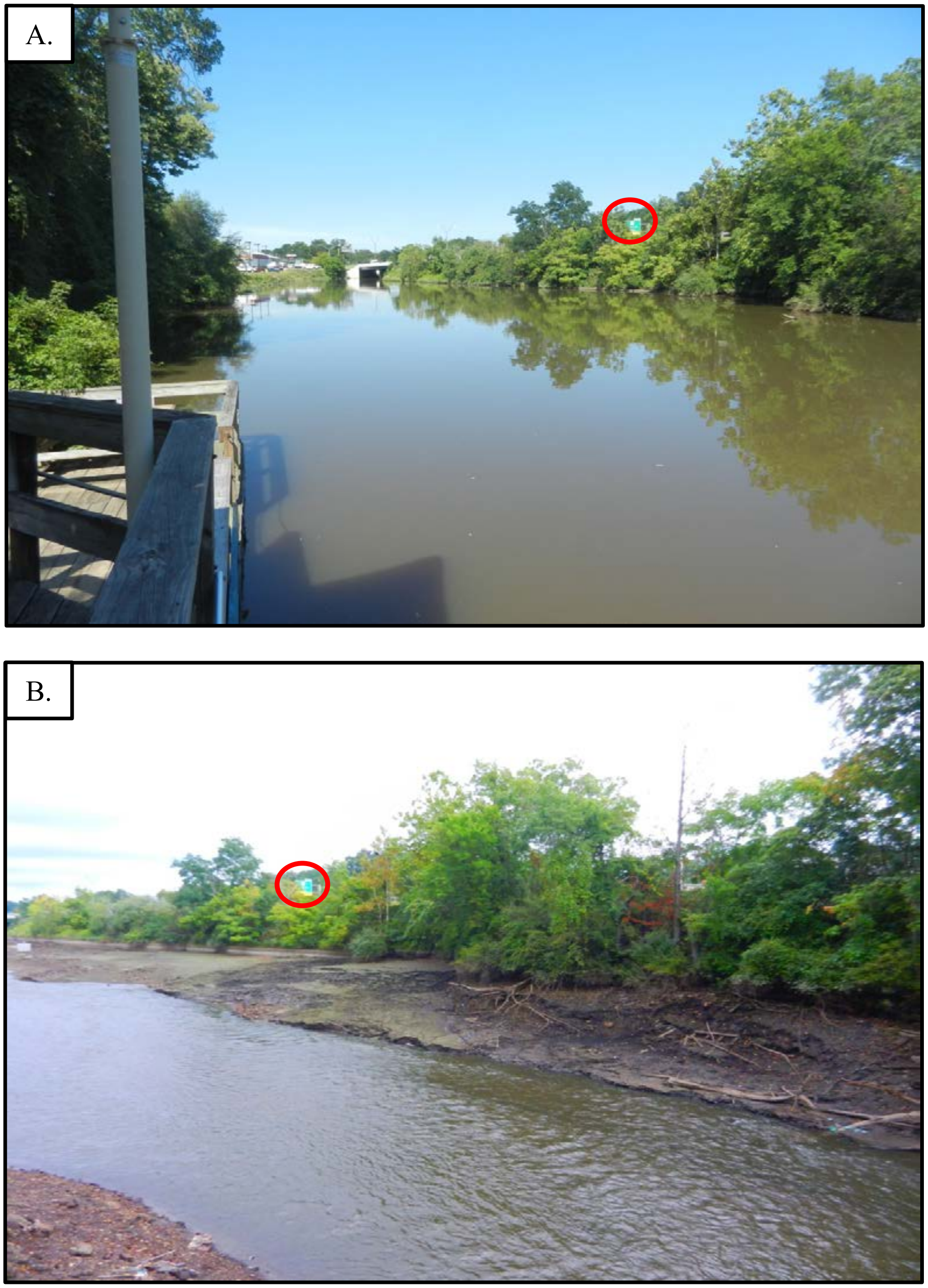

Figure 60. Photographs of the Cuyahoga River near transect D-13 (273 m ULFD). Photo A shows the river pre-LeFever removal on 8-9-13. Photo B was taken 9 days post-removal on 8-28-13 and shows extensive rotational slumping of the subaerially exposed impoundment mud on the channel margins. The red circle marks a stationary highway sign for reference and flow is from left to right.

with superimposed 2.5-D ripples was located just downstream of the Doodlebug railroad bridge (1,146 m ULFD) (Figure 61). This migrating sand wave represents the initial pulse of sediment being remobilized from the upstream portion of the LeFever Dam pool due to increased stream power exerted by the free flowing Cuyahoga River. The sand wave characterizes the aggradation element of Stage D of channel evolution. Doyle et al. (2002) discussed the transport of impounded sediment as a distinct unit which translates downstream as a sediment wave versus sediment dispersal. The sediment moves downstream as a sediment wave if it is finer than the sediment of the preexisting substrate (bedrock in Zone 5) and the thickness of the deposit is less than the depth of the channel (Doyle et al., 2003). It was likely that the sand wave accumulated here because there was a deep water hole immediately downstream of the Doodlebug railroad bridge. This deep water hole was a favorite location for people to jump from the bridge into the former dam pool without injuring themselves. The increased cross-sectional area of the deep water hole would produce the lower velocity conditions needed for sand deposition. This distinct wave morphology was not observed at any other time throughout the study but it affected the channel morphology at transect D-6 as it was transported downstream.

By the March 24, 2014 survey, the channel at 45-50 m on the D-6 profile (843 m ULFD) had aggraded ~0.60 m with sand transported from upstream (Figure 59). The scarp present in the December 2013 survey was buried by this deposition. The wide mud deposit between 17-45 m on the profile was 1.6 m thick on average and vertically eroded and compacted a total of 0.68 m by the March 2014 survey. This geomorphic change represents the transition from Stage D degradation and widening to Stage E aggradation and widening. The progression from Stage C to E was not recorded on specific survey dates but must have occurred sometime between the December 2013 and March 2014 surveys. Part of the 0.68 m vertical lowering of the left bank could be due to the compaction of the mud by sand and gravel deposition as the sediment wave

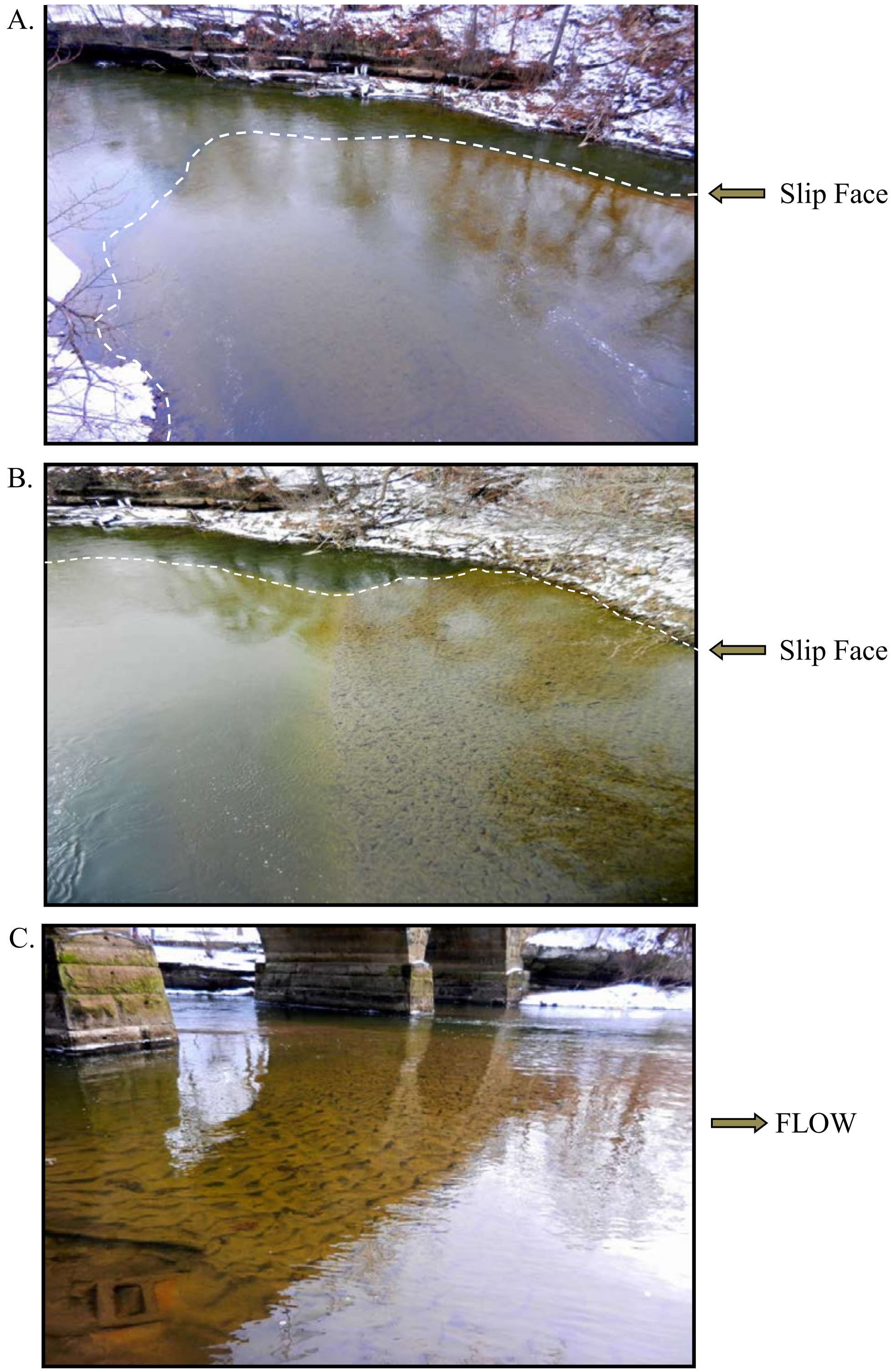

Figure 61. Photos of a migrating sand wave just downstream of the Doodlebug Railroad Bridge (1,146 m ULFD) first observed ~ 4 mo. post-LeFever removal on 12-19-13. A. is looking downstream from the bridge. B. shows the right side of the sand wave. C. is looking upstream and displays 2.5-D ripples in active transport. The white dashed lines mark the slip face of the sand wave.

moved through this location. Sand and gravel are denser than mud which leads to mud compaction. In addition, the loss of pore water in the muds when the left bank is exposed during low flow would further aid in compaction. The magnitude of bank subsidence due to the dewatering of the LeFever Dam pool is comparable to that in the Munroe Falls Dam pool (Zone 3). The 1.9 m thick mud deposit at transect U-2 compacted 0.61 m and at transect U-3, the 1.96 m thick mud deposit compacted 0.59. Channel widening in the former LeFever Dam pool did not occur by mass wasting as the channel evolution model of Doyle et al. (2003) describes. Instead the muddy impoundment sediment of the left bank was eroded vertically downward. This different style of erosion can be attributed to the following site specific conditions.

The muddy channel margins from 450-1,146 m ULFD did not reach their critical bank height (the height at which the over steepened bank collapses) when the LeFever Dam pool was dewatered. One small area on river left just downstream of the Doodlebug railroad bridge did reach its critical bank height and the channel widened by vertical slump block erosion. The exposed impoundment fill along the channel margins gently slope toward the new river channel and did not become stabilized by the growth of riparian vegetation except for the banks farthest inland. These margins are often inundated during moderate to high flows further preventing the growth of new vegetation (Figure 62). The St. Rt. 8 bridge abutments may also cause a ponding effect as the water is backed up behind them. Groundwater discharges at the base of the sandstone cliffs in many locations within the former dam pool which also prevents bank stabilization by plant growth.

Further upstream in Zone 5 is transect D-15 (2,216 m ULFD) and the LeFever impoundment delta (2,415 m ULFD), both of which exhibit morphologic changes consistent with the channel evolution model of Doyle et. al. (2003). Transect D-15 was first surveyed one month after the LeFever Dam was removed on September 7, 2013 and

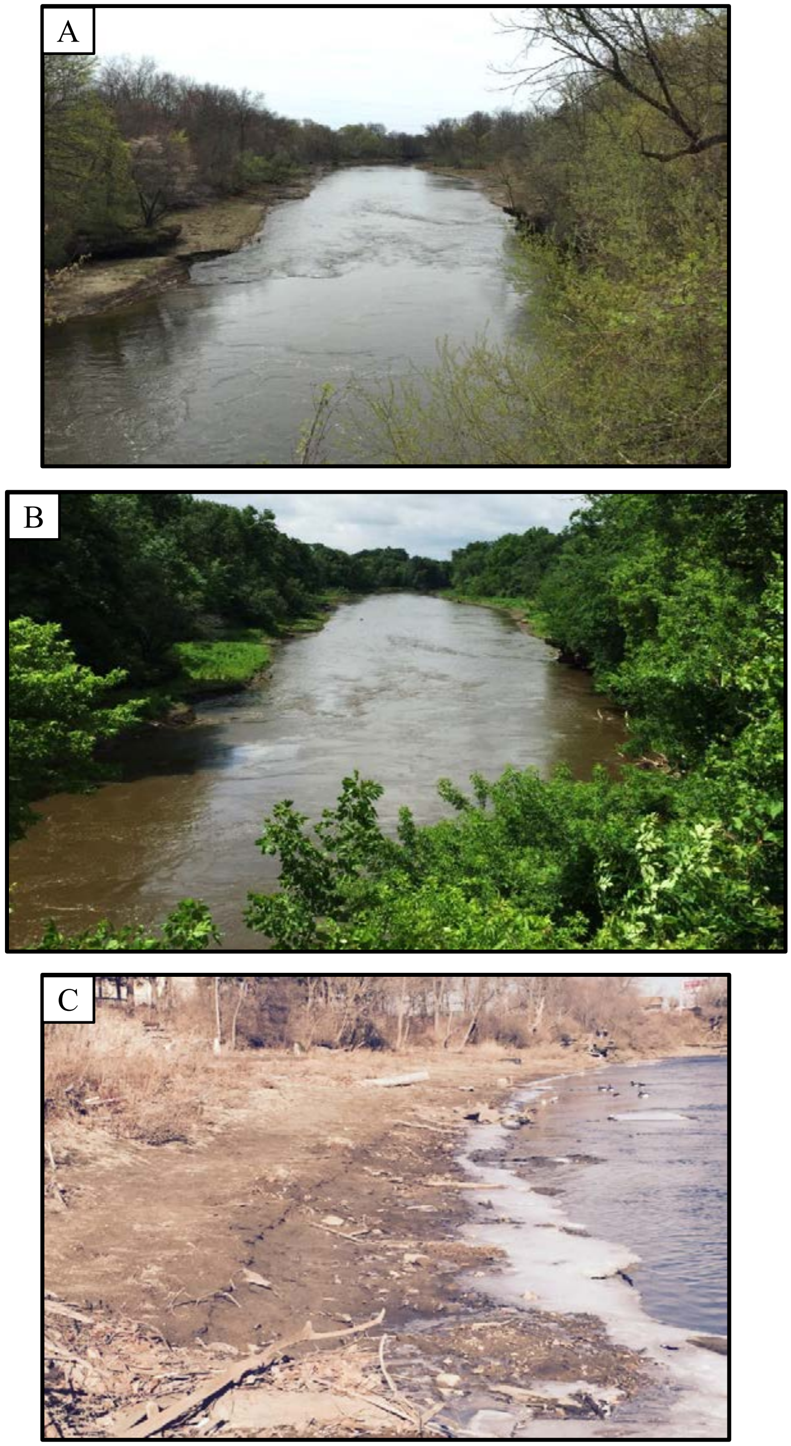

Figure 62. Photographs of the former LeFever Dam pool from 450-1,146 m ULFD. Photo A was taken on 4-19-15 and shows the non-vegetated left and right banks. Photo B was taken on 6-15-15 and shows vegetated banks on the upland but exposed muddy sediment near the river on the left and right bank. Photo C was taken on 1-1-2015 and shows the water lines and extent of inundation of the muddy sediment; note the lack of vegetation near the water's edge.

represents the maximum bed elevation at that location (Figure 40). By the December 2013 survey the channel had vertically incised 0.48 m and Stage C degradation was completed by the March 2014 survey when the river incised to bedrock. It took the Cuyahoga River 7 months to vertically incise a total of 0.7 m to bedrock (complete Stage C) after the LeFever Dam was removed. This is quite different compared to the channel at transect D-6 in which the river incised 1.02 m to bedrock via headcut migration in about 4 months.

Transect D-15 continued to be surveyed in May, July and December of 2014 but showed no geomorphic change because the river was flowing on bedrock. The later stages of the channel evolution model were not observed here because this area is now a zone of transport and with a bedrock channel confined by a bedrock cliff on river left. River right is also a cliff but composed of vegetated soil with large amounts of coarse debris (bricks and cinder blocks) at its base. The river is now wide and shallow at this location so any additional widening is not likely. Temporary aggradation may occur here as upstream sediments are transported through. Overall, transect D-15 reached Stage F quasi-equilibrium by the completion of the December 2014 survey followed by eight months of morphologic stability.

Just upstream of transect D-15 is the LeFever impoundment delta (2,415 m ULFD) deposited at the head of the former LeFever Dam pool. The progression through channel evolution was more complex at this location than at D-15. Prior to the LeFever Dam removal on the May 2013 survey, a large, thick, fairly uniform body of sand spanned the main channel resulting in shallow water depths and no bedrock exposure (Figure 45). There was however, deeper water in the chute on river right because less sand was deposited in that channel. The delta did not undergo significant morphologic change by the August 2013 survey, but Stage B dewatering was complete as the spatial extent of subaerially exposed delta sediments significantly increased (Figure 46). The delta sands continued to erode from the December 2013 through the March 2014 survey where bedrock was first exposed at the downstream end of the delta and along the channel on river left. Consolidated mud deposited in the former LeFever Dam pool was also observed near the mid channel sand island. This clay was buried by the initial deposition of the deltaic sediment after the Munroe Falls Dam was removed. The river has eroded the sandy sediment on top and exposed this resistant impoundment clay.

Significant erosion of all the delta sediment occurred by March 2014 and the thalweg was well established in the area between the mid-channel sand island and larger vegetated island (Figure 48). Stage C degradation was completed by the March 2014 survey and the delta then transitioned into Stage D degradation and widening. By the May 2014 survey, the thalweg reached Stage E aggradation and widening as sand and gravel was transported as bedload on top of bedrock. The areas of the delta beyond the thalweg continued to be eroded but did not undergo significant deposition. Through the duration of the study, sand and gravel continued to be transported as bedload on top of bedrock in the thalweg while the remainder of the deltaic sediments continued to be eroded eventually to reach the underlying bedrock.

By the May 2015 survey virtually all of the deltaic sediment had been eroded and transported downstream (Figure 52). Bedrock was exposed at the downstream end of the delta and on the farthest side of river left. Because impoundment clay is still present in the central channel, the delta is still in Stage E aggradation and widening but once the clay is eroded the transition into Stage F quasi-equilibrium can take place.

4.2.3 Zone 4

The progression through the stages of channel evolution in Zone 4 occurred along a different pathway than in Zone 5. Six transects within Zone 4 displayed morphologic changes consistent with the Stage C degradation in Doyle et al’s. (2003) channel evolution model. These transects include D-5, D-2, D-8, D-10, D-14 and D-12 from 4,607 m (ULFD) to 2,795 m (ULFD). The Cuyahoga River flows over the gravel fill of a glacial buried valley (Figure 57) at the locations of these transects so bedrock did not control the depth to which downcutting occurred.

Transects D-5, D-2, D-8, D-10 and D-12 all experienced significant downcutting with minor channel widening following the LeFever Dam removal. D-14 has also experienced downcutting as well as channel widening. The rates at which the channel reached the pre-Munroe Falls Dam substrate and/or minimum bed elevation differed depending on the upstream distance from the former LeFever Dam and the amount of previously deposited Munroe Falls Dam pool sediment. It took the river 21 months for the channel to reach the pre-Munroe Falls Dam substrate at transects D-5 (4,607 m ULFD), D-2 (4,254 m ULFD), and D-10 (3,310 m ULFD). The channel at these locations had extensive deposits of sandy sediment which spanned the width of the channel. The channel at transect D-12 and at D-8 reached its minimum bed elevation in just 7 months post-removal. Erosion to the pre-dam substrate occurred at D-14 11 months post-removal.

Transect D-2 (4,254 m ULFD) best displays the rate and magnitude of Stage C channel incision resulting from the LeFever Dam removal (Figure 63). It took 21 months for incision to the pre-Munroe Falls substrate to occur at this location. One year post-removal by the August 2014 survey, nearly half of the channel sediment (0.47 m) had been eroded. By the May 2015 survey the river incised to the pre-Munroe Falls substrate therefore transitioning from Stage C degradation to Stage D degradation and widening. However channel widening in the future is not likely to be drastic at this location. In fact, significant channel widening is not likely to occur at any of the transects mentioned above because the river vertically eroded the majority of the preexisting sediment and is nearing equilibrium. In addition, sediments released from the Munroe Falls impoundment did not deposit in large quantities on the channel margins that would have reached a

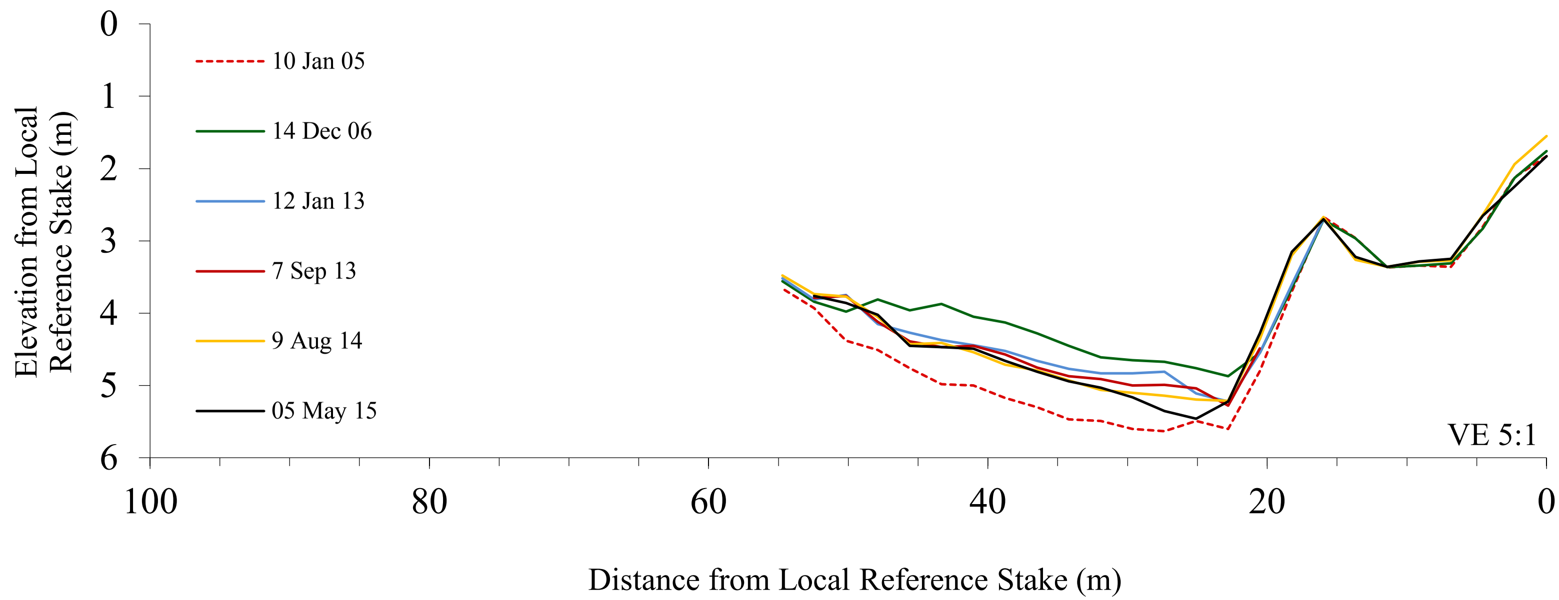

Figure 63. Geomorphic profile of transect D-2 located 4,254 m upstream of the former LeFever Dam, surveyed from January 2005 to May 2015.

critical bank height upon dewatering of the dam pool. But sands did accumulate in chutes on river right near transects D-10, D-14 and D-12 at Water Works Park. The right bank chute environment is most susceptible to lateral erosion in Zone 4 so the magnitude of channel widening should be the greatest at these three transects.

4.3 The Role of Large Woody Debris (LWD)

The channel evolution model describes the first-order change caused by dam removal but this study has also identified an additional element that enhances post-removal sediment dynamics and channel morphology. The presence of large woody debris (LWD) in the Cuyahoga River affected localized channel adjustments in several ways. LWD has both armored channel margins slowing erosion as well as constricted flow which increases bank erosion. As an obstacle scour in the channel, LWD results in both bed aggradation in the lee and obstacle scour erosion.

4.3.1 LWD Related Erosion

At transect U-2 (6,476 m ULFD) LWD that had armored the left bank was dislodged between the June 2008 and May 2009 surveys resulting in 2.75 m of lateral bank erosion (Figure 27) (Peck and Kasper, 2013). Transect U-6 (7,056 m ULFD) best illustrates how LWD constricts flow and enhances bank erosion. LWD was transported and deposited immediately downstream of transect U-6 in the winter of 2011-2012. This LWD directed flow into the right bank which is composed of former Munroe Falls Dam impoundment sediment (Figure 64). Field observations of a vertical scarp and recent slump blocks clearly show the enhanced bank erosion upstream of the LWD (Figure 64). Downstream of the LWD the bank remains vegetated and less prone to erosion. Before the arrival of the LWD obstacle, the right bank at U-6 was relatively stable between 2011 and

Figure 64. Photographs of large woody debris (LWD) related erosion at transect U-6 (7,056 m ULFD) in October 2012 (Peck personal communication). In both photos flow is from right to left and the scale bar is 1.5 m long. (Top) The extent of the LWD and actively eroding vertical scarp upstream (right) and vegetated bank downstream (left). (Bottom) Close up of the actively eroding bank and recent slump blocks. Note the boils on the stream surface upstream of the LWD.

2012 (Figure 26). After the LWD was deposited the right bank laterally eroded 3.5 m (Figure 26). Since the photographs in Figure 64 were taken, the LWD has moved further downstream and the eroding bank scarp has also moved downstream.

4.3.2 LWD Related Deposition

LWD in the channel creates an obstacle that promotes both sediment deposition and erosion. Peck and Kasper (2013) noted that mid-channel sediment deposits associated with LWD were present on profiles U-1 and U-4. Once the LWD at those locations was washed away the sediment deposits were eroded as well.

At Waterworks Park a high flow in the winter of 2013 brought LWD to the location of transect D-8 (Figure 65). Sediment was continually deposited in the low velocity lee thus temporarily storing sediment as a mid channel bar. Furthermore, this LWD redirected flow to the right side of the channel and accelerated the erosion of sands that had been previously deposited following the removal of the Munroe Falls

At Waterworks Park, LWD appeared at the location of transect D-14 (3,146 m ULFD) in the fall of 2014. The log directed flow towards the right bank promoting 2.36 m of erosion to the right bank (Figure 66). Where the tree trunk crossed the profile line at 30 m, flow was directed to the channel floor and scoured the channel to its lowest elevation (Figure 66). However, between the December 2014 and April 2015 profile the channel aggraded 0.69 m where the tree trunk intersects the profile line. The sediment dynamics associated with the presence of LWD have been variable at this particular location as well as the other transects described above.

The channel evolution model of Doyle et al. (2003) has been sufficient for describing the response of the Cuyahoga River to dam removal but LWD placement is unpredictable and has a significant local effect on channel erosion and deposition. LWD has additional implications in fluvial environments. LWD can form deep, shaded pools on their

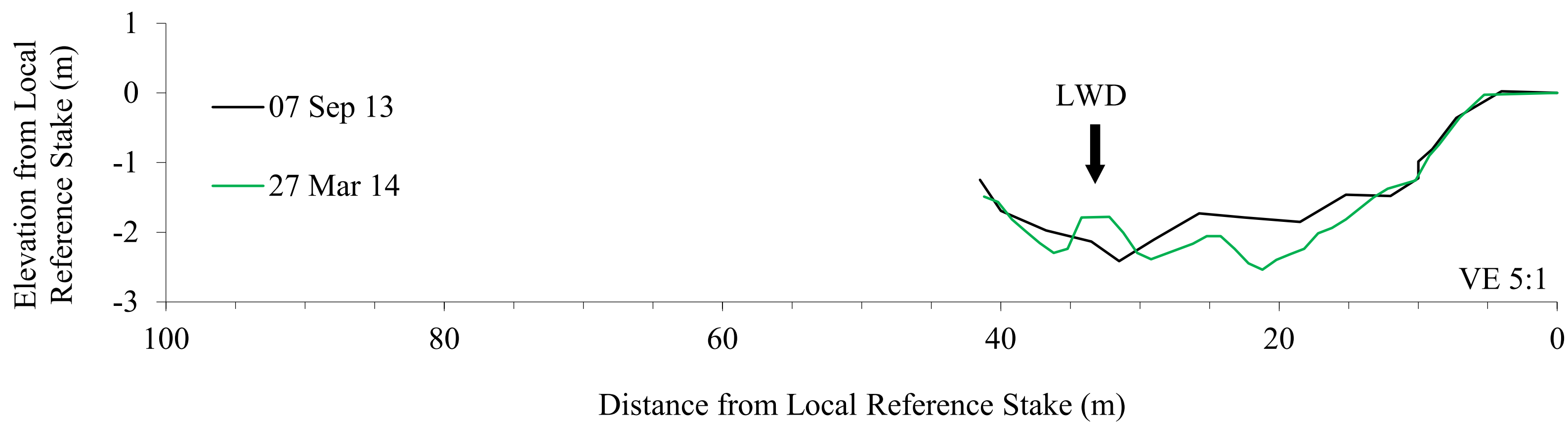

Figure 65. Geomorphic profile of transect D-8 located 4,023 m upstream of the former LeFever Dam, surveyed from September 2013 to March 2014. Large woody debris (LWD) deposited at about 30-35 m on the profile line and promoted erosion of the right side of the channel and deposition on the left.

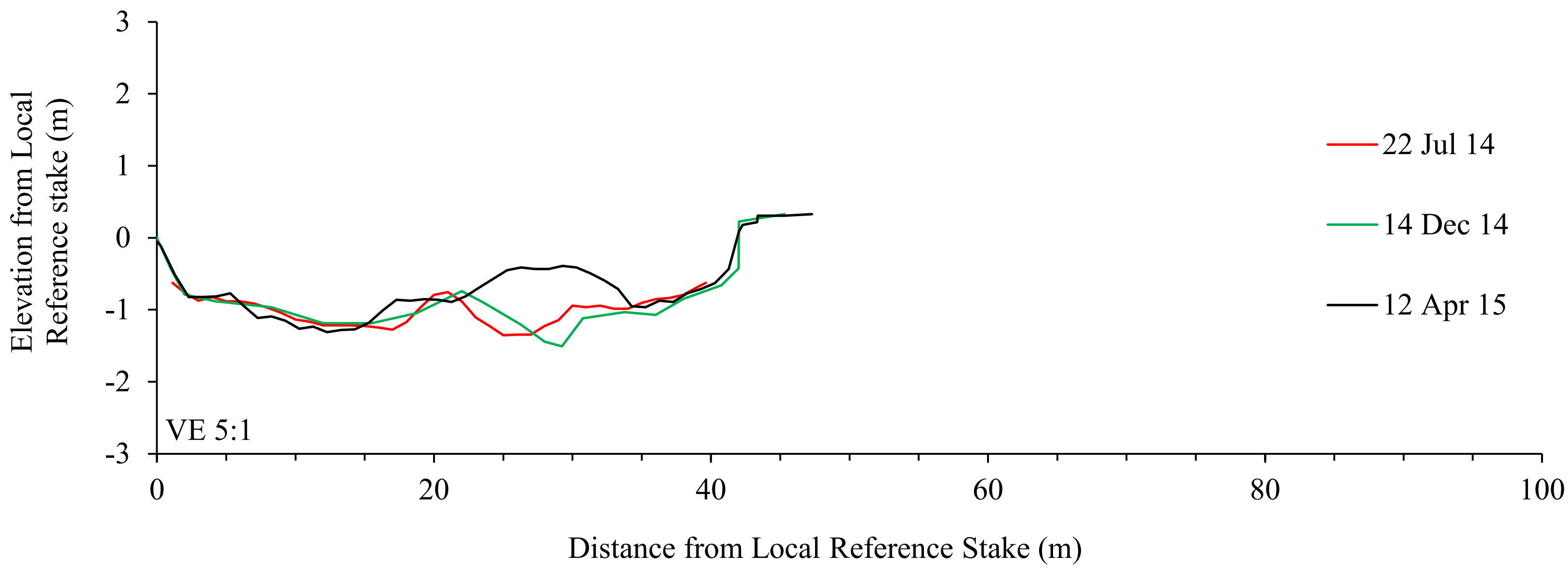

Figure 66. Geomorphic profile of transect D-14 located 3,146 m upstream of the former LeFever Dam, surveyed from July 2014 to April 2015. The survey dates included above show how large woody debris (LWD) can cause bed degradation and aggradation.

upstream end which provides a favorable, nutrient rich habitat for anadromous fish and invertebrates (Abbe and Montgomery, 1996). In fact, from 1950-1980s LWD was widely removed from rivers to attempt to improve fish habitat, but today LWD is known to be a healthy part of the riparian system (Abbe and Montgomery, 1996). Removing LWD from rivers increases flow velocity and reduces the amount in-channel materials available for natural bank stabilization (McBroom et al., 2014). LWD has also been used as a cost effective, natural construction material for bank stabilization in many states throughout the U.S. as well as in Australia and British Columbia (Shields et al., 2004).

4.4 High Discharge Events

With increased flow velocities and large volumes of water in the channel; high discharge events erode and transport larger quantities of coarser grained sediment. Flooding events are frequently accompanied by prolonged precipitation which saturates the land surrounding the river increasing the potential for mass wasting. Oversaturated river banks/valleys and high flows can impact natural river systems in a profound way as well as accelerate the rate of channel evolution in a river reach recovering from dam removal. Since 2003, the frequency and magnitude of floods on the Cuyahoga River has increased (Liberatore, 2013) (Figure 67). In fact, since data collection began in the spring of 1922, six of the top ten historical floods on the Cuyahoga have occurred in 2003 or later (Figure 67) (waterdata.USGS.gov). Since the completion of the Munroe Falls Dam removal on October 31, 2005, there have been 42 days greater than 80 m^3/s mean daily discharge on the middle Cuyahoga River (waterdata.USGS.gov) (Table 13). Following the study of Liberatore (2013) this study also chose 80 m^3/s as the threshold for high flow. The middle Cuyahoga River has undergone significant geomorphic and sedimentologic

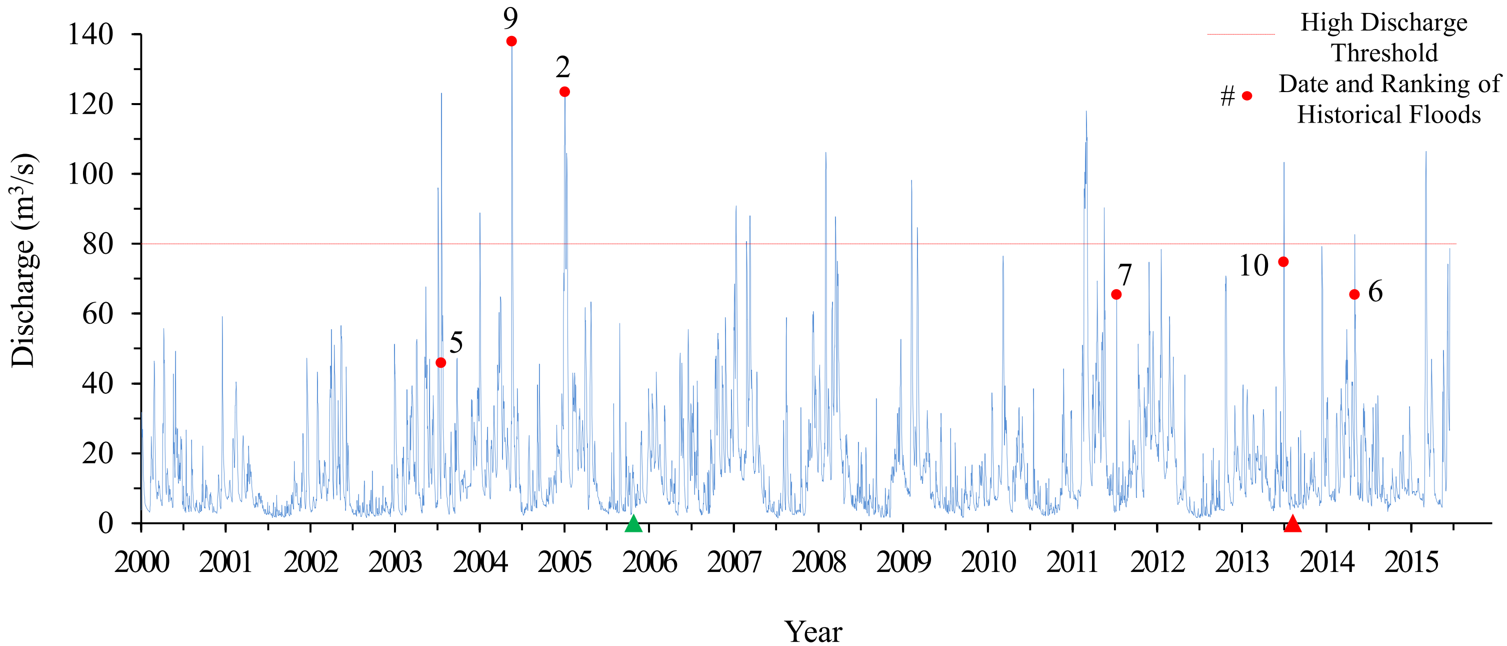

Figure 67. Stream hydrograph showing the mean daily discharge of the Cuyahoga River recorded at the Old Portage stream gauging station USGS 04206000 (waterdata.usgs.gov). In this study 80 m^3/sec was chosen as the threshold for high discharge events and is represented by the red line. The numbered red dots represent the date and ranking of a historical flood based on instantaneous discharge (waterdata.usgs.gov). The 2005 Munroe Falls Dam removal (green triangle) and 2013 LeFever Dam removal (red triangle) are also shown.

change resulting from the Munroe Falls and LeFever Dam removals and high discharge events have aided in the process.

4.4.1 Upstream Changes

The river reach upstream of the former Munroe Falls Dam is characterized by thick, near-vertical banks of former impoundment mud. Transects U8-U1 are all located along this reach and display this channel morphology. The lateral erosion rates were the greatest within the first year after the Munroe Falls Dam was removed and rapidly decreased in the second year as the banks dewatered and were vegetated (Peck and Kasper, 2013) (Figure 68). These banks eroded by episodic, near vertical slump blocks. Between the spring of 2009 and January 2011 there were no high discharge events (Figure 68) and the bank erosion was near 0.0 m/mo for all transects except U-2 which declined from the previous years (Figure 68).

In February to March, 2011 there were fifteen consecutive days of high mean daily flow (> 80 m^3/s) (Table 13). This prolonged period of high discharge resulted in marked increases in the lateral erosion rates at transects U-8, U-1, U-6, U-2, and U-3. Transects U-1 and U-3 were the most affect by the high flow as their lateral erosions rates increased by six-fold and nine-fold respectively (Figure 68). The channel at U-1 widened by 1.66 m and the channel at U-3 widened by 1.25 m between the May 2010 and July 2011 surveys.

Additional high discharge events occurred in the summer of 2013 and in the winter/ spring of 2014 causing accelerated lateral erosion at transects U-8, U-1, U-7 and U-3 (Table 13) (Figure 68). The channel at all of these locations experienced 0.5 m or more of channel widening. The most severe lateral erosion occurred at transect U-1 where the channel widened by 1.5 m. Due to irregular time intervals between surveys, transects U-6 and U-2 were affected not only by the two previously mentioned high flows but also five consecutive days of high flow in the spring of 2015. Between the October 2012 and May

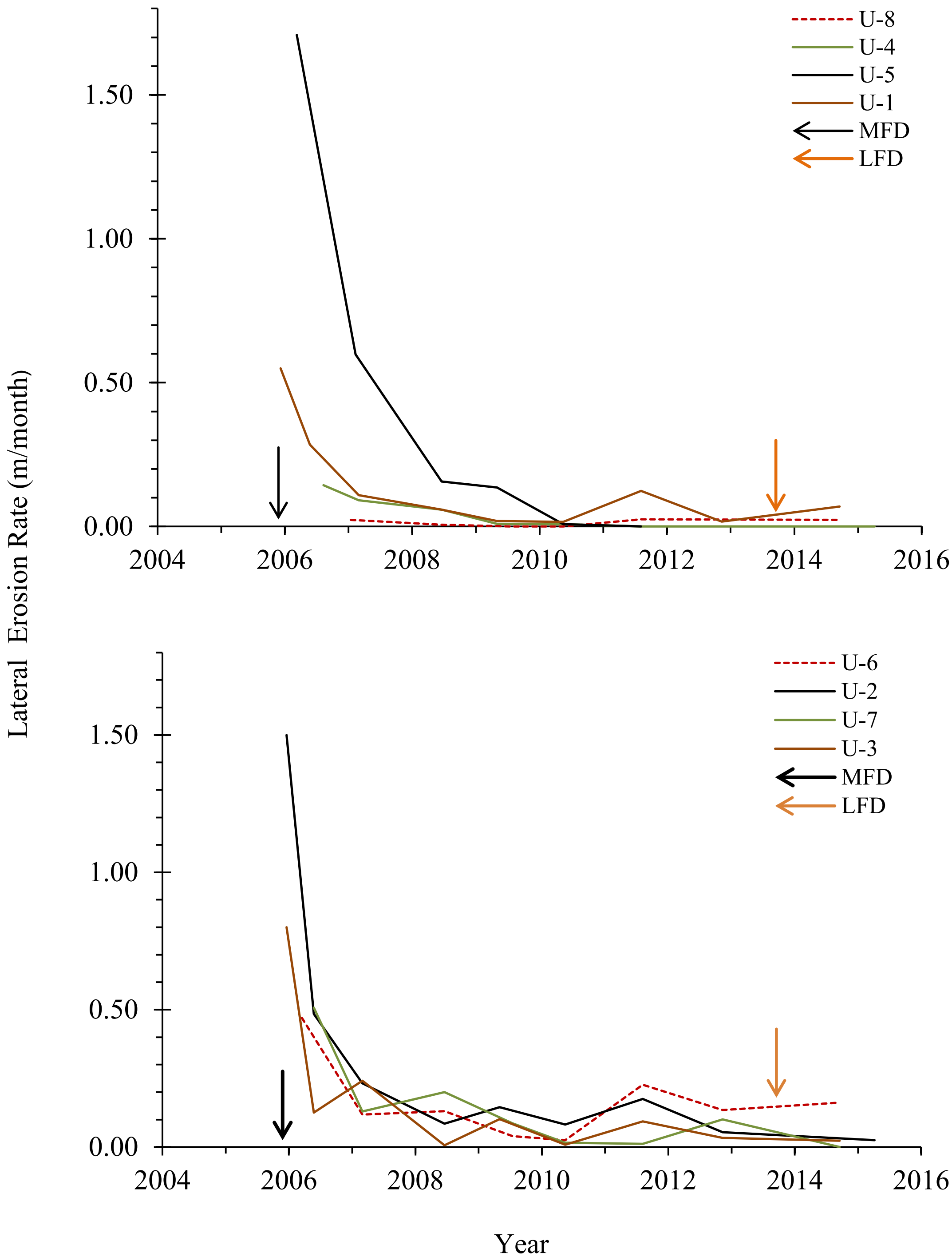

Figure 68. Lateral erosion rates per year at transects U1-U8 located 10,107-7,325 m (ULFD). The downward pointing arrows indicate the times of the Monroe Falls (MFD) and LeFever Dam (LFD) removals. The legend in each graph is arranged in decreasing distance from the former LeFever Dam and the top graph displays the four upstream most transects. Data collected after 2010 has been added to the post-Munroe Falls erosion rates (Kasper, 2010; Peck and Kasper, 2013).

Table 13. Dates when the high discharge threshold of 80 m^3/s was surpassed on the middle Cuyahoga River recorded by the Old Portage stream gauging station USGS 04206000 (waterdata.USGS.gov). The threshold was not surpassed until 1/15/2007, two years after the Munroe Falls Dam removal.

Date	Mean Daily Discharge (m^3/s)
1/15/2007	89
1/16/2007	91
1/17/2007	84
3/2/2007	81
3/16/2007	84
3/17/2007	88
3/18/2007	83
2/6/2008	101
2/7/2008	102
2/8/2008	106
2/9/2008	103
3/20/2008	88
3/21/2008	84
3/22/2008	84
2/12/2009	98
2/13/2009	95
2/14/2009	86
3/9/2009	85
3/10/2009	80
2/28/2011	96
3/1/2011	96
3/2/2011	93
3/3/2011	101
3/4/2011	90
3/5/2011	104
3/6/2011	109
3/7/2011	99
3/8/2011	97
3/9/2011	99
3/10/2011	118
3/11/2011	115
3/12/2011	110
3/13/2011	110
3/14/2011	94
5/26/2011	90

Table 13. Dates when the high discharge threshold of 80 m^3/s was surpassed on the middle Cuyahoga River recorded by the Old Portage stream gauging station USGS 04206000 (waterdata.USGS.gov). The threshold was not surpassed until 1/15/2007, two years after the Munroe Falls Dam removal (Continued).

Date	Mean Daily Discharge (m^3/s)
7/11/2013	103
5/13/2014	83
3/14/2015	85
3/15/2015	97
3/16/2015	102
3/17/2015	106
3/18/2015	91

2015 surveys, the channel at U-6 widened by 3.5 m and by 0.75 m at U-2. Lateral erosion at transect U-6 was however enhanced by the presence of LWD.

The present day, long-term (10 years) relationship between high discharge events, the placement of LWD and channel erosion/deposition has been exemplified in Zones 1-3. This study has highlighted the local effect of these factors within the study reach and can be applied to the Cuyahoga River as whole. Although the Cuyahoga River is small compared to the large rivers of the world, the interplay of floods and LWD can be applied to other river systems. However, the mean annual discharge of a river and vegetative cover within its watershed changes based on geographic location. Also, higher discharge and LWD deposits composed of larger tree types exacerbates the sedimentologic and geomorphic impacts on the channel and flood plain. In a greater context, the modern analogue in this study provides quantitative information (which is lacking) (Colombera et al., 2013) for incorporating site specific occurrences into traditional alluvial facies models to better understand the ancient fluvial sedimentary record. Cross bedding and deep scour holes (erosional surfaces) are often used as indicators for fluvial environments in the sedimentary record (Latrubesse, 2015). This study has shown the LWD can cause obstacle scour and bar forms to accumulate in the channel that, if preserved, would closely resemble the cross beds and erosional surfaces that are often attributed to other mechanisms such as sharp meander bends, lithologic differences and tributary confluence (Latrubesse, 2015).

4.4.2 Downstream Changes

While channel widening has characterized the effects of high discharge events in the upstream Zones 1, 2, 3, vertical changes in downcutting and aggradation have resulted from flooding events in Zone 4 and 5. In order to accurately assess the role of flooding, it was important to determine the erosion rate induced purely by the LeFever Dam removal.

A high discharge event occurred between nearly all consecutive survey dates. However, when a flood did not occur between surveys, the erosion that took place was attributed to the increased stream energy resulting from the LeFever Dam removal alone. The total amount of erosion between consecutive surveys often exceeded the rate caused by the LeFever Dam removal therefore indicating that flooding events accelerate stream erosion.

The 6th (July 10, 2013) and 10th (May 13, 2014) largest floods on record on the Cuyahoga River and a five-day flood in March of 2015 increased stream erosion in Zones 4 and 5. The rate of downcutting already established by the LeFever Dam removal was accelerated during one or more of these flooding events at transect D-5, D-2, D-8, D-10, D-12, D-14 and D-6 (Table 14). Flooding events often doubled the rate of downcutting at most of the transects above and even caused channel aggradation as the former Munroe Falls impoundment sediment was transported downstream (Table 14). Transect D-6 experienced the greatest increase in the rate of downcutting and aggradation because it was located closest to the former LeFever Dam while the other transects were upstream of the dam pool. However, the rate of downcutting did not increase as drastically during the March 2015 flood at transects D-12 and D-6 because the highest erosion rates tends to occur immediately after dam removal, then decay in the long-term (Figure 69) (Kasper, 2013; Peck and Kasper, 2013). The long-term decrease in erosion is often interrupted during times of high discharge when erosion becomes more intense like in the year 2011 (Figure 69).

Although erosion rates have slowed in both the former Munroe Falls and LeFever Dam pools, the May 2014 flood mobilized a very large rotation slump which protruded into the left side of the river just downstream of transect D-6. The rotation slump was first observed on the May 23, 2014 survey and also exposed a portion of buried fiber optic cable (Figure 70). The former LeFever Dam pool provided support to the toe of the failed slope but saturated the land mass at the same time. Once the dam pool was

Table 14. Rates of downcutting due to floods (Flood Erosion) and the LeFever Dam removal (Non-Flood Erosion) at seven transects in Zones 4 and 5. Mean daily discharge values greater than 80 m^3/s are considered a flooding event. The time between surveys was normalized using a 31-day month. When no floods occurred between consecutive surveys, the erosion was attributed to the LeFever Dam removal. * indicates the mean daily discharge on 12/22/13 was 79 m^3/s. Bold values were affected by LWD and (+) values indicate channel aggradation rather than erosion.

Transect	Survey Date	No.Days Between Surveys	No. Days > 80 m^3/s	Flood Rank	Flood Erosion (m/mo)	Non-Flood Erosion (m/mo)
D-5	Mar 2014 - Jul 2014	123	1	6th	0.05	-
	Jul 2014 - Dec 2014	142	0	-	-	0.02
	Dec 2014 - May 2015	140	5	-	0.06	-
D-2	Sep 2013 - Mar 2014	201	0 *	-	-	0.01
	Mar 2014 - Aug 2014	135	1	6th	0.01	-
	Aug 2014 - May 2015	269	5	-	0.03	
D-8	May 2012 - Sep 2013	481	1	10th	0.03	-
	Sep 2013 - Mar 2014	201	0	-	-	**0.07**
	Aug 2014 - Dec 2014	117	0 *	-	-	**0.08**
D-10	May 2012 - May 2013	371	0	-	+ 0.03	-
	May 2013 - Sep 2013	110	1	10th	0.09	-
	Sep 2013 - Mar 2014	198	0 *	-	-	0.03
	Mar 2014 - Aug 2014	143	1	6th	0.03	-
	Aug 2014 - Dec 2014	117	0	-	-	0.04
D-14	May 2013 - Sep 2013	110	1	10th	0.14	-
	Sep 2013 - Oct 2013	52	0	-	-	0.06
	Oct 2013 - Mar 2014	146	0 *	-	-	0.08
	Mar 2014 - Jul 2014	120	1	6th	0.19	-
	Jul 2014 - Dec 2014	145	0	-	-	**0.08**
D-12	Sep 2013 - Mar 2014	198	0 *	-		0.08
	Mar 2014 - Aug 2014	143	1	6th	0.13	-
	Aug 2014 - Dec 2014	117	0	-	-	+ 0.03
	Dec 2014 - Apr 2015	119	5	-	0.07	
D-6	May 2012 - Dec 2013	548	1 *	10th	0.06	-
	Dec 2013 - Mar 2014	97	0 *	-		0.03, + 0.22
	Mar 2014 - May 2014	60	1	6th	0.31	-
	May 2014 - Aug 2014	80	0	-	-	0.07
	Aug 2014 - Apr 2015	244	5	-	0.02	+ 0.02

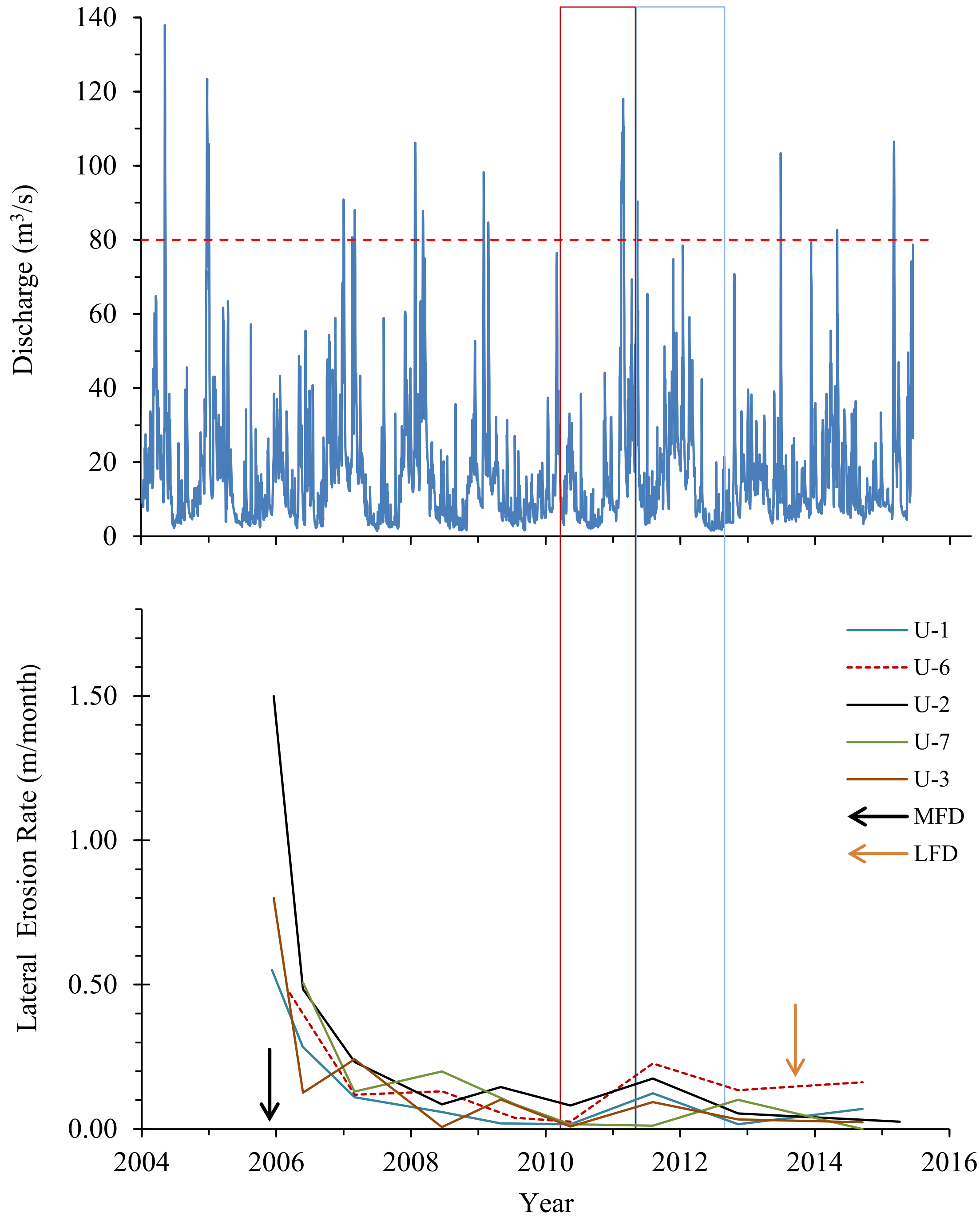

Figure 69. (Top) Stream hydrograph showing the mean daily discharge from 2004 - 2016 at Old Portage stream gauging station USGS 04206000 (waterdata.usgs.gov). (Bottom) Lateral erosion rates per year at five transects upstream of the former Munroe Falls Dam (MFD) (Peck and Kasper, 2013). The removal of the former LeFever Dam is also shown (LFD). The blue rectangles border portions of the years 2009 through 2011 and highlight the relationship between frequent high discharge events and elevated lateral erosion in the long-term following the Munroe Falls Dam removal.

Figure 70. Photograph of rotational slump just downstream of transect D-6 (843 m ULFD) taken on November 30, 2014. The slump was first observed in the former dam pool on May 23, 2014 and occurred during a heavy precipitation event and the 6th largest flood on the Cuyahoga River on May 13, 2014.

dewatered, the pore fluid pressure in the saturated bank material decreased which could have caused the mass wasting to occur (Jiao et. al., 2014). On the other hand, prolonged precipitation during the May 13, 2014 flood may have led to soil oversaturation therefore causing the slumping event (Liang et. al. 2014). The specific conditions that caused this rotational slump cannot be ascertained but it is likely a combination of both scenarios. Mass wasting like this could have happened anywhere in the downstream end of Zone 5. The right side of this reach is bordered by the urban infrastructure of Cuyahoga Falls which easily could have been subjected to this slope failure. Assessing slope stability is important in the dam removal process because mass wasting could lead to property damage and human injury.

4.5 Future Conditions

Based upon the ten years of data collection in Zones 1-3 and the current rate of channel of evolution in Zones 4 and 5, the likely future conditions of the Cuyahoga River can be predicted. Transects U-3 and D-6 are located immediately upstream of the former Munroe Falls Dam and LeFever Dam respectively. While the dams were in place, these transects represented dam pool locations having the deepest water, greatest channel width, and largest quantities of impounded sediment. The long term response of the Cuyahoga River to the Munroe Falls Dam removal has been assessed with continued geomorphic surveys so those data can aid in predicting the future conditions within the LeFever Dam pool. During low flow on the August 2014 (~10 years post-Munroe Falls removal), the channel at transect U-3 was ~30 m wide, ~0.5 m deep, floored by bedrock and had vegetated banks of impoundment mud (Figure 71). During the August 2014 survey (~1 year post-LeFever removal) the channel at transect D-6 was also ~30 m wide and ~0.5 m deep (Figure 71). The river was not flowing on bed rock because

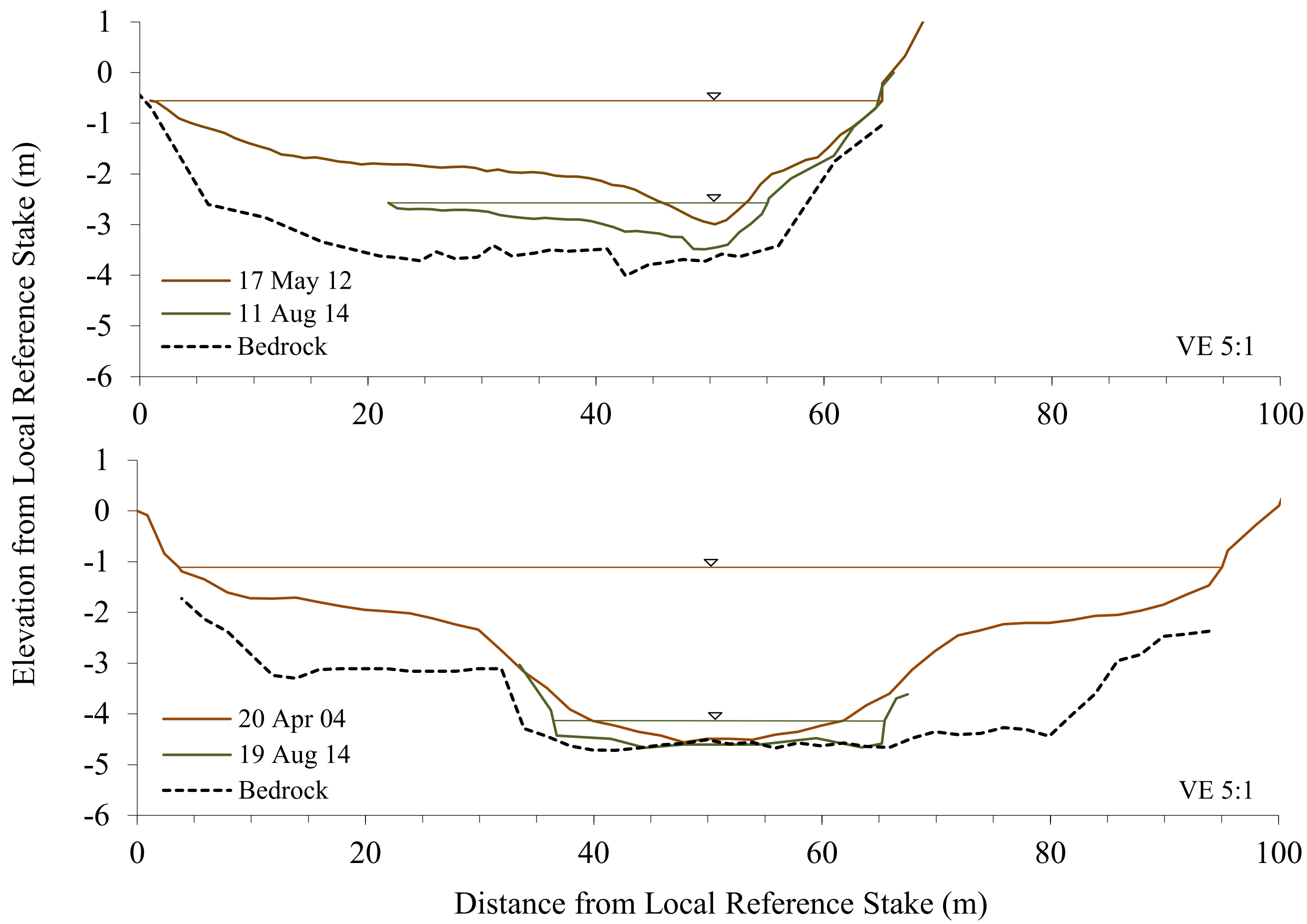

Figure 71. Comparison between the geomorphology at transect D-6 (843 m ULFD) (top) and transect U-3 (5,765 m ULFD) (bottom). The channel at transect U-3 has had ~10 years to adjust after the Munroe Falls Dan removal and the channel at transect D-6 has had ~2 years to adjust after the LeFever Dam removal. The elevation of the future water surface at D-6 is likely to be attained within ~5 years post removal.

the thalweg had aggraded with sand and gravel transported from upstream. However, as the impoundment sediment continues to be transported downstream it is likely that the channel will be floored by bedrock in the future (Figure 57). Impoundment mud occupies the channel margins but is not as extensively vegetated as the banks at U-3, nor do the banks have vertical scarps. Once the impoundment sediment from the former LeFever Dam is entirely transported downstream, the river should flow on top of bedrock as it does at transect U-3 (Figure 71). The channel will also widen episodically during seasonal floods. Furthermore, because no significant tributaries enter the Cuyahoga River between U-3 and U-6 both locations should have similar low flow widths (30 m) and depths (0.5 m) (Figure 71).

Predicating future channel conditions after dam removal is important for a number of reasons including the health and safety of wild life downstream of the dam, risk assessment for property damage and flood control. The channel in former LeFever Dam pool should be ~30 m wide, ~0.5 m deep, flow on top of bedrock and be flanked by partially vegetated banks of impoundment mud (Figure 72). Because dam removal has been shown to improve water quality, potential recreation opportunities are also considered after dam removal. In fact, this study has aided in the planning of a boat launch construction project at Waterfront Park just upstream of transect D-6. These data were presented to a panel of professionals at City Hall in Cuyahoga Falls, Ohio. The city of Cuyahoga Falls desired to build a boat ramp on the right bank. Because only ~1 m of impoundment mud underlain by bedrock remains, it was concluded that the construction of this ramp was feasible (Figure 72). The City successfully gained the funding to complete this project and will begin the construction process within two years.

Because the banks of impoundment mud are often inundated during medium to high flows and wetted by groundwater discharge, there will always be portions of the banks that are saturated. From the Waterfront Park standpoint, the saturated banks are not safe

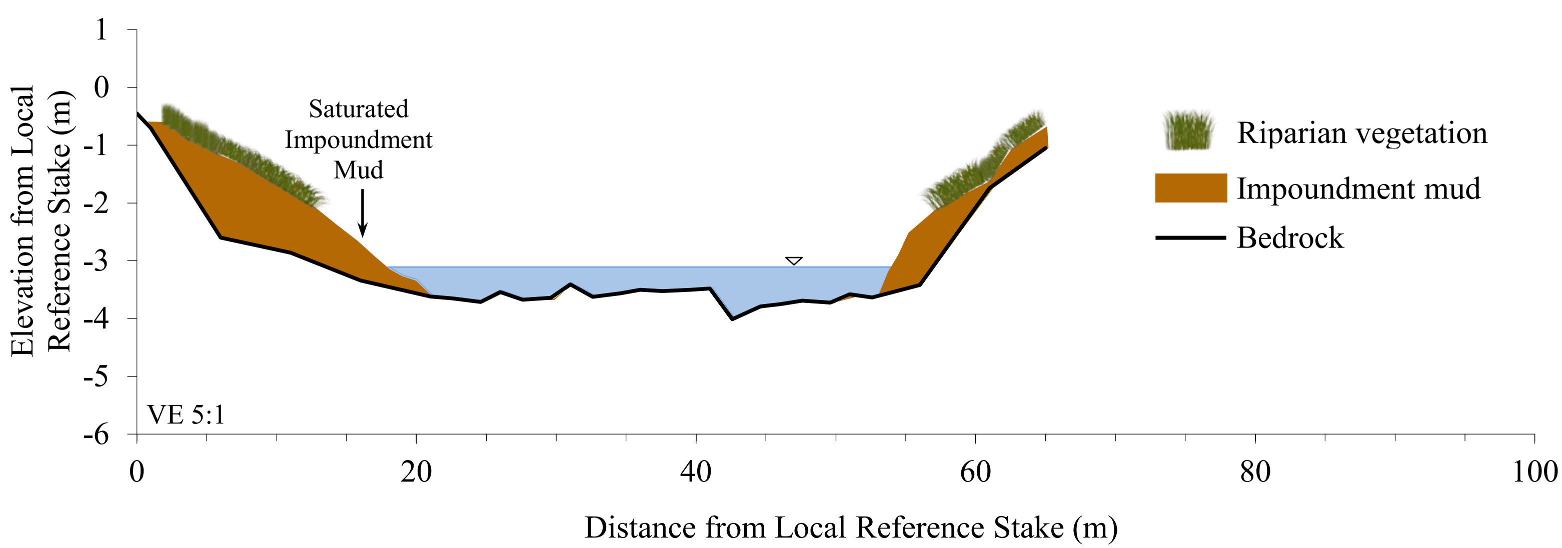

Figure 72. Geomorphic profile of transect D-6 (843 m ULFD) representing the future conditions within the former LeFever Dam pool. The river will flow on top of bedrock and former impoundment mud will occupy the channel margins. It is likely that the banks closest to the water's edge will always be saturated.

for children because it is very easy to sink into the impoundment mud. The mud is also polluted (Kasper, 2013) and contains a large amount of litter and debris which is also not a safe environment for recreation. Furthermore, there are locations that are dewatered and safe to walk on so in time, the conditions of the former dam pool will improve and Waterfront Park will become a safer and cleaner place for recreation.

CHAPTER V

CONCLUSIONS

Summary

The growing trend of removing dams as a river restoration technique necessitates a deeper understanding of how a river system will equilibrate following dam removal. Predicting how a river system will adjust to dam removal is also of great importance because rivers provide the habitat for an abundance of biota. This thesis quantified the response of the Cuyahoga River in the 1.5 years following the LeFever Dam removal and furthered the understanding of the long-term adjustments following the Munroe Falls Dam removal upstream. The major findings of this thesis research are:

- The LeFever Dam removal increased stream power by about 26 times within the former dam pool (Zone 5) due to an increase in river slope from 0.00029 to 0.0072 m/m and an 87 % decrease in channel cross-sectional area.
- The peak stream velocity in the former dam pool increased from 0.06 to 0.53 m/s post-removal. This increase in velocity is great enough to erode and transport consolidated mud to granules and transport small cobbles as bedload whereas the pre-removal dam pool could only transport unconsolidated mud to coarse sand as bedload.
- Stage C incision to the pre-dam substrate occurred two months sooner in the former LeFever Dam pool (D-6) than at a comparable location in the former Munroe Falls Dam pool (U-3). Stage D degradation and widening is still

occurring within the former Munroe Falls Dam pool (10 years post-removal) and aggradation of sand is not likely because the channel has become a gravel lag deposit. Stage E aggradation and widening occurred in the former LeFever Dam pool within 4 months post removal and reached stage F quasi-equilibrium within 7 months at transect D-15.

- The LeFever impoundment delta was almost completely eroded by the May 2015 survey. This location will likely reach Stage F quasi equilibrium by May 2016. Bedrock with very thin deposits of sand and gravel in active transport will comprise the channel substrate near the Zone 4/Zone 5 boundary.
- Large woody debris has had a significant local effect on channel erosion/ deposition throughout the study reach and should be considered in channel evolution models.
- High discharge events have been shown to nearly double the rate of downcutting induced by the LeFever Dam removal in Zones 4 and 5. Flooding has also temporarily increased the rate of lateral erosion of the former Munroe Falls impoundment mud in Zones 1-3. Even though lateral erosion is increased episodically in Zones 1-3, the overall trend of lateral erosion has decreased in the long-term.
- Channel coarsening and depletion of organic rich mud was the prevailing sedimentological change following the LeFever and Munroe Falls Dam removals because flow velocity significantly increased post-removal. The mean grain size increased from 2.41 ϕ in 2003-04 to -3.39 ϕ in 2014 upstream of the former Munroe Falls Dam and increased from 1.99 ϕ in 2008-09 to -1.26 ϕ in 2014 upstream of the LeFever Dam.
- Based upon the long-term morphological response of the Munroe Falls Dam removal and short-term response of the LeFever Dam removal, the likely future

conditions within the former LeFever Dam pool can be predicated. During low flow, the channel will likely be ~30 m wide, ~0.5 m deep, flow on top of bedrock and be flanked by partially vegetated banks of former impoundment mud.

- These future conditions are favorable for recreation along the waterfront and this research has aided the city of Cuyahoga Falls in the planning of a boat ramp construction project within the former LeFever Dam pool.

REFERENCES

Abbe, T. B., Montgomery, D. R., 1996, Large woody debris jams, channel hydraulics and habitat formation in large rivers, Regulated Rivers: Research & Management. v. 12, p. 201-221.

Ager, D. V., The Nature of the Stratigraphic Record, second edition, New York, Halsted Press. 1981: p. 36-48

BBC&M Engineering, Inc, 2008,Hydrologic Engineering Report-Cuyahoga River Study Cuyahoga Falls, Ohio, no. 1, 31 p.

Bednarek, A. T., 2001, Undamming Rivers: A review of the Ecological Impacts of Dam Removal. Environmental Management 27, no. 6, p. 803-814.

Burroughs, B. A., Hayes, D. B., Klomp, K.D., Hansen, J. F., Mitak, J., 2009, Effects of Stronach Dam removal on fluvial geomorphology in the Pine River, Michigan, United States.Geomorphology 110, no. ¾, p. 96-107.

Boggs, S., Jr., Principles of Sedimentation and Stratigraphy, fourth edition, Upper Saddle River, New Jersey, Pearson Prentice Hall: p 21-47.

Cannatelli, K. M., Curran, J, C., 2012, Importance of Hydrology on Channel Evolution Following Dam Removal: Case Study and Conceptual Model. Journal Of Hydraulic Engineering 138, no.5, p. 377-390.

Colombera, L., Mountney, N. P., McCaffrey, W. D., 2013, A quantitative approach to fluvial facies models: Methods and example results. Sedimentology, no. 60, p. 1526-1558.

Csiki, S., Rhoads, B. L., 2010, Hydraulic and geomorphological effects of run-of-river dams. Progress In Physical Geography 34, no. 6, p. 755-780.

Csiki, S., Rhoads, B. L., 2013, Influence of four run-of-river dams on channel morphology and sediment characteristics in Illinois, USA. No. 206, p. 215-229.

Dean, W. E., Jr., 1974, Determination of carbonate and organic matter in calcareous sediments and sedimentary rocks by loss on ignition; comparison with other methods: Journal of Sedimentary Petrology, v. 44, p. 242-248.

Demasi, T., 2011, Finding no significant impacts to all interested citizens, organizations and government agencies. Ohio Environmental Protection Agency Environmental Assessment-Cuyahoga Falls Dam Removal. WRRSP no. WR390296-0004, 6 p.

Doyle, M. W., Stanley, E. H., Harbor, J. M., 2003, Channel adjustments following two dam removals in Wisconsin. Water Resources Research v. 39, no. 1, 1011.

Doyle, M. W., Stanley, E. H., Orr, C.H., Selle, A. R., Sethi, S. A., Harbor, J. M., 2005,Stream Ecosystem response to small dam removal: Lessons from the Heartland. Geomorphology v.71 p. 227-244.

Evans, J. E., 2007, Sediment impacts of the 1994 failure of IVEX dam (Chagrin River, NE Ohio); a test of channel evolution models. Journal of Great Lakes Research 33, no. Special issue 2, p. 90-102.

Folk, R. L., 1980, Petrology of Sedimentary Rocks: Austin, TX Hemphill Publishing Company, p. 15-84.

Green, S. L., Krause, A. J., Knox. J. C., 2013, A decade of geomorphic and hydraulic response to the LaValle Dam project, Baraboo River, Wisconsin. Journal of the American Water Resources Association, v. 49 no. 6, p. 1473-1484.

Hardlines Design Company (HDC), 2011, Phase I History/Architecture Evaluation of Two Concrete Dams on the Cuyahoga River. HDC 1168, p. 8-13, 26-28.

Harris, N., Evans, J., 2014. Channel Evolution of Sandy Reservoir Sediments following low-head dam removal, Ottawa River, Northwestern Ohio, U.S.A. Open Journal of Modern Hydrology no.4, p. 44-56.

Heinz Center, 2002, Dam Removal Science and Decision Making, The H. John Heinz III Center for Science, Economics and the Environment, 263 p.

ICF Consulting, 2005, A summary of existing research on low-head dam removal projects, NCHRP Project 25-25, Task 14, National Cooperative Highway Research Program,Transportation Research Board, no. 1, 170 p.

Kasper, N. A., An assessment of the LaFever Dam pool, middle Cuyahoga River, Summit County, Ohio. Master’s Thesis. Department of Geology, University of Akron, 2010.

Krieger, K. A., Zawiski B., 2013, Changes in biotic and habitat indices in response to dam removals in Ohio. Reviews In Engineering Geology v. 21, p. 105-116.

Latrubesse, M. E., 2015, Large rivers, megafans and other quaternary avulsive fluvial systems: A potential “who’s who” in the geological record, Earth-Science Reviews. no. 146, p. 1-30.

Liberatore, S., Changes in Geomorphic Equilibrium on Furnace Run, Summit County, Ohio., Masters Thesis. Department of Geology, University of Akron, 2013.

McBroom, M., Ringer, .M, Zhang, Y., 2014, Instream woody debris and riparian forest characteristics in the Sabine River Texas. Proceedings of the 5th Big Thicket Science Conference: Changing Landscapes and changing Climate, Southeastern Naturalist, v. 13, p. 1-14.

Ohio Environmental Protection Agency Division of Surface Water, 2003, Total Maximum Daily Loads for the Lower Cuyahoga River, Final report. 102 p.

Raub, E. J., The Walsh Industries in Cuyahoga Falls. Unpublished report from the Cuyahoga Falls Historical Society, 1984.

Rumschlag, J. H., The sediment and morphologic response of the Cuyahoga River to the removal of the Munroe Falls Dam, Summit County, Ohio. Master's Thesis. Department of Geology, University of Akron, 2007.

Rumschlag, J, H., Peck J. A., 2007, Short-term sediment and morphologic response of the middle Cuyahoga River to the removal of the Munroe Falls dam, Summit County, Ohio. Journal Of Great Lakes Research 33, no. Special issue 2, p. 142-153.

Peck, J, A., Kasper N. R., 2013, Multiyear assessment of the sedimentological impacts of the removal of the Munroe Falls Dam on the middle Cuyahoga River, Ohio. Reviews In Engineering Geology v. 21, p. 81-92.

Peck, J. A., Mullen, A., Moore, A., Rumschlag, J. H., 2007, The legacy sediment record within the Munroe Falls dam pool, Cuyahoga River, Summit County, Ohio. Journal of Great Lakes Research 33, no. Special issue 2, p. 127-141.

Peck, M., 2012, Middle Cuyahoga River Watershed Action Plan, Northeast Ohio Four County Regional Planning and Development Organization, no. 1, 491 p.

Press, F., Siever, R., Earth, fourth edition, New York, W.H. Freeman and Company, 1986.

Schiefer, M. C., 2002, Basin Descriptions and flow Characteristics of Ohio Streams. Ohio Department of Natural resources Division of Water, Bulletin 47, p. 12-26.

Shields, F. D. Jr., Morin, N., Cooper, C. M., 2004, Large woody debris structures for sand-bed channels, Journal of Hydraulic Engineering v. 217, p. 1-12.

Stanley, E. H., Doyle, M. W., 2002, A Geomorphic Perspective on Nutrient Retention Following Dam Removal. Bioscience v. 52, no. 8 p. 693.

Summit County Interactive GIS Database, 2014. scids.summitoh.net

Surface Water data for USA, 2014, Old Portage Stream Gauge USGS 04206000USGS, Surface- Water Daily Statistics. http://waterdata.usgs.gov.

Szabo, J, P., 1987, Wisconsinan stratigraphy of the Cuyahoga Valley in the Erie Basin, northeastern Ohio. Canadian Journal of Earth Science. v. 24, p. 279-290.

Szabo, J. P., Ryan, D. E., 1981, Quaternary Stratigraphy of the Lower Mud Brook Basin,Northampton Township, Summit County, Ohio. Ohio Journal of Science. v. 81 no. 6, p. 239.

Szabo, J. P., Huth-Pyscher, C. G., Kushner, V. A., 2013, Vertical Variability and Latera Distribution of Late Wisconsinan Sediments Parallel to the Axis of the Buried Valley of Mud Brook North of Akron, Summit County, Ohio. Ohio Journal of Science v. 111 no. 2-5, p.18-27.

USGS., 1994, 7.5 minute Hudson Quadrangle 2 ft. topographic contour map.

Jiao, Yu-Yong, Zhang, Huan-Qiang, Tang, Hui-Ming, Zhang, Xiu-Li, Adoko, Amoussou Coffi, Tian, Hu-Nan., 2014, Simulating the process of reservoir impoundment- induced landslide using the extended DDA method, Engineering Geology, v. 39, no. 1, 1011.

APPENDICES

APPENDIX A

GRAIN SIZE DATA OF SEDIMENT SAMPLES FROM THE DEEP WATER CHANNEL ENVIRONMENT

Grain size analysis was performed on deep water sediment samples collected from 2013 through 2014 following the method of Folk (1980). Samples were sieved at half phi intervals. Mud fractions (> 4 ϕ) were measured using the pipette method. Sample identifications ending in "R" are the replicate samples.

Sample ID	CR13-G1
Initial wt. (g)	259.034
% error	0.285

m_ϕ	phi (ϕ)	Individual wt. (g)	Individual wt. %	% G S M	Cummulative wt. %	fm_ϕ	m_ϕ-x	$(m_\phi-x)^2$	$f(m_\phi-x)^2$	$(m_\phi-x)^3$	$f(m_\phi-x)^3$
-5.75	-5.5	132.941	51.468		51.468	-295.944	-2.572	6.614	340.413	-17.010	-875.464
-3.675	-3.35	5.129	1.986	73.190	53.454	-7.297	-0.497	0.247	0.490	-0.123	-0.243
-3.175	-3	2.702	1.046		54.500	-3.321	0.003	0.000	0.000	0.000	0.000
-2.75	-2.5	4.720	1.827		56.328	-5.025	0.428	0.183	0.335	0.079	0.143
-2.25	-2	18.642	7.217		63.545	-16.239	0.928	0.862	6.218	0.800	5.772
-1.75	-1.5	11.850	4.588		68.133	-8.029	1.428	2.040	9.358	2.913	13.366
-1.25	-1	13.062	5.057		73.190	-6.321	1.928	3.718	18.802	7.169	36.255
-0.75	-0.5	7.836	3.034		76.223	-2.275	2.428	5.896	17.888	14.318	43.436
-0.25	0	7.870	3.047		79.270	-0.762	2.928	8.575	26.126	25.108	76.502
0.25	0.5	7.159	2.772		82.042	0.693	3.428	11.753	32.574	40.291	111.672
0.75	1	12.439	4.816		86.858	3.612	3.928	15.431	74.312	60.616	291.916
1.25	1.5	13.926	5.391		92.249	6.739	4.428	19.609	105.723	86.834	468.165
1.75	2	11.211	4.340	26.667	96.590	7.596	4.928	24.287	105.416	119.694	519.516
2.25	2.5	5.437	2.105		98.695	4.736	5.428	29.466	62.024	159.946	336.679
2.75	3	2.104	0.815		99.509	2.240	5.928	35.144	28.627	208.341	169.708
3.25	3.5	0.711	0.275		99.784	0.895	6.428	41.322	11.375	265.628	73.118
3.75	4	0.188	0.073		99.857	0.273	6.928	48.000	3.494	332.557	24.205
4.25	> 4	0.369	0.143	0.143	100.000	0.607	7.428	55.179	7.883	409.879	58.555
	TOTAL	258.296				-317.823			851.058		1353.301
meanϕ	-3.178	SKϕ	13.533								
σϕ	2.917	D50	-5.514								

Sample ID	CR13-G2
Initial wt. (g)	123.365
% error	0.765

m_{ϕ}	phi (ϕ)	Individual wt. (g)	Individual wt. %	% G S M	Cummulative wt. %	fm_{ϕ}	m_{ϕ}-x	$(m_{\phi}-x)^2$	$f(m_{\phi}-x)^2$	$(m_{\phi}-x)^3$	$f(m_{\phi}-x)^3$
-3.175	-3	5.331	4.355	18.052	4.355	-13.826	-3.683	13.563	59.063	-49.951	-217.520
-2.75	-2.5	1.814	1.482		5.836	-4.075	-3.258	10.613	15.727	-34.577	-51.235
-2.25	-2	4.977	4.065		9.902	-9.147	-2.758	7.606	30.921	-20.975	-85.274
-1.75	-1.5	3.290	2.687		12.589	-4.703	-2.258	5.098	13.700	-11.510	-30.933
-1.25	-1	6.687	5.462		18.052	-6.828	-1.758	3.090	16.878	-5.432	-29.669
-0.75	-0.5	6.487	5.299		23.351	-3.974	-1.258	1.582	8.384	-1.990	-10.545
-0.25	0	10.017	8.182		31.533	-2.046	-0.758	0.574	4.699	-0.435	-3.561
0.25	0.5	9.934	8.115		39.648	2.029	-0.258	0.066	0.539	-0.017	-0.139
0.75	1	17.430	14.238		53.885	10.678	0.242	0.059	0.835	0.014	0.202
1.25	1.5	18.962	15.489		69.375	19.361	0.742	0.551	8.532	0.409	6.332
1.75	2	19.201	15.684	81.748	85.059	27.448	1.242	1.543	24.201	1.917	30.061
2.25	2.5	14.311	11.690		96.749	26.302	1.742	3.035	35.481	5.288	61.813
2.75	3	3.065	2.504		99.253	6.885	2.242	5.027	12.587	11.272	28.221
3.25	3.5	0.549	0.448		99.701	1.457	2.742	7.519	3.372	20.620	9.247
3.75	4	0.121	0.099		99.800	0.371	3.242	10.512	1.039	34.080	3.368
4.25	> 4	0.245	0.200	0.200	100.000	0.851	3.742	14.004	2.803	52.405	10.488
	TOTAL	122.421				50.783			238.760		-279.144
$mean_{\phi}$	0.508	SKϕ	-2.791								
σϕ	1.545	D50	0.864								

Sample ID	CR13-G3
Initial wt. (g)	124.795
% error	-0.059

m_ϕ	phi (ϕ)	Individual wt. (g)	Individual wt. %	% G S M	Cummulative wt. %	fm_ϕ	m_ϕ-x	$(m_\phi-x)^2$	$f(m_\phi-x)^2$	$(m_\phi-x)^3$	$f(m_\phi-x)^3$
-3.175	-3	8.926	7.148	55.108	7.148	-22.696	-2.294	5.263	37.623	-12.075	-86.313
-2.75	-2.5	7.457	5.972		13.120	-16.423	-1.869	3.494	20.864	-6.530	-38.999
-2.25	-2	21.301	17.059		30.179	-38.382	-1.369	1.875	31.978	-2.567	-43.784
-1.75	-1.5	15.954	12.777		42.955	-22.359	-0.869	0.755	9.652	-0.657	-8.389
-1.25	-1	15.175	12.153		55.108	-15.191	-0.369	0.136	1.656	-0.050	-0.611
-0.75	-0.5	10.755	8.613		63.721	-6.460	0.131	0.017	0.147	0.002	0.019
-0.25	0	10.32	8.265		71.986	-2.066	0.631	0.398	3.289	0.251	2.075
0.25	0.5	8.37	6.703		78.689	1.676	1.131	1.279	8.572	1.446	9.693
0.75	1	6.584	5.273		83.962	3.955	1.631	2.660	14.023	4.337	22.870
1.25	1.5	6.625	5.306		89.267	6.632	2.131	4.540	24.090	9.675	51.331
1.75	2	6.974	5.585	44.649	94.852	9.774	2.631	6.921	38.656	18.209	101.697
2.25	2.5	3.691	2.956		97.808	6.651	3.131	9.802	28.974	30.689	90.713
2.75	3	1.615	1.293		99.101	3.557	3.631	13.183	17.050	47.865	61.907
3.25	3.5	0.603	0.483		99.584	1.569	4.131	17.064	8.240	70.488	34.039
3.75	4	0.216	0.173		99.757	0.649	4.631	21.445	3.710	99.306	17.178
4.25	> 4	0.303	0.243	0.243	100.000	1.031	5.131	26.325	6.388	135.072	32.776
	TOTAL	124.869				-88.083			254.913		246.201
meanϕ	-0.881	SKϕ	2.462								
$\sigma\phi$	1.597	D50	-1.297								

					Sample ID	CR13-G4					
					Initial wt. (g)	131.649					
					% error	0.032					
m_ϕ	phi (ϕ)	Individual wt. (g)	Individual wt. %	% G S M	Cummulative wt. %	fm_ϕ	m_ϕ-x	$(m_\phi\text{-}x)^2$	$f(m_\phi\text{-}x)^2$	$(m_\phi\text{-}x)^3$	$f(m_\phi\text{-}x)^3$
-3.675	-3.35	4.278	3.251	58.473	3.251	-11.946	-2.673	7.144	23.222	-19.095	-62.069
-3.175	-3	15.044	11.431		14.682	-36.293	-2.173	4.721	53.968	-10.258	-117.262
-2.75	-2.5	4.927	3.744		18.425	-10.295	-1.748	3.055	11.437	-5.339	-19.989
-2.25	-2	22.533	17.121		35.547	-38.523	-1.248	1.557	26.659	-1.943	-33.266
-1.75	-1.5	17.195	13.065		48.612	-22.864	-0.748	0.559	7.307	-0.418	-5.464
-1.25	-1	12.978	9.861		58.473	-12.326	-0.248	0.061	0.606	-0.015	-0.150
-0.75	-0.5	9.017	6.851		65.325	-5.139	0.252	0.064	0.436	0.016	0.110
-0.25	0	7.069	5.371		70.696	-1.343	0.752	0.566	3.039	0.426	2.286
0.25	0.5	6.075	4.616		75.312	1.154	1.252	1.568	7.238	1.963	9.063
0.75	1	6.772	5.146		80.458	3.859	1.752	3.070	15.798	5.379	27.680
1.25	1.5	10.548	8.015		88.472	10.018	2.252	5.072	40.653	11.424	91.559
1.75	2	10.409	7.909	41.253	96.382	13.841	2.752	7.574	59.908	20.846	164.877
2.25	2.5	2.727	2.072		98.454	4.662	3.252	10.577	21.916	34.397	71.274
2.75	3	1.020	0.775		99.229	2.131	3.752	14.079	10.912	52.826	40.942
3.25	3.5	0.481	0.365		99.594	1.188	4.252	18.081	6.608	76.884	28.100
3.75	4	0.174	0.132		99.726	0.496	4.752	22.583	2.986	107.319	14.189
4.25	> 4	0.360	0.274	0.274	100.000	1.163	5.252	27.585	7.546	144.883	39.632
	TOTAL	131.607				-100.218			300.236		251.511
meanϕ	-1.002	SKϕ	2.515								
σϕ	1.733	D50	-1.430								

Sanmple ID	CR13-G5
Initial wt. (g)	109.556
% error	0.183

m_ϕ	phi (ϕ)	Individual wt. (g)	Individual wt. %	% G S M	Cummulative wt. %	fm_ϕ	m_ϕ-x	$(m_\phi-x)^2$	$f(m_\phi-x)^2$	$(m_\phi-x)^3$	$f(m_\phi-x)^3$
-3.675	-3.35	0.202	0.185	24.589	0.185	-0.679	-3.674	13.497	2.493	-49.588	-9.160
-3.175	-3	0.645	0.590		0.775	-1.873	-3.174	10.073	5.942	-31.972	-18.858
-2.75	-2.5	1.823	1.667		2.442	-4.584	-2.749	7.556	12.597	-20.771	-34.627
-2.25	-2	5.480	5.011		7.453	-11.275	-2.249	5.057	25.344	-11.374	-56.995
-1.75	-1.5	7.501	6.859		14.312	-12.004	-1.749	3.059	20.979	-5.349	-36.690
-1.25	-1	11.239	10.277		24.589	-12.847	-1.249	1.560	16.030	-1.948	-20.019
-0.75	-0.5	11.282	10.317		34.906	-7.738	-0.749	0.561	5.786	-0.420	-4.333
-0.25	0	14.629	13.377		48.284	-3.344	-0.249	0.062	0.829	-0.015	-0.206
0.25	0.5	15.574	14.242		62.525	3.560	0.251	0.063	0.898	0.016	0.226
0.75	1	14.205	12.990		75.515	9.742	0.751	0.564	7.329	0.424	5.505
1.25	1.5	13.044	11.928		87.443	14.910	1.251	1.565	18.671	1.958	23.360
1.75	2	8.311	7.600	75.175	95.043	13.300	1.751	3.066	23.305	5.370	40.810
2.25	2.5	3.581	3.275		98.317	7.368	2.251	5.068	16.594	11.408	37.356
2.75	3	0.947	0.866		99.183	2.381	2.751	7.569	6.554	20.822	18.032
3.25	3.5	0.462	0.422		99.606	1.373	3.251	10.570	4.465	34.364	14.518
3.75	4	0.173	0.158		99.764	0.593	3.751	14.071	2.226	52.782	8.350
4.25	> 4	0.258	0.236	0.236	100.000	1.003	4.251	18.072	4.264	76.827	18.125
	TOTAL	109.356				-0.112			174.305		-14.606
meanϕ	-0.001	SKϕ	-0.146								
σϕ	1.320	D50	0.060								

Sample ID	CR13-G6
Initial wt. (g)	111.433
% error	0.434

m_ϕ	phi (ϕ)	Individual wt. (g)	Individual wt. %	% G S M	Cummulative wt. %	fm_ϕ	m_ϕ-x	$(m_\phi-x)^2$	$f(m_\phi-x)^2$	$(m_\phi-x)^3$	$f(m_\phi-x)^3$
-3.675	-3.35	3.154	2.843	44.443	2.843	-10.447	-3.011	9.063	25.765	-27.285	-77.566
-3.175	-3	4.909	4.425		7.267	-14.048	-2.511	6.303	27.887	-15.823	-70.012
-2.75	-2.5	1.841	1.659		8.927	-4.563	-2.086	4.349	7.217	-9.071	-15.052
-2.25	-2	11.255	10.144		19.071	-22.825	-1.586	2.514	25.502	-3.986	-40.434
-1.75	-1.5	13.735	12.380		31.450	-21.664	-1.086	1.178	14.588	-1.279	-15.836
-1.25	-1	14.415	12.992		44.443	-16.241	-0.586	0.343	4.455	-0.201	-2.608
-0.75	-0.5	11.989	10.806		55.249	-8.104	-0.086	0.007	0.079	-0.001	-0.007
-0.25	0	11.061	9.969		65.218	-2.492	0.414	0.172	1.713	0.071	0.710
0.25	0.5	10.493	9.457		74.676	2.364	0.914	0.836	7.909	0.765	7.232
0.75	1	10.613	9.566		84.241	7.174	1.414	2.001	19.138	2.830	27.070
1.25	1.5	10.837	9.768		94.009	12.209	1.914	3.665	35.800	7.017	68.537
1.75	2	5.145	4.637	55.289	98.646	8.115	2.414	5.830	27.034	14.075	65.272
2.25	2.5	0.618	0.557		99.203	1.253	2.914	8.494	4.731	24.756	13.789
2.75	3	0.219	0.197		99.401	0.543	3.414	11.659	2.301	39.808	7.858
3.25	3.5	0.228	0.205		99.606	0.668	3.914	15.323	3.149	59.981	12.326
3.75	4	0.140	0.126		99.732	0.473	4.414	19.487	2.459	86.027	10.855
4.25	> 4	0.297	0.268	0.268	100.000	1.138	4.914	24.152	6.465	118.694	31.773
	TOTAL	110.949				-66.446			216.191		23.908
meanϕ	-0.664	SKϕ	0.239								
$\sigma\phi$	1.470	D50	-0.763								

Sample ID	CR13-G7
Initial wt. (g)	69.204
% error	-0.389

m_ϕ	phi (ϕ)	Individual wt. (g)	Individual wt. %	% G S M	Cummulative wt. %	fm_ϕ	m_ϕ-x	$(m_\phi-x)^2$	$f(m_\phi-x)^2$	$(m_\phi-x)^3$	$f(m_\phi-x)^3$
-3.175	-3	1.565	2.253	8.170	2.253	-7.152	-3.884	15.083	33.978	-58.579	-131.960
-2.75	-2.5	0.702	1.010		3.263	-2.779	-3.459	11.963	12.088	-41.376	-41.809
-2.25	-2	0.268	0.386		3.649	-0.868	-2.959	8.754	3.377	-25.901	-9.991
-1.75	-1.5	0.948	1.365		5.013	-2.388	-2.459	6.045	8.249	-14.864	-20.282
-1.25	-1	2.193	3.157		8.170	-3.946	-1.959	3.837	12.111	-7.515	-23.721
-0.75	-0.5	2.923	4.207		12.377	-3.156	-1.459	2.128	8.953	-3.104	-13.059
-0.25	0	5.831	8.393		20.771	-2.098	-0.959	0.919	7.714	-0.881	-7.396
0.25	0.5	7.325	10.544		31.314	2.636	-0.459	0.210	2.219	-0.097	-1.018
0.75	1	14.753	21.236		52.550	15.927	0.041	0.002	0.036	0.000	0.001
1.25	1.5	17.379	25.015		77.565	31.269	0.541	0.293	7.329	0.159	3.967
1.75	2	12.135	17.467	91.467	95.033	30.568	1.041	1.084	18.939	1.129	19.721
2.25	2.5	2.669	3.842		98.874	8.644	1.541	2.376	9.126	3.661	14.066
2.75	3	0.014	0.020		98.895	0.055	2.041	4.167	0.084	8.506	0.171
3.25	3.5	0.233	0.335		99.230	1.090	2.541	6.458	2.166	16.412	5.504
3.75	4	0.283	0.407		99.637	1.528	3.041	9.249	3.768	28.130	11.459
4.25	> 4	0.252	0.363	0.363	100.000	1.542	3.541	12.541	4.549	44.410	16.109
	TOTAL	69.473				70.872			134.686		-178.237
meanϕ	0.709	SKϕ	-1.782								
σϕ	1.161	D50	0.940								

Sample ID	CR13-G8
Initial wt. (g)	123.685
% error	0.169

m_ϕ	phi (ϕ)	Individual wt. (g)	Individual wt. %	% G S M	Cummulative wt. %	fm_ϕ	m_ϕ-x	$(m_\phi\text{-}x)^2$	$f(m_\phi\text{-}x)^2$	$(m_\phi\text{-}x)^3$	$f(m_\phi\text{-}x)^3$
-2.75	-2.5	7.174	5.810	24.559	5.810	-15.978	-2.653	7.038	40.892	-18.672	-108.486
-2.25	-2	5.687	4.606		10.416	-10.363	-2.153	4.635	21.349	-9.980	-45.963
-1.75	-1.5	8.121	6.577		16.993	-11.510	-1.653	2.732	17.970	-4.516	-29.704
-1.25	-1	9.343	7.567		24.559	-9.458	-1.153	1.329	10.059	-1.533	-11.597
-0.75	-0.5	11.592	9.388		33.947	-7.041	-0.653	0.426	4.003	-0.278	-2.614
-0.25	0	17.358	14.058		48.005	-3.514	-0.153	0.023	0.329	-0.004	-0.050
0.25	0.5	18.147	14.697		62.702	3.674	0.347	0.120	1.770	0.042	0.614
0.75	1	19.873	16.095		78.797	12.071	0.847	0.717	11.547	0.608	9.781
1.25	1.5	16.005	12.962		91.759	16.203	1.347	1.815	23.520	2.444	31.682
1.75	2	7.621	6.172	75.209	97.931	10.801	1.847	3.412	21.056	6.301	38.892
2.25	2.5	1.835	1.486		99.417	3.344	2.347	5.509	8.186	12.929	19.214
2.75	3	0.221	0.179		99.596	0.492	2.847	8.106	1.451	23.077	4.130
3.25	3.5	0.137	0.111		99.707	0.361	3.347	11.203	1.243	37.496	4.160
3.75	4	0.076	0.062		99.768	0.231	3.847	14.800	0.911	56.935	3.504
4.25	> 4	0.286	0.232	0.232	100.000	0.984	4.347	18.897	4.377	82.145	19.027
	TOTAL	123.476				-9.704			168.663		-67.411
meanϕ	-0.097	SKϕ	-0.674								
σϕ	1.299	D50	0.068								

Sample ID	CR13-G9
Initial wt. (g)	73.254
% error	-0.564

m_ϕ	phi (ϕ)	Individual wt. (g)	Individual wt. %	% G S M	Cummulative wt. %	fm_ϕ	m_ϕ-x	$(m_\phi-x)^2$	$f(m_\phi-x)^2$	$(m_\phi-x)^3$	$f(m_\phi-x)^3$
-3.175	-3	1.551	2.105	4.803	2.105	-6.685	-4.636	21.488	45.241	-99.608	-209.717
-2.75	-2.5	0.000	0.000		2.105	0.000	-4.211	17.728	0.000	-74.646	0.000
-2.25	-2	0.292	0.396		2.502	-0.892	-3.711	13.768	5.457	-51.086	-20.249
-1.75	-1.5	0.565	0.767		3.269	-1.342	-3.211	10.307	7.905	-33.092	-25.381
-1.25	-1	1.130	1.534		4.803	-1.917	-2.711	7.347	11.270	-19.914	-30.547
-0.75	-0.5	0.449	0.609		5.412	-0.457	-2.211	4.886	2.978	-10.801	-6.583
-0.25	0	0.645	0.876		6.288	-0.219	-1.711	2.926	2.562	-5.005	-4.382
0.25	0.5	1.197	1.625		7.913	0.406	-1.211	1.465	2.381	-1.774	-2.882
0.75	1	6.488	8.807		16.720	6.605	-0.711	0.505	4.446	-0.359	-3.159
1.25	1.5	17.100	23.213		39.932	29.016	-0.211	0.044	1.029	-0.009	-0.217
1.75	2	25.502	34.618	93.938	74.550	60.581	0.289	0.084	2.901	0.024	0.840
2.25	2.5	16.393	22.253		96.803	50.069	0.789	0.623	13.870	0.492	10.950
2.75	3	1.175	1.595		98.398	4.386	1.289	1.663	2.652	2.144	3.420
3.25	3.5	0.201	0.273		98.671	0.887	1.789	3.202	0.874	5.730	1.564
3.75	4	0.051	0.069		98.740	0.260	2.289	5.242	0.363	12.001	0.831
4.25	> 4	0.928	1.260	1.260	100.000	5.354	2.789	7.781	9.802	21.706	27.343
	TOTAL	73.667				146.052			113.731		-258.170
meanϕ	1.461	SKϕ	-2.582								
σϕ	1.066	D50	1.855								

					Sample ID	CR13-G9-R					
					Initial wt. (g)	71.850					
					% error	0.214					
m_ϕ	phi (ϕ)	Individual wt. (g)	Individual wt. %	% G S M	Cummulative wt. %	fm_ϕ	m_ϕ-x	$(m_\phi\text{-x})^2$	$f(m_\phi\text{-x})^2$	$(m_\phi\text{-x})^3$	$f(m_\phi\text{-x})^3$
-2.75	-2.5	0.082	0.114	1.557	0.114	-0.315	-4.323	18.686	2.137	-80.777	-9.239
-2.25	-2	0.181	0.252		0.367	-0.568	-3.823	14.614	3.689	-55.864	-14.103
-1.75	-1.5	0.322	0.449		0.816	-0.786	-3.323	11.041	4.959	-36.686	-16.476
-1.25	-1	0.531	0.741		1.557	-0.926	-2.823	7.968	5.901	-22.492	-16.658
-0.75	-0.5	0.337	0.470		2.027	-0.353	-2.323	5.395	2.536	-12.532	-5.891
-0.25	0	0.484	0.675		2.702	-0.169	-1.823	3.322	2.243	-6.056	-4.088
0.25	0.5	1.376	1.919		4.621	0.480	-1.323	1.750	3.358	-2.314	-4.442
0.75	1	5.491	7.659		12.280	5.744	-0.823	0.677	5.185	-0.557	-4.266
1.25	1.5	17.838	24.880		37.160	31.100	-0.323	0.104	2.592	-0.034	-0.837
1.75	2	28.817	40.193	98.205	77.353	70.338	0.177	0.031	1.262	0.006	0.224
2.25	2.5	14.481	20.198		97.551	45.445	0.677	0.459	9.263	0.311	6.273
2.75	3	1.370	1.911		99.462	5.255	1.177	1.386	2.648	1.631	3.118
3.25	3.5	0.154	0.215		99.676	0.698	1.677	2.813	0.604	4.718	1.013
3.75	4	0.061	0.085		99.761	0.319	2.177	4.740	0.403	10.321	0.878
4.25	> 4	0.171	0.239	0.239	100.000	1.014	2.677	7.168	1.710	19.189	4.577
	TOTAL	71.696				157.277			48.491		-59.917
$mean_\phi$	1.573	SKϕ	-0.599								
$\sigma\phi$	0.696	D50	1.660								

					Sample ID	CR13-G10					
					Initial wt. (g)	70.412					
					% error	0.528					
m_ϕ	phi (ϕ)	Individual wt. (g)	Individual wt. %	% G S M	Cummulative wt. %	fm_ϕ	m_ϕ-x	$(m_\phi-x)^2$	$f(m_\phi-x)^2$	$(m_\phi-x)^3$	$f(m_\phi-x)^3$
-2.25	-2	0.196	0.280	1.298	0.280	-0.630	-3.359	11.282	3.157	-37.892	-10.604
-1.75	-1.5	0.116	0.166		0.445	-0.290	-2.859	8.173	1.354	-23.364	-3.870
-1.25	-1	0.597	0.852		1.298	-1.065	-2.359	5.564	4.743	-13.124	-11.187
-0.75	-0.5	0.735	1.049		2.347	-0.787	-1.859	3.455	3.626	-6.422	-6.740
-0.25	0	3.847	5.493		7.840	-1.373	-1.359	1.846	10.141	-2.509	-13.780
0.25	0.5	8.111	11.581		19.420	2.895	-0.859	0.738	8.541	-0.633	-7.335
0.75	1	13.112	18.721		38.141	14.041	-0.359	0.129	2.410	-0.046	-0.865
1.25	1.5	21.181	30.241		68.382	37.802	0.141	0.020	0.603	0.003	0.085
1.75	2	16.523	23.591	98.507	91.973	41.284	0.641	0.411	9.699	0.264	6.219
2.25	2.5	4.884	6.973		98.946	15.690	1.141	1.302	9.081	1.486	10.364
2.75	3	0.479	0.684		99.630	1.881	1.641	2.694	1.842	4.421	3.023
3.25	3.5	0.072	0.103		99.733	0.334	2.141	4.585	0.471	9.817	1.009
3.75	4	0.050	0.071		99.804	0.268	2.641	6.976	0.498	18.425	1.315
4.25	> 4	0.137	0.196	0.196	100.000	0.831	3.141	9.867	1.930	30.995	6.063
	TOTAL	70.040				110.879			58.096		-26.300
meanϕ	1.109	SKϕ	-0.263								
σϕ	0.762	D50	1.317								

					Sample ID	CR13-G10 R				
					Initial wt. (g)	78.554				
					% error	0.284				
m_ϕ	phi (ϕ)	Individual wt. (g)	Individual wt. %	% G S M	Cummulative wt. %	fm_ϕ	m_ϕ-x	$(m_\phi\text{-x})^2$	$f(m_\phi\text{-x})^2$	$(m_\phi\text{-x})^3$
-1.75	-1.5	0.089	0.114	0.712	0.114	-0.199	-2.883	8.314	0.945	-23.973
-1.25	-1	0.469	0.599		0.712	-0.748	-2.383	5.681	3.401	-13.540
-0.75	-0.5	1.451	1.852		2.565	-1.389	-1.883	3.547	6.571	-6.681
-0.25	0	3.501	4.469		7.034	-1.117	-1.383	1.914	8.554	-2.648
0.25	0.5	8.962	11.441		18.475	2.860	-0.883	0.780	8.929	-0.689
0.75	1	15.228	19.441		37.916	14.580	-0.383	0.147	2.858	-0.056
1.25	1.5	22.656	28.923		66.839	36.154	0.117	0.014	0.393	0.002
1.75	2	19.801	25.279	98.995	92.118	44.238	0.617	0.380	9.610	0.234
2.25	2.5	5.177	6.609		98.727	14.871	1.117	1.247	8.240	1.392
2.75	3	0.601	0.767		99.494	2.110	1.617	2.613	2.005	4.225
3.25	3.5	0.091	0.116		99.611	0.378	2.117	4.480	0.520	9.482
3.75	4	0.076	0.097		99.708	0.364	2.617	6.846	0.664	17.914
4.25	> 4	0.229	0.292	0.292	100.000	1.242	3.117	9.713	2.840	30.271
	TOTAL	78.331				113.343			55.531	
$mean_\phi$	1.133	SKϕ	-0.139							
$\sigma\phi$	0.745	D50	1.209							

					Sample ID	CR13-G11					
					Initial wt. (g)	71.836					
					% error	-0.093					
m_ϕ	phi (ϕ)	Individual wt. (g)	Individual wt. %	% G S M	Cummulative wt. %	fm_ϕ	m_ϕ-x	$(m_\phi\text{-}x)^2$	$f(m_\phi\text{-}x)^2$	$(m_\phi\text{-}x)^3$	$f(m_\phi\text{-}x)^3$
-2.75	-2.5	0.398	0.55	4.252	0.554	-1.522	-3.793	14.390	7.965	-54.588	-30.216
-2.25	-2	0.576	0.80		1.355	-1.802	-3.293	10.847	8.689	-35.723	-28.617
-1.75	-1.5	0.773	1.08		2.430	-1.881	-2.793	7.803	8.389	-21.798	-23.434
-1.25	-1	1.310	1.82		4.252	-2.277	-2.293	5.260	9.583	-12.063	-21.978
-0.75	-0.5	2.415	3.36		7.610	-2.519	-1.793	3.216	10.803	-5.768	-19.374
-0.25	0	3.699	5.14		12.755	-1.286	-1.293	1.673	8.607	-2.164	-11.132
0.25	0.5	7.476	10.40		23.152	2.599	-0.793	0.630	6.546	-0.500	-5.193
0.75	1	12.284	17.08		40.236	12.813	-0.293	0.086	1.471	-0.025	-0.432
1.25	1.5	18.937	26.34		66.573	32.921	0.207	0.043	1.124	0.009	0.232
1.75	2	15.315	21.30	95.061	87.873	37.274	0.707	0.499	10.633	0.353	7.513
2.25	2.5	6.793	9.45		97.320	21.257	1.207	1.456	13.754	1.757	16.595
2.75	3	1.050	1.46		98.780	4.016	1.707	2.912	4.253	4.970	7.258
3.25	3.5	0.238	0.33		99.111	1.076	2.207	4.869	1.612	10.744	3.556
3.75	4	0.145	0.20		99.313	0.756	2.707	7.325	1.477	19.827	3.998
4.25	> 4	0.494	0.69	0.687	100.000	2.920	3.207	10.282	7.064	32.970	22.652
	TOTAL	71.903				104.344			101.969		-78.573
meanϕ	1.043	SKϕ	-0.786								
σϕ	1.010	D50	1.185								

Sample ID	CR13-G12
Initial wt. (g)	68.486
% error	-0.092

m_ϕ	phi (ϕ)	Individual wt. (g)	Individual wt. %	% G S M	Cummulative wt. %	fm_ϕ	m_ϕ-x	$(m_\phi-x)^2$	$f(m_\phi-x)^2$	$(m_\phi-x)^3$	$f(m_\phi-x)^3$
-3.175	-3	0.979	1.428	8.547	1.428	-4.534	-3.951	15.608	22.291	-61.661	-88.063
-2.75	-2.5	0.343	0.500		1.929	-1.376	-3.526	12.430	6.220	-43.825	-21.929
-2.25	-2	1.655	2.414		4.343	-5.432	-3.026	9.155	22.102	-27.699	-66.874
-1.75	-1.5	1.242	1.812		6.155	-3.171	-2.526	6.379	11.558	-16.111	-29.191
-1.25	-1	1.640	2.392		8.547	-2.991	-2.026	4.103	9.817	-8.312	-19.886
-0.75	-0.5	1.942	2.833		11.380	-2.125	-1.526	2.328	6.594	-3.551	-10.061
-0.25	0	4.085	5.959		17.339	-1.490	-1.026	1.052	6.269	-1.079	-6.430
0.25	0.5	5.834	8.511		25.850	2.128	-0.526	0.276	2.352	-0.145	-1.236
0.75	1	15.961	23.284		49.134	17.463	-0.026	0.001	0.015	0.000	0.000
1.25	1.5	18.209	26.563		75.698	33.204	0.474	0.225	5.977	0.107	2.835
1.75	2	13.563	19.786	91.141	95.484	34.625	0.974	0.949	18.783	0.925	18.301
2.25	2.5	2.453	3.578		99.062	8.052	1.474	2.174	7.778	3.205	11.468
2.75	3	0.271	0.395		99.457	1.087	1.974	3.898	1.541	7.696	3.042
3.25	3.5	0.089	0.130		99.587	0.422	2.474	6.122	0.795	15.149	1.967
3.75	4	0.069	0.101		99.688	0.377	2.974	8.847	0.890	26.313	2.649
4.25	> 4	0.214	0.312	0.312	100.000	1.327	3.474	12.071	3.768	41.939	13.093
	TOTAL	68.549				77.567			126.751		-190.316
meanϕ	0.776	SKϕ	-1.903								
σϕ	1.126	D50	1.016								

	Sample ID	CR13-G13
	Initial wt. (g)	112.803
	% error	0.127

m_ϕ	phi (ϕ)	Individual wt. (g)	Individual wt. %	% G S M	Cummulative wt. %	fm_ϕ	m_ϕ-x	$(m_\phi\text{-x})^2$	$f(m_\phi\text{-x})^2$	$(m_\phi\text{-x})^3$	$f(m_\phi\text{-x})^3$
-3.675	-3.35	2.229	1.979	18.959	1.979	-7.271	-4.152	17.243	34.115	-71.599	-141.660
-3.175	-3	0.903	0.802		2.780	-2.545	-3.652	13.340	10.693	-48.724	-39.054
-2.75	-2.5	2.196	1.949		4.729	-5.360	-3.227	10.416	20.304	-33.618	-65.529
-2.25	-2	5.819	5.165		9.894	-11.621	-2.727	7.439	38.422	-20.289	-104.794
-1.75	-1.5	5.083	4.512		14.406	-7.896	-2.227	4.961	22.385	-11.051	-49.861
-1.25	-1	5.129	4.553		18.959	-5.691	-1.727	2.984	13.585	-5.155	-23.467
-0.75	-0.5	4.708	4.179		23.138	-3.134	-1.227	1.507	6.296	-1.849	-7.728
-0.25	0	5.617	4.986		28.124	-1.246	-0.727	0.529	2.638	-0.385	-1.919
0.25	0.5	6.509	5.778		33.901	1.444	-0.227	0.052	0.299	-0.012	-0.068
0.75	1	18.099	16.065		49.966	12.049	0.273	0.074	1.194	0.020	0.325
1.25	1.5	28.802	25.565		75.532	31.957	0.773	0.597	15.259	0.461	11.789
1.75	2	22.188	19.695	80.440	95.226	34.466	1.273	1.619	31.894	2.061	40.588
2.25	2.5	3.861	3.427		98.653	7.711	1.773	3.142	10.768	5.569	19.087
2.75	3	0.410	0.364		99.017	1.001	2.273	5.165	1.880	11.737	4.271
3.25	3.5	0.237	0.210		99.228	0.684	2.773	7.687	1.617	21.313	4.484
3.75	4	0.193	0.171		99.399	0.642	3.273	10.710	1.835	35.048	6.004
4.25	> 4	0.677	0.601	0.601	100.000	2.554	3.773	14.232	8.553	53.692	32.265
	TOTAL	112.660				47.743			221.736		-315.266
meanϕ	0.477	SKϕ	-3.153								
σϕ	1.489	D50	1.001								

Sample ID	CR13-G14
Initial wt. (g)	19.437
% error	0.880

m_ϕ	phi (ϕ)	Individual wt. (g)	Individual wt. %	% G S M	Cummulative wt. %	fm_ϕ	m_ϕ-x	$(m_\phi-x)^2$	$f(m_\phi-x)^2$	$(m_\phi-x)^3$	$f(m_\phi-x)^3$
-2.75	-2.5	0.146	0.758	23.129	0.758	-2.084	-3.346	11.194	8.483	-37.452	-28.382
-2.25	-2	0.556	2.886		3.644	-6.493	-2.846	8.098	23.371	-23.045	-66.507
-1.75	-1.5	1.441	7.479		11.123	-13.089	-2.346	5.502	41.156	-12.907	-96.541
-1.25	-1	2.313	12.006		23.129	-15.007	-1.846	3.407	40.900	-6.288	-75.491
-0.75	-0.5	2.591	13.449		36.577	-10.086	-1.346	1.811	24.356	-2.437	-32.776
-0.25	0	2.232	11.585		48.163	-2.896	-0.846	0.715	8.287	-0.605	-7.008
0.25	0.5	1.515	7.864		56.026	1.966	-0.346	0.120	0.940	-0.041	-0.325
0.75	1	0.914	4.744		60.770	3.558	0.154	0.024	0.113	0.004	0.017
1.25	1.5	1.496	7.765		68.535	9.706	0.654	0.428	3.324	0.280	2.175
1.75	2	1.244	6.457	72.257	74.992	11.300	1.154	1.332	8.603	1.538	9.930
2.25	2.5	0.804	4.173		79.165	9.390	1.654	2.737	11.420	4.527	18.892
2.75	3	0.617	3.203		82.368	8.807	2.154	4.641	14.862	9.998	32.018
3.25	3.5	1.512	7.848		90.216	25.506	2.654	7.045	55.290	18.700	146.754
3.75	4	0.996	5.170		95.386	19.386	3.154	9.949	51.436	31.383	162.241
4.25	> 4	0.889	4.614	4.614	100.000	19.611	3.654	13.354	61.618	48.798	225.169
	TOTAL	19.266				59.574			354.158		290.166
meanϕ	0.596	SKϕ	2.902								
σϕ	1.882	D50	0.117								

					Sample ID	CR13-G15					
					Initial wt. (g)	62.020					
					% error	0.255					
m_{ϕ}	phi (ϕ)	Individual wt. (g)	Individual wt. %	% G S M	Cummulative wt. %	fm_{ϕ}	m_{ϕ}-x	$(m_{\phi}-x)^2$	$f(m_{\phi}-x)^2$	$(m_{\phi}-x)^3$	$f(m_{\phi}-x)^3$
-1.75	-1.5	0.195	0.315	0.823	0.315	-0.552	-3.787	14.340	4.520	-54.304	-17.117
-1.25	-1	0.314	0.508		0.823	-0.634	-3.287	10.803	5.484	-35.509	-18.023
-0.75	-0.5	0.138	0.223		1.046	-0.167	-2.787	7.766	1.733	-21.644	-4.828
-0.25	0	0.245	0.396		1.442	-0.099	-2.287	5.230	2.071	-11.959	-4.736
0.25	0.5	0.436	0.705		2.147	0.176	-1.787	3.193	2.250	-5.705	-4.021
0.75	1	1.041	1.683		3.829	1.262	-1.287	1.656	2.787	-2.131	-3.586
1.25	1.5	4.184	6.763		10.593	8.454	-0.787	0.619	4.187	-0.487	-3.295
1.75	2	27.315	44.155	96.416	54.748	77.271	-0.287	0.082	3.633	-0.024	-1.042
2.25	2.5	17.551	28.371		83.119	63.835	0.213	0.045	1.289	0.010	0.275
2.75	3	5.555	8.980		92.099	24.694	0.713	0.509	4.567	0.363	3.257
3.25	3.5	1.940	3.136		95.235	10.192	1.213	1.472	4.616	1.786	5.599
3.75	4	1.240	2.004		97.239	7.517	1.713	2.935	5.883	5.028	10.079
4.25	> 4	1.708	2.761	2.761	100.000	11.734	2.213	4.898	13.524	10.840	29.930
	TOTAL	61.862				203.683			56.543		-7.509
meanϕ	2.037	SKϕ	-0.075								
σϕ	0.752	D50	1.946								

					Sample ID	CR14-G1					
					Initial wt. (g)	979.883					
					% error	0.023					
m_ϕ	phi (ϕ)	Individual wt. (g)	Individual wt. %	% G S M	Cummulative wt. %	fm_ϕ	m_ϕ-x	$(m_\phi-x)^2$	$f(m_\phi-x)^2$	$(m_\phi-x)^3$	$f(m_\phi-x)^3$
-6.25	-6	641.770	65.510		65.510	-409.436	-0.666	0.443	29.029	-0.295	-19.323
-5.75	-5.5	111.148	11.346		76.855	-65.237	-0.166	0.027	0.311	-0.005	-0.052
-5.25	-5	88.400	9.024		85.879	-47.374	0.334	0.112	1.009	0.037	0.337
-4.75	-4.5	23.990	2.449		88.328	-11.632	0.834	0.696	1.705	0.581	1.422
-4.25	-4	20.781	2.121		90.449	-9.015	1.334	1.780	3.777	2.376	5.039
-3.675	-3.35	15.243	1.556	97.098	92.005	-5.718	1.909	3.646	5.672	6.961	10.830
-3.175	-3	14.051	1.434		93.439	-4.554	2.409	5.805	8.326	13.986	20.060
-2.75	-2.5	10.823	1.105		94.544	-3.038	2.834	8.033	8.875	22.769	25.155
-2.25	-2	13.209	1.348		95.892	-3.034	3.334	11.118	14.990	37.070	49.983
-1.75	-1.5	5.567	0.568		96.461	-0.994	3.834	14.702	8.355	56.373	32.034
-1.25	-1	6.247	0.638		97.098	-0.797	4.334	18.786	11.980	81.426	51.923
-0.75	-0.5	4.626	0.472		97.570	-0.354	4.834	23.371	11.036	112.982	53.351
-0.25	0	2.855	0.291		97.862	-0.073	5.334	28.455	8.293	151.789	44.236
0.25	0.5	3.015	0.308		98.170	0.077	5.834	34.039	10.476	198.597	61.120
0.75	1	4.077	0.416		98.586	0.312	6.334	40.124	16.698	254.157	105.772
1.25	1.5	5.195	0.530		99.116	0.663	6.834	46.708	24.769	319.218	169.278
1.75	2	5.620	0.574	2.889	99.690	1.004	7.334	53.792	30.859	394.531	226.331
2.25	2.5	2.302	0.235		99.925	0.529	7.834	61.377	14.422	480.845	112.989
2.75	3	0.420	0.043		99.968	0.118	8.334	69.461	2.978	578.911	24.819
3.25	3.5	0.128	0.013		99.981	0.042	8.834	78.045	1.020	689.478	9.009
3.75	4	0.064	0.007		99.987	0.024	9.334	87.130	0.569	813.297	5.313
4.25	> 4	0.125	0.013	0.013	100.000	0.054	9.834	96.714	1.234	951.117	12.136
	TOTAL	979.656				-558.433			216.381		1001.762
meanϕ	-5.584	SKϕ	10.018								
σϕ	1.471	D50	-6.118								

Sample ID	CR14-G2
Initial wt. (g)	297.147
% error	0.177

m_ϕ	phi (ϕ)	Individual wt. (g)	Individual wt. %	% G S M	Cummulative wt. %	fm_ϕ	m_ϕ-x	$(m_\phi-x)^2$	$f(m_\phi-x)^2$	$(m_\phi-x)^3$	$f(m_\phi-x)^3$
-5.75	-5.5	93.933	31.668		31.668	-182.089	-1.956	3.824	121.108	-7.479	-236.838
-5.25	-5	43.389	14.628		46.295	-76.796	-1.456	2.119	30.993	-3.084	-45.113
-4.75	-4.5	0.000	0.000		46.295	0.000	-0.956	0.913	0.000	-0.873	0.000
-4.25	-4	40.814	13.760		60.055	-58.478	-0.456	0.208	2.856	-0.095	-1.301
-3.675	-3.35	10.742	3.621	87.458	63.677	-13.309	0.119	0.014	0.052	0.002	0.006
-3.175	-3	22.537	7.598		71.274	-24.123	0.619	0.384	2.915	0.238	1.806
-2.75	-2.5	12.078	4.072		75.346	-11.198	1.044	1.091	4.442	1.139	4.639
-2.25	-2	18.667	6.293		81.640	-14.160	1.544	2.385	15.011	3.684	23.182
-1.75	-1.5	8.226	2.773		84.413	-4.853	2.044	4.180	11.591	8.545	23.697
-1.25	-1	9.034	3.046		87.458	-3.807	2.544	6.474	19.717	16.473	50.169
-0.75	-0.5	5.959	2.009		89.467	-1.507	3.044	9.268	18.620	28.217	56.687
-0.25	0	4.510	1.520		90.988	-0.380	3.544	12.563	19.101	44.528	67.703
0.25	0.5	3.994	1.346		92.334	0.337	4.044	16.357	22.025	66.155	89.078
0.75	1	5.401	1.821		94.155	1.366	4.544	20.652	37.603	93.849	170.885
1.25	1.5	7.387	2.490		96.646	3.113	5.044	25.446	63.370	128.360	319.666
1.75	2	7.615	2.567	12.510	99.213	4.493	5.544	30.740	78.918	170.438	437.556
2.25	2.5	1.777	0.599		99.812	1.348	6.044	36.535	21.887	220.832	132.296
2.75	3	0.299	0.101		99.913	0.277	6.544	42.829	4.317	280.292	28.254
3.25	3.5	0.100	0.034		99.946	0.110	7.044	49.624	1.673	349.569	11.785
3.75	4	0.066	0.022		99.969	0.083	7.544	56.918	1.266	429.413	9.555
4.25	> 4	0.093	0.031	0.031	100.000	0.133	8.044	64.712	2.029	520.574	16.322
	TOTAL	296.621				-379.441			479.495		1160.032
meanϕ	-3.794	SKϕ	11.600								
σϕ	2.190	D50	-4.365								

					Sample ID	CR14-G3					
					Initial wt. (g)	1027.241					
					% error	0.082					
m_ϕ	phi (ϕ)	Individual wt. (g)	Individual wt. %	% G S M	Cummulative wt. %	fm_ϕ	m_ϕ-x	$(m_\phi-x)^2$	$f(m_\phi-x)^2$	$(m_\phi-x)^3$	$f(m_\phi-x)^3$
-6.25	-6	526.800	51.325		51.325	-320.782	-0.923	0.852	43.712	-0.786	-40.340
-5.75	-5.5	172.219	16.779		68.104	-96.479	-0.423	0.179	3.000	-0.076	-1.269
-5.25	-5	134.494	13.103		81.208	-68.793	0.077	0.006	0.078	0.000	0.006
-4.75	-4.5	61.574	5.999		87.207	-28.495	0.577	0.333	1.998	0.192	1.153
-3.675	-3.35	27.787	2.707	95.319	89.914	-9.949	1.652	2.730	7.390	4.510	12.209
-3.175	-3	14.497	1.412		91.326	-4.484	2.152	4.632	6.542	9.968	14.079
-2.75	-2.5	7.203	0.702		92.028	-1.930	2.577	6.642	4.661	17.116	12.012
-2.25	-2	15.998	1.559		93.587	-3.507	3.077	9.469	14.759	29.137	45.414
-1.75	-1.5	9.303	0.906		94.493	-1.586	3.577	12.796	11.598	45.773	41.487
-1.25	-1	8.480	0.826		95.319	-1.033	4.077	16.623	13.734	67.775	55.995
-0.75	-0.5	6.067	0.591		95.910	-0.443	4.577	20.950	12.384	95.892	56.681
-0.25	0	4.900	0.477		96.388	-0.119	5.077	25.777	12.306	130.875	62.479
0.25	0.5	5.519	0.538		96.925	0.134	5.577	31.104	16.725	173.474	93.278
0.75	1	6.780	0.661		97.586	0.495	6.077	36.932	24.396	224.439	148.256
1.25	1.5	8.716	0.849		98.435	1.061	6.577	43.259	36.735	284.519	241.608
1.75	2	9.407	0.917	4.658	99.352	1.604	7.077	50.086	45.904	354.465	324.869
2.25	2.5	5.044	0.491		99.843	1.106	7.577	57.413	28.214	435.027	213.784
2.75	3	1.025	0.100		99.943	0.275	8.077	65.240	6.515	526.954	52.624
3.25	3.5	0.285	0.028		99.971	0.090	8.577	73.567	2.043	630.997	17.521
3.75	4	0.064	0.006		99.977	0.023	9.077	82.394	0.514	747.906	4.663
4.25	> 4	0.237	0.023	0.023	100.000	0.098	9.577	91.722	2.118	878.431	20.283
	TOTAL	1026.399				-532.714			295.324		1376.792
meanϕ	-5.327	SKϕ	13.768								
σϕ	1.718	D50	-6.013								

					Sample ID	CR14-G4					
					Initial wt. (g)	495.122					
					% error	0.162					
m_ϕ	phi (ϕ)	Individual wt. (g)	Individual wt. %	% G S M	Cummulative wt. %	fm_ϕ	m_ϕ-x	$(m_\phi\text{-}x)^2$	$f(m_\phi\text{-}x)^2$	$(m_\phi\text{-}x)^3$	$f(m_\phi\text{-}x)^3$
-5.25	-5	259.963	52.590		52.590	-276.097	-1.010	1.019	53.613	-1.029	-54.131
-4.75	-4.5	52.130	10.546		63.136	-50.092	-0.510	0.260	2.739	-0.132	-1.396
-4.25	-4	57.758	11.684		74.820	-49.658	-0.010	0.000	0.001	0.000	0.000
-3.675	-3.35	14.940	3.022	94.029	77.842	-11.107	0.565	0.320	0.966	0.181	0.546
-3.175	-3	42.576	8.613		86.455	-27.346	1.065	1.135	9.775	1.209	10.414
-2.75	-2.5	11.335	2.293		88.748	-6.306	1.490	2.221	5.093	3.310	7.590
-2.25	-2	14.604	2.954		91.703	-6.647	1.990	3.961	11.703	7.884	23.293
-1.75	-1.5	6.599	1.335		93.038	-2.336	2.490	6.202	8.279	15.444	20.618
-1.25	-1	4.898	0.991		94.029	-1.239	2.990	8.942	8.860	26.740	26.495
-0.75	-0.5	2.436	0.493		94.521	-0.370	3.490	12.182	6.003	42.520	20.954
-0.25	0	1.864	0.377		94.898	-0.094	3.990	15.923	6.004	63.537	23.959
0.25	0.5	2.359	0.477		95.376	0.119	4.490	20.163	9.622	90.538	43.207
0.75	1	3.950	0.799		96.175	0.599	4.990	24.903	19.900	124.276	99.306
1.25	1.5	7.432	1.503		97.678	1.879	5.490	30.144	45.320	165.498	248.823
1.75	2	6.782	1.372	5.943	99.050	2.401	5.990	35.884	49.232	214.957	294.917
2.25	2.5	4.234	0.857		99.907	1.927	6.490	42.124	36.081	273.400	234.175
2.75	3	0.034	0.007		99.914	0.019	6.990	48.865	0.335	341.579	2.343
3.25	3.5	0.218	0.044		99.958	0.143	7.490	56.105	2.474	420.244	18.533
3.75	4	0.071	0.014		99.972	0.054	7.990	63.845	0.917	510.144	7.327
4.25	> 4	0.138	0.028	0.028	100.000	0.119	8.490	72.086	2.012	612.030	17.086
	TOTAL	494.321				-424.032			278.931		1044.057
meanϕ	-4.240	SKϕ	10.441								
σϕ	1.670	D50	-5.025								

Sample ID	CR14-G5
Initial wt. (g)	88.992
% error	0.225

m_ϕ	phi (ϕ)	Individual wt. (g)	Individual wt. %	% G S M	Cummulative wt. %	fm_ϕ	m_ϕ-x	$(m_\phi-x)^2$	$f(m_\phi-x)^2$	$(m_\phi-x)^3$	$f(m_\phi-x)^3$
-1.75	-1.5	0.127	0.143	0.955	0.143	-0.250	-3.084	9.509	1.360	-29.325	-4.194
-1.25	-1	0.721	0.812		0.955	-1.015	-2.584	6.676	5.421	-17.248	-14.006
-0.75	-0.5	1.148	1.293		2.248	-0.970	-2.084	4.342	5.614	-9.048	-11.698
-0.25	0	2.608	2.937		5.185	-0.734	-1.584	2.508	7.367	-3.972	-11.668
0.25	0.5	4.425	4.984		10.169	1.246	-1.084	1.174	5.853	-1.273	-6.343
0.75	1	14.760	16.623		26.792	12.467	-0.584	0.341	5.664	-0.199	-3.307
1.25	1.5	23.564	26.538		53.330	33.173	-0.084	0.007	0.186	-0.001	-0.016
1.75	2	30.479	34.326	98.726	87.657	60.071	0.416	0.173	5.948	0.072	2.476
2.25	2.5	9.328	10.505		98.162	23.637	0.916	0.840	8.820	0.769	8.081
2.75	3	1.058	1.192		99.354	3.277	1.416	2.006	2.390	2.841	3.385
3.25	3.5	0.198	0.223		99.577	0.725	1.916	3.672	0.819	7.037	1.569
3.75	4	0.093	0.105		99.681	0.393	2.416	5.838	0.611	14.107	1.478
4.25	> 4	0.283	0.319	0.319	100.000	1.355	2.916	8.505	2.711	24.802	7.905
	TOTAL	88.792				133.374			52.764		-26.338
meanϕ	1.334	SKϕ	-0.263								
σϕ	0.726	D50	1.437								

					Sample ID	CR14-G5-R					
					Initial wt. (g)	76.008					
					% error	0.093					
m_ϕ	phi (ϕ)	Individual wt. (g)	Individual wt. %	% G S M	Cummulative wt. %	fm_ϕ	m_ϕ-x	$(m_\phi\text{-x})^2$	$f(m_\phi\text{-x})^2$	$(m_\phi\text{-x})^3$	$f(m_\phi\text{-x})^3$
-2.25	-2	0.126	0.166	1.325	0.166	-0.373	-3.470	12.044	1.998	-41.798	-6.935
-1.75	-1.5	0.198	0.261		0.427	-0.456	-2.970	8.824	2.301	-26.210	-6.834
-1.25	-1	0.682	0.898		1.325	-1.123	-2.470	6.103	5.481	-15.078	-13.541
-0.75	-0.5	1.818	2.394		3.719	-1.796	-1.970	3.883	9.296	-7.651	-18.316
-0.25	0	2.418	3.184		6.903	-0.796	-1.470	2.162	6.885	-3.179	-10.124
0.25	0.5	5.237	6.897		13.800	1.724	-0.970	0.942	6.495	-0.914	-6.303
0.75	1	12.164	16.019		29.818	12.014	-0.470	0.221	3.545	-0.104	-1.668
1.25	1.5	23.296	30.678		60.496	38.348	0.030	0.001	0.027	0.000	0.001
1.75	2	23.559	31.024	98.400	91.521	54.293	0.530	0.280	8.700	0.148	4.607
2.25	2.5	5.534	7.288		98.808	16.397	1.030	1.060	7.725	1.091	7.953
2.75	3	0.567	0.747		99.555	2.053	1.530	2.340	1.747	3.578	2.672
3.25	3.5	0.070	0.092		99.647	0.300	2.030	4.119	0.380	8.360	0.771
3.75	4	0.059	0.078		99.725	0.291	2.530	6.399	0.497	16.186	1.258
4.25	> 4	0.209	0.275	0.275	100.000	1.170	3.030	9.178	2.526	27.806	7.653
	TOTAL	75.937				122.046			57.602		-38.809
$mean_\phi$	1.220	SKϕ	-0.388								
σϕ	0.759	D50	1.329								

Sample ID	CR14-G6
Initial wt. (g)	135.818
% error	0.149

m_ϕ	phi (ϕ)	Individual wt. (g)	Individual wt. %	% G S M	Cummulative wt. %	fm_ϕ	m_ϕ-x	$(m_\phi-x)^2$	$f(m_\phi-x)^2$	$(m_\phi-x)^3$	$f(m_\phi-x)^3$
-3.675	-3.35	13.927	10.270	63.246	10.270	-37.740	-2.447	5.988	61.495	-14.653	-150.482
-3.175	-3	14.320	10.559		20.829	-33.526	-1.947	3.791	40.031	-7.381	-77.943
-2.75	-2.5	8.024	5.917		26.746	-16.271	-1.522	2.317	13.707	-3.526	-20.863
-2.25	-2	21.451	15.818		42.563	-35.590	-1.022	1.045	16.523	-1.068	-16.888
-1.75	-1.5	15.974	11.779		54.342	-20.613	-0.522	0.273	3.210	-0.142	-1.676
-1.25	-1	12.075	8.904		63.246	-11.130	-0.022	0.000	0.004	0.000	0.000
-0.75	-0.5	7.329	5.404		68.650	-4.053	0.478	0.228	1.234	0.109	0.590
-0.25	0	6.767	4.990		73.640	-1.247	0.978	0.956	4.772	0.935	4.667
0.25	0.5	4.966	3.662		77.302	0.915	1.478	2.184	7.999	3.228	11.821
0.75	1	5.960	4.395		81.697	3.296	1.978	3.912	17.193	7.738	34.008
1.25	1.5	9.700	7.153		88.849	8.941	2.478	6.140	43.918	15.215	108.827
1.75	2	7.754	5.718	36.391	94.567	10.006	2.978	8.868	50.705	26.409	150.996
2.25	2.5	4.299	3.170		97.737	7.133	3.478	12.096	38.345	42.069	133.360
2.75	3	1.857	1.369		99.106	3.766	3.978	15.824	21.668	62.947	86.194
3.25	3.5	0.576	0.425		99.531	1.380	4.478	20.052	8.517	89.791	38.137
3.75	4	0.144	0.106		99.637	0.398	4.978	24.780	2.631	123.353	13.098
4.25	> 4	0.492	0.363	0.363	100.000	1.542	5.478	30.008	10.887	164.381	59.636
	TOTAL	135.615				-122.794			342.840		373.481
meanϕ	-1.228	SKϕ	3.735								
σϕ	1.852	D50	-1.684								

Sample ID	CR14-G7
Initial wt. (g)	128.648
% error	0.191

m_ϕ	phi (ϕ)	Individual wt. (g)	Individual wt. %	% G S M	Cummulative wt. %	fm_ϕ	m_ϕ-x	$(m_\phi-x)^2$	$f(m_\phi-x)^2$	$(m_\phi-x)^3$	$f(m_\phi-x)^3$
-3.675	-3.35	5.543	4.317	28.588	4.317	-15.865	-3.820	14.595	63.006	-55.758	-240.704
-3.175	-3	2.924	2.277		6.594	-7.230	-3.320	11.025	25.106	-36.606	-83.360
-2.75	-2.5	3.437	2.677		9.271	-7.361	-2.895	8.383	22.439	-24.272	-64.970
-2.25	-2	8.965	6.982		16.253	-15.709	-2.395	5.738	40.061	-13.744	-95.959
-1.75	-1.5	7.421	5.780		22.032	-10.114	-1.895	3.592	20.762	-6.809	-39.351
-1.25	-1	8.417	6.555		28.588	-8.194	-1.395	1.947	12.763	-2.717	-17.809
-0.75	-0.5	7.843	6.108		34.696	-4.581	-0.895	0.802	4.897	-0.718	-4.384
-0.25	0	9.602	7.478		42.174	-1.870	-0.395	0.156	1.169	-0.062	-0.462
0.25	0.5	9.030	7.033		49.206	1.758	0.105	0.011	0.077	0.001	0.008
0.75	1	12.677	9.873		59.079	7.405	0.605	0.366	3.610	0.221	2.182
1.25	1.5	17.027	13.261		72.340	16.576	1.105	1.220	16.181	1.348	17.875
1.75	2	13.561	10.561	70.918	82.901	18.482	1.605	2.575	27.194	4.132	43.637
2.25	2.5	17.586	13.696		96.597	30.816	2.105	4.430	60.667	9.323	127.683
2.75	3	3.075	2.395		98.992	6.586	2.605	6.784	16.247	17.670	42.318
3.25	3.5	0.488	0.380		99.372	1.235	3.105	9.639	3.663	29.925	11.373
3.75	4	0.171	0.133		99.505	0.499	3.605	12.993	1.730	46.837	6.238
4.25	> 4	0.635	0.495	0.495	100.000	2.102	4.105	16.848	8.332	69.156	34.200
	TOTAL	128.402				14.535			327.904		-261.485
meanϕ	0.145	SKϕ	-2.615								
σϕ	1.811	D50	0.540								

					Sample ID	CR14-G7-R					
					Initial wt. (g)	82.227					
					% error	0.126					
m_ϕ	phi (ϕ)	Individual wt. (g)	Individual wt. %	% G S M	Cummulative wt. %	fm_ϕ	m_ϕ-x	$(m_\phi\text{-}x)^2$	$f(m_\phi\text{-}x)^2$	$(m_\phi\text{-}x)^3$	$f(m_\phi\text{-}x)^3$
-3.175	-3	0.557	0.678	29.175	0.678	-2.153	-3.188	10.163	6.893	-32.397	-21.973
-2.75	-2.5	4.269	5.198		5.877	-14.295	-2.763	7.634	39.681	-21.091	-109.635
-2.25	-2	5.363	6.530		12.407	-14.694	-2.263	5.121	33.440	-11.587	-75.671
-1.75	-1.5	6.587	8.021		20.428	-14.037	-1.763	3.108	24.927	-5.479	-43.943
-1.25	-1	7.183	8.747		29.175	-10.933	-1.263	1.595	13.950	-2.014	-17.617
-0.75	-0.5	8.071	9.828		39.002	-7.371	-0.763	0.582	5.720	-0.444	-4.364
-0.25	0	6.251	7.612		46.614	-1.903	-0.263	0.069	0.526	-0.018	-0.138
0.25	0.5	7.874	9.588		56.202	2.397	0.237	0.056	0.539	0.013	0.128
0.75	1	9.613	11.706		67.908	8.779	0.737	0.543	6.360	0.401	4.688
1.25	1.5	11.375	13.851		81.759	17.314	1.237	1.530	21.199	1.893	26.225
1.75	2	7.769	9.460	70.438	91.219	16.555	1.737	3.018	28.547	5.242	49.589
2.25	2.5	5.413	6.591		97.811	14.830	2.237	5.005	32.988	11.196	73.797
2.75	3	1.255	1.528		99.339	4.203	2.737	7.492	11.449	20.506	31.337
3.25	3.5	0.127	0.155		99.493	0.503	3.237	10.479	1.621	33.921	5.246
3.75	4	0.098	0.119		99.613	0.447	3.737	13.966	1.667	52.193	6.228
4.25	> 4	0.318	0.387	0.387	100.000	1.646	4.237	17.953	6.952	76.070	29.456
	TOTAL	82.123				1.288			236.457		-46.647
$mean_\phi$	0.013	SKϕ	-0.466								
σϕ	1.538	D50	0.177								

Sample ID	CR14-G8
Initial wt. (g)	78.449
% error	0.150

m_ϕ	phi (ϕ)	Individual wt. (g)	Individual wt. %	% G S M	Cummulative wt. %	fm_ϕ	m_ϕ-x	$(m_\phi\text{-x})^2$	$f(m_\phi\text{-x})^2$	$(m_\phi\text{-x})^3$	$f(m_\phi\text{-x})^3$
-2.25	-2	0.082	0.105	0.540	0.105	-0.236	-3.286	10.801	1.131	-35.496	-3.716
-1.25	-1	0.341	0.435		0.540	-0.544	-2.286	5.228	2.276	-11.953	-5.203
-0.75	-0.5	0.823	1.051		1.591	-0.788	-1.786	3.191	3.353	-5.701	-5.990
-0.25	0	3.042	3.884		5.474	-0.971	-1.286	1.655	6.427	-2.129	-8.268
0.25	0.5	7.326	9.353		14.827	2.338	-0.786	0.618	5.784	-0.486	-4.549
0.75	1	21.684	27.683		42.509	20.762	-0.286	0.082	2.271	-0.023	-0.651
1.25	1.5	30.937	39.495		82.005	49.369	0.214	0.046	1.801	0.010	0.385
1.75	2	11.736	14.983	99.243	96.987	26.220	0.714	0.509	7.629	0.363	5.444
2.25	2.5	1.895	2.419		99.406	5.443	1.214	1.473	3.563	1.787	4.324
2.75	3	0.193	0.246		99.653	0.678	1.714	2.936	0.723	5.032	1.240
3.25	3.5	0.060	0.077		99.729	0.249	2.214	4.900	0.375	10.846	0.831
3.75	4	0.042	0.054		99.783	0.201	2.714	7.363	0.395	19.981	1.071
4.25	> 4	0.170	0.217	0.217	100.000	0.922	3.214	10.327	2.241	33.187	7.202
	TOTAL	78.331				103.643			37.970		-7.880
meanϕ	1.036	SKϕ	-0.079								
σϕ	0.616	D50	1.095								

Sample ID	CR14-G9
Initial wt. (g)	204.028
% error	-0.258

m_{ϕ}	phi (ϕ)	Individual wt. (g)	Individual wt. %	% G S M	Cummulative wt. %	fm_{ϕ}	m_{ϕ}-x	$(m_{\phi}-x)^2$	$f(m_{\phi}-x)^2$	$(m_{\phi}-x)^3$	$f(m_{\phi}-x)^3$
-4.75	-4.5	32.325	15.803		15.803	-75.062	-1.072	1.150	18.169	-1.233	-19.482
-4.25	-4	19.762	9.661		25.464	-41.059	-0.572	0.327	3.164	-0.187	-1.811
-3.675	-3.35	120.824	59.067	96.583	84.530	-217.070	0.003	0.000	0.000	0.000	0.000
-3.175	-3	21.861	10.687		95.217	-33.932	0.503	0.253	2.701	0.127	1.358
-2.75	-2.5	2.699	1.319		96.537	-3.628	0.928	0.861	1.136	0.798	1.054
-2.25	-2	0.000	0.000		96.537	0.000	1.428	2.038	0.000	2.910	0.000
-1.75	-1.5	0.000	0.000		96.537	0.000	1.928	3.716	0.000	7.164	0.000
-1.25	-1	0.094	0.046		96.583	-0.057	2.428	5.894	0.271	14.309	0.658
-0.75	-0.5	0.098	0.048		96.631	-0.036	2.928	8.572	0.411	25.095	1.202
-0.25	0	0.140	0.068		96.699	-0.017	3.428	11.749	0.804	40.274	2.756
0.25	0.5	5.143	2.514		99.213	0.629	3.928	15.427	38.787	60.593	152.346
0.75	1	0.122	0.060		99.273	0.045	4.428	19.605	1.169	86.805	5.177
1.25	1.5	0.121	0.059		99.332	0.074	4.928	24.283	1.436	119.658	7.078
1.75	2	0.145	0.071	3.084	99.403	0.124	5.428	29.460	2.088	159.902	11.335
2.25	2.5	0.140	0.068		99.472	0.154	5.928	35.138	2.405	208.288	14.256
2.75	3	0.105	0.051		99.523	0.141	6.428	41.316	2.121	265.566	13.632
3.25	3.5	0.135	0.066		99.589	0.214	6.928	47.993	3.167	332.485	21.943
3.75	4	0.159	0.078		99.667	0.291	7.428	55.171	4.288	409.796	31.853
4.25	> 4	0.682	0.333	0.333	100.000	1.417	7.928	62.849	20.954	498.249	166.120
	TOTAL	204.555				-367.773			103.073		409.474
meanφ	-3.678	SKφ	4.095								
σφ	1.015	D50	-3.418								

					Sample ID	CR14-G10					
					Initial wt. (g)	111.568					
					% error	1.402					
m_ϕ	phi (ϕ)	Individual wt. (g)	Individual wt. %	% G S M	Cummulative wt. %	fm_ϕ	m_ϕ-x	$(m_\phi-x)^2$	$f(m_\phi-x)^2$	$(m_\phi-x)^3$	$f(m_\phi-x)^3$
-2.25	-2	0.536	0.487	2.594	0.487	-1.096	-3.224	10.393	5.064	-33.506	-16.326
-1.75	-1.5	0.916	0.833		1.320	-1.457	-2.724	7.419	6.178	-20.209	-16.828
-1.25	-1	1.402	1.274		2.594	-1.593	-2.224	4.945	6.303	-10.998	-14.017
-0.75	-0.5	3.526	3.205		5.800	-2.404	-1.724	2.972	9.525	-5.123	-16.420
-0.25	0	7.068	6.425		12.225	-1.606	-1.224	1.498	9.624	-1.833	-11.778
0.25	0.5	12.534	11.394		23.619	2.849	-0.724	0.524	5.970	-0.379	-4.321
0.75	1	25.768	23.425		47.044	17.568	-0.224	0.050	1.174	-0.011	-0.263
1.25	1.5	27.014	24.557		71.601	30.697	0.276	0.076	1.873	0.021	0.517
1.75	2	23.922	21.746	97.078	93.348	38.056	0.776	0.602	13.101	0.468	10.168
2.25	2.5	5.760	5.236		98.584	11.781	1.276	1.629	8.528	2.078	10.883
2.75	3	0.862	0.784		99.367	2.155	1.776	3.155	2.472	5.603	4.391
3.25	3.5	0.224	0.204		99.571	0.662	2.276	5.181	1.055	11.793	2.401
3.75	4	0.112	0.102		99.673	0.382	2.776	7.707	0.785	21.396	2.178
4.25	> 4	0.360	0.327	0.327	100.000	1.391	3.276	10.733	3.513	35.164	11.508
	TOTAL	110.004				97.384			75.163		-37.905
meanϕ	0.974	SKϕ	-0.379								
σϕ	0.867	D50	1.060								

					Sample ID	CR14-G10-R				
					Initial wt. (g)	72.779				
					% error	0.176				
m_ϕ	phi (ϕ)	Individual wt. (g)	Individual wt. %	% G S M	Cummulative wt. %	fm_ϕ	m_ϕ-x	$(m_\phi\text{-}x)^2$	$f(m_\phi\text{-}x)^2$	$(m_\phi\text{-}x)^3$
-2.75	-2.5	0.168	0.231	2.659	0.231	-0.636	-3.718	13.821	3.196	-51.382
-2.25	-2	0.188	0.259		0.490	-0.582	-3.218	10.353	2.679	-33.314
-1.75	-1.5	0.364	0.501		0.991	-0.877	-2.718	7.386	3.700	-20.072
-1.25	-1	1.212	1.668		2.659	-2.085	-2.218	4.918	8.205	-10.907
-0.75	-0.5	2.079	2.862		5.521	-2.146	-1.718	2.950	8.443	-5.068
-0.25	0	4.096	5.638		11.159	-1.409	-1.218	1.483	8.359	-1.805
0.25	0.5	9.264	12.751		23.910	3.188	-0.718	0.515	6.567	-0.370
0.75	1	15.061	20.731		44.641	15.548	-0.218	0.047	0.982	-0.010
1.25	1.5	21.155	29.119		73.759	36.398	0.282	0.080	2.321	0.023
1.75	2	15.699	21.609	96.975	95.368	37.815	0.782	0.612	13.226	0.479
2.25	2.5	2.729	3.756		99.125	8.452	1.282	1.644	6.177	2.109
2.75	3	0.235	0.323		99.448	0.890	1.782	3.177	1.028	5.662
3.25	3.5	0.06	0.083		99.531	0.268	2.282	5.209	0.430	11.889
3.75	4	0.075	0.103		99.634	0.387	2.782	7.741	0.799	21.539
4.25	> 4	0.266	0.366	0.366	100.000	1.556	3.282	10.774	3.945	35.363
	TOTAL	72.651				96.766			70.057	
$mean_\phi$	0.968	SKϕ	-0.415							
$\sigma\phi$	0.837	D50	1.092							

Sample ID	CR14-G11
Initial wt. (g)	140.674
% error	-1.211

m_ϕ	phi (ϕ)	Individual wt. (g)	Individual wt. %	% G S M	Cummulative wt. %	fm_ϕ	m_ϕ-x	$(m_\phi-x)^2$	$f(m_\phi-x)^2$	$(m_\phi-x)^3$	$f(m_\phi-x)^3$
-3.675	-3.35	11.945	8.390	30.668	8.390	-30.832	-3.654	13.348	111.986	-48.767	-409.141
-3.175	-3	1.997	1.403		9.792	-4.453	-3.154	9.945	13.948	-31.360	-43.986
-2.75	-2.5	2.572	1.806		11.599	-4.968	-2.729	7.445	13.449	-20.313	-36.695
-2.25	-2	11.020	7.740		19.339	-17.415	-2.229	4.966	38.438	-11.067	-85.660
-1.75	-1.5	6.556	4.605		23.943	-8.058	-1.729	2.988	13.757	-5.164	-23.780
-1.25	-1	9.574	6.724		30.668	-8.405	-1.229	1.509	10.149	-1.854	-12.468
-0.75	-0.5	10.188	7.156		37.823	-5.367	-0.729	0.531	3.798	-0.387	-2.767
-0.25	0	9.282	6.519		44.343	-1.630	-0.229	0.052	0.340	-0.012	-0.078
0.25	0.5	9.202	6.463		50.806	1.616	0.271	0.074	0.476	0.020	0.129
0.75	1	14.468	10.162		60.967	7.621	0.771	0.595	6.048	0.459	4.666
1.25	1.5	17.510	12.298		73.266	15.373	1.271	1.617	19.883	2.056	25.281
1.75	2	23.420	16.449	68.779	89.715	28.786	1.771	3.138	51.621	5.559	91.446
2.25	2.5	11.088	7.788		97.502	17.522	2.271	5.160	40.182	11.720	91.274
2.75	3	2.000	1.405		98.907	3.863	2.771	7.681	10.790	21.288	29.904
3.25	3.5	0.506	0.355		99.263	1.155	3.271	10.703	3.804	35.014	12.444
3.75	4	0.262	0.184		99.447	0.690	3.771	14.224	2.617	53.646	9.872
4.25	> 4	0.788	0.553	0.553	100.000	2.352	4.271	18.246	10.098	77.936	43.134
	TOTAL	142.378				-2.149			351.384		-306.424
meanϕ	-0.021	SKϕ	-3.064								
σϕ	1.875	D50	0.438								

					Sample ID	CR14-G12					
					Initial wt. (g)	135.228					
					% error	-2.264					
m_{ϕ}	phi (ϕ)	Individual wt. (g)	Individual wt. %	% G S M	Cummulative wt. %	fm_{ϕ}	m_{ϕ}-x	$(m_{\phi}-x)^2$	$f(m_{\phi}-x)^2$	$(m_{\phi}-x)^3$	$f(m_{\phi}-x)^3$
-3.175	-3	4.498	3.253	33.295	3.253	-10.327	-2.861	8.188	26.632	-23.429	-76.206
-2.75	-2.5	1.220	0.882		4.135	-2.426	-2.436	5.936	5.237	-14.464	-12.760
-2.25	-2	11.938	8.633		12.767	-19.423	-1.936	3.750	32.371	-7.261	-62.685
-1.75	-1.5	13.178	9.529		22.297	-16.676	-1.436	2.063	19.663	-2.964	-28.245
-1.25	-1	15.210	10.999		33.295	-13.748	-0.936	0.877	9.645	-0.821	-9.032
-0.75	-0.5	15.418	11.149		44.444	-8.362	-0.436	0.190	2.124	-0.083	-0.927
-0.25	0	14.918	10.787		55.232	-2.697	0.064	0.004	0.044	0.000	0.003
0.25	0.5	16.470	11.910		67.142	2.977	0.564	0.318	3.782	0.179	2.132
0.75	1	20.960	15.157		82.298	11.367	1.064	1.131	17.144	1.203	18.233
1.25	1.5	14.144	10.228		92.526	12.785	1.564	2.445	25.004	3.822	39.094
1.75	2	7.470	5.402	66.398	97.928	9.453	2.064	4.258	23.002	8.787	47.465
2.25	2.5	1.708	1.235		99.163	2.779	2.564	6.572	8.117	16.847	20.808
2.75	3	0.392	0.283		99.446	0.780	3.064	9.385	2.660	28.752	8.150
3.25	3.5	0.184	0.133		99.579	0.432	3.564	12.699	1.690	45.253	6.021
3.75	4	0.158	0.114		99.693	0.428	4.064	16.512	1.887	67.099	7.666
4.25	> 4	0.424	0.307	0.307	100.000	1.303	4.564	20.826	6.385	95.040	29.140
	TOTAL	138.290				-31.355			185.385		-11.143
meanϕ	-0.314	SKϕ	-0.111								
σϕ	1.362	D50	-0.242								

Sample ID	CR14-G13
Initial wt. (g)	146.991
% error	2.141

m_ϕ	phi (ϕ)	Individual wt. (g)	Individual wt. %	% G S M	Cummulative wt. %	fm_ϕ	m_ϕ-x	$(m_\phi-x)^2$	$f(m_\phi-x)^2$	$(m_\phi-x)^3$	$f(m_\phi-x)^3$
-3.175	-3	0.644	0.448	5.195	0.448	-1.421	-3.943	15.550	6.962	-61.316	-27.452
-2.75	-2.5	0.234	0.163		0.610	-0.447	-3.518	12.378	2.014	-43.551	-7.085
-2.25	-2	1.512	1.051		1.662	-2.365	-3.018	9.110	9.576	-27.497	-28.903
-1.75	-1.5	1.810	1.258		2.920	-2.202	-2.518	6.342	7.980	-15.970	-20.096
-1.25	-1	3.272	2.275		5.195	-2.843	-2.018	4.073	9.266	-8.221	-18.701
-0.75	-0.5	5.226	3.633		8.828	-2.725	-1.518	2.305	8.375	-3.500	-12.716
-0.25	0	9.302	6.467		15.294	-1.617	-1.018	1.037	6.705	-1.056	-6.828
0.25	0.5	18.324	12.739		28.033	3.185	-0.518	0.269	3.422	-0.139	-1.774
0.75	1	42.480	29.532		57.565	22.149	-0.018	0.000	0.010	0.000	0.000
1.25	1.5	35.252	24.507		82.072	30.634	0.482	0.232	5.687	0.112	2.739
1.75	2	20.796	14.457	94.391	96.530	25.300	0.982	0.964	13.933	0.946	13.679
2.25	2.5	3.428	2.383		98.913	5.362	1.482	2.195	5.232	3.253	7.753
2.75	3	0.548	0.381		99.294	1.048	1.982	3.927	1.496	7.783	2.965
3.25	3.5	0.242	0.168		99.462	0.547	2.482	6.159	1.036	15.285	2.571
3.75	4	0.178	0.124		99.586	0.464	2.982	8.891	1.100	26.509	3.280
4.25	> 4	0.596	0.414	0.414	100.000	1.761	3.482	12.122	5.023	42.207	17.488
	TOTAL	143.844				76.829			87.817		-73.078
meanϕ	0.768	SKϕ	-0.731								
σϕ	0.937	D50	0.872								

Sample ID	CR14-G14
Initial wt. (g)	168.051
% error	0.451

m_ϕ	phi (ϕ)	Individual wt. (g)	Individual wt. %	% G S M	Cummulative wt. %	fm_ϕ	m_ϕ-x	$(m_\phi-x)^2$	$f(m_\phi-x)^2$	$(m_\phi-x)^3$	$f(m_\phi-x)^3$
-4.25	-4	17.022	10.175		10.175	-43.244	-3.388	11.477	116.781	-38.883	-395.634
-3.675	-3.35	13.696	8.187	56.983	18.362	-30.087	-2.813	7.912	64.774	-22.255	-182.197
-3.175	-3	31.659	18.924		37.286	-60.085	-2.313	5.349	101.229	-12.372	-234.124
-2.75	-2.5	7.271	4.346		41.632	-11.952	-1.888	3.564	15.490	-6.728	-29.241
-2.25	-2	12.755	7.624		49.257	-17.155	-1.388	1.926	14.685	-2.673	-20.380
-1.75	-1.5	6.929	4.142		53.399	-7.248	-0.888	0.788	3.265	-0.700	-2.898
-1.25	-1	5.997	3.585		56.983	-4.481	-0.388	0.150	0.539	-0.058	-0.209
-0.75	-0.5	4.587	2.742		59.725	-2.056	0.112	0.013	0.035	0.001	0.004
-0.25	0	3.782	2.261		61.986	-0.565	0.612	0.375	0.847	0.229	0.519
0.25	0.5	3.667	2.192		64.178	0.548	1.112	1.237	2.711	1.376	3.015
0.75	1	6.874	4.109		68.287	3.082	1.612	2.599	10.680	4.190	17.218
1.25	1.5	6.704	4.007		72.294	5.009	2.112	4.461	17.878	9.423	37.761
1.75	2	8.965	5.359	36.286	77.653	9.378	2.612	6.823	36.566	17.824	95.517
2.25	2.5	9.554	5.711		83.364	12.850	3.112	9.686	55.314	30.144	172.148
2.75	3	7.318	4.374		87.738	12.029	3.612	13.048	57.076	47.131	206.169
3.25	3.5	5.314	3.176		90.915	10.324	4.112	16.910	53.714	69.537	220.882
3.75	4	3.939	2.355		93.269	8.830	4.612	21.272	50.086	98.111	231.008
4.25	> 4	11.260	6.731	6.731	100.000	28.606	5.112	26.134	175.903	133.604	899.247
	TOTAL	167.293				-86.218			777.572		1018.803
meanϕ	-0.862	SKϕ	10.188								
σϕ	2.788	D50	-1.910								

Sample ID	CR14-G15
Initial wt. (g)	74.638
% error	0.114

m_ϕ	phi (ϕ)	Individual wt. (g)	Individual wt. %	% G S M	Cummulative wt. %	fm_ϕ	m_ϕ-x	$(m_\phi\text{-}x)^2$	$f(m_\phi\text{-}x)^2$	$(m_\phi\text{-}x)^3$	$f(m_\phi\text{-}x)^3$
-3.675	-3.35	1.366	1.832	4.888	1.832	-6.734	-4.602	21.176	38.801	-97.449	-178.551
-3.175	-3	1.128	1.513		3.345	-4.804	-4.102	16.825	25.456	-69.011	-104.415
-2.75	-2.5	0.000	0.000		3.345	0.000	-3.677	13.519	0.000	-49.705	0.000
-2.25	-2	0.243	0.326		3.671	-0.733	-3.177	10.092	3.289	-32.060	-10.450
-1.75	-1.5	0.464	0.622		4.294	-1.089	-2.677	7.165	4.459	-19.180	-11.937
-1.25	-1	0.443	0.594		4.888	-0.743	-2.177	4.738	2.816	-10.314	-6.129
-0.75	-0.5	0.841	1.128		6.016	-0.846	-1.677	2.812	3.172	-4.714	-5.318
-0.25	0	2.365	3.172		9.188	-0.793	-1.177	1.385	4.393	-1.630	-5.170
0.25	0.5	6.302	8.453		17.641	2.113	-0.677	0.458	3.872	-0.310	-2.620
0.75	1	16.901	22.670		40.311	17.002	-0.177	0.031	0.708	-0.006	-0.125
1.25	1.5	27.037	36.265		76.576	45.332	0.323	0.104	3.789	0.034	1.225
1.75	2	14.217	19.070	94.857	95.646	33.372	0.823	0.678	12.923	0.558	10.639
2.25	2.5	2.777	3.725		99.371	8.381	1.323	1.751	6.522	2.317	8.630
2.75	3	0.162	0.217		99.588	0.598	1.823	3.324	0.722	6.061	1.317
3.25	3.5	0.074	0.099		99.687	0.323	2.323	5.397	0.536	12.539	1.245
3.75	4	0.043	0.058		99.745	0.216	2.823	7.971	0.460	22.503	1.298
4.25	> 4	0.190	0.255	0.255	100.000	1.083	3.323	11.044	2.815	36.701	9.353
	TOTAL	74.553				92.678			114.732		-291.009
meanϕ	0.927	SKϕ	-2.910								
σϕ	1.071	D50	1.134								

					Sample ID	CR14-G15-R				
					Initial wt. (g)	75.704				
					% error	0.141				
m_ϕ	phi (ϕ)	Individual wt. (g)	Individual wt. %	% G S M	Cummulative wt. %	fm_ϕ	m_ϕ-x	$(m_\phi-x)^2$	$f(m_\phi-x)^2$	$(m_\phi-x)^3$
-2.75	-2.5	0.189	0.250	2.435	0.250	-0.688	-3.741	13.995	3.499	-52.354
-2.25	-2	0.482	0.638		0.888	-1.435	-3.241	10.504	6.697	-34.042
-1.75	-1.5	0.493	0.652		1.540	-1.141	-2.741	7.513	4.899	-20.592
-1.25	-1	0.677	0.896		2.435	-1.119	-2.241	5.022	4.497	-11.254
-0.75	-0.5	1.341	1.774		4.209	-1.330	-1.741	3.031	5.376	-5.277
-0.25	0	2.691	3.560		7.769	-0.890	-1.241	1.540	5.482	-1.911
0.25	0.5	7.992	10.572		18.341	2.643	-0.741	0.549	5.804	-0.407
0.75	1	17.988	23.795		42.135	17.846	-0.241	0.058	1.382	-0.014
1.25	1.5	27.233	36.024		78.159	45.030	0.259	0.067	2.417	0.017
1.75	2	14.533	19.224	97.362	97.383	33.643	0.759	0.576	11.076	0.437
2.25	2.5	1.608	2.127		99.511	4.786	1.259	1.585	3.372	1.996
2.75	3	0.118	0.156		99.667	0.429	1.759	3.094	0.483	5.443
3.25	3.5	0.044	0.058		99.725	0.189	2.259	5.103	0.297	11.529
3.75	4	0.055	0.073		99.798	0.273	2.759	7.612	0.554	21.003
4.25	> 4	0.153	0.202	0.202	100.000	0.860	3.259	10.621	2.150	34.616
	TOTAL	75.597				99.096			57.985	
$mean_\phi$	0.991	SKϕ	-0.558							
σϕ	0.761	D50	1.165							

Sample ID	CR14-G16
Initial wt. (g)	602.906
% error	-0.586

m_ϕ	phi (ϕ)	Individual wt. (g)	Individual wt. %	% G S M	Cummulative wt. %	fm_ϕ	m_ϕ-x	$(m_\phi-x)^2$	$f(m_\phi-x)^2$	$(m_\phi-x)^3$	$f(m_\phi-x)^3$
-5.75	-5.5	301.060	49.644		49.644	-285.452	-1.185	1.405	69.761	-1.666	-82.696
-5.25	-5	133.410	21.999		71.643	-115.494	-0.685	0.470	10.335	-0.322	-7.084
-3.675	-3.35	44.027	7.260	92.951	78.902	-26.680	0.890	0.791	5.745	0.704	5.111
-3.175	-3	27.837	4.590		83.493	-14.574	1.390	1.931	8.863	2.683	12.316
-2.75	-2.5	13.449	2.218		85.710	-6.099	1.815	3.293	7.302	5.975	13.250
-2.25	-2	19.093	3.148		88.859	-7.084	2.315	5.357	16.867	12.400	39.039
-1.75	-1.5	14.880	2.454		91.312	-4.294	2.815	7.922	19.438	22.297	54.708
-1.25	-1	9.934	1.638		92.951	-2.048	3.315	10.986	17.997	36.415	59.651
-0.75	-0.5	9.399	1.550		94.500	-1.162	3.815	14.551	22.552	55.506	86.027
-0.25	0	7.469	1.232		95.732	-0.308	4.315	18.616	22.927	80.318	98.921
0.25	0.5	5.752	0.948		96.680	0.237	4.815	23.180	21.986	111.603	105.853
0.75	1	5.492	0.906		97.586	0.679	5.315	28.245	25.579	150.109	135.940
1.25	1.5	3.526	0.581		98.168	0.727	5.815	33.809	19.658	196.587	114.301
1.75	2	3.853	0.635	6.679	98.803	1.112	6.315	39.874	25.334	251.787	159.972
2.25	2.5	2.312	0.381		99.184	0.858	6.815	46.438	17.704	316.459	120.647
2.75	3	0.625	0.103		99.287	0.283	7.315	53.503	5.514	391.352	40.333
3.25	3.5	0.224	0.037		99.324	0.120	7.815	61.068	2.256	477.218	17.627
3.75	4	1.853	0.306		99.630	1.146	8.315	69.132	21.124	574.805	175.634
4.25	> 4	2.246	0.370	0.370	100.000	1.574	8.815	77.697	28.776	684.864	253.645
	TOTAL	606.441				-456.458			369.716		1403.195
$mean_\phi$	-4.565	SKϕ	14.032								
σϕ	1.923	D50	-5.492								

Sample ID	CR14-G17
Initial wt. (g)	1460.130
% error	0.000

m_ϕ	phi (ϕ)	Individual wt. (g)	Individual wt. %	% G S M	Cummulative wt. %	fm_ϕ	m_ϕ-x	$(m_\phi-x)^2$	$f(m_\phi-x)^2$	$(m_\phi-x)^3$	$f(m_\phi-x)^3$
-7.25	-7	784.400	53.721		53.721	-389.479	-4.475	20.030	1076.026	-89.643	-4815.722
-6.25	-6	331.460	22.701	100.000	76.422	-141.879	-3.475	12.079	274.199	-41.980	-952.971
-5.75	-5.5	344.270	23.578		100.000	-135.574	-2.975	8.853	208.746	-26.343	-621.117
	TOTAL	1460.130				-277.453			482.945		-1574.088
meanϕ	-2.775	SKϕ	-15.741								
σϕ	2.198	D50	-7.035								

					Sample ID	CR14-G18					
					Initial wt. (g)	132.440					
					% error	-0.163					

m_ϕ	phi (ϕ)	Individual wt. (g)	Individual wt. %	% G S M	Cummulative wt. %	fm_ϕ	m_ϕ-x	$(m_\phi-x)^2$	$f(m_\phi-x)^2$	$(m_\phi-x)^3$	$f(m_\phi-x)^3$
-3.675	-3.35	6.950	5.239	26.286	5.239	-19.254	-3.949	15.597	81.717	-61.600	-322.731
-3.175	-3	12.562	9.470		14.709	-30.066	-3.449	11.898	112.671	-41.041	-388.642
-2.75	-2.5	5.382	4.057		18.766	-11.157	-3.024	9.147	37.110	-27.663	-112.233
-2.25	-2	5.108	3.851		22.616	-8.664	-2.524	6.372	24.537	-16.086	-61.941
-1.75	-1.5	2.700	2.035		24.652	-3.562	-2.024	4.098	8.341	-8.296	-16.885
-1.25	-1	2.168	1.634		26.286	-2.043	-1.524	2.324	3.798	-3.542	-5.789
-0.75	-0.5	2.447	1.845		28.131	-1.383	-1.024	1.049	1.936	-1.075	-1.983
-0.25	0	2.953	2.226		30.357	-0.557	-0.524	0.275	0.612	-0.144	-0.321
0.25	0.5	4.571	3.446		33.802	0.861	-0.024	0.001	0.002	0.000	0.000
0.75	1	12.881	9.710		43.513	7.283	0.476	0.226	2.197	0.108	1.045
1.25	1.5	24.553	18.509		62.021	23.136	0.976	0.952	17.618	0.929	17.188
1.75	2	35.913	27.072	73.575	89.094	47.376	1.476	2.177	58.950	3.213	86.988
2.25	2.5	12.923	9.742		98.835	21.919	1.976	3.903	38.023	7.711	75.120
2.75	3	1.181	0.890		99.726	2.448	2.476	6.129	5.456	15.173	13.508
3.25	3.5	0.000	0.000		99.726	0.000	2.976	8.854	0.000	26.347	0.000
3.75	4	0.180	0.136		99.861	0.509	3.476	12.080	1.639	41.986	5.697
4.25	> 4	0.184	0.139	0.139	100.000	0.589	3.976	15.806	2.192	62.838	8.716
	TOTAL	132.656				27.437			396.798		-702.263
meanϕ	0.274	SKϕ	-7.023								
σϕ	1.992	D50	1.175								

					Sample ID	CR14-G19					
					Initial wt. (g)	829.400					
					% error	0.000					
m_ϕ	phi (ϕ)	Individual wt. (g)	Individual wt. %	% G S M	Cummulative wt. %	fm_ϕ	m_ϕ-x	$(m_\phi-x)^2$	$f(m_\phi-x)^2$	$(m_\phi-x)^3$	$f(m_\phi-x)^3$
-6.25	-6	745.600	89.896		89.896	-561.852	-0.101	0.010	0.918	-0.001	-0.093
-5.25	-5	83.800	10.104	100.000	100.000	-53.044	0.899	0.808	8.165	0.726	7.340
-3.675	-3.35	0.000	0.000		100.000	0.000	2.474	6.120	0.000	15.142	0.000
	TOTAL	829.400				-614.896			9.083		7.247
meanϕ	-6.149	SKϕ	0.072								
σϕ	0.301	D50	-6.222								

Sample ID	CR14-G20
Initial wt. (g)	429.118
% error	0.035

m_ϕ	phi (ϕ)	Individual wt. (g)	Individual wt. %	% G S M	Cummulative wt. %	fm_ϕ	m_ϕ-x	$(m_\phi-x)^2$	$f(m_\phi-x)^2$	$(m_\phi-x)^3$	$f(m_\phi-x)^3$
-5.75	-5.5	90.400	21.074		21.074	-121.175	-1.791	3.208	67.606	-5.746	-121.089
-5.25	-5	178.000	41.495		62.569	-217.848	-1.291	1.667	69.170	-2.152	-89.305
-3.675	-3.35	28.606	6.669	87.134	69.237	-24.507	0.284	0.081	0.537	0.023	0.153
-3.175	-3	22.351	5.210		74.448	-16.543	0.784	0.614	3.202	0.482	2.510
-2.75	-2.5	11.720	2.732		77.180	-7.513	1.209	1.461	3.993	1.767	4.827
-2.25	-2	19.800	4.616		81.796	-10.385	1.709	2.920	13.479	4.991	23.035
-1.75	-1.5	13.236	3.086		84.881	-5.400	2.209	4.879	15.055	10.778	33.255
-1.25	-1	9.664	2.253		87.134	-2.816	2.709	7.338	16.532	19.878	44.783
-0.75	-0.5	9.052	2.110		89.244	-1.583	3.209	10.297	21.729	33.042	69.725
-0.25	0	7.004	1.633		90.877	-0.408	3.709	13.756	22.460	51.019	83.302
0.25	0.5	6.714	1.565		92.442	0.391	4.209	17.715	27.726	74.560	116.698
0.75	1	8.260	1.926		94.368	1.444	4.709	22.174	42.697	104.414	201.054
1.25	1.5	7.496	1.747		96.115	2.184	5.209	27.133	47.413	141.331	246.969
1.75	2	8.869	2.068	12.798	98.183	3.618	5.709	32.592	67.384	186.062	384.686
2.25	2.5	4.792	1.117		99.300	2.513	6.209	38.550	43.065	239.356	267.384
2.75	3	1.946	0.454		99.753	1.248	6.709	45.009	20.418	301.963	136.985
3.25	3.5	0.594	0.138		99.892	0.450	7.209	51.968	7.196	374.634	51.876
3.75	4	0.173	0.040		99.932	0.151	7.709	59.427	2.397	458.118	18.476
4.25	> 4	0.291	0.068	0.068	100.000	0.288	8.209	67.386	4.571	553.165	37.525
	TOTAL	428.968				-395.890			496.629		1512.848
meanϕ	-3.959	SKϕ	15.128								
σϕ	2.229	D50	-5.151								

					Sample ID	CR14-G21					
					Initial wt. (g)	470.361					
					% error	-0.018					
m_ϕ	phi (ϕ)	Individual wt. (g)	Individual wt. %	% G S M	Cummulative wt. %	fm_ϕ	m_ϕ-x	$(m_\phi\text{-x})^2$	$f(m_\phi\text{-x})^2$	$(m_\phi\text{-x})^3$	$f(m_\phi\text{-x})^3$
-5.75	-5.5	257.110	54.652		54.652	-314.251	-1.674	2.804	153.237	-4.695	-256.590
-5.25	-5	44.100	9.374		64.026	-49.214	-1.174	1.379	12.930	-1.620	-15.186
-3.675	-3.35	36.277	7.711	84.368	71.738	-28.339	0.401	0.160	1.237	0.064	0.495
-3.175	-3	14.171	3.012		74.750	-9.564	0.901	0.811	2.443	0.730	2.200
-2.75	-2.5	10.879	2.312		77.062	-6.359	1.326	1.757	4.063	2.329	5.386
-2.25	-2	14.884	3.164		80.226	-7.119	1.826	3.333	10.544	6.084	19.248
-1.75	-1.5	10.115	2.150		82.376	-3.763	2.326	5.408	11.628	12.577	27.041
-1.25	-1	9.372	1.992		84.368	-2.490	2.826	7.984	15.905	22.558	44.939
-0.75	-0.5	8.365	1.778		86.146	-1.334	3.326	11.059	19.664	36.778	65.394
-0.25	0	7.384	1.570		87.716	-0.392	3.826	14.635	22.970	55.985	87.873
0.25	0.5	9.012	1.916		89.632	0.479	4.326	18.710	35.842	80.932	155.035
0.75	1	14.993	3.187		92.819	2.390	4.826	23.286	74.211	112.366	358.107
1.25	1.5	14.571	3.097		95.916	3.872	5.326	28.361	87.842	151.039	467.808
1.75	2	11.337	2.410	15.551	98.326	4.217	5.826	33.937	81.782	197.700	476.424
2.25	2.5	4.895	1.040		99.366	2.341	6.326	40.012	41.633	253.099	263.350
2.75	3	1.808	0.384		99.750	1.057	6.826	46.588	17.904	317.987	122.207
3.25	3.5	0.581	0.123		99.874	0.401	7.326	53.663	6.627	393.113	48.549
3.75	4	0.212	0.045		99.919	0.169	7.826	61.239	2.760	479.227	21.596
4.25	> 4	0.381	0.081	0.081	100.000	0.344	8.326	69.314	5.614	577.080	46.736
	TOTAL	470.447				-407.553			608.836		1940.611
meanϕ	-4.076	SKϕ	19.406								
σϕ	2.467	D50	-5.543								

Sample ID	CR14-G22
Initial wt. (g)	330.172
% error	0.259

m_ϕ	phi (ϕ)	Individual wt. (g)	Individual wt. %	% G S M	Cummulative wt. %	fm_ϕ	m_ϕ-x	$(m_\phi-x)^2$	$f(m_\phi-x)^2$	$(m_\phi-x)^3$	$f(m_\phi-x)^3$
-5.25	-5	155.200	47.128		47.128	-247.421	-1.901	3.612	170.245	-6.866	-323.574
-4.25	-4	14.831	4.504		51.631	-19.140	-0.901	0.811	3.653	-0.731	-3.290
-3.675	-3.35	46.796	14.210	81.721	65.841	-52.222	-0.326	0.106	1.507	-0.035	-0.491
-3.175	-3	19.056	5.787		71.628	-18.372	0.174	0.030	0.176	0.005	0.031
-2.75	-2.5	6.950	2.110		73.738	-5.804	0.599	0.359	0.758	0.215	0.454
-2.25	-2	15.017	4.560		78.298	-10.260	1.099	1.209	5.511	1.329	6.059
-1.75	-1.5	6.745	2.048		80.347	-3.584	1.599	2.558	5.239	4.091	8.379
-1.25	-1	4.525	1.374		81.721	-1.718	2.099	4.407	6.056	9.253	12.714
-0.75	-0.5	3.548	1.077		82.798	-0.808	2.599	6.757	7.280	17.563	18.922
-0.25	0	2.610	0.793		83.591	-0.198	3.099	9.606	7.613	29.773	23.596
0.25	0.5	3.146	0.955		84.546	0.239	3.599	12.955	12.376	46.631	44.547
0.75	1	7.881	2.393		86.939	1.795	4.099	16.805	40.216	68.889	164.861
1.25	1.5	14.560	4.421		91.360	5.527	4.599	21.154	93.528	97.296	430.171
1.75	2	19.335	5.871	18.210	97.232	10.275	5.099	26.004	152.673	132.601	778.535
2.25	2.5	6.954	2.112		99.343	4.751	5.599	31.353	66.206	175.556	370.712
2.75	3	1.436	0.436		99.779	1.199	6.099	37.202	16.222	226.910	98.945
3.25	3.5	0.377	0.114		99.894	0.372	6.599	43.552	4.986	287.413	32.903
3.75	4	0.121	0.037		99.930	0.138	7.099	50.401	1.852	357.815	13.147
4.25	> 4	0.229	0.070	0.070	100.000	0.296	7.599	57.750	4.016	438.866	30.518
	TOTAL	329.317				-334.937			600.114		1707.140
meanϕ	-3.349	SKϕ	17.071								
σϕ	2.450	D50	-4.181								

					Sample ID	CR14-G23					
					Initial wt. (g)	2700.795					
					% error	0.017					
m_ϕ	phi (ϕ)	Individual wt. (g)	Individual wt. %	% G S M	Cummulative wt. %	fm_ϕ	m_ϕ-x	$(m_\phi-x)^2$	$f(m_\phi-x)^2$	$(m_\phi-x)^3$	$f(m_\phi-x)^3$
-7.25	-7	2624.400	97.188	97.348	97.188	-704.614	-7.287	53.093	5160.053	-386.867	-37598.869
-2.75	-2.5	1.219	0.045		97.233	-0.124	-2.787	7.765	0.351	-21.637	-0.977
-2.25	-2	1.620	0.060		97.293	-0.135	-2.287	5.228	0.314	-11.954	-0.717
-1.75	-1.5	0.416	0.015		97.309	-0.027	-1.787	3.192	0.049	-5.702	-0.088
-1.25	-1	1.076	0.040		97.348	-0.050	-1.287	1.655	0.066	-2.129	-0.085
-0.75	-0.5	0.984	0.036		97.385	-0.027	-0.787	0.619	0.023	-0.487	-0.018
-0.25	0	1.672	0.062		97.447	-0.015	-0.287	0.082	0.005	-0.024	-0.001
0.25	0.5	2.548	0.094		97.541	0.024	0.213	0.046	0.004	0.010	0.001
0.75	1	6.716	0.249		97.790	0.187	0.713	0.509	0.127	0.363	0.090
1.25	1.5	21.271	0.788		98.578	0.985	1.213	1.473	1.160	1.787	1.408
1.75	2	26.438	0.979	2.613	99.557	1.713	1.713	2.936	2.875	5.031	4.925
2.25	2.5	9.121	0.338		99.894	0.760	2.213	4.899	1.655	10.845	3.663
2.75	3	1.152	0.043		99.937	0.117	2.713	7.363	0.314	19.979	0.852
3.25	3.5	0.480	0.018		99.955	0.058	3.213	10.326	0.184	33.184	0.590
3.75	4	0.189	0.007		99.962	0.026	3.713	13.790	0.097	51.208	0.358
4.25	> 4	1.029	0.038	0.038	100.000	0.162	4.213	17.753	0.677	74.803	2.850
	TOTAL	2700.331				3.653			7.898		12.853
meanϕ	0.037	SKϕ	0.129								
σϕ	0.281	D50	-7.243								

					Sample ID	CR14-G24					
					Initial wt. (g)	1602.978					
					% error	-0.017					
m_ϕ	phi (ϕ)	Individual wt. (g)	Individual wt. %	% G S M	Cummulative wt. %	fm_ϕ	m_ϕ-x	$(m_\phi\text{-x})^2$	$f(m_\phi\text{-x})^2$	$(m_\phi\text{-x})^3$	$f(m_\phi\text{-x})^3$
-5.75	-5.5	669.923	41.785		41.785	-240.265	-0.857	0.735	30.722	-0.630	-26.343
-5.25	-5	553.458	34.521		76.306	-181.235	-0.357	0.128	4.411	-0.046	-1.577
-4.75	-4.5	190.014	11.852		88.158	-56.296	0.143	0.020	0.241	0.003	0.034
-4.25	-4	16.499	1.029		89.187	-4.374	0.643	0.413	0.425	0.265	0.273
-3.675	-3.35	22.893	1.428	94.841	90.615	-5.248	1.218	1.482	2.117	1.805	2.577
-3.175	-3	14.755	0.920		91.535	-2.922	1.718	2.950	2.715	5.067	4.663
-2.75	-2.5	8.845	0.552		92.087	-1.517	2.143	4.590	2.533	9.835	5.426
-2.25	-2	22.025	1.374		93.461	-3.091	2.643	6.983	9.593	18.453	25.350
-1.75	-1.5	13.917	0.868		94.329	-1.519	3.143	9.876	8.572	31.034	26.939
-1.25	-1	8.212	0.512		94.841	-0.640	3.643	13.268	6.796	48.329	24.755
-0.75	-0.5	5.932	0.370		95.211	-0.277	4.143	17.161	6.349	71.088	26.303
-0.25	0	4.110	0.256		95.467	-0.064	4.643	21.553	5.525	100.061	25.651
0.25	0.5	3.525	0.220		95.687	0.055	5.143	26.446	5.814	135.998	29.901
0.75	1	6.044	0.377		96.064	0.283	5.643	31.838	12.002	179.648	67.724
1.25	1.5	12.044	0.751		96.815	0.939	6.143	37.731	28.344	231.762	174.105
1.75	2	24.173	1.508	5.080	98.323	2.639	6.643	44.123	66.527	293.090	441.906
2.25	2.5	17.117	1.068		99.391	2.402	7.143	51.016	54.467	364.382	389.029
2.75	3	6.331	0.395		99.786	1.086	7.643	58.408	23.065	446.388	176.272
3.25	3.5	1.678	0.105		99.890	0.340	8.143	66.301	6.939	539.857	56.503
3.75	4	0.491	0.031		99.921	0.115	8.643	74.693	2.288	645.540	19.770
4.25	> 4	1.268	0.079	0.079	100.000	0.336	9.143	83.586	6.611	764.187	60.439
	TOTAL	1603.254				-489.253			286.056		1529.698
meanϕ	-4.893	SKϕ	15.297								
σϕ	1.691	D50	-5.381								

Sample ID	CR14-G25
Initial wt. (g)	103.863
% error	-0.022

m_ϕ	phi (ϕ)	Individual wt. (g)	Individual wt. %	% G S M	Cummulative wt. %	fm_ϕ	m_ϕ-x	$(m_\phi-x)^2$	$f(m_\phi-x)^2$	$(m_\phi-x)^3$	$f(m_\phi-x)^3$
-2.25	-2	0.711	0.684	6.022	0.684	-1.540	-3.100	9.609	6.576	-29.786	-20.386
-1.75	-1.5	1.845	1.776		2.460	-3.108	-2.600	6.759	12.004	-17.573	-31.209
-1.25	-1	3.700	3.562		6.022	-4.452	-2.100	4.409	15.704	-9.259	-32.976
-0.75	-0.5	6.832	6.576		12.598	-4.932	-1.600	2.559	16.832	-4.095	-26.929
-0.25	0	8.898	8.565		21.164	-2.141	-1.100	1.210	10.361	-1.330	-11.395
0.25	0.5	11.213	10.794		31.957	2.698	-0.600	0.360	3.884	-0.216	-2.330
0.75	1	18.291	17.607		49.564	13.205	-0.100	0.010	0.176	-0.001	-0.018
1.25	1.5	20.855	20.075		69.639	25.094	0.400	0.160	3.215	0.064	1.286
1.75	2	21.639	20.830	93.388	90.468	36.452	0.900	0.810	16.878	0.729	15.193
2.25	2.5	7.593	7.309		97.777	16.445	1.400	1.960	14.329	2.745	20.063
2.75	3	1.289	1.241		99.018	3.412	1.900	3.611	4.480	6.861	8.513
3.25	3.5	0.261	0.251		99.269	0.817	2.400	5.761	1.447	13.827	3.474
3.75	4	0.146	0.141		99.410	0.527	2.900	8.411	1.182	24.393	3.428
4.25	> 4	0.613	0.590	0.590	100.000	2.508	3.400	11.561	6.822	39.310	23.195
	TOTAL	103.886				84.984			113.890		-50.091
meanϕ	0.850	SKϕ	-0.501								
σϕ	1.067	D50	1.011								

					Sample ID	CR14-G26					
					Initial wt. (g)	490.591					
					% error	0.015					
m_ϕ	phi (ϕ)	Individual wt. (g)	Individual wt. %	% G S M	Cummulative wt. %	fm_ϕ	m_ϕ-x	$(m_\phi-x)^2$	$f(m_\phi-x)^2$	$(m_\phi-x)^3$	$f(m_\phi-x)^3$
-5.75	-5.5	165.340	33.707		33.707	-193.817	-1.422	2.022	68.144	-2.874	-96.891
-5.25	-5	150.460	30.674		64.381	-161.037	-0.922	0.850	26.067	-0.783	-24.030
-4.75	-4.5	0.000	0.000		64.381	0.000	-0.422	0.178	0.000	-0.075	0.000
-4.25	-4	68.048	13.873		78.254	-58.959	0.078	0.006	0.085	0.000	0.007
-3.675	-3.35	28.531	5.817	89.318	84.070	-21.376	0.653	0.427	2.481	0.279	1.621
-3.175	-3	16.886	3.442		87.513	-10.930	1.153	1.330	4.578	1.533	5.279
-2.75	-2.5	1.528	0.312		87.824	-0.857	1.578	2.491	0.776	3.930	1.224
-2.25	-2	3.813	0.777		88.602	-1.749	2.078	4.319	3.357	8.975	6.977
-1.75	-1.5	2.175	0.443		89.045	-0.776	2.578	6.647	2.947	17.137	7.599
-1.25	-1	1.340	0.273		89.318	-0.341	3.078	9.475	2.588	29.166	7.967
-0.75	-0.5	1.543	0.315		89.633	-0.236	3.578	12.803	4.027	45.812	14.411
-0.25	0	1.419	0.289		89.922	-0.072	4.078	16.631	4.811	67.825	19.621
0.25	0.5	2.209	0.450		90.372	0.113	4.578	20.959	9.439	95.956	43.213
0.75	1	6.053	1.234		91.606	0.926	5.078	25.788	31.822	130.953	161.597
1.25	1.5	8.814	1.797		93.403	2.246	5.578	31.116	55.911	173.569	311.882
1.75	2	17.948	3.659	10.510	97.062	6.403	6.078	36.944	135.178	224.551	821.631
2.25	2.5	8.911	1.817		98.879	4.087	6.578	43.272	78.610	284.650	517.111
2.75	3	2.979	0.607		99.486	1.670	7.078	50.100	30.427	354.617	215.365
3.25	3.5	1.201	0.245		99.731	0.796	7.578	57.428	14.061	435.201	106.556
3.75	4	0.477	0.097		99.828	0.365	8.078	65.257	6.346	527.152	51.263
4.25	> 4	0.842	0.172	0.172	100.000	0.730	8.578	73.585	12.631	631.221	108.353
	TOTAL	490.517				-432.815			494.287		2280.755
meanϕ	-4.328	SKϕ	22.808								
σϕ	2.223	D50	-5.234								

Sample ID	CR14-G27
Initial wt. (g)	1549.121
% error	-0.018

m_ϕ	phi (ϕ)	Individual wt. (g)	Individual wt. %	% G S M	Cummulative wt. %	fm_ϕ	m_ϕ-x	$(m_\phi-x)^2$	$f(m_\phi-x)^2$	$(m_\phi-x)^3$	$f(m_\phi-x)^3$
-6.75	-6.5	995.300	64.237		64.237	-433.603	-4.961	24.614	1581.140	-122.116	-7844.430
-6.25	-6	269.400	17.387		81.625	-108.671	-4.461	19.903	346.055	-88.791	-1543.836
-5.25	-5	132.400	8.545		90.170	-44.862	-3.461	11.980	102.374	-41.467	-354.340
-4.75	-4.5	37.840	2.442		92.612	-11.601	-2.961	8.769	21.416	-25.967	-63.418
-4.25	-4	12.559	0.811		93.423	-3.445	-2.461	6.058	4.910	-14.910	-12.085
-3.675	-3.35	12.114	0.782	97.912	94.205	-2.873	-1.886	3.558	2.782	-6.711	-5.247
-3.175	-3	21.619	1.395		95.600	-4.430	-1.386	1.922	2.681	-2.664	-3.717
-2.75	-2.5	6.648	0.429		96.029	-1.180	-0.961	0.924	0.396	-0.888	-0.381
-2.25	-2	15.020	0.969		96.998	-2.181	-0.461	0.213	0.206	-0.098	-0.095
-1.75	-1.5	8.266	0.533		97.532	-0.934	0.039	0.002	0.001	0.000	0.000
-1.25	-1	5.885	0.380		97.912	-0.475	0.539	0.290	0.110	0.156	0.059
-0.75	-0.5	4.565	0.295		98.206	-0.221	1.039	1.079	0.318	1.121	0.330
-0.25	0	3.682	0.238		98.444	-0.059	1.539	2.368	0.563	3.643	0.866
0.25	0.5	3.413	0.220		98.664	0.055	2.039	4.157	0.916	8.474	1.867
0.75	1	5.127	0.331		98.995	0.248	2.539	6.445	2.133	16.363	5.415
1.25	1.5	5.956	0.384		99.380	0.481	3.039	9.234	3.550	28.060	10.786
1.75	2	6.209	0.401	2.071	99.780	0.701	3.539	12.523	5.018	44.315	17.759
2.25	2.5	2.230	0.144		99.924	0.324	4.039	16.312	2.348	65.878	9.482
2.75	3	0.586	0.038		99.962	0.104	4.539	20.600	0.779	93.499	3.536
3.25	3.5	0.221	0.014		99.976	0.046	5.039	25.389	0.362	127.929	1.825
3.75	4	0.105	0.007		99.983	0.025	5.539	30.678	0.208	169.917	1.151
4.25	> 4	0.262	0.017	0.017	100.000	0.072	6.039	36.467	0.617	220.212	3.724
	TOTAL	1549.407				-178.875			497.742		-1926.321
meanϕ	-1.789	SKϕ	-19.263								
σϕ	2.231	D50	-6.611								

					Sample ID	CR14-G28				
					Initial wt. (g)	388.577				
					% error	0.058				

m_ϕ	phi (ϕ)	Individual wt. (g)	Individual wt. %	% G S M	Cummulative wt. %	fm_ϕ	m_ϕ-x	$(m_\phi-x)^2$	$f(m_\phi-x)^2$	$(m_\phi-x)^3$	$f(m_\phi-x)^3$
-6.25	-6	95.600	24.617		24.617	-153.855	-2.023	4.093	100.763	-8.281	-203.862
-5.75	-5.5	62.000	15.965		40.582	-91.798	-1.523	2.320	37.040	-3.534	-56.418
-5.25	-5	0.000	0.000		40.582	0.000	-1.023	1.047	0.000	-1.071	0.000
-4.75	-4.5	73.258	18.864		59.445	-89.603	-0.523	0.274	5.163	-0.143	-2.701
-4.25	-4	18.613	4.793		64.238	-20.369	-0.023	0.001	0.003	0.000	0.000
-3.675	-3.35	17.299	4.454	90.984	68.693	-16.370	0.552	0.305	1.356	0.168	0.748
-3.175	-3	31.247	8.046		76.739	-25.546	1.052	1.106	8.901	1.164	9.363
-2.75	-2.5	14.308	3.684		80.423	-10.132	1.477	2.181	8.035	3.221	11.867
-2.25	-2	21.068	5.425		85.848	-12.206	1.977	3.908	21.200	7.725	41.908
-1.75	-1.5	11.840	3.049		88.897	-5.335	2.477	6.135	18.703	15.194	46.324
-1.25	-1	8.108	2.088		90.984	-2.610	2.977	8.861	18.501	26.379	55.074
-0.75	-0.5	7.012	1.806		92.790	-1.354	3.477	12.088	21.826	42.029	75.886
-0.25	0	5.363	1.381		94.171	-0.345	3.977	15.815	21.840	62.894	86.854
0.25	0.5	4.980	1.282		95.453	0.321	4.477	20.042	25.700	89.724	115.056
0.75	1	5.962	1.535		96.989	1.151	4.977	24.769	38.025	123.269	189.243
1.25	1.5	4.865	1.253		98.241	1.566	5.477	29.996	37.576	164.280	205.798
1.75	2	3.916	1.008	8.932	99.250	1.765	5.977	35.722	36.021	213.506	215.291
2.25	2.5	1.662	0.428		99.678	0.963	6.477	41.949	17.953	271.697	116.276
2.75	3	0.550	0.142		99.819	0.389	6.977	48.676	6.894	339.603	48.096
3.25	3.5	0.251	0.065		99.884	0.210	7.477	55.903	3.613	417.975	27.015
3.75	4	0.128	0.033		99.917	0.124	7.977	63.630	2.097	507.562	16.729
4.25	> 4	0.323	0.083	0.083	100.000	0.353	8.477	71.856	5.976	609.114	50.661
	TOTAL	388.353				-422.682			437.188		1049.207
$mean_\phi$	-4.227	SKϕ	10.492								
σϕ	2.091	D50	-4.750								

Sample ID	CR14-G29
Initial wt. (g)	384.559
% error	0.120

m_ϕ	phi (ϕ)	Individual wt. (g)	Individual wt. %	% G S M	Cummulative wt. %	fm_ϕ	m_ϕ-x	$(m_\phi-x)^2$	$f(m_\phi-x)^2$	$(m_\phi-x)^3$	$f(m_\phi-x)^3$
-5.75	-5.5	106.500	27.727		27.727	-159.433	-2.054	4.221	117.032	-8.671	-240.436
-5.25	-5	91.200	23.744		51.472	-124.656	-1.554	2.416	57.373	-3.756	-89.184
-4.25	-4	29.304	7.629		59.101	-32.425	-0.554	0.307	2.345	-0.170	-1.300
-3.675	-3.35	29.516	7.685	84.721	66.785	-28.241	0.021	0.000	0.003	0.000	0.000
-3.175	-3	19.587	5.100		71.885	-16.191	0.521	0.271	1.382	0.141	0.719
-2.75	-2.5	5.436	1.415		73.300	-3.892	0.946	0.894	1.265	0.845	1.196
-2.25	-2	17.725	4.615		77.915	-10.383	1.446	2.090	9.643	3.021	13.939
-1.75	-1.5	15.432	4.018		81.933	-7.031	1.946	3.785	15.208	7.364	29.587
-1.25	-1	10.709	2.788		84.721	-3.485	2.446	5.981	16.675	14.626	40.779
-0.75	-0.5	9.260	2.411		87.132	-1.808	2.946	8.676	20.917	25.556	61.612
-0.25	0	6.458	1.681		88.813	-0.420	3.446	11.872	19.961	40.905	68.775
0.25	0.5	5.375	1.399		90.212	0.350	3.946	15.567	21.785	61.422	85.953
0.75	1	6.396	1.665		91.878	1.249	4.446	19.763	32.909	87.857	146.300
1.25	1.5	6.326	1.647		93.525	2.059	4.946	24.458	40.283	120.960	199.220
1.75	2	10.301	2.682	15.042	96.206	4.693	5.446	29.654	79.528	161.482	433.076
2.25	2.5	8.163	2.125		98.332	4.782	5.946	35.350	75.127	210.172	446.668
2.75	3	3.454	0.899		99.231	2.473	6.446	41.545	37.360	267.781	240.803
3.25	3.5	1.517	0.395		99.626	1.284	6.946	48.241	19.053	335.057	132.332
3.75	4	0.526	0.137		99.763	0.514	7.446	55.436	7.592	412.752	56.524
4.25	> 4	0.911	0.237	0.237	100.000	1.008	7.946	63.132	14.974	501.616	118.973
	TOTAL	384.096				-369.555			590.413		1745.537
$mean_\phi$	-3.696	SKϕ	17.455								
σϕ	2.430	D50	-5.031								

Sample ID	CR14-G30
Initial wt. (g)	1173.700
% error	0.000

m_ϕ	phi (ϕ)	Individual wt. (g)	Individual wt. %	% G S M	Cummulative wt. %	fm_ϕ	m_ϕ-x	$(m_\phi-x)^2$	$f(m_\phi-x)^2$	$(m_\phi-x)^3$	$f(m_\phi-x)^3$
-6.25	-6	981.800	83.650	100.000	83.650	-522.812	-0.082	0.007	0.559	-0.001	-0.046
-5.75	-5.5	191.900	16.350		100.000	-94.013	0.418	0.175	2.860	0.073	1.196
	TOTAL	1173.700				-616.825			3.419		1.151
$mean_\phi$	-6.168	SKϕ	0.012								
$\sigma\phi$	0.185	D50	-6.201								

Sample ID	CR14-G31
Initial wt. (g)	494.213
% error	-0.001

m_ϕ	phi (ϕ)	Individual wt. (g)	Individual wt. %	% G S M	Cummulative wt. %	fm_ϕ	m_ϕ-x	$(m_\phi-x)^2$	$f(m_\phi-x)^2$	$(m_\phi-x)^3$	$f(m_\phi-x)^3$
-5.25	-5	325.500	65.861		65.861	-345.773	-0.643	0.414	27.259	-0.266	-17.537
-4.75	-4.5	64.477	13.046		78.908	-61.970	-0.143	0.021	0.268	-0.003	-0.038
-4.25	-4	9.020	1.825		80.733	-7.757	0.357	0.127	0.232	0.045	0.083
-3.675	-3.35	42.961	8.693	95.936	89.426	-31.946	0.932	0.868	7.545	0.809	7.029
-3.175	-3	16.522	3.343		92.769	-10.614	1.432	2.050	6.852	2.934	9.810
-2.75	-2.5	3.825	0.774		93.543	-2.128	1.857	3.447	2.668	6.400	4.953
-2.25	-2	6.620	1.339		94.882	-3.014	2.357	5.554	7.439	13.088	17.532
-1.75	-1.5	2.573	0.521		95.403	-0.911	2.857	8.160	4.249	23.312	12.137
-1.25	-1	2.638	0.534		95.936	-0.667	3.357	11.267	6.014	37.820	20.187
-0.75	-0.5	1.781	0.360		96.297	-0.270	3.857	14.874	5.360	57.363	20.672
-0.25	0	1.933	0.391		96.688	-0.098	4.357	18.980	7.424	82.691	32.342
0.25	0.5	2.244	0.454		97.142	0.114	4.857	23.587	10.710	114.555	52.013
0.75	1	3.009	0.609		97.751	0.457	5.357	28.694	17.470	153.703	93.580
1.25	1.5	4.630	0.937		98.688	1.171	5.857	34.300	32.134	200.886	188.196
1.75	2	3.725	0.754	4.032	99.441	1.319	6.357	40.407	30.455	256.854	193.595
2.25	2.5	1.894	0.383		99.825	0.862	6.857	47.014	18.017	322.357	123.537
2.75	3	0.488	0.099		99.923	0.272	7.357	54.120	5.344	398.145	39.314
3.25	3.5	0.153	0.031		99.954	0.101	7.857	61.727	1.911	484.968	15.014
3.75	4	0.070	0.014		99.968	0.053	8.357	69.834	0.989	583.576	8.266
4.25	> 4	0.156	0.032	0.032	100.000	0.134	8.857	78.440	2.476	694.720	21.929
	TOTAL	494.219				-460.666			194.816		842.613
$mean_\phi$	-4.607	SKϕ	8.426								
σϕ	1.396	D50	-5.120								

Sample ID	CR14-G32
Initial wt. (g)	229.623
% error	0.150

m_ϕ	phi (ϕ)	Individual wt. (g)	Individual wt. %	% G S M	Cummulative wt. %	fm_ϕ	m_ϕ-x	$(m_\phi\text{-x})^2$	$f(m_\phi\text{-x})^2$	$(m_\phi\text{-x})^3$	$f(m_\phi\text{-x})^3$
-4.75	-4.5	45.722	19.942		19.942	-94.723	-2.638	6.961	138.814	-18.366	-366.242
-4.25	-4	32.249	14.065		34.007	-59.778	-2.138	4.573	64.316	-9.778	-137.531
-3.675	-3.35	6.111	2.665	68.055	36.673	-9.795	-1.563	2.444	6.514	-3.821	-10.184
-3.175	-3	12.395	5.406		42.079	-17.164	-1.063	1.131	6.113	-1.202	-6.500
-2.75	-2.5	12.765	5.567		47.646	-15.311	-0.638	0.408	2.269	-0.260	-1.448
-2.25	-2	16.433	7.167		54.813	-16.126	-0.138	0.019	0.137	-0.003	-0.019
-1.75	-1.5	14.720	6.420		61.234	-11.235	0.362	0.131	0.840	0.047	0.304
-1.25	-1	15.641	6.822		68.055	-8.527	0.862	0.742	5.065	0.640	4.364
-0.75	-0.5	12.676	5.529		73.584	-4.146	1.362	1.854	10.250	2.525	13.957
-0.25	0	14.263	6.221		79.805	-1.555	1.862	3.466	21.559	6.452	40.136
0.25	0.5	11.465	5.000		84.805	1.250	2.362	5.577	27.889	13.172	65.864
0.75	1	9.055	3.949		88.755	2.962	2.862	8.189	32.341	23.434	92.548
1.25	1.5	6.244	2.723		91.478	3.404	3.362	11.301	30.775	37.988	103.455
1.75	2	6.113	2.666	31.761	94.144	4.666	3.862	14.912	39.759	57.585	153.534
2.25	2.5	8.234	3.591		97.736	8.080	4.362	19.024	68.320	82.975	297.986
2.75	3	3.508	1.530		99.266	4.208	4.862	23.635	36.163	114.907	175.810
3.25	3.5	0.996	0.434		99.700	1.412	5.362	28.747	12.488	154.131	66.956
3.75	4	0.268	0.117		99.817	0.438	5.862	34.359	4.016	201.398	23.541
4.25	> 4	0.420	0.183	0.183	100.000	0.779	6.362	40.470	7.414	257.458	47.162
	TOTAL	229.278				-211.163			515.042		563.692
$mean_\phi$	-2.112	SKϕ	5.637								
σϕ	2.269	D50	-2.336								

Sample ID	CR14-G33
Initial wt. (g)	410.816
% error	0.091

m_ϕ	phi (ϕ)	Individual wt. (g)	Individual wt. %	% G S M	Cummulative wt. %	fm_ϕ	m_ϕ-x	$(m_\phi-x)^2$	$f(m_\phi-x)^2$	$(m_\phi-x)^3$	$f(m_\phi-x)^3$
-5.75	-5.5	184.600	44.976		44.976	-258.610	-1.765	3.116	140.126	-5.499	-247.337
-5.25	-5	42.400	10.330		55.306	-54.234	-1.265	1.600	16.533	-2.025	-20.917
-4.25	-4	49.001	11.939		67.244	-50.739	-0.265	0.070	0.839	-0.019	-0.222
-3.675	-3.35	5.041	1.228	87.934	68.473	-4.514	0.310	0.096	0.118	0.030	0.037
-3.175	-3	17.016	4.146		72.618	-13.163	0.810	0.656	2.719	0.531	2.202
-2.75	-2.5	15.684	3.821		76.440	-10.508	1.235	1.525	5.827	1.883	7.196
-2.25	-2	26.008	6.337		82.776	-14.257	1.735	3.010	19.072	5.222	33.088
-1.75	-1.5	12.029	2.931		85.707	-5.129	2.235	4.995	14.638	11.163	32.715
-1.25	-1	9.139	2.227		87.934	-2.783	2.735	7.480	16.654	20.456	45.548
-0.75	-0.5	4.670	1.138		89.071	-0.853	3.235	10.465	11.906	33.852	38.516
-0.25	0	3.691	0.899		89.971	-0.225	3.735	13.949	12.544	52.100	46.852
0.25	0.5	3.190	0.777		90.748	0.194	4.235	17.934	13.939	75.950	59.029
0.75	1	4.672	1.138		91.886	0.854	4.735	22.419	25.519	106.153	120.832
1.25	1.5	9.561	2.329		94.216	2.912	5.235	27.404	63.836	143.458	334.175
1.75	2	11.327	2.760	11.939	96.975	4.829	5.735	32.889	90.764	188.615	520.520
2.25	2.5	7.914	1.928		98.903	4.338	6.235	38.874	74.955	242.375	467.337
2.75	3	2.687	0.655		99.558	1.800	6.735	45.359	29.694	305.487	199.989
3.25	3.5	1.014	0.247		99.805	0.803	7.235	52.344	12.931	378.701	93.558
3.75	4	0.277	0.067		99.873	0.253	7.735	59.829	4.038	462.768	31.231
4.25	> 4	0.523	0.127	0.127	100.000	0.542	8.235	67.814	8.641	558.437	71.158
	TOTAL	410.444				-398.490			565.296		1835.507
$mean_\phi$	-3.985	SKϕ	18.355								
σϕ	2.378	D50	-5.257								

Sample ID	CR14-G34
Initial wt. (g)	1535.384
% error	0.001

m_ϕ	phi (ϕ)	Individual wt. (g)	Individual wt. %	% G S M	Cummulative wt. %	fm_ϕ	m_ϕ-x	$(m_\phi-x)^2$	$f(m_\phi-x)^2$	$(m_\phi-x)^3$	$f(m_\phi-x)^3$
-5.75	-5.5	720.700	46.940		46.940	-269.903	-0.488	0.238	11.174	-0.116	-5.452
-5.25	-5	558.600	36.382		83.322	-191.005	0.012	0.000	0.005	0.000	0.000
-4.75	-4.5	74.311	4.840		88.162	-22.990	0.512	0.262	1.269	0.134	0.650
-4.25	-4	105.964	6.902		95.063	-29.331	1.012	1.024	7.069	1.037	7.155
-3.675	-3.35	29.177	1.900	99.409	96.963	-6.984	1.587	2.519	4.787	3.998	7.597
-3.175	-3	15.117	0.985		97.948	-3.126	2.087	4.356	4.289	9.091	8.951
-2.75	-2.5	4.448	0.290		98.238	-0.797	2.512	6.311	1.828	15.853	4.593
-2.25	-2	10.543	0.687		98.924	-1.545	3.012	9.073	6.230	27.328	18.765
-1.75	-1.5	4.677	0.305		99.229	-0.533	3.512	12.335	3.757	43.321	13.196
-1.25	-1	2.768	0.180		99.409	-0.225	4.012	16.097	2.902	64.582	11.643
-0.75	-0.5	2.244	0.146		99.555	-0.110	4.512	20.359	2.976	91.861	13.426
-0.25	0	1.978	0.129		99.684	-0.032	5.012	25.121	3.236	125.909	16.221
0.25	0.5	1.546	0.101		99.785	0.025	5.512	30.383	3.059	167.474	16.863
0.75	1	1.133	0.074		99.859	0.055	6.012	36.145	2.667	217.308	16.036
1.25	1.5	0.747	0.049		99.907	0.061	6.512	42.407	2.063	276.160	13.436
1.75	2	0.494	0.032	0.582	99.939	0.056	7.012	49.169	1.582	344.780	11.093
2.25	2.5	0.387	0.025		99.965	0.057	7.512	56.431	1.422	423.918	10.685
2.75	3	0.222	0.014		99.979	0.040	8.012	64.194	0.928	514.324	7.437
3.25	3.5	0.133	0.009		99.988	0.028	8.512	72.456	0.628	616.749	5.343
3.75	4	0.057	0.004		99.992	0.014	9.012	81.218	0.302	731.941	2.717
4.25	> 4	0.130	0.008	0.008	100.000	0.036	9.512	90.480	0.766	860.652	7.287
	TOTAL	1535.376				-526.209			62.941		187.641
$mean_\phi$	-5.262	SKϕ	1.876								
σϕ	0.793	D50	-5.458								

Sample ID	CR14-G35
Initial wt. (g)	263.424
% error	0.129

m_ϕ	phi (ϕ)	Individual wt. (g)	Individual wt. %	% G S M	Cummulative wt. %	fm_ϕ	m_ϕ-x	$(m_\phi-x)^2$	$f(m_\phi-x)^2$	$(m_\phi-x)^3$	$f(m_\phi-x)^3$
-5.75	-5.5	52.060	19.788		19.788	-113.783	-3.647	13.304	263.255	-48.524	-960.199
-4.25	-4	22.630	8.602		28.390	-36.558	-2.147	4.611	39.666	-9.902	-85.179
-3.675	-3.35	7.711	2.931	68.656	31.321	-10.771	-1.572	2.472	7.247	-3.888	-11.395
-3.175	-3	31.894	12.123		43.444	-38.491	-1.072	1.150	13.942	-1.233	-14.952
-2.75	-2.5	13.058	4.963		48.408	-13.649	-0.647	0.419	2.080	-0.271	-1.347
-2.25	-2	22.576	8.581		56.989	-19.308	-0.147	0.022	0.186	-0.003	-0.027
-1.75	-1.5	16.587	6.305		63.294	-11.033	0.353	0.124	0.784	0.044	0.276
-1.25	-1	14.107	5.362		68.656	-6.703	0.853	0.727	3.898	0.620	3.323
-0.75	-0.5	9.032	3.433		72.089	-2.575	1.353	1.830	6.281	2.475	8.495
-0.25	0	8.542	3.247		75.336	-0.812	1.853	3.432	11.144	6.358	20.644
0.25	0.5	6.709	2.550		77.886	0.638	2.353	5.535	14.114	13.021	33.205
0.75	1	7.243	2.753		80.639	2.065	2.853	8.137	22.403	23.212	63.906
1.25	1.5	10.105	3.841		84.480	4.801	3.353	11.240	43.172	37.683	144.738
1.75	2	14.170	5.386	30.871	89.866	9.426	3.853	14.842	79.943	57.182	307.987
2.25	2.5	15.421	5.862		95.728	13.189	4.353	18.945	111.048	82.460	483.348
2.75	3	6.292	2.392		98.119	6.577	4.853	23.548	56.317	114.267	273.284
3.25	3.5	2.954	1.123		99.242	3.649	5.353	28.650	32.169	153.353	172.190
3.75	4	0.748	0.284		99.526	1.066	5.853	34.253	9.739	200.468	56.997
4.25	> 4	1.246	0.474	0.474	100.000	2.013	6.353	40.355	19.113	256.362	121.416
	TOTAL	263.085				-210.259			736.501		616.711
$mean_\phi$	-2.103	SKϕ	6.167								
σϕ	2.714	D50	-2.407								

				Sample ID	CR14-G36						
				Initial wt. (g)	268.948						
				% error	0.309						
m_ϕ	phi (ϕ)	Individual wt. (g)	Individual wt. %	% G S M	Cummulative wt. %	fm_ϕ	m_ϕ-x	$(m_\phi-x)^2$	$f(m_\phi-x)^2$	$(m_\phi-x)^3$	$f(m_\phi-x)^3$
-5.25	-5	52.290	19.503		19.503	-102.389	-2.916	8.500	165.780	-24.783	-483.335
-4.75	-4.5	32.025	11.944		31.447	-56.736	-2.416	5.835	69.693	-14.094	-168.346
-4.25	-4	18.420	6.870		38.317	-29.198	-1.916	3.669	25.208	-7.029	-48.287
-3.675	-3.35	14.420	5.378	68.651	43.696	-19.765	-1.341	1.797	9.665	-2.409	-12.956
-3.175	-3	20.631	7.695		51.390	-24.431	-0.841	0.706	5.436	-0.594	-4.569
-2.75	-2.5	10.072	3.757		55.147	-10.331	-0.416	0.173	0.649	-0.072	-0.270
-2.25	-2	17.381	6.483		61.630	-14.586	0.084	0.007	0.046	0.001	0.004
-1.75	-1.5	10.495	3.914		65.544	-6.850	0.584	0.342	1.337	0.200	0.782
-1.25	-1	8.330	3.107		68.651	-3.884	1.084	1.176	3.654	1.275	3.963
-0.75	-0.5	6.001	2.238		70.889	-1.679	1.584	2.511	5.619	3.978	8.903
-0.25	0	6.016	2.244		73.133	-0.561	2.084	4.345	9.749	9.057	20.322
0.25	0.5	7.549	2.816		75.948	0.704	2.584	6.679	18.807	17.263	48.605
0.75	1	12.379	4.617		80.566	3.463	3.084	9.514	43.926	29.346	135.489
1.25	1.5	22.071	8.232		88.797	10.290	3.584	12.848	105.767	46.055	379.118
1.75	2	19.445	7.252	31.345	96.050	12.692	4.084	16.683	120.992	68.141	494.188
2.25	2.5	7.349	2.741		98.791	6.167	4.584	21.017	57.608	96.353	264.103
2.75	3	1.889	0.705		99.495	1.938	5.084	25.852	18.214	131.443	92.608
3.25	3.5	0.989	0.369		99.864	1.199	5.584	31.186	11.504	174.159	64.242
3.75	4	0.354	0.132		99.996	0.495	6.084	37.021	4.888	225.252	29.741
4.25	> 4	0.010	0.004	0.004	100.000	0.016	6.584	43.355	0.162	285.471	1.065
	TOTAL	268.116				-233.447			678.704		825.367
$mean_\phi$	-2.334	SKϕ	8.254								
σϕ	2.605	D50	-3.063								

Sample ID	CR14-G37
Initial wt. (g)	1265.105
% error	0.030

m_ϕ	phi (ϕ)	Individual wt. (g)	Individual wt. %	% G S M	Cummulative wt. %	fm_ϕ	m_ϕ-x	$(m_\phi-x)^2$	$f(m_\phi-x)^2$	$(m_\phi-x)^3$	$f(m_\phi-x)^3$
-6.75	-6.5	334.040	26.412		26.412	-178.282	-3.146	9.897	261.404	-31.136	-822.369
-5.75	-5.5	755.780	59.759		86.171	-343.612	-2.146	4.605	275.199	-9.883	-590.569
-4.75	-4.5	27.674	2.188		88.359	-10.394	-1.146	1.313	2.874	-1.505	-3.293
-3.675	-3.35	23.334	1.845	93.506	90.204	-6.780	-0.071	0.005	0.009	0.000	-0.001
-3.175	-3	17.637	1.395		91.598	-4.428	0.429	0.184	0.257	0.079	0.110
-2.75	-2.5	6.170	0.488		92.086	-1.342	0.854	0.729	0.356	0.623	0.304
-2.25	-2	7.823	0.619		92.705	-1.392	1.354	1.833	1.134	2.482	1.536
-1.75	-1.5	5.663	0.448		93.153	-0.784	1.854	3.437	1.539	6.373	2.854
-1.25	-1	4.469	0.353		93.506	-0.442	2.354	5.541	1.958	13.045	4.609
-0.75	-0.5	4.180	0.331		93.836	-0.248	2.854	8.145	2.692	23.247	7.683
-0.25	0	6.552	0.518		94.354	-0.130	3.354	11.250	5.828	37.731	19.547
0.25	0.5	8.214	0.649		95.004	0.162	3.854	14.854	9.647	57.246	37.180
0.75	1	11.314	0.895		95.899	0.671	4.354	18.958	16.959	82.542	73.841
1.25	1.5	13.080	1.034		96.933	1.293	4.854	23.562	24.368	114.369	118.282
1.75	2	14.545	1.150	6.403	98.083	2.013	5.354	28.666	32.967	153.477	176.507
2.25	2.5	14.129	1.117		99.200	2.514	5.854	34.270	38.285	200.616	224.120
2.75	3	5.662	0.448		99.648	1.231	6.354	40.374	18.075	256.536	114.848
3.25	3.5	2.628	0.208		99.855	0.675	6.854	46.978	9.762	321.987	66.907
3.75	4	0.670	0.053		99.908	0.199	7.354	54.082	2.865	397.719	21.070
4.25	> 4	1.158	0.092	0.092	100.000	0.389	7.854	61.686	5.648	484.482	44.360
	TOTAL	1264.722				-360.403			450.421		319.894
$mean_\phi$	-3.604	SKϕ	3.199								
$\sigma\phi$	2.122	D50	-5.803								

Sample ID	CR14-G38
Initial wt. (g)	795.833
% error	0.259

m_ϕ	phi (ϕ)	Individual wt. (g)	Individual wt. %	% G S M	Cummulative wt. %	fm_ϕ	m_ϕ-x	$(m_\phi-x)^2$	$f(m_\phi-x)^2$	$(m_\phi-x)^3$	$f(m_\phi-x)^3$
-5.75	-5.5	120.420	15.171		15.171	-87.231	-1.525	2.324	35.259	-3.543	-53.752
-5.25	-5	303.140	38.190		53.361	-200.497	-1.025	1.050	40.085	-1.075	-41.068
-4.75	-4.5	182.660	23.012		76.372	-109.306	-0.525	0.275	6.331	-0.144	-3.321
-4.25	-4	6.236	0.786		77.158	-3.339	-0.025	0.001	0.000	0.000	0.000
-3.675	-3.35	15.562	1.961	89.858	79.118	-7.205	0.550	0.303	0.594	0.167	0.327
-3.175	-3	20.140	2.537		81.656	-8.056	1.050	1.104	2.800	1.159	2.941
-2.75	-2.5	11.527	1.452		83.108	-3.994	1.475	2.177	3.161	3.212	4.665
-2.25	-2	25.346	3.193		86.301	-7.185	1.975	3.903	12.461	7.709	24.617
-1.75	-1.5	17.395	2.191		88.492	-3.835	2.475	6.128	13.429	15.170	33.244
-1.25	-1	10.835	1.365		89.858	-1.706	2.975	8.854	12.085	26.344	35.959
-0.75	-0.5	7.506	0.946		90.803	-0.709	3.475	12.079	11.422	41.980	39.697
-0.25	0	7.929	0.999		91.802	-0.250	3.975	15.804	15.787	62.831	62.762
0.25	0.5	8.857	1.116		92.918	0.279	4.475	20.030	22.350	89.644	100.026
0.75	1	13.157	1.658		94.575	1.243	4.975	24.755	41.033	123.170	204.159
1.25	1.5	18.727	2.359		96.935	2.949	5.475	29.981	70.733	164.160	387.295
1.75	2	15.333	1.932	10.070	98.866	3.380	5.975	35.706	68.973	213.363	412.148
2.25	2.5	6.099	0.768		99.635	1.729	6.475	41.932	32.219	271.530	208.632
2.75	3	1.444	0.182		99.817	0.500	6.975	48.657	8.852	339.409	61.744
3.25	3.5	0.656	0.083		99.899	0.269	7.475	55.883	4.618	417.752	34.525
3.75	4	0.224	0.028		99.927	0.106	7.975	63.608	1.795	507.308	14.316
4.25	> 4	0.576	0.073	0.073	100.000	0.308	8.475	71.834	5.213	608.827	44.180
	TOTAL	793.769				-422.549			409.201		1573.097
$mean_\phi$	-4.225	SKϕ	15.731								
σϕ	2.023	D50	-5.044								

Sample ID	CR14-G39
Initial wt. (g)	381.045
% error	0.128

m_ϕ	phi (ϕ)	Individual wt. (g)	Individual wt. %	% G S M	Cummulative wt. %	fm_ϕ	m_ϕ-x	$(m_\phi\text{-}x)^2$	$f(m_\phi\text{-}x)^2$	$(m_\phi\text{-}x)^3$	$f(m_\phi\text{-}x)^3$
-5.75	-5.5	55.500	14.584		14.584	-83.857	-2.652	7.036	102.605	-18.662	-272.157
-5.25	-5	20.810	5.468		20.052	-28.709	-2.152	4.633	25.335	-9.973	-54.533
-4.75	-4.5	99.581	26.167		46.219	-124.294	-1.652	2.731	71.453	-4.512	-118.073
-4.25	-4	23.476	6.169		52.388	-26.218	-1.152	1.328	8.193	-1.531	-9.442
-3.675	-3.35	19.730	5.184	79.041	57.573	-19.053	-0.577	0.333	1.729	-0.193	-0.998
-3.175	-3	24.798	6.516		64.089	-20.689	-0.077	0.006	0.039	0.000	-0.003
-2.75	-2.5	15.197	3.993		68.082	-10.982	0.348	0.121	0.482	0.042	0.168
-2.25	-2	22.602	5.939		74.021	-13.363	0.848	0.718	4.266	0.609	3.616
-1.75	-1.5	11.808	3.103		77.124	-5.430	1.348	1.816	5.634	2.447	7.592
-1.25	-1	7.296	1.917		79.041	-2.396	1.848	3.413	6.544	6.306	12.091
-0.75	-0.5	4.578	1.203		80.244	-0.902	2.348	5.511	6.629	12.937	15.563
-0.25	0	5.300	1.393		81.637	-0.348	2.848	8.108	11.293	23.089	32.156
0.25	0.5	6.119	1.608		83.245	0.402	3.348	11.206	18.018	37.513	60.317
0.75	1	11.264	2.960		86.205	2.220	3.848	14.804	43.817	56.957	168.586
1.25	1.5	20.629	5.421		91.625	6.776	4.348	18.901	102.458	82.173	445.439
1.75	2	19.131	5.027	20.836	96.653	8.797	4.848	23.499	118.130	113.911	572.639
2.25	2.5	9.440	2.481		99.133	5.581	5.348	28.596	70.935	152.919	379.326
2.75	3	1.945	0.511		99.644	1.406	5.848	34.194	17.476	199.949	102.192
3.25	3.5	0.692	0.182		99.826	0.591	6.348	40.291	7.326	255.750	46.505
3.75	4	0.195	0.051		99.877	0.192	6.848	46.889	2.403	321.073	16.452
4.25	> 4	0.467	0.123	0.123	100.000	0.522	7.348	53.986	6.625	396.667	48.677
	TOTAL	380.558				-309.754			631.390		1456.113
meanϕ	-3.098	SKϕ	14.561								
σϕ	2.513	D50	-4.194								

Sample ID	CR14-G40
Initial wt. (g)	202.893
% error	0.118

m_ϕ	phi (ϕ)	Individual wt. (g)	Individual wt. %	% G S M	Cummulative wt. %	fm_ϕ	m_ϕ-x	$(m_\phi-x)^2$	$f(m_\phi-x)^2$	$(m_\phi-x)^3$	$f(m_\phi-x)^3$
-3.675	-3.35	27.580	13.609	67.941	13.609	-50.015	-2.207	4.871	66.295	-10.751	-146.320
-3.175	-3	30.442	15.022		28.631	-47.694	-1.707	2.914	43.776	-4.975	-74.730
-2.75	-2.5	20.214	9.975		38.606	-27.430	-1.282	1.644	16.396	-2.107	-21.021
-2.25	-2	23.848	11.768		50.374	-26.478	-0.782	0.612	7.198	-0.478	-5.630
-1.75	-1.5	20.331	10.032		60.406	-17.557	-0.282	0.080	0.798	-0.022	-0.225
-1.25	-1	15.270	7.535		67.941	-9.419	0.218	0.047	0.358	0.010	0.078
-0.75	-0.5	8.445	4.167		72.108	-3.125	0.718	0.515	2.148	0.370	1.542
-0.25	0	7.820	3.859		75.967	-0.965	1.218	1.483	5.724	1.806	6.971
0.25	0.5	7.073	3.490		79.457	0.873	1.718	2.951	10.300	5.070	17.695
0.75	1	8.743	4.314		83.771	3.236	2.218	4.919	21.222	10.910	47.069
1.25	1.5	9.435	4.656		88.427	5.820	2.718	7.387	34.392	20.077	93.473
1.75	2	7.924	3.910	31.864	92.337	6.843	3.218	10.355	40.489	33.321	130.289
2.25	2.5	10.253	5.059		97.397	11.384	3.718	13.823	69.935	51.392	260.010
2.75	3	3.911	1.930		99.326	5.307	4.218	17.791	34.334	75.039	144.818
3.25	3.5	0.783	0.386		99.713	1.256	4.718	22.259	8.600	105.014	40.575
3.75	4	0.187	0.092		99.805	0.346	5.218	27.227	2.512	142.065	13.109
4.25	> 4	0.395	0.195	0.195	100.000	0.828	5.718	32.694	6.373	186.943	36.438
	TOTAL	202.654				-146.790			370.849		544.140
$mean_\phi$	-1.468	SKϕ	5.441								
$\sigma\phi$	1.926	D50	-2.016								

Sample ID	CR14-G41
Initial wt. (g)	131.452
% error	0.141

m_ϕ	phi (ϕ)	Individual wt. (g)	Individual wt. %	% G S M	Cummulative wt. %	fm_ϕ	m_ϕ-x	$(m_\phi-x)^2$	$f(m_\phi-x)^2$	$(m_\phi-x)^3$	$f(m_\phi-x)^3$
-3.175	-3	1.498	1.141	23.703	1.141	-3.623	-3.507	12.297	14.033	-43.120	-49.208
-2.75	-2.5	2.886	2.199		3.340	-6.046	-3.082	9.497	20.879	-29.265	-64.342
-2.25	-2	7.054	5.374		8.714	-12.091	-2.582	6.665	35.816	-17.206	-92.464
-1.75	-1.5	8.302	6.325		15.038	-11.068	-2.082	4.333	27.406	-9.020	-57.049
-1.25	-1	11.374	8.665		23.703	-10.831	-1.582	2.502	21.676	-3.957	-34.284
-0.75	-0.5	11.182	8.519		32.222	-6.389	-1.082	1.170	9.966	-1.265	-10.780
-0.25	0	12.800	9.751		41.973	-2.438	-0.582	0.338	3.299	-0.197	-1.919
0.25	0.5	10.891	8.297		50.270	2.074	-0.082	0.007	0.055	-0.001	-0.005
0.75	1	11.204	8.535		58.805	6.402	0.418	0.175	1.494	0.073	0.625
1.25	1.5	14.063	10.713		69.518	13.392	0.918	0.843	9.035	0.775	8.298
1.75	2	19.201	14.628	75.717	84.146	25.598	1.418	2.012	29.427	2.853	41.737
2.25	2.5	17.236	13.131		97.277	29.544	1.918	3.680	48.322	7.060	92.698
2.75	3	2.247	1.712		98.988	4.707	2.418	5.848	10.011	14.144	24.211
3.25	3.5	0.393	0.299		99.288	0.973	2.918	8.517	2.550	24.855	7.441
3.75	4	0.174	0.133		99.420	0.497	3.418	11.685	1.549	39.944	5.295
4.25	> 4	0.761	0.580	0.580	100.000	2.464	3.918	15.353	8.901	60.160	34.877
	TOTAL	131.266				33.165			244.419		-94.868
$mean_\phi$	0.332	SKϕ	-0.949								
σϕ	1.563	D50	0.484								

Sample ID	CR14-G42
Initial wt. (g)	154.709
% error	0.181

m_ϕ	phi (ϕ)	Individual wt. (g)	Individual wt. %	% G S M	Cummulative wt. %	fm_ϕ	m_ϕ-x	$(m_\phi-x)^2$	$f(m_\phi-x)^2$	$(m_\phi-x)^3$	$f(m_\phi-x)^3$
-3.675	-3.35	1.133	0.734	39.752	0.734	-2.696	-3.358	11.274	8.271	-37.853	-27.772
-3.175	-3	3.427	2.219		2.953	-7.046	-2.858	8.166	18.122	-23.336	-51.785
-2.75	-2.5	4.009	2.596		5.549	-7.139	-2.433	5.918	15.362	-14.396	-37.371
-2.25	-2	13.052	8.452		14.001	-19.017	-1.933	3.735	31.568	-7.219	-61.009
-1.75	-1.5	19.992	12.946		26.946	-22.655	-1.433	2.052	26.570	-2.940	-38.066
-1.25	-1	19.776	12.806		39.752	-16.007	-0.933	0.870	11.139	-0.811	-10.388
-0.75	-0.5	15.257	9.880		49.632	-7.410	-0.433	0.187	1.849	-0.081	-0.800
-0.25	0	15.883	10.285		59.917	-2.571	0.067	0.005	0.047	0.000	0.003
0.25	0.5	12.938	8.378		68.295	2.094	0.567	0.322	2.697	0.183	1.530
0.75	1	13.966	9.044		77.338	6.783	1.067	1.139	10.303	1.216	10.997
1.25	1.5	11.734	7.598		84.937	9.498	1.567	2.457	18.666	3.850	29.257
1.75	2	6.726	4.355	59.736	89.292	7.622	2.067	4.274	18.615	8.836	38.484
2.25	2.5	11.474	7.430		96.722	16.717	2.567	6.591	48.974	16.922	125.733
2.75	3	3.516	2.277		98.999	6.261	3.067	9.409	21.422	28.860	65.708
3.25	3.5	0.560	0.363		99.362	1.179	3.567	12.726	4.615	45.399	16.463
3.75	4	0.196	0.127		99.488	0.476	4.067	16.543	2.100	67.288	8.540
4.25	> 4	0.790	0.512	0.512	100.000	2.174	4.567	20.861	10.672	95.279	48.741
	TOTAL	154.429				-31.737			250.991		118.266
$mean_\phi$	-0.317	SKϕ	1.183								
σϕ	1.584	D50	-0.482								

					Sample ID	CR14-G43					
					Initial wt. (g)	159.804					
					% error	0.227					
m_{ϕ}	phi (ϕ)	Individual wt. (g)	Individual wt. %	% G S M	Cummulative wt. %	fm_{ϕ}	m_{ϕ}-x	$(m_{\phi}-x)^2$	$f(m_{\phi}-x)^2$	$(m_{\phi}-x)^3$	$f(m_{\phi}-x)^3$
-3.675	-3.35	6.455	4.049	36.460	4.049	-14.878	-3.299	10.884	44.064	-35.907	-145.371
-3.175	-3	4.165	2.612		6.661	-8.294	-2.799	7.835	20.467	-21.930	-57.288
-2.75	-2.5	4.442	2.786		9.447	-7.661	-2.374	5.636	15.703	-13.381	-37.279
-2.25	-2	13.607	8.534		17.981	-19.202	-1.874	3.512	29.974	-6.582	-56.173
-1.75	-1.5	13.327	8.359		26.340	-14.628	-1.374	1.888	15.782	-2.594	-21.686
-1.25	-1	16.136	10.120		36.460	-12.650	-0.874	0.764	7.732	-0.668	-6.759
-0.75	-0.5	14.284	8.959		45.419	-6.719	-0.374	0.140	1.254	-0.052	-0.469
-0.25	0	16.739	10.499		55.917	-2.625	0.126	0.016	0.166	0.002	0.021
0.25	0.5	16.736	10.497		66.414	2.624	0.626	0.392	4.112	0.245	2.574
0.75	1	15.946	10.001		76.415	7.501	1.126	1.268	12.678	1.427	14.275
1.25	1.5	17.044	10.690		87.105	13.362	1.626	2.644	28.260	4.298	45.948
1.75	2	13.290	8.335	63.392	95.440	14.587	2.126	4.520	37.672	9.608	80.087
2.25	2.5	6.007	3.768		99.208	8.477	2.626	6.895	25.979	18.107	68.218
2.75	3	0.759	0.476		99.684	1.309	3.126	9.771	4.652	30.544	14.540
3.25	3.5	0.172	0.108		99.792	0.351	3.626	13.147	1.418	47.671	5.143
3.75	4	0.096	0.060		99.852	0.226	4.126	17.023	1.025	70.236	4.229
4.25	> 4	0.236	0.148	0.148	100.000	0.629	4.626	21.399	3.167	98.990	14.652
	TOTAL	159.441				-37.591			254.104		-75.338
$mean_{\phi}$	-0.376	SKϕ	-0.753								
$\sigma\phi$	1.594	D50	-0.282								

Sample ID	CR14-G44
Initial wt. (g)	141.465
% error	0.145

m_ϕ	phi (ϕ)	Individual wt. (g)	Individual wt. %	% G S M	Cummulative wt. %	fm_ϕ	m_ϕ-x	$(m_\phi-x)^2$	$f(m_\phi-x)^2$	$(m_\phi-x)^3$	$f(m_\phi-x)^3$
-2.25	-2	0.935	0.662	5.898	0.662	-1.489	-3.039	9.235	6.113	-28.065	-18.576
-1.75	-1.5	2.236	1.583		2.245	-2.770	-2.539	6.446	10.204	-16.367	-25.907
-1.25	-1	5.160	3.653		5.898	-4.566	-2.039	4.157	15.186	-8.477	-30.963
-0.75	-0.5	6.374	4.512		10.410	-3.384	-1.539	2.368	10.687	-3.645	-16.446
-0.25	0	11.182	7.916		18.326	-1.979	-1.039	1.079	8.544	-1.121	-8.877
0.25	0.5	16.143	11.428		29.754	2.857	-0.539	0.290	3.319	-0.157	-1.789
0.75	1	28.963	20.503		50.257	15.377	-0.039	0.002	0.031	0.000	-0.001
1.25	1.5	41.622	29.465		79.722	36.831	0.461	0.213	6.263	0.098	2.888
1.75	2	23.480	16.622	93.870	96.344	29.088	0.961	0.924	15.352	0.888	14.754
2.25	2.5	4.393	3.110		99.453	6.997	1.461	2.135	6.639	3.119	9.699
2.75	3	0.278	0.197		99.650	0.541	1.961	3.846	0.757	7.542	1.484
3.25	3.5	0.103	0.073		99.723	0.237	2.461	6.057	0.442	14.906	1.087
3.75	4	0.063	0.045		99.768	0.167	2.961	8.768	0.391	25.962	1.158
4.25	> 4	0.328	0.232	0.232	100.000	0.987	3.461	11.979	2.781	41.460	9.627
	TOTAL	141.260				78.895			86.709		-61.863
$mean_\phi$	0.789	SKϕ	-0.619								
σϕ	0.931	D50	0.994								

Sample ID	CR14-G45
Initial wt. (g)	159.478
% error	0.224

m_ϕ	phi (ϕ)	Individual wt. (g)	Individual wt. %	% G S M	Cummulative wt. %	fm_ϕ	m_ϕ-x	$(m_\phi-x)^2$	$f(m_\phi-x)^2$	$(m_\phi-x)^3$	$f(m_\phi-x)^3$
-3.175	-3	0.943	0.593	18.750	0.593	-1.882	-3.141	9.863	5.845	-30.976	-18.358
-2.75	-2.5	2.928	1.840		2.433	-5.060	-2.716	7.374	13.570	-20.026	-36.850
-2.25	-2	3.772	2.371		4.803	-5.334	-2.216	4.909	11.636	-10.876	-25.782
-1.75	-1.5	8.025	5.043		9.847	-8.826	-1.716	2.943	14.844	-5.049	-25.466
-1.25	-1	14.167	8.903		18.750	-11.129	-1.216	1.478	13.156	-1.796	-15.992
-0.75	-0.5	17.766	11.165		29.915	-8.374	-0.716	0.512	5.717	-0.366	-4.091
-0.25	0	30.030	18.872		48.787	-4.718	-0.216	0.046	0.877	-0.010	-0.189
0.25	0.5	30.177	18.965		67.752	4.741	0.284	0.081	1.534	0.023	0.436
0.75	1	25.707	16.156		83.908	12.117	0.784	0.615	9.941	0.483	7.798
1.25	1.5	16.773	10.541		94.449	13.176	1.284	1.650	17.390	2.119	22.336
1.75	2	5.882	3.697	80.849	98.145	6.469	1.784	3.184	11.770	5.682	21.003
2.25	2.5	1.538	0.967		99.112	2.175	2.284	5.219	5.044	11.921	11.523
2.75	3	0.403	0.253		99.365	0.696	2.784	7.753	1.964	21.587	5.467
3.25	3.5	0.237	0.149		99.514	0.484	3.284	10.787	1.607	35.430	5.277
3.75	4	0.134	0.084		99.598	0.316	3.784	14.322	1.206	54.200	4.564
4.25	> 4	0.639	0.402	0.402	100.000	1.707	4.284	18.356	7.372	78.646	31.583
	TOTAL	159.121				-3.441			123.472		-16.740
$mean_\phi$	-0.034	SKϕ	-0.167								
σϕ	1.111	D50	0.032								

Sample ID	CR14-G46
Initial wt. (g)	241.975
% error	0.777

m_ϕ	phi (ϕ)	Individual wt. (g)	Individual wt. %	% G S M	Cummulative wt. %	fm_ϕ	m_ϕ-x	$(m_\phi-x)^2$	$f(m_\phi-x)^2$	$(m_\phi-x)^3$	$f(m_\phi-x)^3$
-3.175	-3	7.822	3.258	24.428	3.258	-10.344	-3.536	12.503	40.733	-44.210	-144.032
-2.75	-2.5	10.724	4.467		7.724	-12.283	-3.111	9.678	43.228	-30.108	-134.480
-2.25	-2	16.953	7.061		14.785	-15.887	-2.611	6.817	48.135	-17.799	-125.680
-1.75	-1.5	10.276	4.280		19.065	-7.490	-2.111	4.456	19.072	-9.407	-40.261
-1.25	-1	12.875	5.362		24.428	-6.703	-1.611	2.595	13.917	-4.181	-22.419
-0.75	-0.5	10.135	4.221		28.649	-3.166	-1.111	1.234	5.210	-1.371	-5.788
-0.25	0	15.419	6.422		35.071	-1.606	-0.611	0.373	2.397	-0.228	-1.465
0.25	0.5	17.011	7.085		42.156	1.771	-0.111	0.012	0.087	-0.001	-0.010
0.75	1	28.648	11.932		54.088	8.949	0.389	0.151	1.806	0.059	0.703
1.25	1.5	34.033	14.175		68.263	17.719	0.889	0.790	11.204	0.703	9.960
1.75	2	44.368	18.479	75.266	86.742	32.339	1.389	1.929	35.655	2.680	49.525
2.25	2.5	22.967	9.566		96.308	21.523	1.889	3.568	34.135	6.741	64.483
2.75	3	5.555	2.314		98.622	6.363	2.389	5.707	13.205	13.635	31.548
3.25	3.5	1.969	0.820		99.442	2.665	2.889	8.347	6.845	24.113	19.775
3.75	4	0.604	0.252		99.693	0.943	3.389	11.486	2.889	38.925	9.792
4.25	> 4	0.736	0.307	0.307	100.000	1.303	3.889	15.125	4.636	58.820	18.031
	TOTAL	240.095				36.096			283.155		-270.317
$mean_\phi$	0.361	SKϕ	-2.703								
σϕ	1.683	D50	0.829								

Sample ID	CR14-G47
Initial wt. (g)	606.990
% error	0.175

m_{ϕ}	phi (ϕ)	Individual wt. (g)	Individual wt. %	% G S M	Cummulative wt. %	fm_{ϕ}	m_{ϕ}-x	$(m_{\phi}-x)^2$	$f(m_{\phi}-x)^2$	$(m_{\phi}-x)^3$	$f(m_{\phi}-x)^3$
-3.675	-3.35	79.519	13.124	71.955	13.124	-48.229	-2.044	4.176	54.808	-8.535	-112.006
-3.175	-3	132.546	21.875		34.999	-69.453	-1.544	2.383	52.122	-3.678	-80.456
-2.75	-2.5	46.979	7.753		42.752	-21.321	-1.119	1.251	9.701	-1.400	-10.852
-2.25	-2	90.160	14.880		57.632	-33.479	-0.619	0.383	5.694	-0.237	-3.522
-1.75	-1.5	50.110	8.270		65.902	-14.473	-0.119	0.014	0.116	-0.002	-0.014
-1.25	-1	36.679	6.053		71.955	-7.567	0.381	0.145	0.881	0.055	0.336
-0.75	-0.5	21.136	3.488		75.443	-2.616	0.881	0.777	2.710	0.685	2.388
-0.25	0	14.131	2.332		77.775	-0.583	1.381	1.908	4.450	2.636	6.148
0.25	0.5	10.318	1.703		79.478	0.426	1.881	3.540	6.027	6.659	11.340
0.75	1	13.710	2.263		81.741	1.697	2.381	5.671	12.832	13.505	30.557
1.25	1.5	34.718	5.730		87.471	7.162	2.881	8.302	47.571	23.923	137.071
1.75	2	48.600	8.021	27.851	95.491	14.036	3.381	11.434	91.708	38.662	310.103
2.25	2.5	18.595	3.069		98.560	6.905	3.881	15.065	46.233	58.474	179.449
2.75	3	6.271	1.035		99.595	2.846	4.381	19.197	19.867	84.108	87.047
3.25	3.5	1.278	0.211		99.806	0.685	4.881	23.828	5.026	116.314	24.533
4.25	> 4	1.175	0.194	0.194	100.000	0.824	5.881	34.591	6.708	203.442	39.451
	TOTAL	605.925				-163.140			366.455		621.572
$mean_{\phi}$	-1.631	SKϕ	6.216								
σϕ	1.914	D50	-2.256								

Sample ID	CR14-G48
Initial wt. (g)	146.207
% error	0.103

m_ϕ	phi (ϕ)	Individual wt. (g)	Individual wt. %	% G S M	Cummulative wt. %	fm_ϕ	m_ϕ-x	$(m_\phi-x)^2$	$f(m_\phi-x)^2$	$(m_\phi-x)^3$	$f(m_\phi-x)^3$
-3.175	-3	1.503	1.029	37.993	1.029	-3.267	-2.529	6.398	6.583	-16.182	-16.652
-2.75	-2.5	2.118	1.450		2.479	-3.988	-2.104	4.428	6.422	-9.319	-13.513
-2.25	-2	10.718	7.338		9.817	-16.511	-1.604	2.574	18.888	-4.129	-30.303
-1.75	-1.5	15.637	10.706		20.524	-18.736	-1.104	1.220	13.057	-1.347	-14.419
-1.25	-1	25.515	17.469		37.993	-21.837	-0.604	0.365	6.380	-0.221	-3.856
-0.75	-0.5	27.732	18.987		56.980	-14.240	-0.104	0.011	0.207	-0.001	-0.022
-0.25	0	27.913	19.111		76.091	-4.778	0.396	0.157	2.992	0.062	1.184
0.25	0.5	15.164	10.382		86.474	2.596	0.896	0.802	8.329	0.719	7.460
0.75	1	9.786	6.700		93.174	5.025	1.396	1.948	13.051	2.719	18.215
1.25	1.5	5.692	3.897		97.071	4.871	1.896	3.594	14.004	6.812	26.548
1.75	2	2.748	1.881	61.785	98.952	3.293	2.396	5.739	10.798	13.749	25.869
2.25	2.5	0.862	0.590		99.543	1.328	2.896	8.385	4.949	24.280	14.329
2.75	3	0.155	0.106		99.649	0.292	3.396	11.530	1.224	39.154	4.155
3.25	3.5	0.122	0.084		99.732	0.271	3.896	15.176	1.268	59.121	4.938
3.75	4	0.066	0.045		99.777	0.169	4.396	19.322	0.873	84.932	3.838
4.25	> 4	0.325	0.223	0.223	100.000	0.946	4.896	23.967	5.333	117.337	26.109
	TOTAL	146.056				-64.566			114.357		53.880
$mean_\phi$	-0.646	SKϕ	0.539								
σϕ	1.069	D50	-0.684								

					Sample ID	CR14-G49					
					Initial wt. (g)	1481.741					
					% error	0.016					
m_ϕ	phi (ϕ)	Individual wt. (g)	Individual wt. %	% G S M	Cummulative wt. %	fm_ϕ	m_ϕ-x	$(m_\phi-x)^2$	$f(m_\phi-x)^2$	$(m_\phi-x)^3$	$f(m_\phi-x)^3$
-7.5	-6	1326.300	89.524		89.524	-671.432	-0.522	0.272	24.372	-0.142	-12.716
-3.675	-3.35	64.527	4.356	98.397	93.880	-16.007	3.303	10.911	47.525	36.043	156.986
-3.175	-3	26.001	1.755		95.635	-5.572	3.803	14.465	25.386	55.012	96.549
-2.75	-2.5	8.925	0.602		96.237	-1.657	4.228	17.878	10.770	75.592	45.539
-2.25	-2	15.565	1.051		97.288	-2.364	4.728	22.356	23.488	105.706	111.057
-1.75	-1.5	9.280	0.626		97.914	-1.096	5.228	27.334	17.122	142.911	89.519
-1.25	-1	7.154	0.483		98.397	-0.604	5.728	32.813	15.845	187.959	90.763
-0.75	-0.5	5.263	0.355		98.752	-0.266	6.228	38.791	13.780	241.599	85.828
-0.25	0	4.542	0.307		99.059	-0.077	6.728	45.269	13.879	304.582	93.379
0.25	0.5	2.714	0.183		99.242	0.046	7.228	52.247	9.571	377.657	69.184
0.75	1	2.775	0.187		99.430	0.140	7.728	59.726	11.187	461.574	86.458
1.25	1.5	3.548	0.239		99.669	0.299	8.228	67.704	16.214	557.084	133.415
1.75	2	2.664	0.180	1.567	99.849	0.315	8.728	76.182	13.699	664.936	119.567
2.25	2.5	1.017	0.069		99.918	0.154	9.228	85.160	5.846	785.880	53.948
2.75	3	0.341	0.023		99.941	0.063	9.728	94.639	2.178	920.667	21.191
3.25	3.5	0.235	0.016		99.956	0.052	10.228	104.617	1.659	1070.046	16.973
3.75	4	0.117	0.008		99.964	0.030	10.728	115.095	0.909	1234.767	9.751
4.25	> 4	0.529	0.036	0.036	100.000	0.152	11.228	126.073	4.502	1415.581	50.546
	TOTAL	1481.497				-697.824			257.933		1317.938
$mean_\phi$	-6.978	SKϕ	13.179								
σϕ	1.606	D50	-6.221								

					Sample ID	CR14-G50					
					Initial wt. (g)	761.352					
					% error	0.036					

m_ϕ	phi (ϕ)	Individual wt. (g)	Individual wt. %	% G S M	Cummulative wt. %	fm_ϕ	m_ϕ-x	$(m_\phi\text{-}x)^2$	$f(m_\phi\text{-}x)^2$	$(m_\phi\text{-}x)^3$	$f(m_\phi\text{-}x)^3$
-5.75	-5.5	228.154	29.978		29.978	-172.372	-1.277	1.631	48.898	-2.083	-62.450
-5.25	-5	125.638	16.508		46.486	-86.667	-0.777	0.604	9.970	-0.469	-7.749
-4.75	-4.5	266.739	35.048		81.533	-166.476	-0.277	0.077	2.692	-0.021	-0.746
-4.25	-4	11.224	1.475		83.008	-6.268	0.223	0.050	0.073	0.011	0.016
-3.675	-3.35	10.175	1.337	91.932	84.345	-4.913	0.798	0.637	0.851	0.508	0.679
-3.175	-3	19.649	2.582		86.927	-8.197	1.298	1.684	4.349	2.186	5.644
-2.75	-2.5	6.484	0.852		87.779	-2.343	1.723	2.968	2.529	5.114	4.357
-2.25	-2	16.901	2.221		89.999	-4.997	2.223	4.941	10.972	10.983	24.390
-1.75	-1.5	7.973	1.048		91.047	-1.833	2.723	7.414	7.767	20.187	21.148
-1.25	-1	6.733	0.885		91.932	-1.106	3.223	10.387	9.189	33.475	29.614
-0.75	-0.5	4.689	0.616		92.548	-0.462	3.723	13.860	8.539	51.597	31.789
-0.25	0	6.149	0.808		93.356	-0.202	4.223	17.832	14.407	75.303	60.840
0.25	0.5	6.522	0.857		94.213	0.214	4.723	22.305	19.114	105.344	90.274
0.75	1	10.893	1.431		95.644	1.073	5.223	27.278	39.042	142.469	203.910
1.25	1.5	15.064	1.979		97.623	2.474	5.723	32.751	64.824	187.428	370.977
1.75	2	11.734	1.542	8.019	99.165	2.698	6.223	38.724	59.703	240.972	371.521
2.25	2.5	4.756	0.625		99.790	1.406	6.723	45.197	28.244	303.850	189.877
2.75	3	0.830	0.109		99.899	0.300	7.223	52.169	5.689	376.812	41.094
3.25	3.5	0.285	0.037		99.936	0.122	7.723	59.642	2.233	460.608	17.248
3.75	4	0.110	0.014		99.951	0.054	8.223	67.615	0.977	555.988	8.036
4.25	> 4	0.375	0.049	0.049	100.000	0.209	8.723	76.088	3.749	663.703	32.702
	TOTAL	761.077				-447.284			343.812		1433.170
$mean_\phi$	-4.473	SKϕ	14.332								
σϕ	1.854	D50	-4.950								

					Sample ID	CR14-G51	
					Initial wt. (g)	324.671	
					% error	0.051	

m_ϕ	phi (ϕ)	Individual wt. (g)	Individual wt. %	% G S M	Cummulative wt. %	fm_ϕ	m_ϕ-x	$(m_\phi\text{-x})^2$	$f(m_\phi\text{-x})^2$	$(m_\phi\text{-x})^3$	$f(m_\phi\text{-x})^3$
-4.75	-4.5	153.706	47.366		47.366	-224.989	-1.570	2.464	116.694	-3.867	-183.165
-4.25	-4	22.659	6.983		54.349	-29.676	-1.070	1.144	7.989	-1.224	-8.545
-3.675	-3.35	32.353	9.970	82.675	64.318	-36.639	-0.495	0.245	2.439	-0.121	-1.206
-3.175	-3	16.959	5.226		69.545	-16.593	0.005	0.000	0.000	0.000	0.000
-2.75	-2.5	8.657	2.668		72.212	-7.336	0.430	0.185	0.494	0.080	0.213
-2.25	-2	13.247	4.082		76.295	-9.185	0.930	0.866	3.534	0.805	3.288
-1.75	-1.5	12.053	3.714		80.009	-6.500	1.430	2.046	7.599	2.927	10.870
-1.25	-1	8.651	2.666		82.675	-3.332	1.930	3.726	9.934	7.193	19.177
-0.75	-0.5	6.028	1.858		84.532	-1.393	2.430	5.907	10.972	14.356	26.667
-0.25	0	6.544	2.017		86.549	-0.504	2.930	8.587	17.317	25.164	50.745
0.25	0.5	6.167	1.900		88.449	0.475	3.430	11.768	22.363	40.367	76.715
0.75	1	8.442	2.601		91.051	1.951	3.930	15.448	40.188	60.717	157.953
1.25	1.5	11.652	3.591		94.641	4.488	4.430	19.628	70.479	86.961	312.250
1.75	2	9.986	3.077	17.181	97.719	5.385	4.930	24.309	74.805	119.852	368.817
2.25	2.5	5.168	1.593		99.311	3.583	5.430	29.489	46.964	160.138	255.030
2.75	3	1.166	0.359		99.671	0.988	5.930	35.170	12.637	208.569	74.942
3.25	3.5	0.455	0.140		99.811	0.456	6.430	41.350	5.798	265.896	37.282
3.75	4	0.146	0.045		99.856	0.169	6.930	48.030	2.161	332.869	14.976
4.25	> 4	0.468	0.144	0.144	100.000	0.613	7.430	55.211	7.962	410.237	59.164
	TOTAL	324.507				-318.039			460.329		1275.174
$mean_\phi$	-3.180	SKϕ	12.752								
σϕ	2.146	D50	-4.311								

Sample ID	CR14-G52
Initial wt. (g)	146.975
% error	0.258

m_ϕ	phi (ϕ)	Individual wt. (g)	Individual wt. %	% G S M	Cummulative wt. %	fm_ϕ	m_ϕ-x	$(m_\phi-x)^2$	$f(m_\phi-x)^2$	$(m_\phi-x)^3$	$f(m_\phi-x)^3$
-3.175	-3	10.713	7.308	64.800	7.308	-23.202	-2.149	4.619	33.758	-9.928	-72.554
-2.75	-2.5	14.265	9.731		17.039	-26.760	-1.724	2.973	28.931	-5.126	-49.885
-2.25	-2	28.617	19.521		36.560	-43.922	-1.224	1.499	29.259	-1.835	-35.821
-1.75	-1.5	23.095	15.754		52.314	-27.570	-0.724	0.525	8.264	-0.380	-5.986
-1.25	-1	18.304	12.486		64.800	-15.608	-0.224	0.050	0.628	-0.011	-0.141
-0.75	-0.5	9.229	6.296		71.095	-4.722	0.276	0.076	0.479	0.021	0.132
-0.25	0	6.858	4.678		75.774	-1.170	0.776	0.602	2.815	0.467	2.184
0.25	0.5	4.482	3.057		78.831	0.764	1.276	1.627	4.976	2.076	6.348
0.75	1	4.678	3.191		82.022	2.393	1.776	3.153	10.062	5.599	17.868
1.25	1.5	5.349	3.649		85.671	4.561	2.276	5.179	18.897	11.786	43.004
1.75	2	6.264	4.273	34.947	89.944	7.478	2.776	7.705	32.922	21.386	91.382
2.25	2.5	9.512	6.489		96.432	14.599	3.276	10.730	69.625	35.150	228.073
2.75	3	3.873	2.642		99.074	7.265	3.776	14.256	37.664	53.827	142.209
3.25	3.5	0.817	0.557		99.632	1.811	4.276	18.282	10.189	78.168	43.564
3.75	4	0.169	0.115		99.747	0.432	4.776	22.808	2.629	108.923	12.557
4.25	> 4	0.371	0.253	0.253	100.000	1.076	5.276	27.833	7.044	146.841	37.162
	TOTAL	146.596				-102.573			298.141		460.096
$mean_\phi$	-1.026	SKϕ	4.601								
σϕ	1.727	D50	-1.573								

Sample ID	CR14-G53
Initial wt. (g)	262.200
% error	0.000

m_ϕ	phi (ϕ)	Individual wt. (g)	Individual wt. %	% G S M	Cummulative wt. %	fm_ϕ	m_ϕ-x	$(m_\phi-x)^2$	$f(m_\phi-x)^2$	$(m_\phi-x)^3$	$f(m_\phi-x)^3$
-5.75	-5.5	262.200	100.000	100.000	100.000	-575.000	0.000	0.000	0.000	0.000	0.000
	TOTAL	262.200				-575.000			0.000		0.000
$mean_\phi$	-5.700	SKϕ	0.000								
σϕ	0.000	D50	-5.700								

Sample ID	CR14-G54
Initial wt. (g)	152.248
% error	0.070

m_ϕ	phi (ϕ)	Individual wt. (g)	Individual wt. %	% G S M	Cummulative wt. %	fm_ϕ	m_ϕ-x	$(m_\phi-x)^2$	$f(m_\phi-x)^2$	$(m_\phi-x)^3$	$f(m_\phi-x)^3$
-3.675	-3.35	11.841	7.783	73.015	7.783	-28.602	-1.909	3.642	28.349	-6.952	-54.105
-3.175	-3	27.326	17.961		25.744	-57.026	-1.409	1.984	35.634	-2.794	-50.191
-2.75	-2.5	44.026	28.938		54.682	-79.578	-0.984	0.967	27.992	-0.951	-27.531
-2.25	-2	0.384	0.252		54.934	-0.568	-0.484	0.234	0.059	-0.113	-0.029
-1.75	-1.5	15.279	10.043		64.977	-17.575	0.016	0.000	0.003	0.000	0.000
-1.25	-1	12.229	8.038		73.015	-10.047	0.516	0.267	2.144	0.138	1.107
-0.75	-0.5	7.443	4.892		77.907	-3.669	1.016	1.033	5.055	1.050	5.138
-0.25	0	6.580	4.325		82.232	-1.081	1.516	2.300	9.946	3.487	15.083
0.25	0.5	5.452	3.584		85.815	0.896	2.016	4.066	14.571	8.199	29.382
0.75	1	5.889	3.871		89.686	2.903	2.516	6.333	24.512	15.936	61.684
1.25	1.5	6.437	4.231		93.917	5.289	3.016	9.099	38.498	27.447	116.127
1.75	2	5.374	3.532	26.889	97.449	6.181	3.516	12.366	43.678	43.483	153.593
2.25	2.5	3.056	2.009		99.458	4.519	4.016	16.132	32.404	64.794	130.149
2.75	3	0.497	0.327		99.784	0.898	4.516	20.398	6.664	92.129	30.096
3.25	3.5	0.132	0.087		99.871	0.282	5.016	25.165	2.183	126.239	10.953
3.75	4	0.049	0.032		99.903	0.121	5.516	30.431	0.980	167.874	5.407
4.25	> 4	0.147	0.097	0.097	100.000	0.411	6.016	36.198	3.497	217.783	21.042
	TOTAL	152.141				-176.647			276.169		447.903
$mean_\phi$	-1.766	SKϕ	4.479								
σϕ	1.662	D50	-2.581								

Sample ID	CR14-G55
Initial wt. (g)	145.311
% error	0.146

m_ϕ	phi (ϕ)	Individual wt. (g)	Individual wt. %	% G S M	Cummulative wt. %	fm_ϕ	m_ϕ-x	$(m_\phi\text{-}x)^2$	$f(m_\phi\text{-}x)^2$	$(m_\phi\text{-}x)^3$	$f(m_\phi\text{-}x)^3$
-3.675	-3.35	22.731	15.666	69.065	15.666	-57.572	-2.091	4.373	68.512	-9.146	-143.275
-3.175	-3	22.273	15.350		31.016	-48.737	-1.591	2.532	38.868	-4.029	-61.848
-2.75	-2.5	15.442	10.642		41.658	-29.267	-1.166	1.360	14.475	-1.586	-16.881
-2.25	-2	19.030	13.115		54.774	-29.509	-0.666	0.444	5.822	-0.296	-3.879
-1.75	-1.5	12.000	8.270		63.044	-14.473	-0.166	0.028	0.229	-0.005	-0.038
-1.25	-1	8.737	6.021		69.065	-7.527	0.334	0.111	0.671	0.037	0.224
-0.75	-0.5	5.541	3.819		72.884	-2.864	0.834	0.695	2.655	0.580	2.213
-0.25	0	4.702	3.241		76.125	-0.810	1.334	1.779	5.765	2.373	7.689
0.25	0.5	3.952	2.724		78.848	0.681	1.834	3.363	9.159	6.166	16.795
0.75	1	5.682	3.916		82.764	2.937	2.334	5.446	21.328	12.711	49.774
1.25	1.5	10.885	7.502		90.266	9.377	2.834	8.030	60.240	22.755	170.706
1.75	2	9.541	6.576	30.749	96.841	11.507	3.334	11.114	73.080	37.051	243.629
2.25	2.5	3.499	2.411		99.253	5.426	3.834	14.698	35.443	56.347	135.879
2.75	3	0.539	0.371		99.624	1.022	4.334	18.781	6.977	81.394	30.235
3.25	3.5	0.197	0.136		99.760	0.441	4.834	23.365	3.172	112.941	15.334
3.75	4	0.078	0.054		99.814	0.202	5.334	28.449	1.529	151.740	8.157
4.25	> 4	0.270	0.186	0.186	100.000	0.791	5.834	34.033	6.333	198.538	36.944
	TOTAL	145.099				-158.375			354.255		491.658
$mean_\phi$	-1.584	SKϕ	4.917								
$\sigma\phi$	1.882	D50	-2.182								

Sample ID	CR14-G56
Initial wt. (g)	108.676
% error	0.127

m_ϕ	phi (ϕ)	Individual wt. (g)	Individual wt. %	% G S M	Cummulative wt. %	fm_ϕ	m_ϕ-x	$(m_\phi-x)^2$	$f(m_\phi-x)^2$	$(m_\phi-x)^3$	$f(m_\phi-x)^3$
-4.25	-4	12.395	11.420		11.420	-48.535	-3.893	15.152	173.038	-58.982	-673.568
-3.675	-3.35	1.241	1.143	43.968	12.563	-4.202	-3.318	11.006	12.585	-36.515	-41.750
-3.175	-3	2.528	2.329		14.892	-7.395	-2.818	7.939	18.491	-22.368	-52.099
-2.75	-2.5	2.834	2.611		17.504	-7.180	-2.393	5.724	14.947	-13.696	-35.762
-2.25	-2	9.924	9.143		26.647	-20.573	-1.893	3.582	32.751	-6.779	-61.984
-1.75	-1.5	10.978	10.114		36.761	-17.700	-1.393	1.939	19.615	-2.701	-27.316
-1.25	-1	7.822	7.207		43.968	-9.008	-0.893	0.797	5.742	-0.711	-5.125
-0.75	-0.5	4.280	3.943		47.911	-2.957	-0.393	0.154	0.608	-0.061	-0.239
-0.25	0	3.774	3.477		51.388	-0.869	0.107	0.012	0.040	0.001	0.004
0.25	0.5	3.108	2.864		54.252	0.716	0.607	0.369	1.056	0.224	0.642
0.75	1	4.447	4.097		58.349	3.073	1.107	1.226	5.025	1.358	5.564
1.25	1.5	9.183	8.461		66.810	10.576	1.607	2.584	21.860	4.153	35.138
1.75	2	18.795	17.317	55.615	84.126	30.304	2.107	4.441	76.906	9.359	162.071
2.25	2.5	14.345	13.217		97.343	29.737	2.607	6.799	89.854	17.727	234.286
2.75	3	1.830	1.686		99.029	4.637	3.107	9.656	16.280	30.005	50.590
3.25	3.5	0.463	0.427		99.455	1.386	3.607	13.013	5.551	46.945	20.026
3.75	4	0.138	0.127		99.583	0.477	4.107	16.871	2.145	69.295	8.811
4.25	> 4	0.453	0.417	0.417	100.000	1.774	4.607	21.228	8.860	97.807	40.821
	TOTAL	108.538				-35.741			505.353		-339.890
$mean_\phi$	-0.357	SKϕ	-3.399								
$\sigma\phi$	2.248	D50	-0.200								

Sample ID	CR14-G57
Initial wt. (g)	144.575
% error	0.108

m_ϕ	phi (ϕ)	Individual wt. (g)	Individual wt. %	% G S M	Cummulative wt. %	fm_ϕ	m_ϕ-x	$(m_\phi-x)^2$	$f(m_\phi-x)^2$	$(m_\phi-x)^3$	$f(m_\phi-x)^3$
-3.175	-3	8.134	5.632	39.966	5.632	-17.882	-2.753	7.577	42.673	-20.855	-117.459
-2.75	-2.5	6.475	4.483		10.116	-12.330	-2.328	5.418	24.289	-12.610	-56.535
-2.25	-2	13.525	9.365		19.481	-21.072	-1.828	3.340	31.279	-6.104	-57.164
-1.75	-1.5	14.877	10.301		29.782	-18.027	-1.328	1.762	18.155	-2.340	-24.102
-1.25	-1	14.707	10.184		39.966	-12.729	-0.828	0.685	6.974	-0.567	-5.772
-0.75	-0.5	11.793	8.166		48.131	-6.124	-0.328	0.107	0.876	-0.035	-0.287
-0.25	0	13.070	9.050		57.182	-2.263	0.172	0.030	0.269	0.005	0.046
0.25	0.5	12.296	8.514		65.696	2.129	0.672	0.452	3.850	0.304	2.589
0.75	1	15.995	11.075		76.771	8.307	1.172	1.375	15.225	1.612	17.850
1.25	1.5	16.992	11.766		88.537	14.707	1.672	2.797	32.910	4.678	55.040
1.75	2	10.377	7.185	59.838	95.722	12.574	2.172	4.720	33.911	10.253	73.671
2.25	2.5	4.915	3.403		99.125	7.657	2.672	7.142	24.306	19.087	64.957
2.75	3	0.734	0.508		99.634	1.398	3.172	10.064	5.115	31.929	16.228
3.25	3.5	0.177	0.123		99.756	0.398	3.672	13.487	1.653	49.530	6.070
3.75	4	0.068	0.047		99.803	0.177	4.172	17.409	0.820	72.639	3.420
4.25	> 4	0.284	0.197	0.197	100.000	0.836	4.672	21.832	4.293	102.008	20.060
	TOTAL	144.419				-42.245			246.598		-1.388
$mean_\phi$	-0.422	SKϕ	-0.014								
σϕ	1.570	D50	-0.397								

Sample ID	CR14-G58
Initial wt. (g)	152.656
% error	0.107

m_ϕ	phi (ϕ)	Individual wt. (g)	Individual wt. %	% G S M	Cummulative wt. %	fm_ϕ	m_ϕ-x	$(m_\phi\text{-}x)^2$	$f(m_\phi\text{-}x)^2$	$(m_\phi\text{-}x)^3$	$f(m_\phi\text{-}x)^3$
-3.675	-3.35	14.925	9.787	87.213	9.787	-35.968	-1.593	2.538	24.841	-4.044	-39.576
-3.175	-3	24.511	16.074		25.861	-51.033	-1.093	1.195	19.207	-1.306	-20.996
-2.75	-2.5	22.850	14.984		40.845	-41.207	-0.668	0.446	6.689	-0.298	-4.469
-2.25	-2	44.832	29.399		70.245	-66.149	-0.168	0.028	0.831	-0.005	-0.140
-1.75	-1.5	17.688	11.599		81.844	-20.299	0.332	0.110	1.277	0.037	0.424
-1.25	-1	8.188	5.369		87.213	-6.712	0.832	0.692	3.716	0.576	3.091
-0.75	-0.5	3.121	2.047		89.260	-1.535	1.332	1.774	3.630	2.363	4.835
-0.25	0	2.114	1.386		90.646	-0.347	1.832	3.356	4.652	6.147	8.522
0.25	0.5	1.696	1.112		91.758	0.278	2.332	5.438	6.048	12.680	14.102
0.75	1	2.104	1.380		93.138	1.035	2.832	8.019	11.065	22.710	31.334
1.25	1.5	2.905	1.905		95.043	2.381	3.332	11.101	21.148	36.988	70.462
1.75	2	2.988	1.959	12.464	97.002	3.429	3.832	14.683	28.771	56.264	110.245
2.25	2.5	2.986	1.958		98.961	4.406	4.332	18.765	36.744	81.287	159.170
2.75	3	0.663	0.435		99.395	1.196	4.832	23.347	10.151	112.809	49.046
3.25	3.5	0.273	0.179		99.574	0.582	5.332	28.429	5.089	151.578	27.136
3.75	4	0.157	0.103		99.677	0.386	5.832	34.011	3.502	198.345	20.421
4.25	> 4	0.492	0.323	0.323	100.000	1.371	6.332	40.092	12.935	253.859	81.905
	TOTAL	152.493				-208.186			200.296		515.511
$mean_\phi$	-2.082	SKϕ	5.155								
σϕ	1.415	D50	-2.344								

Sample ID	CR14-G59
Initial wt. (g)	78.361
% error	0.106

m_ϕ	phi (ϕ)	Individual wt. (g)	Individual wt. %	% G S M	Cummulative wt. %	fm_ϕ	m_ϕ-x	$(m_\phi-x)^2$	$f(m_\phi-x)^2$	$(m_\phi-x)^3$	$f(m_\phi-x)^3$
-2.25	-2	0.350	0.447	2.559	0.447	-1.006	-3.422	11.708	5.235	-40.059	-17.912
-1.75	-1.5	0.396	0.506		0.953	-0.885	-2.922	8.536	4.318	-24.939	-12.616
-1.25	-1	1.257	1.606		2.559	-2.007	-2.422	5.864	9.417	-14.201	-22.805
-0.75	-0.5	1.627	2.078		4.637	-1.559	-1.922	3.693	7.675	-7.096	-14.749
-0.25	0	3.690	4.714		9.351	-1.178	-1.422	2.021	9.527	-2.873	-13.544
0.25	0.5	5.642	7.208		16.559	1.802	-0.922	0.849	6.122	-0.783	-5.643
0.75	1	12.142	15.511		32.070	11.634	-0.422	0.178	2.758	-0.075	-1.163
1.25	1.5	24.042	30.714		62.784	38.392	0.078	0.006	0.189	0.000	0.015
1.75	2	19.985	25.531	97.281	88.315	44.679	0.578	0.334	8.540	0.193	4.939
2.25	2.5	8.149	10.410		98.725	23.423	1.078	1.163	12.106	1.254	13.054
2.75	3	0.715	0.913		99.638	2.512	1.578	2.491	2.275	3.932	3.592
3.25	3.5	0.120	0.153		99.792	0.498	2.078	4.320	0.662	8.978	1.376
3.75	4	0.038	0.049		99.840	0.182	2.578	6.648	0.323	17.141	0.832
4.25	> 4	0.125	0.160	0.160	100.000	0.679	3.078	9.476	1.513	29.171	4.658
	TOTAL	78.278				117.164			70.661		-59.966
$mean_\phi$	1.172	SKϕ	-0.600								
σϕ	0.841	D50	1.292								

Sample ID	CR14-G60
Initial wt. (g)	89.252
% error	0.543

m_ϕ	phi (ϕ)	Individual wt. (g)	Individual wt. %	% G S M	Cummulative wt. %	fm_ϕ	m_ϕ-x	$(m_\phi\text{-x})^2$	$f(m_\phi\text{-x})^2$	$(m_\phi\text{-x})^3$	$f(m_\phi\text{-x})^3$
-2.25	-2	1.071	1.207	10.799	1.207	-2.715	-2.506	6.279	7.576	-15.733	-18.982
-1.75	-1.5	2.653	2.989		4.195	-5.230	-2.006	4.023	12.024	-8.069	-24.117
-1.25	-1	5.862	6.604		10.799	-8.255	-1.506	2.267	14.973	-3.414	-22.545
-0.75	-0.5	9.192	10.355		21.154	-7.766	-1.006	1.012	10.475	-1.017	-10.535
-0.25	0	15.849	17.855		39.009	-4.464	-0.506	0.256	4.567	-0.129	-2.310
0.25	0.5	17.101	19.265		58.274	4.816	-0.006	0.000	0.001	0.000	0.000
0.75	1	16.899	19.037		77.311	14.278	0.494	0.244	4.651	0.121	2.299
1.25	1.5	12.439	14.013		91.324	17.516	0.994	0.989	13.852	0.983	13.773
1.75	2	5.412	6.097	88.880	97.421	10.670	1.494	2.233	13.613	3.336	20.341
2.25	2.5	1.722	1.940		99.361	4.365	1.994	3.977	7.715	7.931	15.386
2.75	3	0.130	0.146		99.508	0.403	2.494	6.221	0.911	15.517	2.273
3.25	3.5	0.088	0.099		99.607	0.322	2.994	8.966	0.889	26.845	2.661
3.75	4	0.064	0.072		99.679	0.270	3.494	12.210	0.880	42.664	3.076
4.25	> 4	0.285	0.321	0.321	100.000	1.365	3.994	15.954	5.122	63.724	20.460
	TOTAL	88.767				25.575			97.248		1.779
$mean_\phi$	0.256	SKϕ	0.018								
σϕ	0.986	D50	0.285								

					Sample ID	CR14-G60-R				
					Initial wt. (g)	78.440				
					% error	0.250				
m_{ϕ}	phi (ϕ)	Individual wt. (g)	Individual wt. %	% G S M	Cummulative wt. %	fm_{ϕ}	m_{ϕ}-x	$(m_{\phi}-x)^2$	$f(m_{\phi}-x)^2$	$(m_{\phi}-x)^3$
-3.175	-3	0.096	0.123	12.938	0.123	-0.390	-3.345	11.191	1.373	-37.439
-2.75	-2.5	0.638	0.815		0.938	-2.242	-2.920	8.528	6.954	-24.906
-2.25	-2	1.518	1.940		2.878	-4.365	-2.420	5.858	11.365	-14.178
-1.75	-1.5	2.928	3.742		6.620	-6.549	-1.920	3.688	13.800	-7.082
-1.25	-1	4.943	6.317		12.938	-7.897	-1.420	2.017	12.744	-2.865
-0.75	-0.5	9.586	12.251		25.189	-9.189	-0.920	0.847	10.377	-0.780
-0.25	0	11.416	14.590		39.779	-3.648	-0.420	0.177	2.578	-0.074
0.25	0.5	15.72	20.091		59.870	5.023	0.080	0.006	0.128	0.001
0.75	1	15.028	19.207		79.077	14.405	0.580	0.336	6.454	0.195
1.25	1.5	10.525	13.452		92.529	16.814	1.080	1.166	15.680	1.259
1.75	2	4.561	5.829	86.615	98.358	10.201	1.580	2.495	14.546	3.942
2.25	2.5	0.716	0.915		99.273	2.059	2.080	4.325	3.958	8.995
2.75	3	0.082	0.105		99.378	0.288	2.580	6.655	0.697	17.167
3.25	3.5	0.056	0.072		99.449	0.233	3.080	9.484	0.679	29.209
3.75	4	0.081	0.104		99.553	0.388	3.580	12.814	1.327	45.870
4.25	> 4	0.35	0.447	0.447	100.000	1.901	4.080	16.644	7.445	67.901
	TOTAL	78.244				17.034			110.104	
$mean_{\phi}$	0.170	SKϕ	-0.167							
σϕ	1.049	D50	0.254							

					Sample ID	CR14-G61					
					Initial wt. (g)	150.826					
					% error	0.106					
m_ϕ	phi (ϕ)	Individual wt. (g)	Individual wt. %	% G S M	Cummulative wt. %	fm_ϕ	m_ϕ-x	$(m_\phi-x)^2$	$f(m_\phi-x)^2$	$(m_\phi-x)^3$	$f(m_\phi-x)^3$
-3.675	-3.35	10.505	6.972	75.338	6.972	-25.623	-2.084	4.344	30.289	-9.054	-63.130
-3.175	-3	19.682	13.063		20.036	-41.476	-1.584	2.510	32.788	-3.976	-51.944
-2.75	-2.5	22.915	15.209		35.245	-41.825	-1.159	1.344	20.439	-1.558	-23.695
-2.25	-2	29.804	19.782		55.026	-44.508	-0.659	0.435	8.598	-0.287	-5.668
-1.75	-1.5	17.516	11.626		66.652	-20.345	-0.159	0.025	0.295	-0.004	-0.047
-1.25	-1	13.087	8.686		75.338	-10.858	0.341	0.116	1.008	0.040	0.344
-0.75	-0.5	6.605	4.384		79.722	-3.288	0.841	0.707	3.099	0.594	2.605
-0.25	0	4.145	2.751		82.473	-0.688	1.341	1.798	4.945	2.410	6.630
0.25	0.5	1.967	1.306		83.779	0.326	1.841	3.388	4.424	6.237	8.143
0.75	1	2.339	1.552		85.331	1.164	2.341	5.479	8.506	12.825	19.910
1.25	1.5	5.466	3.628		88.959	4.535	2.841	8.070	29.276	22.924	83.166
1.75	2	8.459	5.614	24.372	94.573	9.825	3.341	11.161	62.660	37.284	209.330
2.25	2.5	5.764	3.826		98.399	8.608	3.841	14.751	56.434	56.656	216.747
2.75	3	1.394	0.925		99.324	2.544	4.341	18.842	17.433	81.788	75.672
3.25	3.5	0.434	0.288		99.612	0.936	4.841	23.433	6.750	113.432	32.674
3.75	4	0.147	0.098		99.710	0.366	5.341	28.523	2.783	152.336	14.863
4.25	> 4	0.437	0.290	0.290	100.000	1.233	5.841	34.114	9.895	199.252	57.792
	TOTAL	150.666				-159.074			299.621		583.392
$mean_\phi$	-1.591	SKϕ	5.834								
σϕ	1.731	D50	-2.366								

Sample ID	CR14-G62
Initial wt. (g)	91.549
% error	0.208

m_ϕ	phi (ϕ)	Individual wt. (g)	Individual wt. %	% G S M	Cummulative wt. %	fm_ϕ	m_ϕ-x	$(m_\phi-x)^2$	$f(m_\phi-x)^2$	$(m_\phi-x)^3$	$f(m_\phi-x)^3$
-3.175	-3	0.661	0.724	15.252	0.724	-2.297	-3.313	10.974	7.940	-36.353	-26.302
-2.25	-2	2.049	2.243		2.966	-5.046	-2.388	5.701	12.786	-13.612	-30.529
-1.75	-1.5	4.134	4.525		7.491	-7.919	-1.888	3.563	16.124	-6.726	-30.437
-1.25	-1	7.090	7.761		15.252	-9.701	-1.388	1.926	14.944	-2.672	-20.738
-0.75	-0.5	8.767	9.596		24.848	-7.197	-0.888	0.788	7.562	-0.699	-6.712
-0.25	0	14.408	15.771		40.619	-3.943	-0.388	0.150	2.370	-0.058	-0.919
0.25	0.5	16.522	18.085		58.704	4.521	0.112	0.013	0.228	0.001	0.026
0.75	1	19.427	21.264		79.968	15.948	0.612	0.375	7.973	0.230	4.882
1.25	1.5	13.187	14.434		94.402	18.043	1.112	1.237	17.859	1.376	19.865
1.75	2	3.856	4.221	84.434	98.623	7.386	1.612	2.600	10.972	4.191	17.690
2.25	2.5	0.726	0.795		99.418	1.788	2.112	4.462	3.546	9.425	7.490
2.75	3	0.102	0.112		99.529	0.307	2.612	6.824	0.762	17.827	1.990
3.25	3.5	0.082	0.090		99.619	0.292	3.112	9.687	0.869	30.148	2.706
3.75	4	0.061	0.067		99.686	0.250	3.612	13.049	0.871	47.137	3.147
4.25	> 4	0.287	0.314	0.314	100.000	1.335	4.112	16.911	5.313	69.544	21.847
	TOTAL	91.359				13.768			110.119		-35.995
$mean_\phi$	0.138	SKϕ	-0.360								
$\sigma\phi$	1.049	D50	0.259								

					Sample ID	CR14-G62-R				
					Initial wt. (g)	81.496				
					% error	0.341				
m_{ϕ}	phi (ϕ)	Individual wt. (g)	Individual wt. %	% G S M	Cummulative wt. %	fm_{ϕ}	m_{ϕ}-x	$(m_{\phi}-x)^2$	$f(m_{\phi}-x)^2$	$(m_{\phi}-x)^3$
-3.175	-3	0.34	0.419	21.698	0.419	-1.329	-3.049	9.294	3.891	-28.334
-2.75	-2.5	3.144	3.871		4.290	-10.645	-2.624	6.883	26.646	-18.059
-2.25	-2	3.14	3.866		8.156	-8.699	-2.124	4.510	17.435	-9.577
-1.75	-1.5	4.402	5.420		13.576	-9.485	-1.624	2.636	14.287	-4.280
-1.25	-1	6.597	8.123		21.698	-10.153	-1.124	1.262	10.255	-1.419
-0.75	-0.5	10.124	12.465		34.164	-9.349	-0.624	0.389	4.847	-0.243
-0.25	0	10.931	13.459		47.622	-3.365	-0.124	0.015	0.206	-0.002
0.25	0.5	14.817	18.243		65.866	4.561	0.376	0.142	2.585	0.053
0.75	1	15.475	19.054		84.920	14.290	0.876	0.768	14.635	0.673
1.25	1.5	9.676	11.914		96.833	14.892	1.376	1.894	22.570	2.608
1.75	2	2.057	2.533	78.022	99.366	4.432	1.876	3.521	8.917	6.607
2.25	2.5	0.115	0.142		99.507	0.319	2.376	5.647	0.800	13.420
2.75	3	0.053	0.065		99.573	0.179	2.876	8.274	0.540	23.798
3.25	3.5	0.049	0.060		99.633	0.196	3.376	11.400	0.688	38.491
3.75	4	0.071	0.087		99.721	0.328	3.876	15.026	1.314	58.249
4.25	> 4	0.227	0.279	0.279	100.000	1.188	4.376	19.153	5.353	83.821
	TOTAL	81.218				-12.640			134.967	
$mean_{\phi}$	-0.126	SKϕ	-0.607							
σϕ	1.162	D50	0.065							

Sample ID	CR14-G63
Initial wt. (g)	264.347
% error	0.000

m_ϕ	phi (ϕ)	Individual wt. (g)	Individual wt. %	% G S M	Cummulative wt. %	fm_ϕ	m_ϕ-x	$(m_\phi-x)^2$	$f(m_\phi-x)^2$	$(m_\phi-x)^3$	$f(m_\phi-x)^3$
-4.75	-4.5	214.972	81.322		81.322	-386.279	-0.111	0.012	1.008	-0.001	-0.112
-4.25	-4	41.123	15.556	100.000	96.878	-66.115	0.389	0.151	2.350	0.059	0.913
-3.675	-3.35	8.252	3.122		100.000	-11.472	0.964	0.929	2.899	0.895	2.794
	TOTAL	264.347				-463.866			6.257		3.595
$mean_\phi$	-4.639	SKϕ	0.036								
σϕ	0.250	D50	-4.693								

Sample ID	CR14-G64
Initial wt. (g)	231.434
% error	0.043

m_ϕ	phi (ϕ)	Individual wt. (g)	Individual wt. %	% G S M	Cummulative wt. %	fm_ϕ	m_ϕ-x	$(m_\phi\text{-x})^2$	$f(m_\phi\text{-x})^2$	$(m_\phi\text{-x})^3$	$f(m_\phi\text{-x})^3$
-4.75	-4.5	99.606	43.057		43.057	-204.521	-1.692	2.864	123.309	-4.846	-208.674
-3.675	-3.35	31.486	13.611	81.958	56.668	-50.019	-0.617	0.381	5.186	-0.235	-3.201
-3.175	-3	29.596	12.794		69.461	-40.620	-0.117	0.014	0.176	-0.002	-0.021
-2.75	-2.5	6.069	2.623		72.085	-7.215	0.308	0.095	0.248	0.029	0.076
-2.25	-2	12.038	5.204		77.288	-11.708	0.808	0.652	3.395	0.527	2.742
-1.75	-1.5	5.626	2.432		79.720	-4.256	1.308	1.710	4.159	2.236	5.439
-1.25	-1	5.176	2.237		81.958	-2.797	1.808	3.268	7.312	5.907	13.217
-0.75	-0.5	4.633	2.003		83.960	-1.502	2.308	5.326	10.666	12.290	24.613
-0.25	0	5.269	2.278		86.238	-0.569	2.808	7.883	17.955	22.134	50.413
0.25	0.5	5.149	2.226		88.464	0.556	3.308	10.941	24.352	36.189	80.550
0.75	1	6.803	2.941		91.405	2.206	3.808	14.499	42.637	55.207	162.349
1.25	1.5	8.530	3.687		95.092	4.609	4.308	18.556	68.423	79.935	294.745
1.75	2	6.663	2.880	17.957	97.972	5.040	4.808	23.114	66.574	111.126	320.069
2.25	2.5	3.501	1.513		99.486	3.405	5.308	28.172	42.635	149.528	226.293
2.75	3	0.704	0.304		99.790	0.837	5.808	33.729	10.265	195.891	59.614
3.25	3.5	0.225	0.097		99.887	0.316	6.308	39.787	3.870	250.966	24.409
3.75	4	0.063	0.027		99.914	0.102	6.808	46.345	1.262	315.503	8.592
4.25	> 4	0.198	0.086	0.086	100.000	0.364	7.308	53.403	4.571	390.251	33.402
	TOTAL	231.335				-305.771			436.994		1094.627
$mean_\phi$	-3.058	SKϕ	10.946								
$\sigma\phi$	2.090	D50	-3.668								

Sample ID	CR14-G65
Initial wt. (g)	144.081
% error	0.136

m_ϕ	phi (ϕ)	Individual wt. (g)	Individual wt. %	% G S M	Cummulative wt. %	fm_ϕ	m_ϕ-x	$(m_\phi\text{-x})^2$	$f(m_\phi\text{-x})^2$	$(m_\phi\text{-x})^3$	$f(m_\phi\text{-x})^3$
-3.675	-3.35	3.327	2.312	46.393	2.312	-8.498	-3.066	9.400	21.736	-28.821	-66.642
-3.175	-3	3.850	2.676		4.988	-8.495	-2.566	6.584	17.618	-16.895	-45.208
-2.75	-2.5	12.128	8.429		13.417	-23.180	-2.141	4.584	38.637	-9.814	-82.722
-2.25	-2	18.161	12.622		26.039	-28.399	-1.641	2.693	33.989	-4.419	-55.776
-1.75	-1.5	14.120	9.813		35.852	-17.173	-1.141	1.302	12.776	-1.485	-14.577
-1.25	-1	15.167	10.541		46.393	-13.176	-0.641	0.411	4.331	-0.263	-2.776
-0.75	-0.5	12.039	8.367		54.760	-6.275	-0.141	0.020	0.166	-0.003	-0.023
-0.25	0	11.938	8.297		63.057	-2.074	0.359	0.129	1.069	0.046	0.384
0.25	0.5	9.404	6.536		69.593	1.634	0.859	0.738	4.823	0.634	4.143
0.75	1	10.754	7.474		77.067	5.606	1.359	1.847	13.804	2.510	18.759
1.25	1.5	13.532	9.405		86.472	11.756	1.859	3.456	32.502	6.425	60.421
1.75	2	12.242	8.508	53.303	94.980	14.889	2.359	5.565	47.347	13.128	111.693
2.25	2.5	5.590	3.885		98.865	8.741	2.859	8.174	31.756	23.369	90.791
2.75	3	0.828	0.575		99.441	1.583	3.359	11.283	6.493	37.899	21.810
3.25	3.5	0.253	0.176		99.616	0.571	3.859	14.892	2.619	57.468	10.105
3.75	4	0.115	0.080		99.696	0.300	4.359	19.001	1.519	82.825	6.620
4.25	> 4	0.437	0.304	0.304	100.000	1.291	4.859	23.610	7.171	114.721	34.842
	TOTAL	143.885				-60.901			278.355		91.844
$mean_\phi$	-0.609	SKϕ	0.918								
σϕ	1.668	D50	-0.784								

					Sample ID	CR14-G66					
					Initial wt. (g)	262.793					
					% error	0.381					
m_ϕ	phi (ϕ)	Individual wt. (g)	Individual wt. %	% G S M	Cummulative wt. %	fm_ϕ	m_ϕ-x	$(m_\phi-x)^2$	$f(m_\phi-x)^2$	$(m_\phi-x)^3$	$f(m_\phi-x)^3$
-4.75	-4.5	91.434	34.926		34.926	-165.899	-1.896	3.595	125.546	-6.815	-238.028
-4.25	-4	27.114	10.357		45.283	-44.017	-1.396	1.949	20.182	-2.720	-28.174
-3.675	-3.35	28.441	10.864	79.748	56.147	-39.925	-0.821	0.674	7.322	-0.553	-6.011
-3.175	-3	20.664	7.893		64.040	-25.061	-0.321	0.103	0.813	-0.033	-0.261
-2.75	-2.5	8.156	3.115		67.156	-8.567	0.104	0.011	0.034	0.001	0.004
-2.25	-2	15.143	5.784		72.940	-13.015	0.604	0.365	2.111	0.220	1.275
-1.75	-1.5	10.056	3.841		76.781	-6.722	1.104	1.219	4.682	1.346	5.169
-1.25	-1	7.767	2.967		79.748	-3.709	1.604	2.573	7.634	4.127	12.245
-0.75	-0.5	5.422	2.071		81.819	-1.553	2.104	4.427	9.169	9.315	19.292
-0.25	0	5.503	2.102		83.921	-0.526	2.604	6.781	14.254	17.658	37.119
0.25	0.5	4.869	1.860		85.781	0.465	3.104	9.635	17.920	29.908	55.625
0.75	1	6.312	2.411		88.192	1.808	3.604	12.989	31.318	46.814	112.871
1.25	1.5	9.892	3.779		91.971	4.723	4.104	16.843	63.643	69.126	261.195
1.75	2	10.937	4.178	20.116	96.148	7.311	4.604	21.197	88.557	97.594	407.719
2.25	2.5	8.445	3.226		99.374	7.258	5.104	26.051	84.037	132.968	428.931
2.75	3	0.877	0.335		99.709	0.921	5.604	31.405	10.521	175.998	58.959
3.25	3.5	0.296	0.113		99.822	0.367	6.104	37.259	4.213	227.434	25.715
3.75	4	0.108	0.041		99.864	0.155	6.604	43.614	1.799	288.026	11.882
4.25	> 4	0.357	0.136	0.136	100.000	0.580	7.104	50.468	6.882	358.524	48.891
	TOTAL	261.793				-285.405			500.636		1214.419
$mean_\phi$	-2.854	SKϕ	12.144								
$\sigma\phi$	2.237	D50	-3.718								

Sample ID	CR14-G67
Initial wt. (g)	329.839
% error	0.078

m_ϕ	phi (ϕ)	Individual wt. (g)	Individual wt. %	% G S M	Cummulative wt. %	fm_ϕ	m_ϕ-x	$(m_\phi-x)^2$	$f(m_\phi-x)^2$	$(m_\phi-x)^3$	$f(m_\phi-x)^3$
-4.75	-4.5	180.780	54.851		54.851	-260.543	-1.568	2.457	134.784	-3.852	-211.283
-4.25	-4	29.376	8.913		63.764	-37.881	-1.068	1.140	10.158	-1.217	-10.845
-3.675	-3.35	4.162	1.263	78.982	65.027	-4.641	-0.493	0.243	0.306	-0.120	-0.151
-3.175	-3	10.552	3.202		68.229	-10.165	0.007	0.000	0.000	0.000	0.000
-2.75	-2.5	3.404	1.033		69.261	-2.840	0.432	0.187	0.193	0.081	0.084
-2.25	-2	8.655	2.626		71.888	-5.909	0.932	0.869	2.283	0.811	2.129
-1.75	-1.5	11.882	3.605		75.493	-6.309	1.432	2.052	7.397	2.939	10.596
-1.25	-1	11.501	3.490		78.982	-4.362	1.932	3.734	13.031	7.216	25.182
-0.75	-0.5	10.156	3.081		82.064	-2.311	2.432	5.917	18.232	14.392	44.349
-0.25	0	10.609	3.219		85.283	-0.805	2.932	8.599	27.680	25.216	81.170
0.25	0.5	9.819	2.979		88.262	0.745	3.432	11.782	35.100	40.440	120.478
0.75	1	11.476	3.482		91.744	2.611	3.932	15.464	53.845	60.811	211.743
1.25	1.5	12.128	3.680		95.424	4.600	4.432	19.646	72.295	87.082	320.443
1.75	2	8.468	2.569	20.902	97.993	4.496	4.932	24.329	62.508	120.001	308.318
2.25	2.5	4.714	1.430		99.423	3.218	5.432	29.511	42.210	160.318	229.302
2.75	3	1.054	0.320		99.743	0.879	5.932	35.194	11.255	208.785	66.769
3.25	3.5	0.328	0.100		99.843	0.323	6.432	41.376	4.118	266.150	26.487
3.75	4	0.137	0.042		99.884	0.156	6.932	48.059	1.998	333.163	13.849
4.25	> 4	0.382	0.116	0.116	100.000	0.493	7.432	55.241	6.403	410.575	47.587
	TOTAL	329.583				-318.243			503.797		1286.207
$mean_\phi$	-3.182	SKϕ	12.862								
σϕ	2.245	D50	-4.544								

					Sample ID	CR14-G68					
					Initial wt. (g)	80.174					
					% error	0.258					
m_ϕ	phi (ϕ)	Individual wt. (g)	Individual wt. %	% G S M	Cummulative wt. %	fm_ϕ	m_ϕ-x	$(m_\phi-x)^2$	$f(m_\phi-x)^2$	$(m_\phi-x)^3$	$f(m_\phi-x)^3$
-2.75	-2.5	0.206	0.258	16.009	0.258	-0.708	-2.910	8.470	2.182	-24.652	-6.351
-2.25	-2	1.583	1.980		2.237	-4.454	-2.410	5.810	11.501	-14.005	-27.723
-1.75	-1.5	2.930	3.664		5.901	-6.412	-1.910	3.650	13.372	-6.972	-25.546
-1.25	-1	8.083	10.108		16.009	-12.635	-1.410	1.989	20.107	-2.806	-28.359
-0.75	-0.5	11.382	14.233		30.242	-10.675	-0.910	0.829	11.797	-0.755	-10.740
-0.25	0	14.594	18.250		48.493	-4.563	-0.410	0.168	3.074	-0.069	-1.262
0.25	0.5	11.419	14.280		62.772	3.570	0.090	0.008	0.115	0.001	0.010
0.75	1	10.235	12.799		75.571	9.599	0.590	0.348	4.449	0.205	2.623
1.25	1.5	8.138	10.177		85.748	12.721	1.090	1.187	12.082	1.294	13.165
1.75	2	6.220	7.778	83.648	93.526	13.612	1.590	2.527	19.654	4.017	31.242
2.25	2.5	4.023	5.031		98.557	11.319	2.090	4.366	21.967	9.124	45.902
2.75	3	0.655	0.819		99.376	2.252	2.590	6.706	5.493	17.366	14.224
3.25	3.5	0.157	0.196		99.572	0.638	3.090	9.546	1.874	29.492	5.790
3.75	4	0.068	0.085		99.657	0.319	3.590	12.885	1.096	46.253	3.933
4.25	> 4	0.274	0.343	0.343	100.000	1.456	4.090	16.725	5.731	68.398	23.436
	TOTAL	79.967				16.040			134.494		40.345
$mean_\phi$	0.160	SKϕ	0.403								
$\sigma\phi$	1.160	D50	0.053								

Sample ID	CR14-G68-R
Initial wt. (g)	82.005
% error	0.215

m_ϕ	phi (ϕ)	Individual wt. (g)	Individual wt. %	% G S M	Cummulative wt. %	fm_ϕ	m_ϕ-x	$(m_\phi-x)^2$	$f(m_\phi-x)^2$	$(m_\phi-x)^3$	$f(m_\phi-x)^3$
-2.75	-2.5	0.136	0.166	20.025	0.166	-0.457	-2.595	6.736	1.120	-17.482	-2.906
-2.25	-2	1.111	1.358		1.524	-3.055	-2.095	4.391	5.961	-9.200	-12.491
-1.75	-1.5	4.2	5.133		6.657	-8.982	-1.595	2.545	13.063	-4.060	-20.841
-1.25	-1	10.939	13.368		20.025	-16.710	-1.095	1.200	16.039	-1.314	-17.569
-0.75	-0.5	18.764	22.931		42.955	-17.198	-0.595	0.354	8.128	-0.211	-4.839
-0.25	0	14.246	17.409		60.365	-4.352	-0.095	0.009	0.158	-0.001	-0.015
0.25	0.5	11.845	14.475		74.840	3.619	0.405	0.164	2.370	0.066	0.959
0.75	1	8.615	10.528		85.368	7.896	0.905	0.818	8.616	0.740	7.794
1.25	1.5	6.058	7.403		92.772	9.254	1.405	1.973	14.607	2.771	20.517
1.75	2	4.279	5.229	79.686	98.001	9.151	1.905	3.628	18.970	6.909	36.131
2.25	2.5	1.123	1.372		99.373	3.088	2.405	5.782	7.935	13.904	19.082
2.75	3	0.147	0.180		99.553	0.494	2.905	8.437	1.516	24.506	4.402
3.25	3.5	0.055	0.067		99.620	0.218	3.405	11.592	0.779	39.465	2.653
3.75	4	0.074	0.090		99.710	0.339	3.905	15.246	1.379	59.531	5.384
4.25	> 4	0.237	0.290	0.290	100.000	1.231	4.405	19.401	5.619	85.454	24.750
	TOTAL	81.829				-15.464			106.260		63.012
$mean_\phi$	-0.155	SKϕ	0.630								
σϕ	1.031	D50	-0.298								

APPENDIX B

LOSS ON IGNITION DATA OF SEDIMENT SAMPLES FROM THE DEEP WATER CHANNEL ENVIRONMENT

Sediment wet and dry bulk density and organic content were measured by Dean's (1974) method of loss on ignition (LOI). The measured sediment samples were collected during the years 2012, 2013 and 2014.

Sample ID	Latitude	Longitude	Distance from LeFever (m)	Water Depth (m)	WBD (g/cc)	DBD (g/cc)	Water (%)	Organic Matter (%)	Comments
CR12-G28	41.1410	-81.4768	603	2.04	1.369	0.568	58.503	14.657	Mud
CR12-G27	41.1419	-81.4758	726	1.65	1.480	0.670	54.748	11.503	Mud
CR14-G68	41.1425	-81.4753	809	0.97	2.076	1.665	24.645	1.378	Coarse sand
CR14-G15	41.1425	-81.4753	811	0.91	2.015	1.584	27.258	1.725	Sand and gravel
CR14-G14	41.1428	-81.4751	847	0	1.637	0.978	67.318	7.757	Sand, gravel and mud
CR13-G16	41.14382	-81.47453	964	0	1.444	0.648	55.161	9.326	Mud
CR14-G67	41.1441	-81.4740	1016	0.74	2.055	1.677	22.535	0.974	Sand and granules
CR13-G15	41.14457	-81.47368	1076	0.65	1.800	1.321	26.610	3.636	Little sand, no bed forms.
CR14-G13	41.1448	-81.4735	1106	1.08	1.958	1.446	35.412	5.464	Sand
CR14-G12	41.1464	-81.4708	1391	0.28	2.053	1.601	28.220	2.881	Sandy granules
CR13-G14	41.14642	-81.47067	1406	0.55	1.346	0.648	51.837	36.792	Mud, sticks and leaves
CR12-G26	41.1428	-81.4750	1455	1.3	1.285	0.455	64.628	14.712	Mud
CR14-G66	41.1466	-81.4702	1457	0.9	2.036	1.652	23.200	7.094	Little sand on bedrock
CR13-G13	41.14792	-81.46847	1655	0.36	1.740	1.234	29.071	3.703	Sand
CR12-G25	41.1447	-81.4737	1687	2.75	1.849	1.396	24.526	1.553	Sand
CR12-G24	41.1453	-81.4725	1818	2.48	1.865	1.401	24.896	2.740	Sand
CR14-G11	41.1482	-81.4652	1957	0.38	2.114	1.612	31.152	3.844	Sand
CR12-G23	41.1465	-81.4706	2023	1.9	1.669	1.125	32.577	19.865	Sand and leaves
CR13-G12	41.1478	-81.46447	2039	0.48	1.860	1.439	22.623	1.776	Small dunes.
CR14-G65	41.1474	-81.4640	2095	0.71	2.057	1.676	22.787	0.461	Sand, granules with shells
CR12-G22	41.1478	-81.4686	2248	1.55	1.071	0.134	87.518	26.036	Mud
CR13-G10	41.14642	-81.46168	2337	0.24	1.928	1.497	22.367	1.032	Sand
CR14-G64	41.1458	-81.4619	2356	0.62	2.093	1.724	21.362	0.880	Sand and gravel
CR14-G10	41.1458	-81.4617	2366	0.42	1.995	1.503	32.770	2.498	Sand

Sample ID	Latitude	Longitude	Distance from LeFever (m)	Water Depth (m)	WBD (g/cc)	DBD (g/cc)	Water (%)	Organic Matter (%)	Comments
CR13-G11	41.1456	-81.46168	2378	0.4	1.898	1.471	22.506	1.987	Sand
CR12-G20	41.1484	-81.4654	2546	0.76	1.983	1.536	22.516	1.256	Sand
CR14-G9	41.1444	-81.4599	2582	0.5	1.972	1.348	46.305	4.668	Sand, gravel with leaves
CR13-G9	41.14537	-81.45872	2751	0.6	1.930	1.510	21.792	0.780	Sand
CR14-G48	41.1455	-81.4588	2774	0.56	1.912	1.430	33.757	5.010	Sand to pebbles with shells
CR14-G62	41.1456	-81.4588	2778	0.72	1.984	1.582	25.374	1.272	Coarse sand
CR12-G19	41.1468	-81.4628	2831	0.76	1.992	1.570	21.181	1.021	Sand
CR12-G17	41.1463	-81.4624	2887	1.14	2.027	1.597	21.215	1.718	Sand
CR12-G18	41.1459	-81.4618	2962	0.14	1.994	1.573	21.119	0.484	Sand
CR14-G61	41.1457	-81.4572	3132	0.42	2.252	1.913	17.690	9.068	Sand and pebbles
CR12-G16	41.1456	-81.4590	3398	0.41	2.051	1.620	20.992	0.508	Sand
CR13-G8	41.14708	-81.45637	3430	0.52	2.044	1.634	20.041	1.045	Coarse sand and granules
CR12-G15	41.1461	-81.4591	3453	1.32	1.968	1.494	24.084	2.977	Coarse sand
CR14-G60	41.1472	-81.4563	3458	0.71	1.999	1.558	28.344	2.559	Sand and granules
CR14-G8	41.1474	-81.4564	3473	0.57	2.081	1.600	30.051	1.057	Sand and 2.5-D ripples
CR14-G45	41.1477	-81.4563	3513	0.84	1.951	1.438	35.616	18.466	Sand, granules with shells
CR12-G14	41.1457	-81.4573	3719	0.86	2.068	1.645	20.493	4.713	Sand
CR13-G7	41.14952	-81.46048	3742	0.45	1.939	1.527	21.258	2.231	Sand
CR14-G44	41.1496	-81.4546	3819	1.27	1.983	1.711	15.907	1.898	Cobbles and sand
CR14-G59	41.1496	-81.4544	3834	0.96	2.058	1.623	26.847	0.811	Sand with leaves and shells
CR12-G13	41.1460	-81.4557	3908	0.76	2.080	1.616	22.321	0.793	Sand
CR14-G43	41.1487	-81.4531	3976	0.96	2.019	1.612	25.226	2.363	Sand to pebbles with shells
CR14-G58	41.1487	-81.4530	3985	1.38	2.170	1.821	19.176	1.112	Sand, coarse pebbles, shells
CR13-G6	41.14845	-81.45192	4069	0.54	2.006	1.576	21.474	1.747	Sand, granules with shells

Sample ID	Latitude	Longitude	Distance from LeFever (m)	Water Depth (m)	WBD (g/cc)	DBD (g/cc)	Water (%)	Organic Matter (%)	Comments
CR12-G12	41.1474	-81.4562	4071	1.08	1.996	1.584	20.619	1.042	Sand
CR14-G42	41.1485	-81.4520	4073	0.54	2.044	1.619	26.305	3.826	Sand, gravel with shells
CR14-G57	41.1484	-81.4515	4118	0.94	2.058	1.680	22.439	0.970	Sand, granules with shells
CR14-G7	41.1480	-81.4499	4262	0.76	2.131	1.685	26.452	1.946	Sand and granules
CR14-G56	41.1478	-81.4497	4281	1.1	1.996	1.592	25.428	2.046	Sand, granules with shells
CR13-G5	41.14778	-81.44928	4305	1.2	2.051	1.634	20.323	1.780	Sand to pebbles
CR14-G41	41.1473	-81.4486	4393	0.66	2.083	1.630	27.818	3.232	Sand, granules with shells
CR14-G55	41.1462	-81.4476	4540	0.56	2.141	1.787	19.843	4.910	Sand, pebbles with shells
CR13-G4	41.14603	-81.44753	4547	0.28	2.088	1.736	16.839	2.481	Sand and granules
CR14-G6	41.1459	-81.4473	4588	0.42	2.147	1.748	22.841	5.326	Sand to pebbles with shells
CR12-G11	41.1486	-81.4528	4603	1.3	2.027	1.620	20.080	0.986	Sand
CR14-G40	41.1456	-81.4470	4622	0.63	2.257	1.944	16.106	0.534	Sand to gravel with shells
CR14-G54	41.1453	-81.4467	4667	1.08	2.152	1.801	19.489	0.891	Sand to pebbles
CR13-G3	41.14485	-81.4464	4707	0.84	2.088	1.705	18.309	1.156	Sand, pebbles with shells
CR12-G10	41.1484	-81.4512	4739	0.83	2.067	1.632	21.032	2.377	Sand with granules
CR14-G5	41.1443	-81.4453	4831	0.78	1.987	1.525	30.294	1.110	Sand with cobbles
CR13-G2	41.14417	-81.44453	4887	0.79	2.077	1.693	18.474	1.065	Sand with pebbles
CR12-G9	41.1479	-81.4495	4893	0.56	2.120	1.729	18.431	8.093	Sand with granules
CR14-G52	41.1442	-81.4445	4902	0.76	2.216	1.870	18.471	1.539	Sand to pebbles
CR14-G4	41.1441	-81.4444	4907	0.54	2.281	1.852	23.185	1.499	Sand and gravel
CR12-G8	41.1471	-81.4485	5008	1.15	1.882	1.375	26.915	3.161	Sand with granules
CR14-G51	41.1436	-81.4426	5070	0.74	2.086	1.736	20.140	1.229	Sand with gravel
CR14-G39	41.1436	-81.4425	5076	0.5	2.248	1.862	20.722	1.114	Sand to gravel
CR13-G1	41.14317	-81.44177	5150	0.65	2.126	1.760	17.222	2.412	Sand with pebbles

Sample ID	Latitude	Longitude	Distance from LeFever (m)	Water Depth (m)	WBD (g/cc)	DBD (g/cc)	Water (%)	Organic Matter (%)	Comments
CR14-G3	41.1431	-81.4418	5154	0.56	2.216	1.820	21.767	5.116	Sand and pebbles
CR14-G50	41.1432	-81.4416	5162	0.84	2.132	1.733	22.990	2.167	Sand with gravel
CR12-G7	41.1458	-81.4472	5198	0.69	1.901	1.402	26.230	10.189	Sand
CR12-G6	41.1443	-81.4462	5380	1.18	2.025	1.577	22.115	1.097	Sand with gravel
CR14-G1	41.1423	-81.4383	5466	0.5	2.145	1.746	22.855	1.719	Sand, pebbles with shells
CR14-G2	41.1422	-81.4382	5473	0.5	2.234	1.866	19.726	1.667	Sand, gravel with shells
CR14-G49	41.1420	-81.4379	5507	0.56	2.210	1.821	21.360	2.234	Sand to fine cobbles
CR12-G5	41.1441	-81.4444	5509	0.56	2.190	1.805	17.542	20.466	Sand with pebbles
CR12-G4	41.1441	-81.4443	5523	-	2.144	1.779	17.032	-	Gravel
CR12-G3	41.1435	-81.4425	5682	-	2.173	1.830	15.767	0.983	Pebbly sand
CR12-G2	41.1432	-81.4417	5762	0.89	2.012	1.573	21.821	0.892	Sand
CR12-G1	41.1431	-81.4417	5764	-	2.115	1.747	17.407	4.964	Gravel
CR14-G38	41.1393	-81.4336	5984	0.74	2.212	1.859	18.957	0.582	Red pebbley sand on bedrock
CR12-G51	41.1420	-81.4378	6116	0.22	2.156	1.768	17.967	1.717	Sand, gravel with shells
CR14-G37	41.1379	-81.4310	6246	0.64	2.070	1.634	26.681	1.113	Cobbles and big boulder
CR14-G36	41.1372	-81.4284	6480	1.01	2.207	1.842	19.858	1.522	Sand and gravel
CR12-G50	41.1401	-81.4343	6489	0.78	2.149	1.781	17.113	1.530	Sand to boulders on bedrock
CR12-G49	41.1392	-81.4336	6599	0.58	2.031	1.611	20.679	1.935	Sand and pebbles
CR14-G35	41.1365	-81.4247	6804	0.53	2.278	1.971	15.589	1.266	Sand, mud, Macrophytes
CR12-G48	41.1381	-81.4312	6839	0.53	2.087	1.680	19.470	1.650	Sand
CR14-G34	41.1360	-81.4218	7059	0.41	2.180	1.792	21.619	2.038	Fine cobbles
CR12-G47	41.1373	-81.4286	7070	0.77	2.180	1.819	16.557	1.791	Sand, gravel with shells
CR14-G33	41.1358	-81.4199	7213	0.8	2.302	1.955	17.779	1.505	Gravel with sand and shells
CR14-G32	41.1365	-81.4189	7331	0.59	2.232	1.867	19.527	1.591	Sand to fine cobbles, shells

Sample ID	Latitude	Longitude	Distance from LeFever (m)	Water Depth (m)	WBD (g/cc)	DBD (g/cc)	Water (%)	Organic Matter (%)	Comments
CR12-G46	41.1470	-81.4242	7473	0.42	2.238	1.853	17.218	0.787	Sand with pebbles
CR14-G31	41.1380	-81.4167	7581	0.69	2.126	1.713	24.113	2.926	Cobbles and fines inbetween
CR12-G45	41.1360	-81.4219	7658	0.3	2.175	1.804	17.073	2.925	Sand and gravel
CR12-G44	41.1359	-81.4198	7831	0.68	2.166	1.765	18.489	1.022	Sand and gravel
CR12-G43	41.1365	-81.4189	7934	0.47	2.204	1.829	17.023	3.740	Sand and gravel
CR14-G29	41.1387	-81.4118	7997	0.91	2.267	1.891	19.880	1.803	Sand to gravel
CR14-G28	41.1375	-81.4094	8229	0.88	2.159	1.826	18.243	1.244	Gravel on bedrock.
CR12-G42	41.1381	-81.4157	8267	0.1	2.151	1.756	18.350	1.526	Gravel with shells
CR14-G27	41.1374	-81.4070	8440	0.78	2.209	1.836	20.342	3.460	Gravel with sand
CR12-G41	41.1385	-81.4126	8537	0.84	2.128	1.749	17.832	1.371	San, pebbles with shells
CR14-G26	41.1379	-81.4055	8584	0.6	1.996	1.573	26.942	1.532	Cobbles and boulders
CR14-G25	41.1383	-81.4042	8700	0.8	1.977	1.497	32.093	6.075	Sand
CR12-G40	41.1380	-81.4104	8736	0.58	2.115	1.743	17.573	1.377	Gravel
CR14-G24	41.1391	-81.4027	8849	0.61	2.235	1.864	19.949	1.110	Sand with pebbles and mud
CR12-G39	41.1372	-81.4081	8952	0.68	2.170	1.805	16.821	4.114	Sand and granules
CR12-G38	41.1374	-81.4068	9043	0.81	2.119	1.727	18.495	0.000	Sand, gravel with shells
CR14-G23	41.1401	-81.4006	9056	0.6	1.952	1.488	31.199	1.421	Coarse with sand inbetween
CR14-G22	41.1400	-81.3989	9199	0.54	2.072	1.684	22.993	1.042	Sand to fine cobbles
CR12-G37	41.1380	-81.4031	9235	0.81	2.129	1.762	17.248	1.513	Sand to gravel with shells
CR14-G21	41.1398	-81.3975	9319	0.79	2.124	1.753	21.117	1.169	Sand and pebbles
CR12-G36	41.1388	-81.4031	9411	0.81	2.245	1.899	15.408	1.978	Sand, gravel with shells
CR14-G20	41.1396	-81.3956	9486	0.81	2.130	1.815	17.387	4.634	Sand to fine cobbles
CR14-G18	41.1392	-81.3918	9854	0.84	2.013	1.616	24.602	1.123	Sand with pebbles and shells
CR12-G34	41.1397	-81.3969	9980	1.35	2.015	1.634	18.896	1.783	Sand and pebbles

Sample ID	Latitude	Longitude	Distance from LeFever (m)	Water Depth (m)	WBD (g/cc)	DBD (g/cc)	Water (%)	Organic Matter (%)	Comments
CR14-G16	41.1382	-81.3900	10104	0.72	2.127	1.691	25.773	2.868	Sand to fine cobbles
CR12-G33	41.1397	-81.3951	10130	1.35	2.209	1.842	16.577	1.421	Sand, gravel with shells
CR12-G32	41.1400	-81.3918	10401	0.81	2.110	1.757	16.706	2.039	Sand gravel with shells
CR12-G31	41.1393	-81.3918	10443	1.35	2.160	1.813	16.057	1.929	Sand and pebbles
CR12-G29	41.1382	-81.3900	10719	0.764	2.101	1.752	16.589	1.427	Sand, gravel with shells

APPENDIX C

LOCATION MAPS OF GEOMORPHIC TRANSECTS

These maps aid in locating the local reference stakes (rebars) at the geomorphic transects during field surveys. The latitude and longitude of the rebar locations are given in decimal degrees.

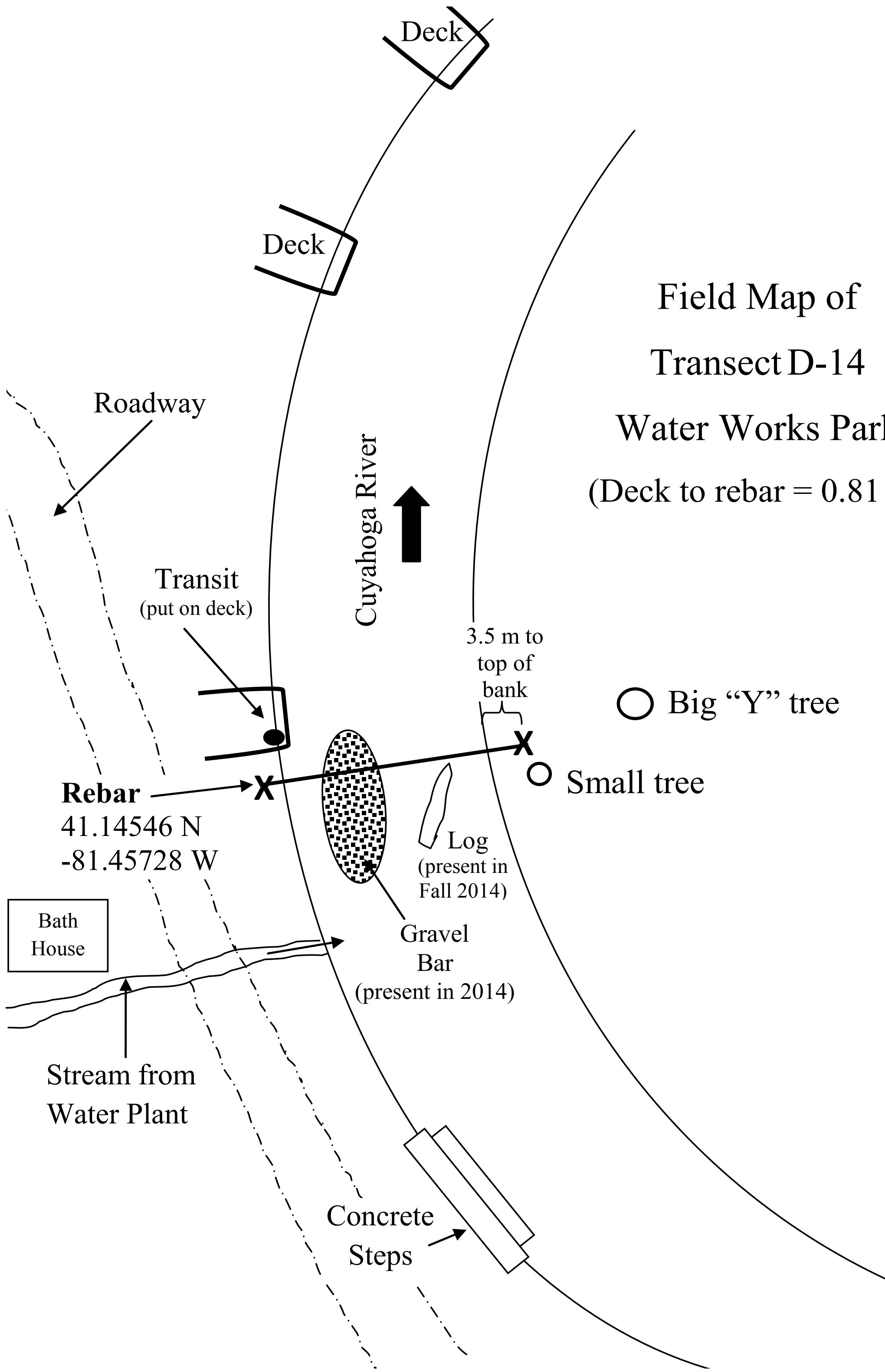
Field Map of
Transect D-14
Water Works Park
(Deck to rebar = 0.81 m)
Deck
Deck
Roadway
Cuyahoga River
Transit
(put on deck)
3.5 m to
top of
bank
Big "Y" tree
Small tree
Rebar
41.14546 N
-81.45728 W
Log
(present in
Fall 2014)
Bath
House
Gravel
Bar
(present in 2014)
Stream from
Water Plant
Concrete
Steps

Field map for L-1 Delta and D-15 profiles.

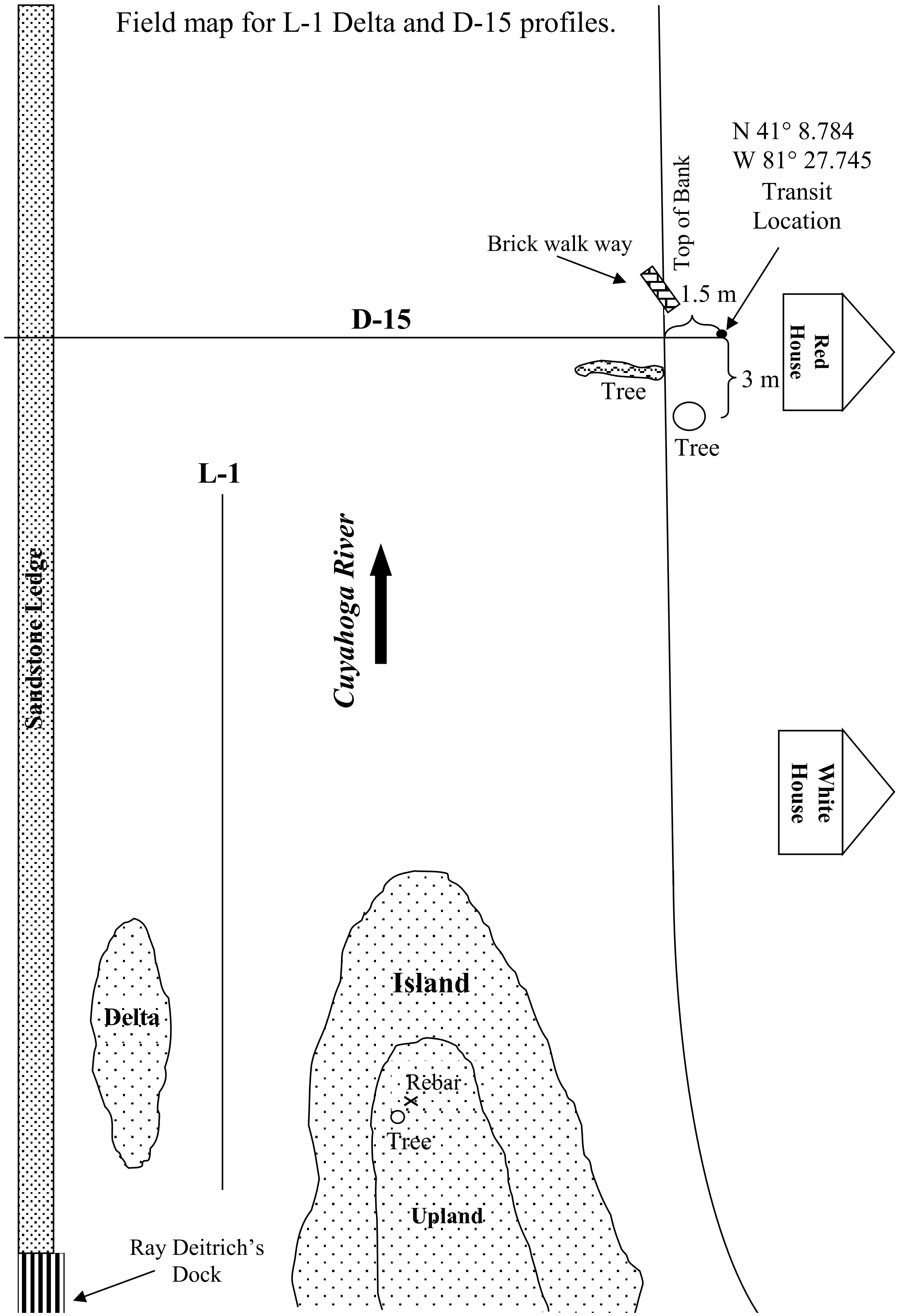

APPENDIX D

SURVEY DATA OF GEOMORPHIC PROFILES

Survey data of geomorphic profiles measured from July 8, 2011 through May 3, 2015. Survey data before 2011 was obtained from Rumschlag (2007), Rumschlag and Peck (2007) Kasper (2010) and Peck and Kasper (2013). Transects D-15 and D-14 were established in 2013. Elevations were measured relative to the local reference stake. These data begin upstream at transect U-8 and end downstream and transect D-13.

Transect U-8
July 7, 2011

Distance (m)	Elevation (m)	Comments
-8.25	1.5025	Eye height
-4	1.415	-
-0.75	0.735	Top of scarp
0	0	Next to rebar
1.5	-0.44	-
2.75	-0.9	Zero water
2.74	-0.9	-
2.84	-0.98	-
3.84	-1.04	-
4.84	-1.11	-
5.84	-1.26	-
6.84	-1.37	-
7.84	-1.48	-
8.84	-1.56	-
9.84	-1.62	-
10.84	-1.62	-
11.84	-1.65	-
12.84	-1.67	-
13.84	-1.72	-
14.84	-1.66	-
15.84	-1.66	-
16.84	-1.63	-
17.84	-1.56	-
18.84	-1.54	-
19.84	-1.6	-
20.84	-1.7	-
21.84	-1.69	-
22.84	-1.67	-
23.84	-1.58	-
24.84	-1.6	-
25.84	-1.48	-
26.84	-1.42	-
27.84	-1.32	-
28.84	-1.14	-
29.84	-1.05	-
30.84	-0.99	-
31.84	-0.93	-
32.3	-0.9	-

Transect U-8
August 19, 2014

Distance (m)	Elevation (m)	Comments
-7.75	1.5975	Instrument height on right bank
-5	1.5225	Parking lot
-1	0.7525	Top of bank
0	-0.21	Rebar
1.1	-0.7025	1.1 m on rope
2	-0.9125	Gravel
3	-1.0025	Gravel
4	-1.1025	Gravel
5	-1.1525	Gravel
6	-1.2525	Gravel
7	-1.3925	Gravel
8	-1.5125	Gravel
9	-1.5825	Gravel
10	-1.6225	Gravel
11	-1.6525	Gravel
12	-1.6625	Gravel
13	-1.7125	Gravel
14	-1.7125	Gravel
15	-1.7025	Gravel
16	-1.7025	-
17	-1.6725	Sand
18	-1.6225	-
19	-1.6225	Sand
20	-1.6625	Gravel
21	-1.5925	Gravel
22	-1.6525	Gravel
23	-1.6025	Gravel
24	-1.6025	Boulder
25	-1.5925	Gravel
26	-1.4925	Gravel
27	-1.3725	Mud begins b/w 26 and 27 m on rope
28	-1.1825	Old dam pool mud
29	-1.0425	Old dam pool mud
30	-0.9825	Old dam pool mud
31	-0.9225	Mud
32	-0.8725	Mud
33	-0.8125	Mud
34	-0.7525	Mud
34.8	-0.7025	Mud
36.25	-0.6275	Edge of the veg. on left bank
39.25	-0.2875	Base of former bank, river left

FC Transect
July 7, 2011

Distance (m)	Elevation (m)	Comments
10.12	-0.58	-
12.37	-0.9825	-
12.87	-1.1875	-
13.87	-1.86	-
14.12	-2.1	-
15.87	-2.0825	-
18.12	-2.145	-
19.87	-2.145	-
20.62	-2.0025	-
21.62	-0.7525	-
23.12	-0.46	-
23.62	-0.0475	-
28.62	0.125	-

FC Transect
August 19, 2014

Distance (m)	Elevation (m)	Comments
10.12	-0.58	Instrument height at 7/7/11 rebar on right bank
11.87	-0.8925	Top of bank
12.12	-1.71	0 water, base of bank
13.12	-1.9375	-
14.37	-1.965	-
16.62	-2.0125	-
19.12	-2.1	-
20.87	-2.03	Base of left bank, 34 cm
21.37	-0.6975	Top of left bank
22.87	-0.47	Base of old bank
23.37	-0.085	
28.12	0.145	-
34.12	0.2	Rebar distance on left bank

Transect U-4
July 7, 2011

Distance (m)	Elevation (m)	Comments
0	0	-
3.75	0.02	-
7	-0.3125	-
8.5	-0.7275	-
11.5	-1.04	-
13.25	-1.3975	-
13.5	-1.7025	-
14.75	-1.9325	-
17.5	-1.7125	-
20	-1.8225	-
24.25	-1.9875	-
28.25	-2.0325	-
32.75	-2.2625	-
37	-2.3725	-
39.5	-2.29	-
41.5	-2.175	-
43.25	-2.305	-
45.5	-1.9925	-
46.75	-1.8525	-

Transect U-4
May 3, 2015

Distance (m)	Elevation (m)	Comments
0	0	Instrument height at right bank rebar
6.5	-0.0925	Top of old bank, starting to roll over
8.5	-0.6325	Bottom of old bank
11.5	-1	Edge of vegetation
14.25	-1.4775	Starting on delta
15.25	-1.76	-
18.25	-1.625	Zero water on right bank is in between 7 and 8
25	-1.8775	-
29	-1.9425	All cobbles
32	-2.1725	Base of delta, all cobbles
35.75	-2.3225	Thalweg
40	-2.2825	Wiggle room on bottom reading (-.5 from bottom)
42	-2.2925	End gravel channel floor, start woody debris and sand
45	-2.0475	LWD and sand
48	-1.6725	Zero water on left bank
51	-0.9425	Edge of vegetation

Transect U-5
July 7, 2011

Distance (m)	Elevation (m)	Comments
0	0	-
7.75	-0.7275	-
11.5	-1	-
12.25	-1.6025	-
15	-1.625	-
17	-2.075	-
20	-2.14	-
22.75	-2.32	-
26	-1.8325	-
27.75	-2.135	-
32	-2.27	-
35.5	-2.575	-
40	-2.5825	-
42.5	-2.4525	-
45	-2.1575	-
46.5	-1.1975	-

Transect U-1
July 7, 2011

Distance (m)	Elevation (m)	Comments
0	0	Eye height at rebar
5.25	-0.6125	-
8	-0.995	-
9.75	-1.3675	-
11.5	-1.9825	-
11.5	-2.4875	-
12	-2.6225	Zero water
13.75	-2.925	-
17	-3.0975	-
22	-3.11	-
26	-3.2175	-
27.5	-2.9	-
30.75	-3.0625	Tree/boat
33	-3.19	-
38.5	-3.255	-
40.25	-2.955	-
42.75	-2.875	-
43.75	-2.64	Zero water
43.75	-2.275	-
46	-1.735	-
48.75	-1.2525	-

Transect U-1
October 13, 2012

Distance (m)	Elevation (m)	Comments
0	0	Instrument height at rebar
2.25	-0.0825	Top of old bank
2.5	-0.31	Bottom of old bank
6.25	-0.835	-
9.75	-1.385	-
11.5	-2.1075	Top of active bank
11.5	-2.61	Bottom of cut bank
13.5	-2.8775	Mud and sticks
16	-3.065	Sticks, some gravel
20.25	-3.16	Sandy gravel
24	-3.1075	Sandy gravel
27.25	-3.1075	Start of tree jam, sandy gravel
28.5	-2.9475	Crest of tree jam
30.5	-3.195	Sandy gravel, end tree jam
35	-3.235	Gravely sand
36.5	-3.2775	-
39.5	-3.0625	Sandy
42	-2.9175	Mud, sand, sticks, in situ tree stump 2 m upstream
43.75	-2.875	Base of bank
44	-2.31	Top of bank
45	-2.02	-

Transect U-1
August 19, 2014

Distance (m)	Elevation (m)	Comments
0	0	Intrument height on right bank
2.25	-0.1025	Top of old bank
2.5	-0.3275	Base of former bank
5.5	-0.78	-
7.5	-1.0325	Old impoundment mud, vegetated
9.75	-1.4025	-
11	-1.8575	Top of active bank
11	-2.2525	10 cm distance at bottom of vertical
11.25	-2.5075	20 cm away from last point
14	-3.0525	LWD and mud
16.25	-3.1125	Gravel, last of LWD
19.75	-3.1475	-
23.25	-3.115	Sand and Gravel
26.5	-3.2125	Start obstruction
27.5	-2.645	On top of rusted metal boat added to tree (ridge)
27.75	-2.8375	25 cm away from last point
28	-2.66	26 cm away from last point
29	-3.18	Stop ridge, Sand
30.75	-3.38	Current crescent, all cobbles
33.75	-3.1925	Sandy Gravel
38	-3.1225	Cobbles
40	-3.0125	End cobbles, start sand and sticks
42.25	-2.8725	-
45.25	-2.655	Base of scarp
45.5	-1.7875	Top of left bank

Transect U-6
July 7, 2011

Distance (m)	Elevation (m)	Comments
6.25	-1.735	-
10.5	-1.965	-
15	-2.06	-
17.5	-2.095	-
17.7	-3.2725	-
19	-3.6	-
20	-3.955	-
20.6	-3.905	-
26	-3.835	-
31.5	-3.83	-
35	-3.73	-
38	-3.61	-
42.5	-3.5225	-
49	-3.11	-

Transect U-6
October 13, 2012

Distance (m)	Elevation (m)	Comments
0	0	Rebar
4.75	-1.47	Old water line
9	-1.8475	-
13.25	-1.985	-
16.75	-2.0375	Top of bank
17	-2.995	Top of slump block
17.75	-3.675	Base of slump block
18	-4.01	Gravely Sand
23.75	-3.88	Gravel
28.5	-3.76	Gravel
32	-3.735	Gravel
33.25	-3.735	Gravel
38	-3.615	Gravel
40	-3.525	Gravel
42.5	-3.425	Edge of clay
46	-3.145	Clay

Transect U-6
August 19, 2014

Distance (m)	Elevation (m)	Comments
0	0	Instrument height at right bank rebar
0.5	-0.2875	Top of old bank
1.25	-0.79	-
3.5	-1.2675	End of boulders
6	-1.705	Break in slope on old dam pool sediment
9	-1.8875	-
12	-1.9825	-
14.5	-2.0275	Top of scarp
14.5	-3.4225	Bottom of scarp
16	-3.6375	~ 6.5 cm away from last point, small slump blocks
18	-4.06	Sandy Gravel
22.5	-3.9725	Cobbles
28.5	-3.8175	Cobbles, good measurement
34.25	-3.7375	Cobbles
41.25	-3.5075	-
44	-3.3475	Left bank, mud
46	-3.135	-
49	-3.0075	~ Distance of old tree stumps, ~ 1 m off edge of veg.

Transect U-2
July 7, 2011

Distance (m)	Elevation (m)	Comments
91.1	-1.925	New rebar
87.85	-2.605	top scarp
87.1	-3.55	-
85.85	-4.2975	Zero water, bottom scarp
84.1	-4.7625	-
80.35	-4.9725	-
75.1	-5.0625	-
69.1	-5.1475	-
65.1	-5.1125	-
62.1	-4.9075	Base of vertical scarp
61.6	-4.0725	Top of scarp
61.1	-3.82	-
58.35	-3.385	-
54.6	-3.1225	-

Transect U-2
October 13, 2012

Distance (m)	Elevation (m)	Comments
91.3	-1.825	Instrument height at new left bank rebar
88.3	-2.48	Top of scarp
88.3	-3.13	Mid way down scarp
86.3	-3.78	Base of scarp, top of another scarp
85.8	-4.1525	Bottom of second scarp, Gravel
84.3	-4.585	Gravel
82.3	-4.9275	Gravel
79.05	-4.8725	Cobbles
75.3	-5.125	Gravel
71.55	-4.985	Sandy Gravel
68.3	-5.045	Gravely sand
65.3	-5.04	Gravely Sand
61.3	-4.7875	Mud, base of scarp
60.3	-3.92	Top of scarp
59.55	-3.515	-

Transect U-2
May 3, 2015

Distance (m)	Elevation (m)	Comments
91.3	-1.825	Instrument height at newer rebar on left bank
88.8	-2.4675	Top of bank, rolling over, stair step slump blocks
87.3	-3.3425	Middle
86.55	-4.0525	2nd reading: Zero water on left bank, 2nd stair step
84.05	-4.645	-
81.3	-4.905	All sand and gravel, really flat
76.55	-4.8925	Flat, cobbles
73.05	-4.9325	-
69.8	-4.9625	Still gravel but more sandy
65.3	-5.0225	Still gravel but more sandy
61.55	-4.9425	Where turtles live
62.3	-4.1025	Zero water on right bank
60.55	-3.48	-
57.55	-3.2375	-

Transect U-7
July 7, 2011

Distance (m)	Elevation (m)	Comments
31.1	-2.82	Eye height (new rebar)
37.6	-3.79	Top old scarp
38.85	-4.0975	Bottom of scarp
39.1	-4.4425	Zero water
41.35	-4.9275	48cm water depth
45.1	-5.1275	-
49.6	-5.18	-
54.35	-5.17	71 cm water depth
59.1	-5.2325	78cm water depth
62.1	-4.9325	51cm water depth
63.6	-3.755	Top of scarp
63.8	-3.64	Fine sand spring flood

Transect U-7
October 13, 2012

Distance (m)	Elevation (m)	Comments
31.1	-2.82	New left bank rebar
35.1	-3.165	Top of old scarp
37.1	-3.6925	-
38.6	-4.1325	Top of active bank
39.1	-4.435	Bottom of active bank, bedrock
41.6	-4.9375	Cobbles
44.1	-5.16	Bedrock and boulders
48.1	-5.11	Bedrock and boulders
53.1	-5.185	Boulders
56.1	-5.285	Boulders
62.1	-5.1025	Point prior to base of scarp remeaseured
63.6	-4.9775	Base of bank
63.85	-3.775	Bank top, ~.3m undercut, under bank
62.1	-5.1025	Point prior to base of scarp remeaseured

Transect U-7
August 19, 2014

Distance (m)	Elevation (m)	Comments
34.1	-2.99	Left bank, back sighted
36.1	-3.305	Instrument height on left bank
38.1	-3.8075	Top of active bank
39.1	-4.26	-
42.1	-4.91	-
45.6	-5.165	Boulders and cobbles on bedrock
50.1	-5.1425	-
53.6	-5.2375	Boulders and cobbles on bedrock
58.1	-5.245	-
60.85	-5.2375	-
63.6	-4.975	Base of undercut scarp
63.6	-3.71	Rght bank

Transect U-3
July 7, 2011

Distance (m)	Elevation (m)	Comments
31.5	-2.756	-
35	-3.421	-
37.25	-3.911	-
37.5	-4.286	-
37.5	-4.4535	-
42.5	-4.6135	-
47.25	-4.5785	-
54	-4.561	-
57.75	-4.616	-
62.5	-4.6485	-
64.5	-4.5735	-
65.25	-4.3935	-
66.25	-3.9735	-

Transect U-3
October 13, 2012

Distance (m)	Elevation (m)	Comments
31.5	-2.756	New left bank rebar
34.25	-3.2635	-
35.5	-3.701	-
37.25	-4.046	Top of active bank
37.25	-4.476	Bottom of active banks, gravel
41.25	-4.5935	Sandy gravel
45.25	-4.801	Bedrock
51.5	-4.571	Bedrock
53.5	-4.601	Bedrock
55.5	-4.811	Bedrock
59.5	-4.696	Bedrock
65.5	-4.651	Base of scarp
66	-3.9385	Top of scarp
68.5	-3.616	-

Transect U-3
August 19, 2014

Distance (m)	Elevation (m)	Comments
33.5	-3.0335	Instrument height on river left
36.25	-3.9285	Top of scarp
36.75	-4.4285	Bottom of scarp
41.5	-4.4885	Gravel on bedrock
44.5	-4.666	All bedrock
47.75	-4.601	-
54.5	-4.606	Flat bedrock, fudged the bottom number
59.5	-4.476	-
63.5	-4.661	-
65.25	-4.586	Base of scarp, rier right
65.5	-4.126	Zero water
66.5	-3.696	-
67.5	-3.616	-

Transect D-3
July 7, 2011

Distance (m)	Elevation (m)	Comments
-11.5	0.42	-
-6.5	0.1475	-
-3.5	0.1225	-
4	-0.33	-
4.5	-0.8875	Zero water
8.25	-1.0325	-
12.5	-1.03	-
17.5	-0.97	-
23.5	-0.995	-
30	-0.8925	Zero water
32.5	-0.4975	-

Transect D-3
October 13, 2012

Distance (m)	Elevation (m)	Comments
-11.5	0.43	Rebar at "Y" shaped tree
-8	0.205	-
-3.5	0.12	-
0	0.3	Reference tree
4	-0.31	Top of bank
4.25	-0.73	Base of bank
8	-0.985	Bedrock
11	-1.09	Gravel
16	-1	Gravel
20	-0.945	Gravel
25.5	-0.9375	Gravel
30.25	-0.83	Zero water
34	-0.34	-

Transect D-3
August 11, 2014

Distance (m)	Elevation (m)	Comments
-11.75	0.43	Rebar at "V" shaped tree
-7	0.195	-
-2.25	0.16	-
0	0.3	Instrument height at river right
2	0.1	-
3.75	-0.375	Top of right bank, may have eroded back
4	-0.6275	Zero water
4.75	-0.8225	Water was 1.4 meters higher in May high flow
7.25	-0.9325	Bedrock
10	-1.14	Cobbles
13.5	-1.0775	Up on cobble bar
17.25	-0.995	Cobbles
23	-0.98	-
27	-0.94	-
30.75	-0.68	Zero water on River left
33.25	-0.3575	Edge of the vegetation, sand
35	-0.3	Sand
36.25	-0.01	-

Transect D-7
July 8, 2011

Distance (m)	Elevation (m)	Comments
0	0	-
3	-0.0425	-
4.75	-1.4725	water edge
5.5	-1.89	-
10.25	-2.0125	-
14.5	-1.9825	-
18.25	-1.9375	-
22.75	-1.825	-
27.5	-1.7275	-
31	-1.4725	water edge
32.5	-0.5025	-
35.75	-0.365	-
38.25	-0.33	-
42.75	-0.27	-
45.25	-0.01	-

Transect D-7
May 14, 2012

Distance (m)	Elevation (m)	Comments
0	0	Instrument height
2.5	-0.0375	Top of bank, 140 cm from rebar
3.9	-1.155	Zero water, same point as last transit
4	-1.225	-
4.2	-1.525	-
5	-1.595	Boulders
6	-1.965	Gravel
7	-2.035	Wood
8	-1.975	Gravel
9	-1.995	Gravel
10	-2.015	Gravel
11	-2.015	Gravel
12	-2.035	Gravel
13	-2.015	Gravel
14	-2.025	Gravel
15	-1.965	Sand
16	-2.045	Sand
17	-1.955	Sand
18	-1.945	Gravel
19	-1.915	Gravel
20	-1.925	Gravel
21	-1.895	Gravel
22	-1.875	Gravel
23	-1.815	Sand and gravel
24	-1.795	Sand and gravel
25	-1.785	Sand and gravel
26	-1.755	Sand and gravel
27	-1.715	Sand and gravel
28	-1.715	Sand and gravel
29	-1.725	Sand and gravel
30	-1.765	Sand and gravel
30.5	-1.735	Mud
31	-1.635	Mud
31.8	-1.155	-
32.5	-0.575	Sand

Transect D-7
September 7, 2013

Distance (m)	Elevation (m)	Comments
0	0	Instrument height
3	-0.0375	Used 2009, 2010, 2011, 2012 Top of bank
4.75	-1.525	Zero Water
4.85	-1.825	-
5.45	-1.885	-
6.45	-2.085	-
7.45	-2.165	-
8.45	-2.245	Gravel
9.45	-2.265	Gravel
10.45	-2.265	Gravel
11.45	-2.265	Gravel
12.45	-2.225	Gravel
13.45	-2.225	Gravel
14.45	-2.225	Gravel
15.45	-2.215	Gravel
16.45	-2.175	Gravel
17.45	-2.165	Gravel
18.45	-2.125	-
19.45	-2.105	-
20.45	-2.045	-
21.45	-2.005	Sandy gravel
22.45	-2.005	-
23.45	-1.995	-
24.45	-1.945	-
25.45	-1.925	-
26.45	-1.855	Sandy gravel
27.45	-1.855	-
28.45	-1.835	-
29.45	-1.865	-
30.45	-1.875	-
31.45	-1.945	Large woody debris
32.45	-1.875	Mud
33.45	-1.565	-
33.55	-1.525	-

Transect D-7
March 24, 2014

Distance (m)	Elevation (m)	Comments
0	0	Instrument Height
3	-0.065	-
4	-0.32	-
4.82	-0.9475	Added from field notes
5	-1.8075	Waters surface, transit rotated slightly upstream
5.5	-1.865	Bottom of scarp
6	-1.9075	-
7	-2.1175	-
8	-2.1575	-
9	-2.2675	-
10	-2.2575	-
11	-2.2675	-
12	-2.2875	Gravel
13	-2.2675	-
14	-2.2675	-
15	-2.2075	-
16	-2.2075	-
17	-2.1875	Gravel
18	-2.1675	-
19	-2.1475	Gravel
20	-2.1075	-
21	-2.0675	-
22	-2.0275	-
23	-1.9875	Gravel
24	-1.9875	-
25	-1.9275	Gravel
26	-1.9075	-
27	-1.8775	-
28	-1.8875	Sand and gravel
29	-1.8875	-
30	-1.9375	-
31	-1.9875	-
32	-1.8475	-
33	-1.5475	-
34	-0.9475	-

Transect D-7
July 25, 2014

Distance (m)	Elevation (m)	Comments
0	0	Instrument height on left bank
1.5	0.025	Top of bank
2.5	-0.03	On bank
3	-1.0725	3 m on rope, right bank rolling over
4	-1.4225	4 m on rope
4.25	-1.5475	5 meters on the rope, Zero water
5.25	-1.9575	Mud
6.25	-2.1275	-
7.25	-2.2275	-
8.25	-2.2475	Sandy pebbles
9.25	-2.2475	Sandy pebbles
10.25	-2.2875	Sand, pebbles and cobbles
11.25	-2.2875	Sand, pebbles and cobbles
12.25	-2.2675	Sand and pebbles
13.25	-2.2475	Sand and pebbles
14.25	-2.2475	Sand and pebbles
15.25	-2.2275	Pebbles
16.25	-2.1475	Sand, pebbles, scattered cobbles
17.25	-2.1475	Sand, pebbles, scattered cobbles
18.25	-2.1175	Sand, pebbles, scattered cobbles
19.25	-2.1075	Sand, pebbles, cobbles
20.25	-2.0675	Sand, pebbles ,cobbles
21.25	-2.0175	Sand, pebbles and cobbles
22.25	-2.0075	Sand, pebbles and cobbles
23.25	-1.9675	-
24.25	-1.9275	Sandy gravel, bedfroms
25.25	-1.8875	Sandy gravel, bedfroms
26.25	-1.8475	Sandy gravel, cobbles
27.25	-1.8275	Sand, some cobbles
28.25	-1.8475	Sand, pebbles, cobbles, 2-D ripples
29.25	-1.9475	Sand, pebbles, 2-D ripples.
30.25	-1.9375	Sand, pebbles, 2-D ripples.
31.25	-1.8775	Sand and mud
32.25	-1.5575	Very fine sand and mud.
32.4	-1.5475	Mud
33.15	-1.5475	Waters edge on right bank.
33.9	-1.24	34 m on the rope.
35.15	-0.7225	35 meters on the rope.
36.65	-0.3325	At rebar
37.9	-0.3275	Top of right bank
39.4	-0.4025	-
40.9	-0.59	-
41.9	-0.6875	Instrument height on right bank.

Transect D-7
December 15, 2014

Distance (m)	Elevation (m)	Comments
Distance (m)	Height (m)	Comments
0	0	Instrument height at left bank rebar
2.25	-0.015	Top of bank
4	-1.185	Zero water on left bank
5	-1.6225	Beginning of boulders
5.5	-1.9075	Cobbles, old channel floor, pre MF
7.75	-2.005	Pebbles
10.75	-2.05	Pebbles and small cobbles
14	-2.04	Flat bottom
18.25	-1.965	More pebbles with cobbles
22	-1.89	Pebbly
23.75	-1.81	Lee of gravel bar at upstream culvert
27.75	-1.74	Sand
30.75	-1.77	Base of slope, eroded roots
31.25	-1.4875	30 cm of water
31.75	-1.2075	Zero water. ~ 30 cm distance
33	-0.6175	-
34.75	-0.3725	Top of right bank

Transect D-7
May 3, 2015

Distance (m)	Elevation (m)	Comments
0	0	Instrument height on left bank rebar
2.25	0.03	Top of bank
4.25	-1.3725	Zero water on left bank
5.75	-1.805	Boulders, bottom of bank
9.75	-2.005	Looks flat
14.75	-2.005	-
19.75	-1.9125	-
23.75	-1.7825	-
28	-1.71	-
30.75	-1.7225	Ramp, top hard to read
32	-1.36	Top > 284, Zero water on right bank
34	-0.395	Top < 192, huge pile of sand
36	-0.225	Top, hard to read
39.75	-0.235	Lots of sand deposition

Transect D-4
July 8, 2011

Distance (m)	Elevation (m)	Comments
0	0	-
2.0006	-0.1456	-
3.7512	-1.8949	-
4.5014	-1.9889	water edge
6.5021	-2.3945	-
8.7528	-2.9165	-
10.0032	-2.8931	-
13.2542	-2.6354	-
18.2558	-2.5470	-
22.7573	-2.5284	-
27.7589	-2.2524	-
29.0093	-2.0091	-
30.7598	-1.9584	water edge
34.5111	-1.6708	-
39.0125	-1.3347	-
42.0135	-1.5306	-
55	-1.4632	-
59.5	-0.2534	-

Transect D-4
September 7, 2013

Distance (m)	Elevation (m)	Comments
0	0	Instrument Height
2.25	-0.0825	Top of bank
4	-1.875	Waters edge
6	-2.3175	All boulders
8.25	-2.9275	-
11.25	-2.8825	All gravel
15	-2.565	Gravel
19.5	-2.5425	Gravel
23.5	-2.54	Sand
27.5	-2.28	Sand
31	-1.89	Mud on top of sand
35.5	-1.625	Edge of vegetation
39	-1.325	Crest of bar
42.25	-1.53	Mud
49.5	-1.535	Third from last
54	-1.545	-
59.5	-0.29	Left bank rebar

Transect D-4
May 14, 2012

Distance (m)	Elevation (m)	Comments
0	0	Instrument Height
2.5	-0.1675	Top of bank
3.9	-1.64	Zero water
3.9	-1.88	Vertical
5	-2.04	Boulders
6	-2.12	Boulders
7	-2.36	Boulders
8	-2.84	Boulders
9	-2.94	Boulders
10	-2.94	Boulders
11	-2.89	Boulders
12	-2.82	Boulders
13	-2.73	Boulders
14	-2.68	Boulders
15	-2.66	Boulders
16	-2.64	Boulders
17	-2.6	Boulders
18	-2.59	Boulders
19	-2.59	Boulders
20	-2.56	Boulders
21	-2.57	Gravel
22	-2.59	Gravel
23	-2.6	Gravel
24	-2.6	Gravel
25	-2.56	Gravel
26	-2.43	Gravel
27	-2.34	Sand
28	-2.2	Sand
29	-2.04	Sand
30	-1.94	Sand
31	-1.88	Muddy sand
32	-1.87	Muddy sand
33	-1.86	Muddy sand
34	-1.76	Muddy sand
35	-1.64	Zero water, 35 m on rope
39	-1.3375	30 m on rope, crest of sand bar
41	-1.5275	-
47	-1.5825	-
53	-1.6025	-
55	-1.4825	-
55	-0.2525	Rebar

Transect D-5
July 8, 2011

Distance (m)	Elevation (m)	Comments
45	0	-
40.5	-0.8425	-
40.25	-1.5575	Water edge
40.25	-1.6075	-
37	-2.015	-
33.5	-2.01	-
30.25	-2.1475	-
25.75	-2.05	-
21.5	-1.93	-
16.75	-1.79	-
12	-1.825	-
11	-2.1	-
9	-2.24	-
5	-2.005	-
3.5	-1.755	-
3.5	-1.58	Water edge

Transect D-5
September 7, 2013

Distance (m)	Elevation (m)	Comments
45	0	Instrument height ar right bank
41.25	-0.565	Top of bank
40.5	-0.88	Middle of bank, I cm mud cracks
40.25	-1.4775	Zero water
40.25	-1.7075	0.23 m vertical drop at root mass
37	-1.99	Mud and sticks
34	-2.0475	Near a tree
30.75	-2.12	Sand
26	-2.0525	Gravely sand
21.5	-1.91	Gravely sand
16.25	-1.825	Gravely sand
12	-1.79	LWD
11	-2.21	Muddy sand in stagnant water behind LWD
7.5	-2.245	Cobbles, old river bottom.
5.5	-1.985	Cobbles
3.75	-1.655	Gravel, base of bank
3.75	-1.495	-

Transect D-5
May 14, 2012

Distance (m)	Elevation (m)	Comments
45	0	Instrument height at rebar
41.5	-0.5625	Top of bank
40	-1.2575	Zero water, 5.2 m on rope
39.9	-1.6875	Mud
39.2	-1.6875	Mud
38.2	-1.8175	Mud
37.2	-1.9975	Mud
36.2	-2.0175	Mud and logs
35.2	-2.0275	Mud
34.2	-1.9775	Tree
33.2	-2.1175	Tree
32.2	-2.0975	Muddy sand
31.2	-2.1675	sand
30.2	-2.1175	Sand
29.2	-2.1775	sand
28.2	-2.0975	Sand
27.2	-2.0775	sand
26.2	-2.0375	sand
25.2	-1.9775	Sand
24.2	-1.9475	Sand, CR12-G7 sample
23.2	-1.9075	Sand with shells
22.2	-1.8975	Sand with shells
21.2	-1.8975	Sand with shells
20.2	-1.8275	Sand with shells
19.2	-1.7975	Sand with shells
18.2	-1.7975	Sand with shells
17.2	-1.7775	Sand with shells
16.2	-1.7475	Sand with shells
15.2	-1.8175	Sand with shells
14.2	-1.8175	Sand with shells
13.2	-1.8175	Sand with shells
12.2	-1.8375	Tree
11.2	-2.0175	-
10.2	-2.1975	Tree limb
9.2	-2.1975	Muddy Sand
8.2	-2.2275	Sand
7.2	-2.2275	Gravel
6.2	-2.0975	Cobbles
5.2	-1.8675	Sand
4.2	-1.6975	Sand
3.76	-1.2575	-

Transect D-5
March 24, 2014

Distance (m)	Elevation (m)	Comments
45	0	Instrument height on right bank, Zero on the rope
41.75	-0.49	3 meters on the rope
40.25	-0.685	4 meters on the rope
40.25	-0.94	Zero water, 4.52 on the rope
39.77	-1.72	Base of scarp
38.77	-1.74	-
37.77	-1.93	-
36.77	-2.02	-
35.77	-2.06	-
34.77	-2.05	-
33.77	-2.08	Wood
32.77	-2.12	-
31.77	-2.16	-
30.77	-2.12	-
29.77	-2.09	Sand
28.77	-2.18	-
27.77	-2.19	-
26.77	-2.18	-
25.77	-2.14	-
24.77	-2.05	Gravely sand
23.77	-2	Gravely sand
22.77	-1.9	Gravely sand
21.77	-1.88	Gravely sand
20.77	-1.9	Gravely sand
19.77	-1.98	Gravely sand
18.77	-1.98	Gravely sand
17.77	-1.95	Gravely sand
16.77	-1.92	Gravely sand
15.77	-1.94	Gravely sand
14.77	-1.88	Gravely sand
13.77	-1.82	Gravely sand
12.77	-1.88	Gravel
11.77	-2	Gravel
10.77	-2.16	Gravel
9.77	-2.22	Gravel
8.77	-2.08	Gravel
7.77	-2.27	Gravel
6.77	-2.16	-
5.77	-1.94	-
4.77	-1.76	-
3.77	-0.94	-

Transect D-5
July 25, 2014

Distance (m)	Elevation (m)	Comments
45	0	Instrument height on right bank
43.5	-0.155	-
42	-0.4225	-
40.75	-0.64	Crest of bank
39.75	-1.21	-
39.75	-1.6175	-
38	-2.005	Very fine sand
34.25	-2.125	Sand
33	-2.015	On top of sand ridge, LWD
29.25	-2.2225	Sandy mud and leaves
27	-2.265	Sand and pebbles
23	-2.095	Sand and pebbles
20	-2.1575	Sand and pebbles
16.75	-1.965	Sand and pebbles, LWD
13	-1.8	Sand an pebble ridge in the lee of LWD
10.5	-1.975	Fine sand, no pebbles
7	-2.1875	Sandy mud, with pebbles, cobbles and leaves
5	-1.94	Sand and pebbles
5	-1.5975	Base of steep bank, on left bank
3	-0.755	Middle of left bank
1.75	0.12	Crest of left bank
0.5	0.31	Top of left bank
0	0.48	At left bank rebar

Transect D-5
December 14, 2014

Distance (m)	Elevation (m)	Comments
45	0	Instrument Height at right bank rebar
42.75	-0.4	-
40.75	-0.6925	Top of right bank
40.25	-1.3675	Zero water, subtracted 1 from bottom
40	-1.7125	20 cm distance, leaves, muds, roots
38.25	-1.9075	Mud
36	-2.13	Mud
34	-2.045	Mud, end mud bar woth sticks
31.5	-2.2325	Muddy sand
28	-2.2775	Sandy gravel
23.75	-2.175	Granules
19.75	-2.1175	-
15.75	-2.0175	-
12.75	-1.805	LWD gravel
9.25	-2.1175	Mud
6.75	-2.165	-
4	-1.6425	Base of bank, 38 cm
3	-0.0775	Top of left bank
0	0.435	Left bank rebar, subtracted .25 from top.

Transect D-5
May 3, 2015

Distance (m)	Elevation (m)	Comments
45	0	Instrument height at right bank rebar
40.75	-0.6725	Top of bank, rolling over
39	-1.6025	Zero water on right bank, bottom of scarp
38	-1.9625	Muddy, sticks
35	-2.13	Trough of mud and sticks, bar behind
33	-2.0775	Sand bar, sticks
31	-2.2075	Off bar, 2-D ripple sands
27	-2.3075	Beautiful 2-D ripples everywhere, 100% sand
23	-2.3425	All pebbles and granules at boundary
19	-2.3675	-
11.5	-1.6025	-
10.5	-1.6025	-
8.5	-2.0125	Zzero warter around LWD bar
7	-2.0975	Coming toward transit
4	-1.6125	Zero water on left bank, base of cliff

Transect D-5
December 14, 2014

Distance (m)	Elevation (m)	Comments
45	0	Instrument Height at right bank rebar
42.75	-0.4	-
40.75	-0.6925	Top of right bank
40.25	-1.3675	Zero water, subtracted 1 from bottom
40	-1.7125	20 cm distance, leaves, muds, roots
38.25	-1.9075	Mud
36	-2.13	Mud
34	-2.045	Mud, end mud bar woth sticks
31.5	-2.2325	Muddy sand
28	-2.2775	Sandy gravel
23.75	-2.175	Granules
19.75	-2.1175	-
15.75	-2.0175	-
12.75	-1.805	LWD gravel
9.25	-2.1175	Mud
6.75	-2.165	-
4	-1.6425	Base of bank, 38 cm
3	-0.0775	Top of left bank
0	0.435	Left bank rebar, subtracted .25 from top.

Transect D-5
May 3, 2015

Distance (m)	Elevation (m)	Comments
45	0	Instrument height at right bank rebar
40.75	-0.6725	Top of bank, rolling over
39	-1.6025	Zero water on right bank, bottom of scarp
38	-1.9625	Muddy, sticks
35	-2.13	Trough of mud and sticks, bar behind
33	-2.0775	Sand bar, sticks
31	-2.2075	Off bar, 2-D ripple sands
27	-2.3075	Beautiful 2-D ripples everywhere, 100% sand
23	-2.3425	All pebbles and granules at boundary
19	-2.3675	-
11.5	-1.6025	-
10.5	-1.6025	-
8.5	-2.0125	Zzero warter around LWD bar
7	-2.0975	Coming toward transit
4	-1.6125	Zero water on left bank, base of cliff

Transect D-2
January 12, 2013

Station	Distance (m)	Bridge Curvature (m)	Bridge to water (m)	Corrected bridge to water (m)	Bridge to bed (m)	Corrected Bridge to bed (m)	Water depth (m)
1	0	-0.31	-	-	-	-	-
2	2.28	-0.26	-	-	-	-	-
3	4.56	-0.21	-	-	-	-	-
4	6.84	-0.17	-	-	-	-	-
5	9.12	-0.14	-	-	-	-	-
6	11.4	-0.11	-	-	-	-	-
7	13.68	-0.06	-	-	-	-	-
8	15.96	-0.04	-	-	2.66	2.7	-
9	18.24	0	-	-	3.6	3.6	-
10	20.52	0.04	-	-	4.59	4.55	-
11	22.8	0.03	-	-	5.25	5.22	-
12	25.08	0.03	-	-	5.14	5.11	-
13	27.36	0.02	-	-	4.83	4.81	-
14	29.64	0	3.01	-	4.83	4.83	-
15	31.92	-0.01	-	-	4.82	4.83	-
16	34.2	-0.02	-	-	4.75	4.77	-
17	36.48	-0.06	-	-	4.6	4.66	-
18	38.76	-0.08	-	-	4.44	4.52	-
19	41.04	-0.1	-	-	4.34	4.44	-
20	43.32	-0.12	-	-	4.25	4.37	-
21	45.6	-0.17	-	-	4.1	4.27	-
22	47.88	-0.21	-	-	3.94	4.15	-
23	50.16	-0.23	-	-	3.52	3.75	-
24	52.44	-0.31	-	-	3.5	3.81	-
25	54.72	-0.32	-	-	3.2	3.52	-

Transect D-2
September 7, 2013

Station	Distance (m)	Bridge Curvature (m)	Bridge to water (m)	Corrected bridge to water (m)	Bridge to bed (m)	Corrected Bridge to bed (m)	Water depth (m)
1	0	-0.31	-	-	-	-	-
2	2.28	-0.26	-	-	-	-	-
3	4.56	-0.21	-	-	-	-	-
4	6.84	-0.17	-	-	-	-	-
5	9.12	-0.14	-	-	-	-	-
6	11.4	-0.11	-	-	-	-	-
7	13.68	-0.06	-	-	-	-	-
8	15.96	-0.04	-	-	-	-	-
9	18.24	0	-	-	-	-	-
10	20.52	0.04	-	-	4.53	4.49	-
11	22.8	0.03	-	-	5.31	5.28	-
12	25.08	0.03	-	-	5.07	5.04	-
13	27.36	0.02	-	-	5.01	4.99	0.4
14	29.64	0	-	-	5.00	5.00	-
15	31.92	-0.01	-	-	4.90	4.91	-
16	34.2	-0.02	-	-	4.85	4.87	-
17	36.48	-0.06	-	-	4.69	4.75	-
18	38.76	-0.08	-	-	4.49	4.57	-
19	41.04	-0.1	-	-	4.35	4.45	-
20	43.32	-0.12	-	-	4.35	4.47	-
21	45.6	-0.17	-	-	4.22	4.39	-
22	47.88	-0.21	-	-	3.91	4.12	-
23	50.16	-0.23	-	-	3.53	3.76	-
24	52.44	-0.31	-	-	3.48	3.79	-
25	54.72	-0.32	-	-	-	-	-

Transect D-2
March 27, 2014

Station	Distance (m)	Bridge Curvature (m)	Bridge to water (m)	Corrected bridge to water (m)	Bridge to bed (m)	Corrected Bridge to bed (m)	Water depth (m)
1	0	-0.31	-	-	-	-	-
2	2.28	-0.26	-	-	-	-	-
3	4.56	-0.21	-	-	-	-	-
4	6.84	-0.17	-	-	-	-	-
5	9.12	-0.14	-	-	-	-	-
6	11.4	-0.11	-	-	-	-	-
7	13.68	-0.06	-	-	-	-	-
8	15.96	-0.04	-	-	2.63	2.67	-
9	18.24	0	-	-	3.01	3.01	-
10	20.52	0.04	-	-	4.51	4.47	-
11	22.8	0.03	-	-	5.25	5.22	-
12	25.08	0.03	-	-	5.22	5.19	-
13	27.36	0.02	-	-	5.10	5.08	-
14	29.64	0	-	-	5.07	5.07	-
15	31.92	-0.01	-	-	4.99	5.00	-
16	34.2	-0.02	-	-	5.16	5.18	-
17	36.48	-0.06	-	-	4.62	4.68	-
18	38.76	-0.08	-	-	4.83	4.91	-
19	41.04	-0.1	-	-	4.40	4.50	-
20	43.32	-0.12	-	-	4.39	4.51	-
21	45.6	-0.17	-	-	4.20	4.37	-
22	47.88	-0.21	-	-	3.85	4.06	-
23	50.16	-0.23	-	-	4.08	4.31	-
24	52.44	-0.31	-	-	3.47	3.78	-
25	54.72	-0.32	-	-	3.18	3.50	-

Transect D-2
August 9, 2014

Station	Distance (m)	Bridge Curvature (m)	Bridge to water (m)	Corrected bridge to water (m)	Bridge to bed (m)	Corrected Bridge to bed (m)	Water depth (m)
1	0	-0.31	-	-	1.24	1.55	-
2	2.28	-0.26	-	-	1.68	1.94	-
3	4.56	-0.21	-	-	2.43	2.64	-
4	6.84	-0.17	-	-	3.1	3.27	-
5	9.12	-0.14	-	-	3.15	3.29	-
6	11.4	-0.11	-	-	3.25	3.36	-
7	13.68	-0.06	-	-	3.2	3.26	-
8	15.96	-0.04	-	-	2.63	2.67	-
9	18.24	0	-	-	3.2	3.2	-
10	20.52	0.04	-	-	4.4	4.36	-
11	22.8	0.03	-	-	5.24	5.21	-
12	25.08	0.03	-	-	5.225	5.195	-
13	27.36	0.02	-	-	5.16	5.14	-
14	29.64	0	-	-	5.1	5.1	-
15	31.92	-0.01	-	-	5.05	5.06	-
16	34.2	-0.02	-	-	4.91	4.93	-
17	36.48	-0.06	-	-	4.73	4.79	-
18	38.76	-0.08	-	-	4.63	4.71	-
19	41.04	-0.1	-	-	4.44	4.54	-
20	43.32	-0.12	-	-	4.29	4.41	-
21	45.6	-0.17	-	-	4.26	4.43	-
22	47.88	-0.21	-	-	3.845	4.055	-
23	50.16	-0.23	-	-	3.54	3.77	-
24	52.44	-0.31	-	-	3.425	3.735	-
25	54.72	-0.32	-	-	3.16	3.48	-

Transect D-2
December 22, 2014

Station	Distance (m)	Bridge Curvature (m)	Bridge to water (m)	Corrected bridge to water (m)	Bridge to bed (m)	Corrected Bridge to bed (m)	Water depth (m)
1	0.00	-0.31	-	-	1.24	1.55	-
2	2.28	-0.26	-	-	1.70	2.01	-
3	4.56	-0.21	-	-	2.40	2.66	-
4	6.84	-0.17	-	-	3.08	3.29	-
5	9.12	-0.14	-	-	3.10	3.27	-
6	11.40	-0.11	-	-	3.22	3.36	-
7	13.68	-0.06	-	-	3.20	3.31	-
8	15.96	-0.04	-	-	2.66	2.72	-
9	18.24	0.00	-	-	3.20	3.24	-
10	20.52	0.04	-	-	4.56	4.56	-
11	22.80	0.03	-	-	5.22	5.18	-
12	25.08	0.03	-	-	5.21	5.18	-
13	27.36	0.02	-	-	5.14	5.11	-
14	29.64	0.00	-	-	5.10	5.08	-
15	31.92	-0.01	-	-	5.00	5.00	-
16	34.20	-0.02	-	-	4.90	4.91	-
17	36.48	-0.06	-	-	4.76	4.78	-
18	38.76	-0.08	-	-	4.62	4.68	-
19	41.04	-0.10	-	-	4.43	4.51	-
20	43.32	-0.12	-	-	4.29	4.39	-
21	45.60	-0.17	-	-	4.26	4.38	-
22	47.88	-0.21	-	-	3.85	4.02	-
23	50.16	-0.23	-	-	3.56	3.77	-
24	52.44	-0.31	-	-	3.46	3.69	-
25	54.72	-0.32	-	-	3.16	3.48	-

Transect D-2
May 2, 2015

Station	Distance (m)	Bridge Curvature (m)	Bridge to water (m)	Corrected bridge to water (m)	Bridge to bed (m)	Corrected Bridge to bed (m)
1	0	-0.31	-	-	1.52	1.83
2	2.28	-0.26	-	-	1.99	2.25
3	4.56	-0.21	-	-	2.44	2.65
4	6.84	-0.17	-	-	3.08	3.25
5	9.12	-0.14	-	-	3.145	3.285
6	11.4	-0.11	-	-	3.25	3.36
7	13.68	-0.06	-	-	3.16	3.22
8	15.96	-0.04	-	-	2.66	2.7
9	18.24	0	-	-	3.15	3.15
10	20.52	0.04	-	-	4.31	4.28
11	22.8	0.03	-	-	5.25	5.22
12	25.08	0.03	-	-	5.48	5.46
13	27.36	0.02	-	-	5.355	5.355
14	29.64	0	-	-	5.155	5.165
15	31.92	-0.01	-	-	5.01	5.03
16	34.2	-0.02	-	-	4.88	4.94
17	36.48	-0.06	-	-	4.73	4.81
18	38.76	-0.08	-	-	4.56	4.66
19	41.04	-0.1	-	-	4.37	4.49
20	43.32	-0.12	3.26	3.38	4.3	4.47
21	45.6	-0.17	-	-	4.24	4.45
22	47.88	-0.21	-	-	3.79	4.02
23	50.16	-0.23	-	-	3.55	3.86
24	52.44	-0.31	-	-	3.44	3.76
25	54.72	-0.32	-	-	2.81	3.12

Transect D-8
July 8, 2011

Distance (m)	Elevation (m)	Comments
0	0	Rebar
6.5	-0.2075	-
8.5	-0.7475	-
16.75	-1.28	Water edge
22.5	-1.57	-
26.75	-1.9	-
31.5	-2.27	-
34.5	-2.43	-
37.75	-2.21	-
40	-1.7525	-
42	-1.405	Base of scarp
42.5	-0.2325	-

Transect D-8
May 14, 2012

Distance (m)	Elevation (m)	Comments
0	0	Eye height at rebar
4	0.11	-
7	-0.2075	Top of bank
8	-0.5825	Mid-bank
10.4	-0.8875	Zero water
11	-1.0575	Muddy sand
11.5	-1.2475	-
12	-1.4275	-
13	-1.7075	-
14	-1.6175	Sand
15	-1.4075	Sand
16	-1.2675	Sand
17	-1.2575	Sand
18	-1.3275	Sand
19	-1.3675	Sand
20	-1.4075	Sand
21	-1.4475	Sand
22	-1.5075	Sand
23	-1.6075	Sand
24	-1.7075	Sand
25	-1.7675	Sand
26	-1.8275	-
27	-1.8875	-
28	-1.9975	-
29	-2.0675	-
30	-2.0975	-
31	-2.1775	-
32	-2.2075	-
33	-2.2575	-
34	-2.3475	-
35	-2.3275	Gravel
36	-2.2175	Gravel
37	-2.0975	-
38	-2.0375	-
39	-1.7675	-
40	-1.5575	-
41	-1.3475	-

Transect D-8
September 7, 2013

Distance (m)	Elevation (m)	Comments
0	0	Instrument Height
4	0.025	Levee sand
7.25	-0.358	Top of bank, sand
9	-0.808	Edge of vegetation
10	-0.985	Top of active scarp
10	-1.228	Bottom of active scarp, sandy
12	-1.478	Sand
15.2	-1.460	Gravely sand
18.5	-1.850	Gravely sand
22.5	-1.790	Gravely sand
25.75	-1.730	Sand bar in lee of a tree
29	-2.105	Same sand bar
31.5	-2.415	Behind tree
33.5	-2.135	Behind Tree, sand
36.75	-1.975	Gravel-cobble, old river bed
40	-1.695	Gravel
41.5	-1.250	At bank, gravel
41.5	-1.250	Vetical bank

Transect D-8
March 27, 2014

Distance (m)	Elevation (m)	Comments
0	0	Instrument Height
5.25	-0.025	Mid bank
7	-0.3525	-
8.5	-0.7375	Waters edge
9.2	-0.8975	-
10.2	-1.2575	-
12.2	-1.3775	-
13.2	-1.4975	-
14.2	-1.6575	Sand
15.2	-1.8175	-
16.2	-1.9375	-
17.2	-2.0175	-
18.2	-2.2375	Sand
19.2	-2.3175	-
20.2	-2.3975	-
21.2	-2.5375	-
22.2	-2.4475	-
23.2	-2.2375	-
24.2	-2.0575	-
25.2	-2.0575	-
26.2	-2.1675	-
29.2	-2.3875	-
30.2	-2.2975	-
31.2	-2.0075	-
32.2	-1.7775	-
34.2	-1.7875	-
35.2	-2.2375	-
36.2	-2.2975	-
37.2	-2.1575	-
38.2	-1.9875	-
39.2	-1.8175	-
40.2	-1.5675	-
41.2	-1.4875	Bottom of bank

Transect D-8
August 19, 2014

Distance (m)	Elevation (m)	Comments
0	0	Instrument height on right bank
3	0.0225	Bank rolling over
5.25	-0.2175	-
8	-0.69	-
8.5	-1.04	Mini-scarp, active
10.5	-1.3	-
13.5	-1.6875	-
16.25	-1.9025	All sand
20.5	-2.395	Sand, active scarp, bed forms
22.5	-2.4975	-
23.75	-2.1325	On sand bar in lee of LWD
27.5	-2.235	On sand bar in lee of LWD
29.5	-1.9825	On sand bar in lee of LWD
32	-1.6425	Crest of sand bar in lee of LWD, 2-D ripples
36.25	-2.1225	All filled in with sand, used to be deep and creepy
38.5	-2.0475	-
41.75	-1.4325	On left bank
43.2	0.1575	At left bank rebar elevation.

Transect D-8
December 14, 2014

Distance (m)	Elevation (m)	Comments
42.34	0	Left bank rebar
41.34	-1.4725	Bottom of bank
40.34	-1.5425	All granules
39.34	-1.7525	Lee of LWD
38.34	-1.9325	-
37.34	-2.0025	Sand
36.34	-1.7925	Sand
35.34	-1.8925	Sand
34.34	-1.7925	Sand and LWD
33.34	-1.7625	Sand
32.34	-1.7325	Sand
31.34	-1.8225	Sand
30.34	-2.3125	Sand and LWD
29.34	-2.3925	Granules
27.34	-2.1525	-
26.34	-2.3925	-
25.34	-2.4725	-
24.34	-2.3725	-
23.34	-2.4525	All granules
22.34	-2.4925	Gravel
21.34	-2.4725	Gravel and pebbles
20.34	-2.3125	Granules
19.34	-2.3325	Pebbles
18.34	-2.3225	Sand
17.34	-1.6225	-
16.34	-1.8725	-
15.34	-1.6725	-
14.34	-1.6925	-
13.34	-1.5925	-
12.34	-1.4025	-
11.34	-1.4025	-
10.34	-1.2725	-
9.72	-1.1125	-
8	-0.695	Inflection point
6.84	-0.2975	Bank starting to roll over
3.34	0.0225	-
0	0	Instrument height ar right bank rebar

Transect D-8
May 3, 2015

Distance (m)	Elevation (m)	Comments
0	0	Instrument height at right bank rebar
5.75	-0.165	Crest, bank starts to roll over
8.5	-0.8475	Top of scarp
9.25	-1.36	Zero water on right bank
12.75	-1.635	All granules
16	-1.94	-
16.25	-1.9575	Sand ribbon behind upstream LWD
19.25	-2.25	-
21.5	-2.55	Deep, pebbles
23	-2.2925	Top of sand bar
26.25	-2.1875	Sand
28	-2.405	All sand, LWD
29.75	-1.94	-
31	-1.605	-
33	-1.44	Sand
36.5	-2.24	Ramp down to gravel
39.25	-1.9	-
42	-1.485	.145 m water depth, rebar is 1 m inland

Transect D-8 Replicate
May 3, 2015

Distance (m)	Elevation (m)	Comments
42	-1.4825	.145 m water depth
38.75	-1.9825	-
37.25	-2.1825	-
36	-2.2275	-
33.75	-1.44	-
31.5	-1.6625	Deer
29.5	-1.86	-
28.75	-2.3725	-
26.75	-2.14	-
24.5	-2.335	-
22.75	-2.3375	Top
21.5	-2.525	-
20.5	-2.355	-
17.5	-2.0325	-
16	-1.9725	-
12	-1.6325	-
10	-1.3675	Zero water on right bank
8.75	-0.8475	Top of scarp
6	-0.1675	Top of roll over
0	0	Instrument height at right bank rebar

Transect D-10
July 8, 2011

Distance (m)	Elevation (m)	Comments
3	0.1	-
4	0.0725	Bank top
6.25	-0.805	-
12.5	-1.305	Water edge
17	-1.7	-
18.25	-1.81	-
19.25	-1.73	-
22.25	-1.5575	-
25.25	-1.785	-
28.75	-2.0025	-
32	-1.9475	-
35.5	-1.8825	-
38.75	-1.8675	-
40	-1.315	Water edge
43	0	-

Transect D-10
May 14, 2012

Distance (m)	Elevation (m)	Comments
3	0.1	Eye height at 2011 rebar
5	-0.1875	-
6.75	-1.035	Zero water
7.05	-1.085	Sand
8.05	-1.335	Sand and sticks
9.05	-1.355	Sand and sticks
10.05	-1.385	Sand
11.05	-1.445	Sand
12.05	-1.475	Sand
13.05	-1.585	Sand
14.05	-1.675	Sand
15.05	-1.665	Sand
16.05	-1.735	Sand
17.05	-1.755	Sand
18.05	-1.755	Sand
19.05	-1.705	-
20.05	-1.695	-
21.05	-1.715	-
22.05	-1.725	-
23.05	-1.705	-
24.05	-1.705	-
25.05	-1.735	-1.735
26.05	-1.795	-
27.05	-1.745	Ripples and dunes
28.05	-1.795	CR12-G13 sample
29.05	-1.865	-
30.05	-1.845	-
31.05	-1.955	-
32.05	-1.975	-
33.05	-2.045	-
34.05	-2.115	-
35.05	-2.095	-
36.05	-2.075	-
37.05	-2.055	-
38.05	-2.045	-
39.05	-1.755	Gravel and sand
40.05	-1.275	Gravel and sand
40.77	-1.035	-

Transect D-10
May 20, 2013

Distance (m)	Elevation (m)	Comments
3	0.1	Instrument height at new rebar
4	-0.1925	Top of right bank
7.25	-1.28	-
10.5	-1.525	-
12.5	-1.575	-
16	-1.5775	-
18.5	-1.6025	-
22.25	-1.5425	-
26.1	-1.5525	-
29.75	-1.54	-
32.5	-1.7375	-
35.75	-1.955	-
38.25	-1.985	-
41	-1.37	-
43	-0.38	At the tree on left bank

Transect D-10
September 7, 2013

Distance (m)	Elevation (m)	Comments
3	0.1	Instrument height
4.75	-0.1775	Top of bank
7.5	-1.28	-
11	-1.525	Sand
15.5	-1.62	Sand
19	-1.9275	Sand
20.5	-1.65	Sand
24.25	-1.6225	Sand
29	-1.845	Sand
33	-1.99	Sand
37.25	-1.975	Sand
40	-1.84	Mud, gravel, sticks
42	-1.275	-

Transect D-10
March 27, 2014

Distance (m)	Elevation (m)	Comments
0	0	Eye height
4	-0.05	Bank sloping
6	-0.87	-
7	-1.2	Sand
8	-1.37	Sand
9	-1.49	Sand
10	-1.55	Sandy gravel
11	-1.6	Gravel
12	-1.61	Gravel
13	-1.68	Gravel
14	-1.74	Gravel
15	-1.76	Gravel
16	-1.76	Sand
17	-1.77	Sand
18	-1.83	Sand
19	-1.71	Sand
20	-1.73	Sand
21	-1.72	Sand
22	-1.73	Sand
23	-1.72	Sand
24	-1.69	Sand
25	-1.78	Gravely sand
26	-1.84	Sand
27	-1.87	Sand
28	-1.92	Sand
29	-2.04	-
30	-2.08	-
31	-2.07	-
32	-2.09	-
33	-2.06	Gravel
34	-2.13	Sand and gravel
35	-2.11	Sand
36	-2.03	Sand
37	-1.95	-
38	-1.91	-
39	-1.57	Gravel
40	-1.15	-
41	-0.87	-

Transect D-10
August 19, 2014

Distance (m)	Elevation (m)	Comments
43.25	-0.84	Base of left bank
41.25	-1.345	Hard to read
38.75	-2.055	Sand
35.5	-2.1975	Sand
31.5	-2.115	Sand
28	-1.995	Sand
24.75	-1.8625	Sand
21.75	-1.82	Sand
19	-1.69	Sand
15.5	-1.7325	Sand, Gravel
11.5	-1.6525	-
8	-1.355	Right bank
7	-1.1175	-
5	-0.555	-
4	-0.0275	-
3	0.1	Eye height

Transect D-10
December 14, 2014

Distance (m)	Elevation (m)	Comments
43.5	0.1925	Left bank, top estimated
42.5	-0.7425	Base of bank
41.75	-1.2225	Zero water
39.25	-1.955	All gravel. Thalwag
37.5	-2.24	-
34.25	-2.1625	Pebbles and granules
31	-2.0775	Sandy
28	-1.8325	-
24.25	-1.715	-
18	-1.7075	Subtracted 10 from top
14.75	-1.6175	-
10.75	-1.565	-
8.25	-1.21	Zero water
6.5	-0.855	-
4.25	0.025	Top of bank
3	0.1	Eye height at right bank, ~ rebar location.

Transect D-14
May 20, 2013

Distance (m)	Elevation (m)	Comments
0	0	Instrument height
1.5	-0.315	Deck = 1.1 m
2.25	-0.715	-
4.5	-0.8375	-
7	-0.9525	-
10	-1.195	-
13	-1.2675	-
15.75	-1.275	-
19.25	-1.2725	-
22.75	-1.06	-
24.25	-0.97	Base of slip face
24.75	-0.615	Top of slip face
27.5	-0.6325	Beginning of subaqueaous point, all gravely sand
30.75	-0.63	Sand with 2-D ripples on 2-D dunes
34	-0.5675	-
37.75	-0.3525	-
41.75	-0.0325	Right bank
42.5	0.25	-
44.5	0.36	-
47	0.35	Right bank rebar

Transect D-14
September 7, 2013

Distance (m)	Elevation (m)	Comments
0	0	-
2.25	-0.735	Boulders
6	-1.004	Gravely sand
11	-1.2275	Gravely sand
15	-1.255	Sand
18	-0.91	Moved up slip face, sand
22	-0.705	Sand
24.5	-0.6475	Pebble Bar
28.75	-0.62	-
32.5	-0.81	-
37	-0.8775	-
39	-0.39	-
41	-0.03	Edge of vegetation
43	0.41	1 cm sand and mud from summer 2013 flood

Transect D-14
October 29, 2013

Distance (m)	Elevation (m)
0	0
0.52	-0.135
1.26	-0.565
2	-0.745
3	-0.775
4	-0.815
5	-0.915
6	-0.995
7	-1.065
8	-1.105
9	-1.155
10	-1.185
11	-1.165
12	-1.205
13	-1.225
14	-1.215
15	-1.245
16	-1.185
17	-1.095
18	-0.935
19	-0.815
20	-0.775
21	-0.755
22	-0.795
23	-0.745
24	-0.615
25	-0.585
26	-0.605
27	-0.655
28	-0.685
29	-0.725
30	-0.745
31	-0.805
32	-0.815
33	-0.845
34	-0.885
35	-0.885
36	-0.825
37	-0.825

Transect D-14
October 29, 2013 continued

Distance (m)	Elevation (m)
38.78	-0.555
38.9	-0.235
40	-0.125
41.5	0.23
44	0.39
47	0.375

Transect D-14
March 24, 2014

Distance (m)	Elevation (m)	Comments
0	0	Left bank
0.25	-0.02	-
1.25	-0.56	-
2.25	-0.78	Gravel
3.25	-0.8	-
4.25	-0.82	-
5.25	-0.88	Sand
6.25	-0.96	Gravel
7.25	-1.04	Gravel
8.25	-1.1	Gravel
9.25	-1.14	Gravel
10.25	-1.2	-
11.25	-1.24	Gravel
12.25	-1.27	-
13.25	-1.25	-
14.25	-1.22	-
15.25	-1.21	Sandy gravel
16.25	-1.2	Sandy gravel
17.25	-1.2	-
18.25	-1.2	Gravel
19.25	-1.2	Gravel
20.25	-1.1	Gravel
21.25	-0.96	Gravel
22.25	-0.78	Gravel
23.25	-0.68	Sandy gravel
24.25	-0.68	Gravel
25.25	-0.64	Gravely sand
26.25	-0.61	Gravely sand
27.25	-0.62	-
28.25	-0.66	Sand, shells
29.25	-0.74	Sand
30.25	-0.78	Sand
31.25	-0.74	Sand
32.25	-0.86	Sand
33.25	-0.93	-
34.25	-0.88	Sand
35.25	-0.86	-
36.25	-0.85	Sandy gravel
37.25	-0.88	Gravel
38.25	-0.73	-
39.25	-0.72	-

Transect D-14
March 24, 2014 continued

Distance (m)	Elevation (m)	Comments
40.25	-0.44	-
40.61	-0.32	Vertical cutbank
40.77	0	-

Transect D-14
July 22, 2014

Distance (m)	Elevation (m)
1.12	-0.625
2	-0.765
3	-0.875
4	-0.825
5	-0.885
6	-0.885
7	-0.915
8	-0.975
9	-1.045
10	-1.135
11	-1.165
12	-1.215
13	-1.215
14	-1.215
15	-1.225
16	-1.245
17	-1.275
18	-1.175
19	-0.975
20	-0.795
21	-0.755
22	-0.885
23	-1.105
24	-1.225
25	-1.355
26	-1.345
27	-1.345
28	-1.225
29	-1.145
30	-0.945
31	-0.965
32	-0.945
33	-0.985
34	-0.985
35	-0.905
36	-0.855
37	-0.835
38	-0.795
39	-0.685
39.64	-0.625

Transect D-14
December 14, 2014

Distance (m)	Elevation (m)	Comments
45.28	0.3275	Right bank rebar
42.02	0.225	Top of bank, clay
42	-0.425	Clay
40.75	-0.66	Clay
38	-0.85	Clay
36	-1.07	Clay
33.75	-1.035	Clay
30.75	-1.1175	Clay
29.25	-1.51	At log, gravel
28	-1.445	-
26.25	-1.2025	-
23.5	-0.89	Crest of bar
22	-0.74	-
18.75	-1.045	-
15.5	-1.185	-
12	-1.185	Sand ripples
8.25	-0.9625	-
4.25	-0.8825	-
2	-0.79	-
1	-0.43	-
0	0	Eye height on deck

Transect D-14
April 12, 2015

Distance (m)	Elevation (m)	Comments
0	-0.0525	Left bank rebar
0.28	-0.1125	-
1.28	-0.5125	-
2.28	-0.8225	At edge of deck
3.28	-0.8225	-
4.28	-0.8125	-
5.28	-0.7725	Sandy
6.28	-0.9525	-
7.28	-1.1125	-
8.28	-1.0925	-
9.28	-1.1525	-
10.28	-1.2625	-
11.28	-1.2325	Hard bottom gravel
12.28	-1.3125	Hard bottom gravel
13.28	-1.2825	Hard bottom gravel
14.28	-1.2725	-
15.28	-1.1825	-
16.28	-1.0125	Gravely
17.28	-0.8625	Sandy gravel
18.28	-0.8725	Sandy gravel
19.28	-0.8525	Sandy gravel
20.28	-0.8625	Sandy gravel
21.28	-0.8925	Sandy gravel
22.28	-0.8125	-
23.28	-0.6925	-
24.28	-0.5725	-
25.28	-0.4525	Pebbly sand
26.28	-0.4125	-
27.28	-0.4325	-
28.28	-0.4325	-
29.28	-0.3925	loose bar sand
30.28	-0.4125	loose bar sand
31.28	-0.4925	loose bar sand
32.28	-0.5925	loose bar sand
33.28	-0.7125	loose bar sand
34.28	-0.9525	Sand, firm bottom
35.28	-0.9625	Firm sand
36.28	-0.8725	Firm sand
37.28	-0.8925	Firm sand
38.28	-0.7725	Firm sand
39.28	-0.7125	Soft sands

Transect D-14
April 12, 2015 continued

Distance (m)	Elevation (m)	Comments
40.28	-0.6325	Soft sands
41.28	-0.4325	-
42.02	0.0875	Scarp
42.28	0.1775	-
43.33	0.2175	-
43.38	0.3075	Little water fall
44.28	0.3075	-
45.28	0.3075	Rebar, right bank
47.28	0.3275	-

Transect D-12
July 8, 2011

Distance (m)	Elevation (m)	Comments
0	0	-
3	-0.1075	-
4.75	-0.9875	Water edge
7.25	-1.12	-
10.25	-1.3725	Tree scour
12	-1.8075	Tree scour
13.5	-1.7875	-
15	-1.4775	-
15.75	-1.5675	-
19.5	-1.3525	-
20.25	-1.0325	-
21.75	-0.965	Water edge
24	-0.7575	-
27	-0.9275	-
28.75	-0.7825	-
30	-0.4175	-
32	-0.0175	-

Transect D-12
May 14, 2012

Distance (m)	Elevation (m)	Comments
0	0	Instrument height
3	-0.04	Top of bank
4	-0.71	Zero water
4.7	-1.07	Mud
5.7	-1.23	-
6.7	-1.01	Sand
7.7	-1.11	Sand
8.7	-1.31	Sand
9.2	-0.71	Tree
9.7	-1.48	Sand
10.5	-0.71	Tree
10.7	-1.85	-
11.7	-1.95	Gravel
12.7	-1.88	Fine gravel
13.2	-1.76	Gravel
13.7	-1.53	Bried tree
14.7	-1.48	Sand
15.7	-1.49	-
16.7	-1.48	-
17.7	-1.51	-
18.7	-1.2	Sand bar
19.7	-1.18	-
20.7	-1.18	2.5-D sand ripples
21.7	-1.1	-
22.7	-1.06	-
23.7	-1.03	-
24.7	-0.99	-
25.1	-0.87	-
25.7	-0.77	-
26.7	-0.78	-
27.54	-0.71	-

Transect D-12
May 20, 2013

Distance (m)	Elevation (m)	Comments
0	0	Eye height
3	-0.02	Top of scarp
5	-0.9475	-
7	-1.1425	Sticks
8.5	-1.5325	-
11	-1.5	LWD gone
12.5	-1.8225	-
15.75	-1.45	-
18.5	-1.45	-
20	-1.175	-
23.5	-1.185	-
25.5	-0.9625	-
30.5	-0.425	Tree, left bank

Transect D-12
March 24, 2014

Distance (m)	Elevation (m)	Comments
0	0	Right bank rebar
3	-0.0475	Top of bank
4.25	-0.7475	-
5.15	-1.1175	LWD
6.15	-1.3275	-
7.15	-1.5075	-
8.15	-1.7275	-
9.15	-1.7475	-
10.15	-1.7475	-
12.15	-2.3475	-
13.15	-2.2975	-
14.15	-2.1675	-
15.15	-2.0475	-
16.15	-2.3475	-
17.15	-1.8275	Sand bar
18.15	-1.7175	Sand bar
19.15	-1.7675	Sand bar
20.15	-1.7875	Sand bar
21.15	-1.7675	-
22.15	-1.6975	-
23.15	-1.7175	-
24.15	-1.6175	-
25.15	-1.4275	-
26.15	-1.3275	-
27.15	-1.1375	-
27.55	-1.0275	-
27.65	-0.8675	Bit of a scarp
28.15	-0.7475	-

Transect D-12
September 7, 2013

Distance (m)	Elevation (m)	Comments
0	-0.0425	Eye Height
2.75	-0.0425	Top of bank
4.5	-1.0175	-
6	-1.1525	Sand
7.75	-1.5425	-
8.25	-1.4025	Sand
11	-1.445	Sand, sticks
13.25	-1.705	Sand, gravel
15.25	-1.5175	Top of slip face
15.5	-1.3425	Sand
22	-1.255	Sand
24.5	-1.04	-
26.25	-0.855	-
28	-0.69	-
29	-0.5	-

Transect D-12
August 19, 2014

Distance (m)	Elevation (m)	Comments
0	0	Eye height, right bank
2.75	-0.025	Top of right bank
4.25	-0.835	~Bottom of bank
6.75	-1.35	-
8	-1.785	-
10	-2.325	-
12.75	-2.22	All gravel
14.75	-2.1175	-
17.5	-1.88	On gravely sand bar
21.25	-1.915	On gravely sand bar
24.5	-1.7375	-
26	-1.555	Base of small scarp
26.5	-1.3825	Top of small scarp
27.5	-1.1825	-
28.5	-0.995	-
29.25	-0.545	Top of left bank
30.25	-0.4575	-

Transect D-12
December 14, 2014

Distance (m)	Elevation (m)	Comments
0	0	Right bank rebar
2.75	-0.01	Top of bank
4	-0.8775	Bottom of bank
6	-1.205	Zero water
7.25	-1.56	Sticks and mud
8.5	-1.9775	Sticks and mud
9.75	-2.33	First gravel
11.5	-2.2625	Cobbles
13.5	-2.1725	Gravely bottom
15.25	-1.955	Sand and LWD
18.75	-2.04	Sand and LWD
20.5	-1.85	-
24.5	-1.68	-
26	-1.575	-
27	-1.2	Zero water
28	-1.02	Base of scarp
28.5	-0.59	Top of scarp
30	-0.41	At tree

Transect D-12
April 12, 2015

Distance (m)	Elevation (m)	Comments
0	0	Right bank rebar
2	0.06	1.5 m on rope
3	-0.0425	Top of bank
3	-0.335	Bottom of scarp
3.75	-0.53	3.3 m on rope, zero water
4.05	-0.76	-
4.25	-0.77	-
3.45	-0.89	-
4.45	-1.03	LWD
5.45	-1.2	Sticky mud, LWD
6.45	-1.36	Old clayey mud, branches
7.45	-1.76	-
8.45	-2.17	-
12.45	-2.25	-
13.45	-2.29	-
14.45	-2.28	-
15.45	-2.23	-
16.45	-2.14	-
17.45	-1.97	-
18.45	-1.82	-
19.45	-1.8	-
20.45	-1.81	-
21.45	-1.65	-
22.45	-1.48	-
23.45	-1.41	Soft sand
24.45	-1.49	Soft sand
25.45	-1.45	Soft sand
26.45	-1.38	Sandy
27.45	-1.09	-
27.77	-0.95	Sloping scarp
28.17	-0.58	Sloping scarp
28.78	-0.53	River left

Transect D-15
September 7, 2013

Distance (m)	Elevation (m)	Comments
0	0	Eye Height
1.5	-0.18	Top of bank
2.5	-0.9	Bottom of bank
3	-1.2325	All bricks
4.75	-1.4975	Sand, ripples
8.5	-1.64	Sand
11.5	-1.71	Sand
16	-1.77	-
18.5	-1.4725	On sand bar
23	-1.415	-
29	-1.35	-
33.5	-1.36	Bar crest
35	-1.535	-
36.5	-1.2525	-

Transect D-15
March 24, 2014

Distance (m)	Elevation (m)	Comments
0	0	Eye Height
1.5	-0.2025	Top of bank
2	-0.875	Base of scarp
2.5	-1.095	Flood sands
4.75	-1.74	-
7.5	-2.07	Bricks, gravel
11	-2.1125	-
15.75	-2.175	Bedrock ledge
20	-2.1	Sand
24	-2.105	Bedrock
28	-1.905	Bedrock
32	-1.785	Bedrock
35.5	-1.155	-
37.25	-0.9575	Base of ss cliff

Transect D-15
December 17, 2013

Distance (m)	Elevation (m)	Comments
0	0	Eye Height
3.25	-1.3775	-
5	-1.725	-
8	-1.76	-
10.25	-1.77	Small dunes
14	-1.9325	-
17.5	-1.955	-
22	-1.915	-
25	-1.7725	-
28.75	-1.6775	-
35	-1.425	-

Transect D-15
May 23, 2014

Distance (m)	Elevation (m)	Comments
0	0	Eye height
1.5	-0.1625	Top of scarp.
2	-0.9425	Base of scarp
3	-1.225	No change.
4.25	-1.625	Sand.
6.75	-2.03	Sand and LWD.
9.5	-2.1125	Sand, dunes.
12	-2.23	Bedrock
15.5	-2.16	Bedrock
19	-2.21	Sand ribbon
23	-2.01	Bedrock
28.5	-1.84	Bedrock
31.5	-1.785	Gravel
35.5	-1.235	-
36.5	-0.935	Base of ss cliff

Transect D-15
July 25, 2014

Distance (m)	Elevation (m)	Comments
0	0	Instrument height on right bank
1.5	-0.1325	Crest of right bank
6	-2.025	Mud, bricks, LWD
9.75	-2.165	Sand on bedrock, some pebbles, 2-D ripples
13.5	-2.105	Sand on bedrock, some pebbles
17	-2.125	Sand on bedrock
20.5	-2.2625	Bedrock
25.25	-2.015	Scattered cobbles on berock
29.75	-1.79	Scattered cobbles on berock
32.5	-1.675	Mud
35.5	-1.18	Mud on left bank
37	-0.8825	Base of ss cliff

Transect D-15
December 15, 2014

Distance (m)	Elevation (m)	Comments
0	0	Right bank
1.75	-0.1175	Top of scarp
1.75	-0.795	Bottom of scarp
3	-1.3125	Turns into ramp, end bricks
3.5	-1.5125	Zero water, mud meets water
6.25	-1.9075	0.43 m of water, mud and leaves
8	-2.0875	Bedrock and LWD
9.75	-2.155	Bedrock with some sand ribbons
13	-2.1475	-
16.75	-2.2575	Bedrock, some gravel and sand ribbons
19.5	-2.095	-
20.75	-2.2475	Bedrock, irregular
22.25	-2.0825	Bedrock, small distance
26	-1.9775	Bedrock
29	-1.8025	Bedrock
32.5	-1.7225	Zero water
35	-1.5125	-
37	-1.0825	Base of cliff, transit rotated upstream

Transect D-6
July 8, 2011

Distance (m)	Elevation (m)
78.85	2.3725
75.85	2.145
73.1	1.955
69.6	1.245
67.6	0.33
65.1	-0.215
64.6	-0.6175
63.8	-0.7775
62.8	-0.9275
61.8	-1.1375
60.8	-1.3475
59.8	-1.4375
58.8	-1.7175
57.8	-1.8075
56.8	-1.8375
55.8	-1.9975
54.8	-2.1175
53.8	-2.3075
52.8	-2.4375
51.8	-2.8375
50.8	-2.8375
49.8	-2.9975
48.8	-2.9475
47.8	-2.7975
46.8	-2.7075
45.8	-2.6475
44.8	-2.5275
43.8	-2.4375
42.8	-2.3475
41.8	-2.2975
40.8	-2.2475
39.8	-2.2875
38.8	-2.1475
37.8	-2.1375
36.8	-2.0875
35.8	-2.0475
34.8	-2.0475
33.8	-1.9975
32.8	-1.9975

Transect D-6
July 8, 2011 continued

Distance (m)	Elevation (m)
30.8	-1.9375
29.8	-1.9575
28.8	-1.9275
27.8	-1.8875
26.8	-1.8775
25.8	-1.8875
24.8	-1.8975
23.8	-1.8475
22.8	-1.8375
21.8	-1.8175
20.8	-1.8175
19.8	-1.7775
18.8	-1.8075
17.8	-1.8075
16.8	-1.7775
15.8	-1.7375
14.8	-1.7075
13.8	-1.6675
12.8	-1.6575
11.8	-1.5775
10.8	-1.5775
9.8	-1.5175
8.8	-1.4575
7.8	-1.3375
6.8	-1.2575
5.8	-1.1875
4.8	-1.1375
3.8	-1.1375
2.8	-1.0775
1.8	-0.9775
0.8	-0.7575
-0.2	-0.6175

Transect D-6
May 17, 2012

Distance (m)	Elevation (m)	Comments
77.6	2.2025	Old picnic table
73.1	2.134	Eye height at tree
69.6	1.4025	-
67.1	0.32	-
65.1	-0.215	Top of Bank
65.1	-0.555	65.68 m on rope
64.42	-0.725	-
63.42	-0.915	-
62.42	-1.085	-
61.42	-1.235	-
60.42	-1.475	-
59.42	-1.675	-
58.42	-1.725	-
57.42	-1.825	-
56.42	-1.935	-
55.42	-2.005	-
54.42	-2.205	Branch
53.42	-2.515	-
52.42	-2.725	-
51.42	-2.915	-
50.42	-2.995	-
49.42	-2.935	-
48.42	-2.855	-
47.42	-2.735	-
46.42	-2.625	-
45.42	-2.535	-
44.42	-2.425	-
43.42	-2.315	-
42.42	-2.245	-
41.42	-2.215	-
40.42	-2.135	-
39.42	-2.085	-
38.42	-2.055	-
37.42	-2.055	-
36.42	-2.035	-
35.42	-1.985	-
34.42	-1.965	-
33.42	-1.975	-
32.42	-1.965	-
31.42	-1.915	-

Transect D-6
May 17, 2012 continued

Distance (m)	Elevation (m)	Comments
30.42	-1.945	-
29.42	-1.885	-
28.42	-1.855	-
27.42	-1.865	-
26.42	-1.875	10:00 a.m.
25.42	-1.855	
24.42	-1.835	-
23.42	-1.815	-
22.42	-1.815	-
21.42	-1.805	-
20.42	-1.795	-
19.42	-1.815	-
18.42	-1.775	-
17.42	-1.755	-
16.42	-1.715	-
15.42	-1.675	-
14.42	-1.685	-
13.42	-1.645	-
12.42	-1.615	-
11.42	-1.515	-
10.42	-1.455	-
9.42	-1.385	-
8.42	-1.305	-
7.42	-1.195	-
6.42	-1.125	-
5.42	-1.065	-
4.42	-0.995	-
3.42	-0.905	-
2.42	-0.735	-
1.42	-0.575	-
0.92	-0.555	-

Transect D-6
December 17, 2013

Distance (m)	Elevation (m)	Depth to Refusal (m)	Comments
66.1	0	-	Instrument Height
65.1	-0.1925	-	Top of old scarp
65.1	-0.5575	-	Bottom of old scarp
61.85	-1.245	-	-
56.85	-1.9025	-	-
55.85	-2.0825	-	Rebar put in
54.1	-2.345	-	-
53.46	-2.825	-	Sticks and mud
52.96	-3.025	-	Mud
51.96	-3.075	-	Mud
50.96	-3.215	-	Mud
49.96	-3.505	-	Mud
48.96	-3.575	-	Mud
47.96	-3.625	1.41	Bedrock
46.96	-3.575	1.38	Bedrock
45.96	-3.195	-	Sand
44.96	-2.945	1.24	Bedrock
43.96	-2.675	-	Mud
42.96	-2.345	-	Mud

Transect D-6
March 24, 2014

Distance (m)	Elevation (m)	Comments
66.1	0	Eye height
65.35	-0.1625	Top of bank
65.1	-0.3025	Top of scarp
64.6	-0.68	Base of scarp
63.1	-0.8975	On bank
61.35	-1.3725	On bank
59.1	-1.73	Base of bank
57.6	-1.97	Zero water
56.85	-2.23	-
56.35	-2.29	Woody
55.35	-2.64	Mud
54.35	-2.83	-
53.35	-3.05	Sand, mud
52.35	-3.11	Sand
51.35	-3.13	Sand, gravel
50.35	-3.17	Sand
49.35	-3.25	-
48.35	-3.15	-
47.35	-3.07	-
46.35	-3.01	-
45.35	-2.96	-
44.35	-3.01	-
43.35	-2.89	-
42.35	-2.81	-
41.35	-2.78	-
40.35	-2.74	-
39.35	-2.72	Sand, gravel
38.35	-2.72	-
37.35	-2.65	-
36.35	-2.66	-
35.35	-2.55	-
34.35	-2.53	-
33.35	-2.5	-
32.35	-2.51	-
31.35	-2.51	-
30.35	-2.5	-
29.35	-2.54	-
28.35	-2.53	-
27.35	-2.48	-
26.35	-2.49	-
25.35	-2.48	Sand, gravel

Transect D-6
March 24, 2014 continued

Distance (m)	Elevation (m)	Comments
24.35	-2.5	-
23.35	-2.41	-
22.35	-2.34	-
21.35	-2.33	-
20.35	-2.27	-
19.35	-2.15	-
18.35	-2.05	River left
17.35	-1.97	-

Transect D-6
May 23, 2014

Distance (m)	Elevation (m)	Comments
68.6	0.9425	Back sighted
66.1	0	Eye height, right bank
65.1	-0.3225	Top of scarp
65.1	-0.71	Bottom of scarp
62.1	-1.095	-
59.6	-1.68	-
56.35	-2.19	197° on transit stage
55.35	-2.54	Dec. 2013 rebar
55.08	-2.63	Mud and LWD
54.08	-2.95	Mud
53.08	-3.11	Mud
52.08	-3.43	Mud
51.08	-3.39	Sand
50.08	-3.32	Sand
49.08	-3.31	Sand
48.08	-3.27	Sand
47.08	-3.15	Sand
46.08	-3.15	Sand, pebbles
45.08	-3.03	Sand
44.08	-3.09	Sand
43.08	-2.99	Sand
42.08	-3.03	Sand
41.08	-2.95	Sand
40.08	-2.95	Sand
39.08	-2.91	Sand
38.08	-2.95	Sand
37.08	-2.85	Sand
36.08	-2.75	Sand
35.08	-2.79	Sand
34.08	-2.71	Sand
33.08	-2.79	Sand
32.08	-2.71	Sand
31.08	-2.73	Sand
30.08	-2.68	Sand
29.08	-2.67	Active ripples, wood
28.08	-2.57	Active ripples
27.08	-2.55	Active ripples
26.08	-2.55	Active ripples
25.08	-2.65	Sand and pebbles
24.08	-2.67	Sand and pebbles
23.08	-2.63	Mud

Transect D-6
May 23, 2014 continued

Distance (m)	Elevation (m)	Comments
22.08	-2.6	Mud
21.08	-2.5	Mud
20.08	-2.44	Mud
19.08	-2.36	Mud
18.4	-2.33	Left bank stick
17.08	-2.19	Left of stick

Transect D-6
August 11, 2014

Distance (m)	Elevation (m)	Comments
66.1	0	Eye height
65.1	-0.27	Top of scarp
64.6	-0.69	-
62.6	-1.0725	-
60.85	-1.6425	-
57.1	-2.09	Edge of the veg.
55.15	-2.485	-
55.05	-2.57	Zero water
54.55	-2.79	-
53.55	-2.99	-
52.55	-3.15	-
51.55	-3.4	-
50.55	-3.45	-
49.55	-3.49	-
48.55	-3.48	-
47.55	-3.25	-
46.55	-3.24	-
45.55	-3.18	-
44.55	-3.15	-
43.55	-3.13	-
42.55	-3.14	-
41.55	-3.05	-
40.55	-2.99	-
39.55	-2.93	-
38.55	-2.9	-
37.55	-2.9	-
36.55	-2.89	-
35.55	-2.87	-
34.55	-2.89	-
33.55	-2.87	-
32.55	-2.84	-
31.55	-2.81	-
30.55	-2.75	-
29.55	-2.72	-
28.55	-2.71	-
27.55	-2.71	-
26.55	-2.72	-
25.55	-2.7	-
24.55	-2.69	-
23.55	-2.7	Estimated
22.55	-2.68	-

Transect D-6
August 11, 2014 continued

Distance (m)	Elevation (m)	Comments
21.8	-2.57	Left bank

Transect D-6
December 15, 2014

Distance (m)	Elevation (m)	Depth to Refusal (m)	Comments
66.1	0	-	Right bank root
65.35	-0.32	-	Top of scarp
64.6	-0.6725	-	Bottom of scarp
62.8	-0.94	-	-
60.85	-1.4075	-	-
58.1	-1.9425	-	-
56.1	-2.1825	-	Edge of veg.
55.1	-2.455	-	Old survey rebar
54.6	-2.5025	-	Zero water
53.6	-2.8625	-	Mud
52.6	-3.0825	-3.6325	-
51.6	-3.2925	-	-
50.6	-3.4425	-	Muddy
49.6	-3.4525	-3.7225	Mud, sand, gravel
48.6	-3.4725	-	Sand
47.6	-3.4325	-3.6925	Sand
46.6	-3.4525	-	Sand
45.6	-3.3825	-	Sand
44.6	-3.2625	-3.7925	Sand
43.6	-3.2425	-	Sand
42.6	-3.1825	-4.0125	Sand
41.6	-3.1525	-	Sand
40.6	-3.0725	-	Sand
39.6	-3.0025	-3.5025	Sand
38.6	-2.9925	-	Sand
37.6	-2.9225	-3.5225	Sand
36.6	-2.9225	-	Sand
35.6	-2.8625	-	Sand
34.6	-2.8025	-3.5625	Sand
33.6	-2.8425	-	Sand
32.6	-2.8525	-3.6225	Sand
31.6	-2.8425	-	Sand
30.6	-2.7925	-	Sand
29.6	-2.7625	-3.6425	Sand
28.6	-2.7425	-	Sand
27.6	-2.6925	-3.6725	Sand
26.6	-2.6825	-	Sand
25.6	-2.6825	-	Sand
24.6	-2.7325	-3.7125	Sand

Transect D-6
December 15, 2014 continued

Distance (m)	Elevation (m)	Depth to Refusal (m)	Comments
23.6	-2.7225	-	Sand
22.6	-2.6825	-3.6525	Sand
21.6	-2.6425	-	Sand, gravel
20.6	-2.5425	-	Sand, gravel
19.8	-2.5025	-	Sand, gravel
16.25	-2.0375	-	Wet mud
13	-1.7475	-	Wet mud
10.5	-1.5425	-	Wet mud
8	-1.3425	-	Wet mud
4.5	-1.0125	-	Dry mud
1.25	-0.6425	-	Dry mud
0	0.0525	-	Left bank rebar, dry mud

Transect D-6
April 12, 2015

Distance (m)	Elevation (m)	Comments
66.1	0	Eye height
64.85	-0.28	Top of old bank
64.85	-0.6625	Bottom of old bank
62.35	-1.06	On flood plain
60.1	-1.48	On flood plain
58.1	-1.78	Zero water
57.8	-1.92	
56.8	-2.17	Sticks and mud
55.8	-2.55	
54.8	-2.64	Muddy
53.8	-2.96	Felt softer
52.8	-3.08	-
51.8	-3.26	-
50.8	-3.3	-
49.8	-3.38	-
48.8	-3.37	-
47.8	-3.42	-
46.8	-3.36	-
45.8	-3.32	-
44.8	-3.28	2.10 m to bedrock
43.8	-3.31	-
42.8	-3.18	-
41.8	-3.18	-
40.8	-3.11	-
39.8	-3.03	-
38.8	-3.03	-
37.8	-3.01	Gravely
36.8	-2.98	-
35.8	-2.96	-
34.8	-2.86	Probe attempted
33.8	-2.86	-
32.8	-2.87	-
31.8	-2.86	-
30.8	-2.83	-
29.8	-2.76	Sand, gravel, mud
28.8	-2.72	Sand on mud
27.8	-2.73	-
26.8	-2.71	-
25.8	-2.74	-

Transect D-6
April 12, 2015 continued

Distance (m)	Elevation (m)	Comments
23.8	-2.74	Gravel
22.8	-2.74	Sandy gravel
21.8	-2.67	-
20.8	-2.62	-
19.8	-2.55	-
18.8	-2.48	Sand on mud
17.8	-2.35	-
16.8	-2.24	-
15.8	-2.2	-
14.8	-2.09	-
13.8	-1.96	-
12.8	-1.8	-
12.2	-1.78	Zero water
9.8	-1.485	-
8.3	-1.43	Quick reading
5.8	-1.175	Begin wet mud
3.8	-0.95	-
1.8	-0.605	Old bank
0	0.185	Left bank tree

APPENDIX E

SPATIAL AND GEOMORPHIC DATA OF LEFEVER IMPOUNDMENT DELTA SURVEYS

GIS and geomorphic survey data for LeFever Impoundment Delta surveys from 2011 through 2015. Geographic coordinates are shown in decimal degrees and elevations were measured relative to the local reference stake.

LeFever Delta
May 17, 2012

Station ID	Latitude	Longitude	Elevation (m)	Comments
0	41.1457	-81.4616	0.00	Instrument at rebar
1	41.1459	-81.4616	-0.61	Medium sand
2	41.1459	-81.4616	-0.53	-
3	41.1459	-81.4617	-0.42	-
4	41.1459	-81.4618	-0.57	-
5	41.1459	-81.4618	-0.63	-
6	41.1460	-81.4619	-0.51	-
7	41.1460	-81.4620	-0.43	-
8	41.1460	-81.4621	-0.59	-
9	41.1460	-81.4622	-0.59	-
10	41.1461	-81.4622	-0.45	-
11	41.1461	-81.4623	-0.48	-
12	41.1461	-81.4624	-0.63	-
13	41.1462	-81.4624	-0.70	-
14	41.1462	-81.4625	-0.58	2-D dunes with 2.5 D ripples
15	41.1462	-81.4625	-0.75	-
16	41.1462	-81.4625	-0.77	-
17	41.1463	-81.4626	-0.87	-
18	41.1463	-81.4626	-0.91	-
19	41.1460	-81.4622	-0.49	-
20	41.1460	-81.4621	-0.43	-
21	41.1459	-81.4621	-0.41	plus
22	41.1459	-81.4620	-0.38	plus
23	41.1458	-81.4620	-0.43	-
24	41.1457	-81.9118	-0.51	-
25	41.1457	-81.4618	-0.57	-
26	41.1456	-81.4617	-0.61	-
27	41.1457	-81.4617	-0.47	Transect
28	41.1457	-81.4617	-0.59	Transect
29	41.1457	-81.4617	-0.57	Transect
30	41.1456	-81.4618	-0.59	Transect
31	41.1456	-81.4619	-0.68	Transect
32	41.1453	-81.4619	-1.20	Transect
33	41.1458	-81.4623	-0.90	Transect, White House
34	41.1460	-81.4623	-1.11	Transect, White House
35	41.1460	-81.4622	-0.89	Transect, White House
36	41.1460	-81.4622	-0.43	Transect, White House
37	41.1459	-81.4615	-1.07	Rebar transect Continued
38	41.1459	-81.4614	-1.55	Rebar transect Continued
39	41.1459	-81.4614	-1.13	Rebar transect continued, Gravel
40	41.1460	-81.4620	-1.61	-

LeFever Delta
May 17, 2012 continued

Station ID	Latitude	Longitude	Elevation (m)	Comments
41	41.1460	-81.4620	-1.63	Bedrock
42	41.1463	-81.4624	-1.66	-
43	41.1463	-81.4624	-1.55	-
44	41.1463	-81.4623	-1.25	-
45	-	-	-0.86	L-1 Transect, Zero water
46	-	-	-0.92	L-1 Transect, Sand
47	-	-	-0.95	L-1 Transect
48	-	-	-1.05	L-1 Transect
49	-	-	-1.07	L-1 Transect
50	-	-	-0.96	L-1 Transect
51	-	-	-1.07	L-1 Transect, Delta Crest
52	41.1460	-81.4620	-1.18	L-1: Halfway down slip face
53	-	-	-1.90	L-1 Transect
54	-	-	-1.94	L-1 Transect
55	-	-	-1.95	L-1 Transect
56	-	-	-2.25	L-1 Transect

LeFever Delta
May 20, 2013

Station ID	Latitude	Longitude	Elevation (m)
1	41.1457	-81.4616	-0.64
2	41.1457	-81.4617	-0.59
3	41.1459	-81.4618	-0.56
4	41.1459	-81.4618	-0.54
5	41.1458	-81.4619	-0.57
6	41.1459	-81.4620	-0.66
7	41.1460	-81.4620	-0.56
8	41.1460	-81.4621	-0.53
9	41.1461	-81.4622	-0.6
10	41.1461	-81.4623	-1.02
11	41.1461	-81.4623	-1.13
12	41.1461	-81.4623	-1.24
13	41.1462	-81.4624	-1.36
14	41.1463	-81.4624	-1.28
15	41.1463	-81.4624	-1.36
16	41.1464	-81.4624	-1.4
17	41.1463	-81.4625	-1.26
18	41.1462	-81.4625	-0.96
19	41.1462	-81.4626	-0.72
20	41.1462	-81.4626	-1.08
21	41.1462	-81.4626	-0.46
22	41.1462	-81.4625	-0.63
23	41.1461	-81.4624	-0.6
24	41.1461	-81.4623	-0.58
25	41.1461	-81.4622	-0.58
26	41.1460	-81.4622	-0.46
27	41.1460	-81.4622	-0.46
28	41.1460	-81.4622	-0.62
29	41.1460	-81.4621	-0.62
30	41.1460	-81.4620	-0.67
31	41.1459	-81.4622	-0.63
32	41.1459	-81.4618	-0.46
33	41.1459	-81.4617	-0.46
34	41.1459	-81.4616	-0.46
35	41.1459	-81.4615	-0.59
36	41.1458	-81.4621	-0.66
37	41.1458	-81.4620	-1.25
38	41.1458	-81.4620	-0.82
39	41.1458	-81.4620	-0.46
40	41.1458	-81.4620	-0.31
41	41.1458	-81.4620	-0.46
42	41.1459	-81.4619	-0.64

LeFever Delta
May 20, 2013 continued

Station ID	Latitude	Longitude	Elevation (m)
43	41.1459	-81.4618	-0.62
44	41.1459	-81.4619	-0.63
45	41.1460	-81.4618	-1.65
46	41.1460	-81.4618	-1.76
47	41.1460	-81.4618	-1.69
48	41.1460	-81.4618	-1.44
49	41.1461	-81.4618	-1.3
50	41.1456	-81.4619	-0.79
51	41.1456	-81.4618	-0.62
52	41.1457	-81.4617	-0.54
53	41.1458	-81.4616	-0.46
54	41.1458	-81.4616	-0.46
55	41.1459	-81.4616	-1.58
56	41.1460	-81.4615	-1.58
57	41.1460	-81.4615	-1.27

LeFever Delta
August 30, 2013

Station ID	Latitude	Longitude	Elevation (m)
1	41.1459	-81.4613	-0.48
2	41.1458	-81.4614	-0.48
3	41.1459	-81.4616	-0.48
4	41.1459	-81.4616	-1.36
5	41.1460	-81.4615	-1.33
6	41.1460	-81.4615	-0.48
7	41.1460	-81.4616	-0.48
8	41.1459	-81.4617	-1.28
9	41.1459	-81.4617	-1.45
10	41.1459	-81.4617	-0.48
11	41.1460	-81.4618	-0.48
12	41.1461	-81.4620	-0.48
13	41.1460	-81.4619	-1.15
14	41.1460	-81.4621	-0.69
15	41.1460	-81.4621	-0.69
16	41.1460	-81.4622	-0.48
17	41.1459	-81.4621	-0.48
18	41.1459	-81.4622	-0.7
19	41.1459	-81.4622	-0.61
20	41.1462	-81.4623	-0.71
21	41.1463	-81.4624	-0.89
22	41.1463	-81.4625	-0.72
23	41.1462	-81.4626	-0.68
24	41.1463	-81.4624	-1
25	41.1463	-81.4624	-1.11
26	41.1459	-81.4622	-0.48
27	41.1458	-81.4621	-0.48
28	41.1458	-81.4621	-0.48
29	41.1458	-81.4620	-0.48
30	41.1457	-81.4621	-0.48
31	41.1457	-81.4619	-0.48
32	41.1456	-81.4619	-0.48
33	41.1455	-81.4618	-0.48
34	41.1455	-81.4618	-0.72
35	41.1456	-81.4617	-0.76
36	41.1456	-81.4617	-0.84
37	41.1457	-81.4616	-0.48
38	41.1459	-81.4620	-0.77
39	41.1459	-81.4619	-0.85
40	41.1458	-81.4618	-0.97
41	41.1457	-81.4617	-1.07
42	41.1456	-81.4617	-0.9

LeFever Delta
August 30, 2013 continued

Station ID	Latitude	Longitude	Elevation (m)
43	41.1456	-81.4616	-0.93
44	41.1456	-81.4616	-0.48

LeFever Delta
Dec. 13, 2013

Station ID	Latitude	Longitude	Elevation (m)
1	41.1456	-81.4615	-0.775
2	41.1456	-81.4616	-1.425
3	41.1455	-81.4616	-1.585
4	41.1456	-81.4616	-1.235
5	41.1456	-81.4616	-1.585
6	41.1455	-81.4616	-1.225
7	41.1455	-81.4616	-1.145
8	41.1454	-81.4617	-1.105
9	41.1454	-81.4617	-0.775
10	41.1455	-81.4619	-1.055
11	41.1455	-81.4619	-1.065
12	41.1456	-81.4618	-0.975
13	41.1456	-81.4618	-0.775
14	41.1456	-81.4617	-1.275
15	41.1456	-81.4617	-1.375
16	41.1456	-81.4617	-0.975
17	41.1456	-81.4617	-1.365
18	41.1456	-81.4617	-1.195
19	41.1456	-81.4616	-0.775
20	41.1458	-81.4617	-0.775
21	41.1458	-81.4617	-1.335
22	41.1457	-81.4618	-1.405
23	41.1457	-81.4618	-1.115
24	41.1457	-81.4618	-1.255
25	41.1457	-81.4619	-0.775
26	41.1456	-81.4619	-0.775
27	41.1457	-81.4620	-1.135
28	41.1457	-81.4620	-0.775
29	41.1458	-81.4621	-0.775
30	41.1458	-81.4621	-1.175
31	41.1458	-81.4621	-1.095
32	41.1459	-81.4620	-0.775
33	41.1458	-81.4620	-0.775
34	41.1458	-81.4619	-1.165
35	41.1459	-81.4619	-1.335
36	41.1459	-81.4619	-1.125
37	41.1459	-81.4619	-1.495
38	41.1459	-81.4618	-1.355
39	41.1460	-81.4618	-0.775
40	41.1460	-81.4618	-1.195
41	41.1460	-81.4618	-1.315
42	41.1460	-81.4618	-1.055

LeFever Delta
Dec. 13, 2013 continued

Station ID	Latitude	Longitude	Elevation (m)
43	41.1461	-81.4617	-0.775
44	41.1459	-81.4615	-0.775
45	41.1459	-81.4615	-1.295
46	41.1460	-81.4615	-1.275
47	41.1460	-81.4615	-1.175
48	41.1460	-81.4615	-0.775
49	41.1459	-81.4613	-0.975
50	41.1459	-81.4613	-0.935
51	41.1459	-81.4613	-0.975
52	41.1460	-81.4615	-1.455
53	41.1460	-81.4616	-1.235
54	41.1459	-81.4616	-1.315
55	41.1459	-81.4617	-1.295
56	41.1459	-81.4617	-0.775
57	41.1461	-81.4619	-0.775
58	41.1460	-81.4620	-1.435
59	41.1460	-81.4620	-1.255
60	41.1460	-81.4621	-1.105
61	41.1460	-81.4621	-1.025
62	41.1459	-81.4622	-0.775
63	41.1459	-81.4622	-0.955
64	41.1459	-81.4622	-1.005
65	41.1459	-81.4623	-0.775
66	41.1460	-81.4624	-0.775
67	41.1461	-81.4624	-0.945
68	41.1461	-81.4624	-1.015
69	41.1462	-81.4623	-1.025
70	41.1462	-81.4623	-1.235
71	41.1462	-81.4622	-1.415
72	41.1462	-81.4622	-1.095
73	41.1463	-81.4622	-0.775
74	41.1461	-81.4622	-1.115

LeFever Delta
March 23, 2014

Station ID	Latitude	Longitude	Elevation (m)
1	41.1457	-81.4623	-0.665
2	41.1457	-81.4616	-1.305
3	41.1456	-81.4616	-1.725
4	41.1456	-81.4617	-1.425
5	41.1456	-81.4617	-1.575
6	41.1455	-81.4618	-1.525
7	41.1455	-81.4617	-1.155
8	41.1456	-81.4618	-1.125
9	41.1455	-81.4618	-1.455
10	41.1455	-81.4618	-1.535
11	41.1455	-81.4618	-1.465
12	41.1455	-81.4619	-1.225
13	41.1456	-81.4619	-0.985
14	41.1456	-81.4619	-1.345
15	41.1456	-81.4619	-1.455
16	41.1456	-81.4618	-0.915
17	41.1456	-81.4618	-0.925
18	41.1456	-81.4618	-1.325
19	41.1457	-81.4618	-1.585
20	41.1457	-81.4618	-1.465
21	41.1457	-81.4617	-1.765
22	41.1457	-81.4617	-1.305
23	41.1457	-81.4617	-1.345
24	41.1457	-81.4617	-1.025
25	41.1457	-81.4616	-0.665
26	41.1458	-81.4616	-0.665
27	41.1458	-81.4617	-1.105
28	41.1458	-81.4618	-1.565
29	41.1458	-81.4618	-1.685
30	41.1459	-81.4617	-0.665
31	41.1459	-81.4617	-1.625
32	41.1460	-81.4617	-1.275
33	41.1460	-81.4617	-1.275
34	41.1459	-81.4615	-1.225
35	41.1460	-81.4615	-1.315
36	41.1459	-81.4615	-1.165
37	41.1459	-81.4615	-0.665
38	41.1451	-81.4617	-1.215
39	41.1458	-81.4618	-1.465
40	41.1459	-81.4618	-1.715
41	41.1460	-81.4618	-1.515
42	41.1460	-81.4618	-1.035

LeFever Delta
March 23, 2014 continued

Station ID	Latitude	Longitude	Elevation (m)
43	41.1460	-81.4618	-1.285
44	41.1459	-81.4619	-1.805
45	41.1459	-81.4619	-1.585
46	41.1459	-81.4620	-1.585
47	41.1459	-81.4620	-1.585
48	41.1459	-81.4620	-1.265
49	41.1459	-81.4620	-1.375
50	41.1458	-81.4621	-1.335
51	41.1458	-81.4621	-1.405
52	41.1458	-81.4621	-1.305
53	41.1458	-81.4621	-0.665
54	41.1460	-81.4623	-1.095
55	41.1460	-81.4623	-1.535
56	41.1461	-81.4622	-1.545
57	41.1461	-81.4622	-1.595
58	41.1461	-81.4622	-1.455
59	41.1461	-81.4621	-1.545
60	41.1462	-81.4621	-1.745
61	41.1462	-81.4621	-1.565
62	41.1462	-81.4621	-1.265
63	41.1461	-81.4620	-1.465
64	41.1460	-81.4619	-1.515
65	41.1458	-81.4619	-1.445
66	41.1458	-81.4619	-1.525
67	41.1458	-81.4618	-1.365
68	41.1458	-81.4617	-1.495
69	41.1458	-81.4617	-1.825
70	41.1458	-81.4617	-1.225

LeFever Delta
May 23, 2014

Station ID	Latitude	Longitude	Elevation (m)
1	41.1455	-81.4617	-0.83
2	41.1455	-81.4617	-0.83
3	41.1456	-81.4617	-0.83
4	41.1456	-81.4617	-0.83
5	41.1456	-81.4618	-0.83
6	41.1457	-81.4618	-0.83
7	41.1458	-81.4618	-0.83
8	41.1458	-81.4618	-0.83
9	41.1459	-81.4617	-0.83
10	41.1459	-81.4616	-0.83
11	41.1458	-81.4616	-0.83
12	41.1459	-81.4614	-0.83
13	41.1459	-81.4615	-1.23
14	41.1459	-81.4614	-1.52
15	41.1460	-81.4615	-1.24
16	41.1460	-81.4615	-0.83
17	41.1460	-81.4615	-0.83
18	41.1459	-81.4616	-1.43
19	41.1458	-81.4616	-1.39
20	41.1459	-81.4616	-1.39
21	41.1458	-81.4616	-1.37
22	41.1458	-81.4617	-1.47
23	41.1459	-81.4617	-1.53
24	41.1459	-81.4617	-1.47
26	41.1460	-81.4617	-1.31
27	41.1462	-81.4622	-1.42
28	41.1462	-81.4622	-1.72
29	41.1461	-81.4623	-1.69
30	41.1460	-81.4624	-1.49
31	41.1460	-81.4624	-1.25
32	41.1460	-81.4625	-0.83
33	41.1459	-81.4622	-0.83
34	41.1458	-81.4622	-1.43
35	41.1459	-81.4622	-1.49
36	41.1459	-81.4621	-1.63
37	41.1460	-81.4621	-1.59
38	41.1460	-81.4621	-1.55
39	41.1460	-81.4620	-1.51
40	41.1461	-81.4620	-0.83
41	41.1460	-81.4618	-0.83
42	41.1460	-81.4618	-1.22
43	41.1459	-81.4619	-1.76

LeFever Delta
May 23, 2014 continued

Station ID	Latitude	Longitude	Elevation (m)
44	41.1459	-81.4619	-1.78
45	41.1459	-81.4620	-1.59
46	41.1458	-81.4620	-1.63
47	41.1458	-81.4621	-1.53
48	41.1458	-81.4621	-1.34
49	41.1457	-81.4621	-1.4
50	41.1457	-81.4621	-0.83
51	41.1452	-81.4619	-0.83
52	41.1455	-81.4619	-1.46
53	41.1455	-81.4618	-1.33
54	41.1455	-81.4618	-1.03
55	41.1455	-81.4619	-0.97
56	41.1456	-81.4618	-1.16
57	41.1456	-81.4619	-1.52
58	41.1456	-81.4619	-1.62
59	41.1456	-81.4620	-1.03
60	41.1456	-81.4619	-1.36
61	41.1457	-81.4619	-1.38
62	41.1459	-81.4619	-1.16
63	41.1458	-81.4620	-1.24
64	41.1458	-81.4619	-1.43
65	41.1458	-81.4619	-1.53
66	41.1458	-81.4619	-1.69
67	41.1458	-81.4618	-1.71
68	41.1458	-81.4618	-1.56
69	41.1458	-81.4618	-1.35
70	41.1458	-81.4618	-1.15
71	41.1457	-81.4617	-1.03
72	41.1457	-81.4618	-1.53
73	41.1457	-81.4618	-1.71
74	41.1457	-81.4618	-1.64
75	41.1456	-81.4618	-1.71
76	41.1456	-81.4618	-1.58
77	41.1456	-81.4619	-1.48
78	41.1456	-81.4619	-1.03
79	41.1456	-81.4619	-0.94
80	41.1456	-81.4619	-0.99
81	41.1456	-81.4619	-1.36
82	41.1454	-81.4618	-0.83
83	41.1455	-81.4618	-1.49
84	41.1456	-81.4617	-1.56
85	41.1455	-81.4618	-1.27

LeFever Delta

May 23, 2014 continued

Station ID	Latitude	Longitude	Elevation (m)
86	41.1455	-81.4617	-1.04
87	41.1455	-81.4617	-1.21
88	41.1455	-81.4617	-1.23
89	41.1455	-81.4617	-1.43
90	41.1455	-81.4617	-1.72
91	41.1456	-81.4617	-1.52
92	41.1456	-81.4616	-1.72
93	41.1456	-81.4616	-1.75
94	41.1456	-81.4616	-1.43
95	41.1456	-81.4616	-1.2
96	41.1456	-81.4616	-0.83
97	41.1456	-81.4616	-0.83
98	41.1458	-81.4617	-0.67
99	41.1458	-81.4617	-0.64
100	41.1458	-81.4616	-0.4825
101	41.1458	-81.4616	-0.465
102	41.1458	-81.4616	-0.5225
103	41.1458	-81.4617	-0.655
104	41.1458	-81.4617	-0.435
105	41.1458	-81.4617	-0.5
106	41.1459	-81.4606	-0.47
107	41.1458	-81.4616	-0.6075
108	41.1458	-81.4616	-0.505
109	41.1458	-81.4617	-0.715
110	41.1458	-81.4616	-0.455
111	41.1457	-81.4616	-0.4475
112	41.1456	-81.4615	-0.44
113	41.1456	-81.4616	-0.44
114	41.1458	-81.4616	-0.4975

LeFever Delta
July 25, 2014

Station ID	Latitude	Longitude	Elevation (m)
1	-	-	-1.2
2	41.1456	-81.4615	-1.2
3	41.1456	-81.4616	-1.49
4	41.1455	-81.4616	-1.76
5	41.1455	-81.4616	-1.34
6	41.1455	-81.4616	-1.6
7	41.1454	-81.4617	-1.7
8	41.1454	-81.4612	-1.59
9	41.1454	-81.4614	-1.2
10	41.1455	-81.4615	-1.2
11	41.1455	-81.4615	-1.56
12	41.1455	-81.4616	-1.61
13	41.1455	-81.4615	-1.66
14	41.1455	-81.4616	-1.52
15	41.1455	-81.4617	-1.64
16	41.1455	-81.4618	-1.52
17	41.1456	-81.4616	-1.77
18	41.1456	-81.4616	-1.46
19	41.1456	-81.4616	-1.2
20	41.1457	-81.4617	-1.7
21	41.1456	-81.4617	-1.69
22	41.1456	-81.4617	-1.7
23	41.1456	-81.4617	-1.54
24	41.1456	-81.4617	-1.35
25	41.1456	-81.4617	-1.4
26	41.1455	-81.4615	-1.2
27	41.1455	-81.4618	-1.37
28	41.1454	-81.4616	-1.2
29	41.1455	-81.4617	-1.2
30	41.1456	-81.4618	-1.2
31	41.1454	-81.4618	-1.37
32	41.1456	-81.4618	-1.48
33	41.1456	-81.4619	-1.42
34	41.1457	-81.4618	-1.7
35	41.1456	-81.4617	-1.2
36	41.1457	-81.4617	-1.72
37	41.1457	-81.4617	-1.71
38	41.1457	-81.4617	-1.76
39	41.1458	-81.4617	-1.2
40	41.1458	-81.4618	-1.2
41	41.1459	-81.4619	-1.55
42	41.1458	-81.4619	-1.38

LeFever Delta
July 25, 2014 continued

Station ID	Latitude	Longitude	Elevation (m)
43	41.1458	-81.4619	-1.64
44	41.1457	-81.4620	-1.61
45	41.1458	-81.4620	-1.32
46	41.1457	-81.4620	-1.2
47	41.1457	-81.4620	-1.41
48	41.1456	-81.4621	-1.2
49	41.1458	-81.4622	-1.2
50	41.1459	-81.4622	-1.2
51	41.1459	-81.4621	-1.48
52	41.1459	-81.4620	-1.32
53	41.1459	-81.4620	-1.46
54	41.1461	-81.4619	-1.7
55	41.1461	-81.4619	-1.4
56	41.1460	-81.4619	-1.2
57	41.1460	-81.4618	-1.26
58	41.1461	-81.4618	-1.2
59	41.1460	-81.4617	-1.2
60	41.1458	-81.4617	-1.35
61	41.1458	-81.4616	-2
62	41.1458	-81.4616	-1.3
63	41.1459	-81.4616	-1.2
64	41.1459	-81.4614	-1.2
65	41.1459	-81.4615	-1.29
66	41.1459	-81.4615	-1.2
67	41.1460	-81.4614	-1.2
68	41.1460	-81.4614	-1.38
69	41.1460	-81.4614	-1.2
70	41.1457	-81.4615	-0.44
71	41.1457	-81.4616	-0.4875
72	41.1457	-81.4617	-0.5725
73	41.1458	-81.4617	-0.5725
74	41.1458	-81.4617	-0.45
75	41.1459	-81.4617	-0.52
76	41.1459	-81.4617	-1.2525
77	41.1458	-81.4617	-0.3875
78	41.1458	-81.4616	-0.5
79	41.1459	-81.4615	-0.55
80	41.1458	-81.4616	-0.4275
81	41.1457	-81.4616	-0.44
82	41.1458	-81.4617	-0.6625
83	41.1458	-81.4618	-0.835
84	41.1459	-81.4618	-1.125

LeFever Delta
Dec. 15, 2014

Station ID	Latitude	Longitude	Elevation (m)
1	41.1458	-81.4616	-
2	41.1458	-81.4616	-
3	41.1458	-81.3915	-
4	41.1457	-81.4617	-0.52
5	41.1458	-81.4615	-
6	41.1458	-81.4616	-0.365
7	41.1458	-81.4616	-0.4525
8	41.1458	-81.4617	-0.665
9	41.1459	-81.4617	-0.655
10	41.1458	-81.4617	-0.565
11	41.1458	-81.4616	-0.585
12	41.1457	-81.4616	-0.585
13	41.1457	-81.4615	-
14	41.1456	-81.4616	-1.105
15	41.1457	-81.4616	-1.105
16	41.1457	-81.4617	-1.625
17	41.1457	-81.4617	-0.3325
18	41.1457	-81.4617	-1.695
19	41.1458	-81.4617	-
20	41.1458	-81.4618	-1.445
21	41.1457	-81.4617	-0.3
22	41.1458	-81.4617	-1.105
23	41.1458	-81.4617	-0.43
24	41.1459	-81.4618	-1.105
25	41.1459	-81.4617	-1.105
26	41.1459	-81.4617	-1.105
27	41.1459	-81.4616	-1.105
28	41.1459	-81.4615	-1.105
29	41.1459	-81.4614	-1.105
30	41.1459	-81.4614	-1.275
31	41.1460	-81.4614	-1.405
32	41.1460	-81.4615	-1.105
33	41.1460	-81.4618	-1.105
34	41.1460	-81.4617	-1.425
35	41.1459	-81.4617	-1.285
36	41.1459	-81.4618	-1.435
37	41.1459	-81.4617	-1.555
38	41.1459	-81.4618	-1.615
39	41.1459	-81.4618	-1.325
40	41.1459	-81.4617	-1.305
41	41.1459	-81.4618	-1.105
42	41.1462	-81.4622	-1.105

LeFever Delta
Dec. 15, 2014 continued

Station ID	Latitude	Longitude	Elevation (m)
43	41.1462	-81.4622	-1.605
44	41.1462	-81.4622	-1.735
45	41.1462	-81.4623	-1.735
46	41.1461	-81.4624	-1.735
47	41.1460	-81.4624	-1.765
48	41.1459	-81.4622	-1.495
49	41.1460	-81.4623	-1.305
50	41.1461	-81.4623	-1.105
51	41.1459	-81.4622	-1.105
52	41.1459	-81.4622	-1.465
53	41.1459	-81.4621	-1.485
54	41.1459	-81.4621	-1.605
55	41.1460	-81.4621	-1.615
56	41.1460	-81.4620	-1.625
57	41.1461	-81.4620	-1.545
58	41.1461	-81.4620	-1.105
59	41.1460	-81.4619	-1.105
60	41.1459	-81.4620	-1.525
61	41.1459	-81.4620	-1.695
62	41.1459	-81.4620	-1.585
63	41.1459	-81.4621	-1.485
64	41.1459	-81.4621	-1.615
65	41.1459	-81.4619	-1.425
66	41.1458	-81.4621	-1.565
67	41.1458	-81.4622	-1.455
68	41.1458	-81.4622	-1.105
69	41.1457	-81.4620	-1.105
70	41.1457	-81.4619	-1.535
71	41.1458	-81.4619	-1.465
72	41.1458	-81.4619	-1.245
73	41.1458	-81.4620	-1.425
74	41.1458	-81.4619	-1.425
75	41.1458	-81.4619	-1.625
76	41.1458	-81.4619	-1.635
77	41.1458	-81.4619	-1.775
78	41.1459	-81.4518	-1.525
79	41.1459	-81.4618	-1.495
80	41.1459	-81.4618	-1.505
81	41.1457	-81.4619	-1.795
82	41.1457	-81.4618	-1.805
83	41.1457	-81.4618	-1.775
84	41.1457	-81.4618	-1.805

LeFever Delta
Dec. 15, 2014 continued

Station ID	Latitude	Longitude	Elevation (m)
85	41.1457	-81.4619	-1.635
86	41.1457	-81.4616	-1.105
87	41.1456	-81.4619	-1.105
88	41.1456	-81.4618	-1.445
89	41.1456	-81.4619	-1.335
90	41.1457	-81.4620	-1.105
91	41.1456	-81.4620	-1.105
92	41.1456	-81.4618	-1.105
93	41.1455	-81.4618	-1.105
94	41.1455	-81.4615	-1.655
95	41.0000	-81.0000	-0.19
96	41.1456	-81.4619	-1.255
97	41.1456	-81.4618	-1.405
98	41.1456	-81.4618	-1.505
99	41.1456	-81.4618	-1.105
100	41.1456	-81.4617	-1.105
101	41.1456	-81.4618	-1.525
102	41.1456	-81.4617	-1.585
103	41.1456	-81.4617	-1.785
104	41.1457	-81.4616	-1.595
105	41.1457	-81.4616	-1.825
106	41.1458	-81.4615	-1.675
107	41.1456	-81.4615	-1.315
108	41.1456	-81.4615	-1.735
109	41.1456	-81.4616	-1.725
110	41.1455	-81.4616	-1.485
111	41.1455	-81.4616	-1.765
112	41.1455	-81.4616	-1.725
113	41.1454	-81.4616	-1.605
114	41.1454	-81.4617	-1.505
115	41.1454	-81.4617	-1.105

LeFever Delta
May 3, 2015

Station ID	Latitude	Longitude	Elevation (m)
0	41.1458	-81.4616	0
1	41.1457	-81.4617	-1.2175
2	41.1458	-81.4616	-0.815
3	41.1459	-81.4617	-0.725
4	41.1459	-81.4617	-1.2175
5	41.1459	-81.4616	-0.4
6	41.1459	-81.4616	-1.2175
7	41.1459	-81.4616	-0.435
8	41.1457	-81.4616	-0.705
9	41.1457	-81.4616	-1.2175
10	41.1456	-81.4615	-1.2175
11	41.1456	-81.4615	-1.8075
12	41.1455	-81.4615	-1.5875
13	41.1455	-81.4616	-1.7775
14	41.1455	-81.4616	-1.7075
15	41.1455	-81.4616	-1.7475
16	41.1454	-81.4616	-1.6175
17	41.1454	-81.4616	-1.2175
18	41.1455	-81.4617	-1.2175
19	41.1454	-81.4617	-1.6075
20	41.1455	-81.4617	-1.6675
21	41.1455	-81.4617	-1.5475
22	41.1622	-81.4617	-1.5775
23	41.1456	-81.4617	-1.7275
24	41.1456	-81.4617	-1.5075
25	41.1456	-81.4616	-1.6575
26	41.1456	-81.4616	-1.7475
27	41.1457	-81.4616	-1.2175
28	41.1457	-81.4617	-1.7375
29	41.1457	-81.4617	-1.6575
30	41.1457	-81.4618	-1.7475
31	41.1457	-81.4618	-1.5875
32	41.1456	-81.4618	-1.5375
33	41.1456	-81.4618	-1.0375
34	41.1455	-81.4619	-1.4775
35	41.1456	-81.4619	-1.4375
36	41.1455	-81.4619	-1.2175
37	41.1457	-81.4620	-1.2175
38	41.1457	-81.4620	-1.3975
39	41.1458	-81.4619	-1.4375
40	41.1458	-81.4619	-1.2275
41	41.1458	-81.4618	-1.4275

LeFever Delta
May 3, 2015 continued

Station ID	Latitude	Longitude	Elevation (m)
42	41.1458	-81.4618	-1.6175
43	41.1459	-81.4618	-1.6975
44	41.1459	-81.4618	-1.6175
45	41.1461	-81.4620	-1.2175
46	41.1461	-81.4620	-1.6375
47	41.1460	-81.4620	-1.6075
48	41.1460	-81.4620	-1.5875
49	41.1460	-81.4621	-1.5575
50	41.1459	-81.4621	-1.3775
51	41.1459	-81.4622	-1.2175
52	41.1460	-81.4624	-1.2175
53	41.1462	-81.4624	-1.7675
54	41.1463	-81.4623	-1.6575
55	41.1463	-81.4622	-1.6575
56	41.1463	-81.4622	-1.7775
57	41.1462	-81.4622	-1.2175
58	41.1459	-81.4619	-1.5575
59	41.1459	-81.4619	-1.7475
60	41.1459	-81.4618	-1.6175
61	41.1460	-81.4618	-1.5775
62	41.1460	-81.0118	-1.5275
63	41.1459	-81.4615	-1.5575
64	41.1459	-81.4615	-1.5375
65	41.1457	-81.4619	-1.1575
66	41.1456	-81.4618	-1.1975
67	41.1457	-81.4618	-1.5675
68	41.1457	-81.4618	-1.5475